PHOSPHORYLATION OF A MAJOR TEGUMENT PROTEIN VP8 AND ITS REGULATORY ROLE IN INFECTION WITH BOVINE HERPESVIRUS TYPE ONE

A Thesis Submitted to
The College of Graduate and Postdoctoral Studies
In Partial Fulfillment of the Requirements
For the Degree of Doctor of Philosophy
In the School of Public Health
University of Saskatchewan
Saskatoon

By

KUAN ZHANG

PERMISSION TO USE

In presenting this thesis/dissertation in partial fulfillment of the requirements for a Postgraduate degree from the University of Saskatchewan, I agree that the Libraries of this University may make it freely available for inspection. I further agree that permission for copying of this thesis in any manner, in whole or in part, for scholarly purposes may be granted by the professor or professors who supervised my thesis work or, in their absence, by the Head of the Department or the Dean of the College in which my thesis work was done. It is understood that any copying or publication or use of this thesis or parts thereof for financial gain shall not be allowed without my written permission. It is also understood that due recognition shall be given to me and to the University of Saskatchewan in any scholarly use which may be made of any material in my thesis/dissertation.

Requests for permission to copy or to make other uses of materials in this thesis/dissertation in whole or part should be addressed to:

Graduate Chair of Vaccinology and Immunotherapeutics Program
School of Public Health
University of Saskatchewan
104 Clinic Place
Saskatoon, Saskatchewan S7N 2Z4
Canada

OR

Dean
College of Graduate and Postdoctoral Studies
University of Saskatchewan
107 Administration Place
Saskatoon, Saskatchewan S7N 5A2
Canada

ABSTRACT

Bovine herpesvirus-1 (BoHV-1) infects bovine species causing respiratory and genital syndromes. VP8, encoded by the *ul47* gene, is a tegument protein essential for BoHV-1 to infect host animals. This protein is abundantly incorporated into the virus and is extensively expressed in BoHV-1-infected cells. VP8 is phosphorylated by a viral kinase, unique short protein 3 (US3), and a cellular kinase, casein kinase 2 (CK2). With the aim to investigate the function of VP8 in the life cycle of BoHV-1, we hypothesized that US3- and CK2-mediated phosphorylation changes the functions of VP8, which in turn affects the replication of BoHV-1.

Using site-directed mutagenesis and liquid chromatography-mass spectrometry we identified minimal amino-acid residues of VP8 required for phosphorylation by US3 and CK2, respectively. US3 phosphorylated VP8 at two residues, serine 16 (S^{16}) and serine 32 (S^{32}). Phosphorylation at S^{16} was essential for subsequent phosphorylation at S^{32}. CK2 phosphorylated at least eleven threonines (T) and serines (S) in VP8. Mutating seven of them (T^{65}, S^{66}, S^{79}, S^{80}, S^{82}, S^{88} and T^{107}) blocked the whole protein being phosphorylated by CK2. By replacing the critical phosphorylation sites for US3 and CK2 in VP8, we generated a mutant VP8 that was not phosphorylated by US3 and CK2. This non-phosphorylated VP8 was studied in parallel with wild-type VP8. Promyelocytic leukemia (PML) protein was redistributed by wild-type VP8 but not by non-phosphorylated VP8 in transfected cells. This implicates that VP8 may be involved in counteracting PML-related host antiviral defenses by redistributing PML protein, and is dependent upon its phosphorylation. VP8-transfected cells developed nuclear lipid droplets (LDs), suggesting that VP8 causes lipid accumulation in host cells. Wild-type VP8 was more abundant around the surface of the droplets compared with the mutant VP8.

We next investigated the roles of phosphorylated VP8 in the life cycle of BoHV-1. A mutant virus (BoHV-1-YmVP8) with non-phosphorylated VP8 was generated by using homologous recombination in mammalian cells. The results showed that the DNA encapsidation was reduced in mutant virus-infected cells, resulting in a lower virus titer, when compared with wild-type virus-infected cells. Capsids without DNA cores were more frequently found in the nuclei and perinuclear spaces of mutant virus-infected cells than that of wild-type virus-infected cells. However, we did not observe obvious restriction of virus egress during the infection with

BoHV-1-YmVP8. Virions lacking DNA core were released into the extracellular medium. Therefore, we conclude that phosphorylated VP8 promotes DNA encapsidation of BoHV-1 in the nuclei of infected cells. VP8 appeared in the Golgi apparatus of cells infected with wild-type virus late during infection. The non-phosphorylated VP8 did not leave the nuclei of BoHV-1-YmVP8-infected cells, suggesting that phosphorylation is critical for the cytoplasmic transport of VP8. By measuring the amount of mature virion-incorporated VP8, we found that mutant BoHV-1 contained lower amounts of VP8 than wild-type virus. Together with the finding that non-phosphorylated VP8 was not able to localize in the Golgi, it implies that phosphorylation is important to place VP8 into a proper cellular location.

Based on the finding that cytoplasmic localization of VP8 was inhibited by mutating phosphorylation residues, we hypothesized that the cellular localization of VP8 is regulated by US3- and/or CK2-dependent phosphorylation. We verified that VP8 was initially localized into the nucleus and then transported into the cytoplasm when BoHV-1 infection progressed to late stages. The cytoplasmic VP8 subsequently accumulated in the Golgi apparatus. We also found that the kinase activity of US3 was critical for VP8 to be exported from the nucleus. Deletion of US3 in BoHV-1 or mutating the essential residue for US3-mediated phosphorylation in VP8 blocked the nuclear-cytoplasmic transport of VP8. In the amino-acid sequence of VP8, US3-phosphorylated residues are closely adjacent to nuclear localization signals (NLSs), providing the possibility that addition of phosphoryl groups to these residues may affect the binding activity of the NLSs, blocking VP8 entering or re-entering the nucleus. The US3-phosphorylated VP8 is transported to the cytoplasm through more than two pathways that require different types of nuclear export signals (NESs). In the cytoplasm, VP8 might experience virus-induced modifications or protein interactions, which led the protein to localize in the *cis*-Golgi cisternae. VP8 was less likely to present in the *trans*-Golgi network (TGN). The *cis*-Golgi localization of VP8 and Golgi accumulation of viral particles suggest that VP8 localizes in the Golgi for incorporation into the virions, and that it may not directly contribute to viral egress.

Altogether, this research described the importance of phosphorylation in regulating the functions of VP8 during BoHV-1 infection. Nuclear VP8 phosphorylated through CK2 is responsible for DNA encapsidation of BoHV-1 and remodeling the cellular antiviral factor PML. When nuclear VP8 is phosphorylated by US3, the cytoplasmic translocation of VP8 is activated

possibly by inactivating the NLSs. Subsequently, VP8 aggregates towards the *cis*-Golgi apparatus where VP8 is abundantly incorporated into virions such that the mature virus contains enough VP8 to benefit future infection.

ACKNOWLEDGEMENTS

I would like to acknowledge the support and cultivations that I have received to accomplish this research. Firstly, I would like to express my sincere appreciation to my graduate supervisor Dr. Sylvia van Drunen Littel-van den Hurk for her mentorship and encouragement. Her wealth of knowledge and willingness to explore new areas have been inspiring me to learn and to search. Her guidance will have great impact in my future life. I am thankful to my advisory committee, Dr. Qiang Liu, Dr. Joyce Willson, Dr. Scott Napper and Dr. Suresh Tikoo, for their scientific guidance and open-door discussions throughout my study.

I obtained expert technical training and assistance from many people during this project. Most of the research techniques I learned are direct results of the masterful training from Ms. Marlene Snider, Ms. Laura Latimer, Dr. Robert Bownlie and Mr. Wayne Connor. I am grateful to them for their love, patience and encouragement. Additionally, I am thankful to many wonderful graduate students and post-doctoral fellows in the lab, Sharmin Afroz, Indranil Sarkar, Elisa Martinez, Amanda Wilson, Sams Sadat, Ravendra Garg, and Yi Wang. The moments that we shared to celebrate our special days and to encourage each other through the difficulties are the best memories during these years.

The scholarship program provided by the China Scholarship Council (CSC) gave me the opportunity to study abroad from China. Research funding is from the Natural Sciences and Engineering Research Council of Canada (NSERC). I would like to express my gratitude to their funding support.

Lastly but most importantly, I would like to thank my beloved family: my grandmother who has raised me as a baby with all her love, my parents who have shaped me with quality education, and my husband who brightens up my life with love and prayers.

TABLE OF CONTENTS

LIST OF FIGURES AND TABLES

LIST OF ABBREVIATIONS

ADD — ATRX-Dnmt3-Dnmt3L domain

ATP — adenosine triphosphate

ATRX — alpha thalassemia/mental retardation syndrome X-linked protein

BAC — bacterial artificial chromosome

BoHV-1— bovine herpesvirus-1

BoHV-5— bovine herpesvirus-5

BFA — brefeldin A

BPIV-3— bovine parainfluenza virus-3

BRSV — bovine respiratory syncytial virus

BVDV — bovine viral diarrhea virus

CAMK2— calmodulin-dependent kinase 2

CDK2— cyclin-dependent kinase 2

CK2— casein kinase 2

COS-7— African green monkey fibroblast-like cells

CRM1— chromosomal maintenance 1

CTMP7 — carboxyl-terminal modulator protein 7

DAXX — death domain-associated protein 6

DDB1— DNA damage binding protein 1

DIVA — differentiating infected from vaccinated animals

DMAT — 2-Dimethylamino-4,5,6,7-tetrabromo-1H-benzimidazole

DYRK1α — dual-specificity Tyr phosphorylation-regulated kinase 1A

EBTr — embryonic bovine tracheal

eEF2 — eukaryotic elongation factor 2

EHV-1— equid herpesvirus-1

ER — endoplasmic reticulum

ERK — extracellular signal-regulated protein kinase

FBT — fetal bovine testis

FTCD — formimidoyltransferase cyclodeaminase

GOLGB1 — golgin subfamily B member 1

GSK3β — glycogen synthase kinase 3β

HAUSP — herpesvirus-associated ubiquitin-specific protease

HDAC — histone deacetylases

Hep-2— human epithelial type 2 cells

HHV-1 — human herpesvirus-1 (or HSV-1, herpes simplex virus-1)

HHV-3 — human herpesvirus-3 (or VZV, varicella-zoster virus)

HHV-4 — human herpesvirus-4 (or EBV, Epstein–Barr virus)

HHV-5 — human herpesvirus-5 (or HCMV, human cytomegalovirus)

HHV-8 — human herpesvirus-8 (or KSAH, Kaposi's sarcoma-associated herpesvirus)

HP1— heterochromatin protein 1

hpi — hour(s) post infection

hpt — hour(s) post transfection

HSR — half-site reaction motif

IBR — infectious bovine rhinotracheitis

IC_{50}— half maximal inhibitory concentration

IFN — interferon

IR — internal repeat

LD — lipid droplet

LC-MS — liquid chromatography–mass spectrometry

LMB — leptomycin B

MDBK — Madin Darby bovine kidney

MEK1— mitogen-activated protein kinase kinase 1

MHV68— murine herpesvirus 68

MOI — multiplicity of infection

MTC— multisubunit tethering complex

ND10— nuclear domain 10 (or PML-NB, promyelocytic leukaemia nuclear body)

NEC — nuclear egress complex

NES — nuclear export signal

NLS — nuclear localization signal

ORF — open reading frame

PAK2— p21-activated kinase 2

PCLS — precision-cut lung slices

PDU — procedure defined unit

PHD — plant homeodomain

PhK — phosphorylase kinase

PKA — protein kinase A

PML — promyelocytic leukemia protein

PLB — phospholamban

RING — really interesting new gene

RhoA — Ras homolog protein family member A

S/T kinase — serine/threonine protein kinase

STAT1— signal transducer and activator of transcription 1

SP100— speckled protein of 100 kDa

SuHV-1—Suid alphaherpesvirus 1 (or PRV, pseudorabies virus)

TBB — 4,5,6,7-tetrabromobenzotriazole

TBCA — tetrabromocinnamic acid

TG — trigeminal ganglion

TGN — trans-Golgi network

TGOLN2 — *trans*-Golgi network integral membrane protein 2

tk — thymidine kinase

TR — terminal repeat

TRIM — tripartite motif-containing protein

UbcH5a — ubiquitin-conjugating enzyme H5a

U_L — unique long region

U_S — unique short region

US3— unique short protein 3

CHAPTER 1

1 LITERATURE REVIEW

Bovine herpesvirus-1 (BoHV-1) is an economically important pathogen in cattle. This virus is one of the major causes of infectious bovine rinotracheitis (IBR), which induces over a billion dollars losses to the cattle industry of USA (1). In addition, BoHV-1 infection restricts international trading (1, 2). This literature review incudes a comprehensive introduction of BoHV-1 classification, the disease caused by BoHV-1, and major viral components. BoHV-1 belongs to the *herpesviridae,* thus it shares common features with other members of the virus family, such as causing lifelong latent infection in host animals, and having a typical herpesvirus structure. Researches of several herpesviruses indicate that tegument proteins play important roles in promoting virus entry (3, 4), DNA encapsidation (5-8), virus assembly (9-11), and egress (12, 13). However, much less is known about the molecular details and biological functions of BoHV-1 tegument proteins. An introduction of tegument proteins of other herpesviruses is included, and it provides important directions to study the functions of BoHV-1 tegument proteins.

This research aims to characterize phosphorylation of VP8, the most abundantly incorporated tegument protein of BoHV-1 (14), and phosphorylation-regulated functions of the protein. A viral kinase, unique short protein 3 (US3), and a cellular kinase, casein kinase 2 (CK2), phosphorylate VP8 (15). The functions and enzyme properties of these two kinases are covered in this literature review. Because specific inhibitors are used to inhibit CK2 activity in this research, an introduction of CK2 inhibitors is also included.

1.1 Introduction of bovine herpesvirus-1 (BoHV-1)

1.1.1 Virus classification of BoHV-1

According to the International Committee on Taxonomy of Viruses (ICTV) BoHV-1 belongs to the genus *varicellovirus*, the *alphaherpesvirinae* subfamily of the *herpesviridae*. The genus *varicellovirus* includes an important human pathogen, human herpesvirus-3 (HHV-3), and pathogens with veterinary importance, such as bovine herpesvirus-5 (BoHV-5) and equid herpesvirus-1 (EHV-1). BoHV-1 has many similarities with other members of the

alphaherpesvirinae, for instance human herpesvirus-1 (HHV-1), with respect to the viral composition, lytic life cycle, and latency infection.

BoHV-1 has been classified as three subtypes (1.1, 1.2a, and 1.2b) based on their genetic and antigenic characteristics (16). Subtype 1.1 is more associated with respiratory infections; subtype 1.2a mostly causes respiratory and genital symptoms; and subtype 1.2b is predominantly associated with genital infections (17). Distinctive diagnosis of infection with these subtypes requires viral DNA analysis (18, 19). Likewise, HHV-1 commonly causes cold sores around the mouth and face in humans (20), whereas HHV-2 is more associated with genital symptoms of human patients (21). However, increasing evidences indicate that HHV-1 also is a sexually transmitted pathogen (22). Subtype BoHV-1.1 is the most common subtype in feedlot cattle, causing respiratory infections (23), thus two BoHV-1.1 isolates were analyzed in this research, a Cooper strain (24) from USA and a 108 strain (25) isolated from Alberta, Canada.

1.1.2 BoHV-1 infection and control strategies

BoHV-1 is responsible for a highly contagious disease in cattle, named infectious bovine rhinotracheitis (IBR) (26). BoHV-1 is effectively transmitted through direct contact or airborne transmission. Transmission is also frequently conducted by mating and artificial insemination within and between breeding groups (27). Animals infected with BoHV-1 may develop respiratory symptoms, conjunctivitis, genital disorders, and abortions (28, 29). On top of that, BoHV-1 also causes immunosuppression in host animals (30). Together with the increased mucous secretion and damaged epithelium it provides a beneficial environment for many other pathogens to replicate; BoHV-1 positive animals are frequently co-infected with bovine viral diarrhea virus (BVDV), bovine parainfluenza virus-3 (BPIV-3), bovine respiratory syncytial virus (BRSV) and several bacterial pathogens, such as *Mannheimia haemolytica*, *Mycoplasma bovis*, *Pastuerella multocida*, and *Histophilus somni* (31), causing bovine respiratory disease complex (1, 32).

1.1.2.1 Epidemiology of BoHV-1

An upper respiratory disease related to BoHV-1 infection was first reported in 1954 on a dairy farm in California (33). The virus was firstly isolated in 1958 by a Canadian research group

and it confirmed that IBR was directly caused by BoHV-1 (26). Infection with BoHV-1 occurs all over the world, but the severity of this pathogen differs between countries and regions (34). For example, serum-neutralizing antibodies against BoHV-1 are present in 10-67% of free-ranging elk and domestic cattle in Western Canada (35, 36). The reported prevalence in different Turkish regions ranges from 2.32% to 79.74% (37). Infection with BoHV-1 has been reported in almost every state in India with a high incidence. For example, the seroprevalence reaches 46.5% in domestic cattle in Uttar Pradesh (38) and the predominant circulating subtype in this region is BoHV-1.1 (39). The prevalence in the Tibetan region of China has been reported to range from 27.9% to 44.6% (40). BoHV-1 has been eradicated in several European regions, including Bavaria of Germany, Bolzano of Italy, Austria, Denmark, Finland, Switzerland, Sweden and Norway (41). With respect to Canada and the United States, eradication would be extremely difficult due to the large number of cattle herds and high prevalence of BoHV-1 (23).

Outbreaks of BoHV-1 in a naive herd are commonly caused by introducing an infected animal without diagnostic tests and proper management, leading to quick spread of the disease within the herd. After the primary infection, animals become latently infected with BoHV-1. In a latently infected herd, disease outbreaks happen in all seasons of the year, with a significant rise from December to February in Northern Hemisphere countries (42). During this time, herds have increased BoHV-1-related respiratory diseases and abortions (42). Generally, BoHV-1 infection occurs in host animals of any age. Calves have a lower rate of seropositivity than the older population, which is possibly due to the latent infection over the years (37). Although cattle are the major host for BoHV-1, it also infects sheep, red deer, reindeer, mule deer, pronghorn antelopes, buffalos, and goats (17, 43).

Infection with BoHV-1 causes significant losses in animal productivity, although it is usually not lethal (44). A study conducted in the UK has reported that the average daily milk production is reduced by 2.6 kg in BoHV-1-positive cows compared with negative cows (45). BoHV-1 infection also increases the abortion rate in a herd. Abortion induced by BoHV-1 occurs between 4 and 8 months after gestation (46). According to a report from India, 21.4% of bovine abortions in the state of Punjab are caused by BoHV-1 (46). This rate is over 50% in Western Turkey (43). Infections with BoHV-1 and BoHV-4 contribute to 42% of the bovine abortions in Morocco of North Africa (47). Moreover, many other important issues are caused by BoHV-1,

including reduction of heard health, increase of management costs, and restrictions of international trading.

1.1.2.2 Pathogenesis of BoHV-1

Epithelial cells in the mucosa of upper respiratory and genital tracts of host animals are the primary target sites for BoHV-1. The virus starts a lytic replication in host cells, resulting in massive virus production. The progeny virus is shed to the extracellular environments or enters the blood stream. Blood-stream circulated BoHV-1 passes through the placenta barrier and may cause abortion (48). In addition, the virus directly infects neighboring cells by cell-to-cell spread. During the primary infection, virus establishes a latent infection in the regional ganglia. It enters the axons of local nerve cells, and travels to the neuron bodies along the axons (2). Reactivation from latency occurs when a host is under stress or in weak immune condition (48). Once the lytic infection is reactivated, the virus enters a new replication cycle and the infected animal starts to shed virus.

1.1.2.3 Prevention of BoHV-1

Vaccination is the major strategy to control BoHV-1 (49-51). In Europe, marker vaccines that differentiate infected from vaccinated animals (DIVA) are commonly used. A marker vaccine is generated by deleting a gene encoding an immunogenic antigen present in a pathogen, thus creating a marker that is negative in vaccinated animals but is positive in infected animals (52). For instance, a marker protein, gE, is omitted in an attenuated live vaccine, which avoids an immune response against gE in vaccinated animals;, hence an infected animal will be distinguished from a vaccinated animal through testing the presence of gE-specific antibodies (52). The marker vaccination and test-slaughter strategies have greatly contributed to eradicate BoHV-1 in many countries (53). Glycoprotein gE was selected as a marker in the DIVA vaccine for the following reasons. Firstly, deletion of gE significantly reduces the virulence of the virus (54), and the vaccine virus preserves high immunogenicity (55). Secondly, vaccine virus without gE has a reduced chance of reactivation from latency, although it can establish latent infection in vaccinated animals (56). Thirdly, deletion of gE allows to distinguish vaccinated animal from virus-infected animals by detecting serum gE-specific antibody (57). However, this marker

vaccine has several weaknesses. The first weakness is that the diagnostic test is fully dependent on detecting serum gE-specific antibody. The limited sensitivity of current gE-specific antibody tests, together with the fact that the gE-specific immune response is relatively low, leading to the possibility of false negative results. More importantly, there are biosafety concerns about using gE-deleted live attenuated vaccine. This vaccine has the potential to cause abortions in pregnant animals and to gain virulence by recombination with field strains (18, 19).

1.2 Comparative composition of alphaherpesviruses and BoHV-1

1.2.1 The genome of alphaherpesviruses and BoHV-1

The herpesvirus genomes are summarized as five major classes, from A to F (58). This classification is based on the structures of the virus genome (59). Class A genome contains a unique (U) sequence which is flanked by a direct repeat (R) (Figure 1.1). Class B genome consists of a U sequence flanked by variable copies of directly repeated sequences (Rs). Class C genome is derived from the class B genome with an internal Rs', which is not related to the terminal Rs. Class D genome is composed of a unique long (U_L) region and a unique short (U_S) region, which is flanked by inverted internal and terminal repeats (IR_S and TR_S). Class E genome is similar to the class D, except that the U_L sequence is flanked by two inverted repeats (TR_L and IR_L). Class F genome is a simple U sequence lacking inverted and direct repeats (58, 59). Alphaherpesviruses HHV-3, EHV-1, SuHV-1, and BoHV-1 represent the class D genome (58). HHV-1 and HHV-2 are examples of the class E genome (58).

The BoHV-1 genome is a double-stranded linear DNA of about 135 kilo base pairs (kbp) (60). It is a class D genome containing a 103-kbp U_L region and a 32-kbp U_S region flanked by 11-kbp IR_S and TR_S (Figure 1.1) (61). The U_L region is fixed in one orientation, named the prototype orientation (62). The U_S region is flanked by large inverted DNA repeats, namely internal repeat (IR) and terminal repeat (TR) (62). Other herpesviruses with class D genomes include HHV-3, Suid alphaherpesvirus 1 (SuHV-1), and EHV-1 (61). The BoHV-1 genome contains 73 open reading frames (ORFs), of which 33 ORFs are essential for viral replication in tissue culture (63). A list of current identified BoHV-1 viral protein components is summarized in Table 1.1. The *ul47* gene, located in the U_L region of the genome, encodes VP8, which is

essential for BoHV-1 replication in host animals but not in tissue culture (64). This high-GC-content gene is flanked by the ORFs of *ul48* and *ul46* encoding VP16 and VP22, respectively.

BoHV-1 DNA replicates in the cell nucleus. The mechanism of replication and cleavage of the BoHV-1 genome is not well understood. However, the rolling circular replication model of the HHV-1 genome (65) may also apply for BoHV-1, because concatemeric DNA is found in BoHV-1 infected cells (61), and several viral proteins important for HHV-1 DNA replication is conserved in BoHV-1, including single-strand DNA-binding protein (U_L29), DNA polymerase catalytic subunit (U_L30) (66), and alkaline deoxyribonuclease (U_L12) (67). Linear BoHV-1 DNA is circularized during infection. DNA replication is initiated at one of the origins where one strand of the DNA is nicked. The DNA is extended as a long continuous DNA concatemer which is subsequently cleaved into individual genomes (Figure 1.2).

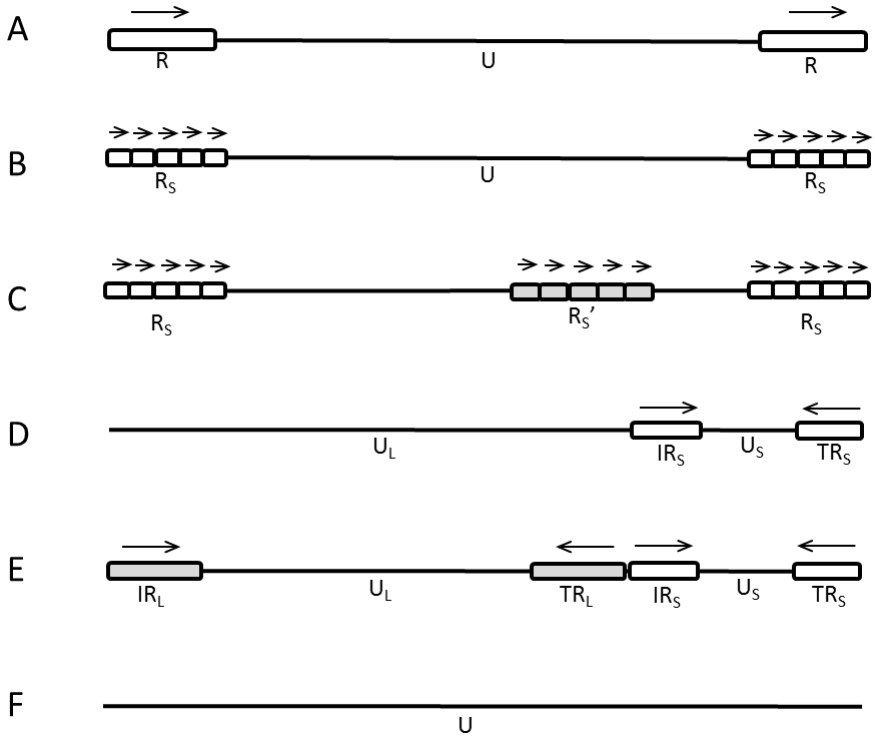

Figure 1.1 Classification of herpesvirus genome structures.

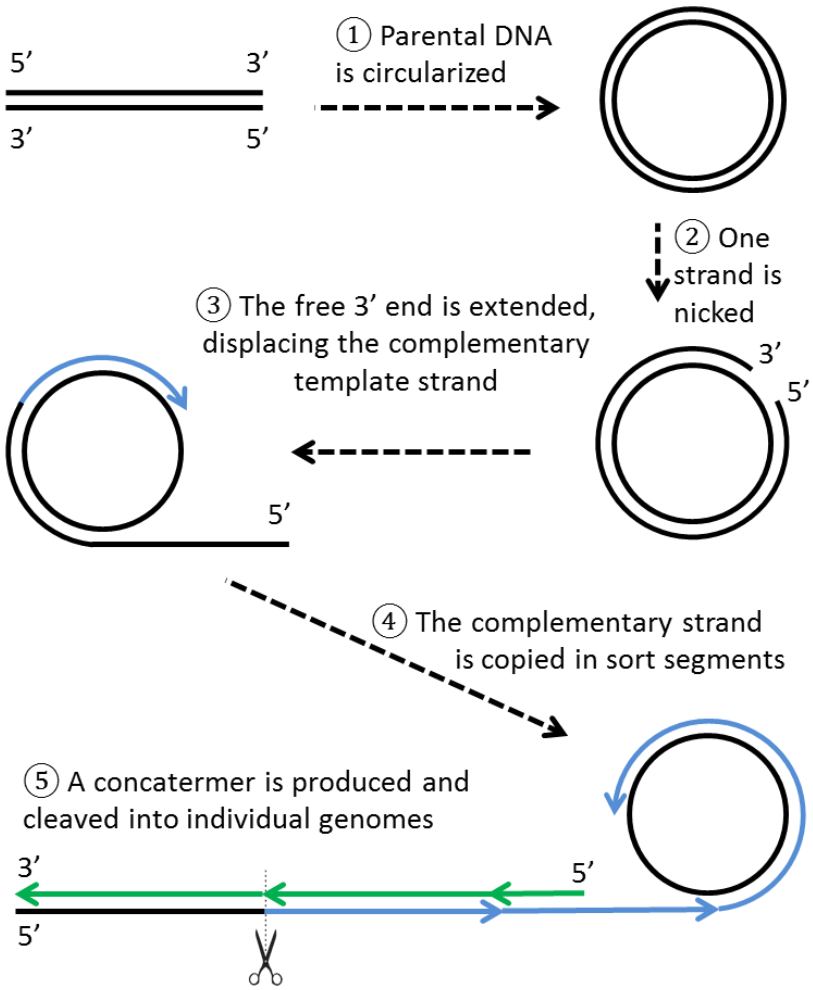

Figure 1.2 Rolling circle model of BoHV-1 DNA replication.

Table 1.1 Viral proteins incorporated into BoHV-1

Protein category	Protein name	BoHV-1 gene	Protein Function	NCBI accession	Reference
Capsid protein	VP5	*ul19*	Major capsid protein	AFV53400	(64)
	U_L6	*ul6*	Portal protein	AFV53413	(68)
	U_L26	*ul26*	Scaffold protein, serine protease	AFV53392	(69)
	$U_L26.5$	*ul26.5*	scaffold protein	CAB01599	(69)
	U_L38	*ul38*	Capsid typlex subunit 1	AFV53380	(68)
	U_L18	*ul18*	Capsid triplex subunit 2	AFV53401	(68)
Tegument protein	ICP4	*icp4*	Transcriptional regulator	AFV53424	(68)
	ICP27	*ul54*	RNA metabolism	AFV53364	(63)
	VP8	*ul47*	Major tegument protein, down-regulates IFN-signaling pathway	AFV53372	(15, 25)
	VP16	*ul48*	Gene expression regulation	AFV53404	(68, 70)
	VP22	*ul49*	Nuclear-cytoplasmic shuttling	AFV53370	(71, 72)
	US3	*us3*	S/T kinase	AFV53428	(15)
	$U_L3.5$	*ul3.5*	Virus maturation	AFV53416	(68, 73, 74)
	VP11/12	*ul46*	Possible gene regulation	AFV53373	(68)
	U_L17	*ul17*	DNA encapsidation	AFV53403	(68)
	U_L25	*ul25*	DNA encapsidation	AFV53394	(68, 75)
	U_L31	*ul31*	Nuclear egress	AFV53387	(68)
	U_L36	*ul36*	Capsid transport	AFV53382	(68)
	U_L37	*ul37*	Capsid transport	AFV53381	(68)
	U_L41	*ul41*	Cellular mRNA degradation	AFV53377	(68)
	U_L42	*ul42*	DNA polymerase prosessivity subunit	AFV53376	(68)
	U_L51	*ul51*	Possible viral maturation and egress	APW77332	(76)
Envelope proteins	gB	*ul27*	Virus entry/ Membrane fusion	AFV53391	(77)
	gC	*ul44*	Virus attachment	AFV53374	(78)
	gD	*us6*	Virus attachment	AFV53430	(78)
	gE	*us28*	Cell-to-cell spread	AFV53432	(79, 80)
	gG	*us4*	Cell-to-cell spread	AFV53429	(80, 81)
	gH	*ul22*	Virus entry/Cell-to-cell spread	AFV53397	(80, 82)
	gI	*us7*	Cell-to-cell spread	AFV53431	(79)
	gK	*ul53*	Virus egress	AFV53365	(63)
	gL	*ul1*	Virus entry/Cell-to-cell spread	AFV53419	(83)
	gM	*ul10*	Membrane fusion	AFV53409	(84)
	gN	*ul49.5*	gM binding partner	ADE08266	(63)

1.2.2 Capsid proteins of alphaherpesviruses and BoHV-1

A capsid of alphaherpesviruses is an icosahedral protein shell that encloses the viral genome. The capsid is assembled and packaged with viral DNA in the host cell nucleus. The process of packaging viral DNA into the capsids is called encapsidation (65). In HHV-1, this process is initiated through recognizing a unique c (Uc) element and is terminated by recognizing a unique b (Ub) element by packaging proteins (85, 86). Modified by nuclease proteins U_L12 (87) and $U_L12.5$ (88), the viral DNA turns into a suitable configuration for encapsidation. Subsequently, the DNA is inserted into a capsid shell through a portal on a unique vertex of the capsid (89). The portal is a ring structure formed with 12 copies of portal protein U_L6 (90) through disulfide bonds in the leucine zipper region of each subunit (90, 91). This leucine zipper region is modulated by U_L32, a non-capsid protein, to optimize the DNA encapsidation (6). When the viral genome is incorporated into a capsid, an additional stabilizing adjustment of the capsid by U_L25 is required to retain the genome (7). U_L25 is exposed on the surface of a capsid (92), forming pentamers on each of the capsid vertices (93). On the one hand it associates with other capsid proteins, such as VP5 (U_L19), to incorporate into the capsids (93). On the other hand, it also interacts with a tegument protein, U_L17, which stabilize U_L25 in the capsids (7). Deletion of U_L25 from HHV-1 results in aberrant truncation of the genome and reduced DNA-containing capsids in infected cells (94). Additionally, many other viral proteins, including capsid protein U_L15, U_L28, and U_L33, as well as tegument protein U_L16 (8), have been reported to facilitate DNA encapsidation (5, 6).

Capsids egress to the cytoplasm through a unique process, which includes several steps: movement of capsids towards the nuclear periphery, disruption of the nuclear lamina, budding through the inner nuclear membrane by obtaining a primary envelope, passing the outer nuclear membrane by de-envelopment (95).

The major protein components of BoHV-1capsids is VP5 (64, 68), alike to HHV-1 capsid (96). Additionally, it also incorporates U_L38 (capsid triplex subunits 1), U_L18 (capsid triplex subunits 2), U_L26 (scaffolding protein), U_L6 (portal protein) (68) and U_L25 (75). A mutant BoHV-1 omitting U_L25 fails to produce virus although it produces viral DNA and late proteins (75).

1.2.3 Tegument proteins of alphaherpesviruses and BoHV-1

1.2.3.1 Dissociation of tegument proteins from alphaherpesviruses

Herpesviruses incorporate large amounts of protein between the envelope and the capsid forming the tegument layer which makes up a significant portion of the virus mass (97). When herpesviruses enter host cells, tegument proteins are released from the viruses into the host cells to modulate the intracellular environment and to initiate viral replication, including suppressing cellular protein transcription (98), controlling cell death signaling (99-102), repressing innate immune responses (103-105), guiding viral capsids to the nuclear pore (106-110), and promoting viral gene transcription (111, 112).

Tegument dissociation is an energy-consuming reaction that requires enzymes, adenosine triphosphate (ATP), and Mg^{+}. The dissociation reaction is completely abolished by inactivating enzymes at 60 °C or lack of ATP (113). Tegument-protein dissociation is regulated by phosphorylation. For example, the dissociation of VP22 from HHV-1 is efficiently promoted by phosphorylation through CK2 (113). Thus several tegument proteins of HHV-1 are non-phosphorylated in the virion but are phosphorylated in infected cells (14, 114, 115). Several HHV-1 kinases are incorporated into the tegument, such as U_L13 (116) and US3 (113, 117, 118). After infection, they are dissociated into infected cells to phosphorylate viral and cellular proteins.

Tegument proteins dissociate from viruses in an order that is related to their locations in the virion and their functions in the infection. VP16 of HHV-1 completely dissociates form virus particles as soon as they enter the host cell (119). Free VP16 travels into the nucleus to stimulate the immediate early gene expression (120). VP13/14 is a minor tegument protein that dissociates quickly after HHV-1 entry (113). In HHV-1-infected cells, VP13/14 colocalizes with ICP4, a viral transcriptional activator, suggesting a role of VP13/14 in viral RNA translation (121). However, VP13/14 does not directly affect the efficacy of reporter RNA translation (122). Instead, it maintains the stability of mRNA by interacting with ICP27 (123). In the mature virions of HHV-1, VP13/14 is incorporated into the tegument layer. VP22 gradually leaves the virus at a slower speed than VP16 (119) and VP13/14 (113). U_L36 and U_L37, localized in the inner tegument layer, are released even more slowly. They are partially dissociated from the capsids, and a residual portion remains associated with the capsid during transit toward the

nucleus in the neuronal cell body (119). This is in line with their major function of precisely guiding the capsids to the nuclear pore complexes (110). A similar dissociation pattern has been described for SuHV-1 (124). The dissociation of SuHV-1 U_L11, U_L47, U_L48 and U_L49 takes place earlier than that of several other tegument proteins, including U_L36, U_L37 and US3 (124).

1.2.3.2 Tegument proteins that facilitate cellular and nuclear entry of alphaherpesviruses

In a host cell, herpesviruses cross the cell membrane and nuclear membrane to transport their genome into the cell nucleus. Multiple viral glycoproteins and cellular receptor proteins are engaged in the viral entry through cell membranes. Two pathways contribute to this stage; one is a pH-dependent endocytic pathway and the other is pH-independent fusion between the virion envelope and the plasma membrane (124, 125). Glycoproteins are important in the viral attachment and entry (124, 126). In the cytoplasm, viruses associate with microtubules for intracellular migration (127).

HHV-1 tegument proteins U_L36 (107) and U_L37 (106) navigate the incoming virus particles towards the nuclear pore complexes. U_L36 in HHV-1 particles is essential to lead the virus towards the nucleus and to inject the viral DNA into the nucleus. It associates with U_L37, which directly contacts the capsids. U_L36 uses a nuclear localization signal (NLS) to enter the nucleus. It takes the capsids towards the nuclear pore complex to inject viral DNA (108). In U_L36, introducing a single-amino-acid mutation in a region that is responsible for HHV-1 DNA entry causes accumulation of viral particles around the nuclear pore area (109). When capsids arrive at the nuclear pore complex, U_L36 is cleaved to promote viral DNA release (128). This cleavage takes place only when the capsids reach the nuclear pore complex (128). U_L37 is required for the optimal incorporation of U_L36 into HHV-1 virions (129). It also transports HHV-1 by mimicking host trafficking machinery (130), although it is not an essential factor for nuclear docking of viral capsids (129). The N-terminal region of U_L37 shares structural similarity with the multisubunit tethering complex (MTC), a cellular protein complex controlling vesicular trafficking to destination membranes (130). The capsid-transporting functionality of U_L36 and U_L37 is also confirmed in SuHV-1 (106), suggesting a conservative capsid-transporting machinery in alphaherpesviruses.

ICP0, well-studied as an immediate early protein, is incorporated into the tegument layer of HHV-1 by interacting with the capsids through its really interesting new gene (RING) finger domain (125). ICP0 contributes to the efficient nuclear delivery of HHV-1 capsids through degrading related cellular or viral proteins by its E3 ubiquitin ligase activity (125).

1.2.3.3 Tegument proteins are bridging molecules for alphaherpesvirus assembly and egress

After incorporation with the viral genome, nuclear capsids leave the nucleus to the cytoplasm. The process of transporting the nuclear capsids through the two-layer nuclear membrane is called nuclear egress, and is mainly accomplished through an envelopment-deenvelopment-reenvelopment pathway (131). If this pathway is not sufficient or is blocked, the nuclear membrane is broken down to allow capsids to be transported to the cytoplasm (9).

HHV-1 tegument proteins U_L31 and U_L34 are essential and sufficient for virus to egress through the envelopment-deenvelopment-reenvelopment mechanism by forming protein complexes docking in the inner nuclear membrane (9). However, U_L31 and U_L34 are independently expressed in the cytoplasm (9) and any interactions between them are inhibited before they arrive in the nucleus (10). When the two proteins are transported into the nucleus, they firmly interact with each other through multiple regions on the surface of each protein, forming a heterocomplex (10, 11). The U_L31-U_L34 complex causes the membrane to curve inwards, forming budding vesicles that enclose nuclear capsids (9). Only when they form a protein complex (132), U_L31 is able to bridge the connection between the nuclear membrane and viral capsids through its C-terminal region, and to activate the virus egress through its N-terminal region (10).

Herpesviruses use several strategies to modify the U_L31-U_L34 complex to maximize the efficiency of U_L31-U_L34-mediated virus egress. A cellular component P32 is attracted to the nuclear egress complex (NEC) and interacts with the U_L31-U_L34 complex to promote the de-envelopment of nuclear capsids during HHV-1 infection (133, 134). Moreover, ICP22 associates with the NEC to optimize the accumulation of the U_L31-U_L34 complex to the NEC (135). HHV-1 US3 is attracted to the NEC. U_L31 phosphorylated by US3 has a better capacity to promote virus egress than the non-phosphorylated form (12, 13). US3 also phosphorylates lamin A, leading to increased permeability of the nuclear membrane (136). During HHV-1 infection a

cellular kinase, protein kinase C (PKC), is attracted to the nuclear membrane (137) by a viral neurovirulent protein, γ134.5 (138). At the nuclear membrane, PKC phosphorylates lamin B and thus disrupts the nuclear lamin network (138).

HHV-1 VP13/14 (133) and ICP34.5 (139) are bridging proteins between P32 protein and the U_L31-U_L34 complex. Deletion of the bridging proteins reduces the amount of primary enveloped virus (133, 139). VP13/14 is encoded by the *ul47* gene of HHV-1. The expression of VP13/14 is activated by ICP8 (140), and a tyrosine kinase-mediated stimulation (141). Cellular VP13/14 is phosphorylated, while viral VP13/14 is associated with O-linked oligosaccharides (14). Similarly, VP8 of BoHV-1 is phosphorylated and glycosylated (25). However, it is not known whether the modification of VP8 is related to virion incorporation.

VP13/14 is predominantly localized in the nuclei of HHV-1-infected cells. It is associated with the nuclear membrane and the nucleoplasm. In the presence of US3, the phosphorylated VP13/14 localizes in the nucleoplasm (142). However, without US3-mediated phosphorylation VP13/14 is predominantly accumulated on the nuclear membrane (142). The nuclear localization of VP13/14 is driven by a NLS contained in the N-terminus of the protein sequence (143). When US3 phosphorylates a residue (S^{77}) near the NLS, the efficacy of the NLS is increased and VP13/14 tends to remain in the nucleoplasm (142). VP13/14 facilitates nuclear egress of HHV-1 by associating with the U_L31-U_L34 protein complex (133). VP13/14 is transiently transported into the cytoplasm (142-144). The transient cytoplasmic localization of VP13/14 is related to two types of NES contained in the sequence (144). One of the NESs localized in the C-terminus acts through the CRM1-dependent pathway (144). The other NES is an N-terminal motif which is regulated by an unidentified mechanism instead of the CRM1-signalling pathway (144). Inferred from the characteristics of VP13/14, the correlation between phosphorylation and cellular localization of BoHV-1 VP8 requires further study.

To egress through the cytoplasmic membrane, HHV-1 virus needs to anchor on the cell membrane. Capsid protein VP26 and tegument protein U_L37 bind with carboxyl-terminal modulator protein 7 (CTMP7), a cytoskeleton cross-linker protein localized in the cell membrane (145, 146) to mediate the interaction between the virus and cell membrane. Subsequently, viral glycoproteins accumulate on the cell membrane to assist virus egress (147). In neurons, gK is essential for virus egress from the cell body (148).

1.2.3.4 Tegument proteins of BoHV-1

Viral proteins incorporated into the tegument layer of BoHV-1 perform various functions during the infection. VP22 shuttles between nucleus and cytoplasm (72) and is an essential tegument protein for BoHV-1 to infect cattle (149). The nuclear localization and nuclear export of VP22 are mediated by NLSs and NESs within the protein sequence (72), which are precisely regulated at different stages of virus infection (150). At early stages of BoHV-1 infection, VP22 mainly localizes in the cytoplasm with accumulation in the perinuclear region (150). When the infection enters late stages VP22 massively enters the nucleus, where it regulates the acetylation of histone protein (149), and this transport is facilitated by phosphorylation of VP22 (150). BoHV-1 incorporates at least two kinase proteins, U_L13 and US3, into virus particles (151), phosphorylating many viral and cellular proteins. The major tegument protein VP8 is one of the substrates of US3 (15). A tegument protein $U_L3.5$ localizes in the Golgi apparatus of BoHV-1-infected cells, where it interacts with VP16 to promote virus maturation and egress (74). More tegument proteins and their functions are listed in Table 1.1.

VP8 is a major tegument protein of BoHV-1, encoded by the *ul47* gene, which is conserved among alphaherpesviruses (14, 152, 153). BoHV-1 incorporates VP8 more than other viral proteins (152). When VP8 is deleted in BoHV-1, a major part of the tegument layer is missing, and the incorporation of several other viral proteins is reduced, causing dramatic morphologic changes of mature virions (64).

In BoHV-1-infected cells, VP8 is initially transported into the nucleus (25, 154). It contains two NLSs (NLS1 and NLS2) near the N-terminus. NLS1 ($P^{11}RPRR^{15}$) is essential but not sufficient to mediate nuclear localization of VP8 (155). It requires a minimal nuclear-transferable peptide (residue 10 to 30) to transport the entire VP8 protein into the nucleus (156). NLS2 ($R^{48}PRVRRPRP^{54}$) may promote the function of NLS1 (156). In transfected cells VP8 shuttles from the nucleus to the cytoplasm, and then enters another nucleus within the same fused cell. The nuclear export of VP8 is mediated by nuclear export signals (NESs). At least two NESs in the sequence of VP8 have been reported. A leucine-rich sequence (NES1, $L^{485}SAYLTLFVAL^{495}$) is able to transport a reporter gene from the nucleus to the cytoplasm (155, 156). The NES1 is a chromosomal maintenance 1 (CRM1)-dependent sequence (144, 156). However, the nuclear export activity of NES1 is weak (144, 156) and is not essential for the

nuclear-cytoplasmic shuttling of VP8 (155), indicating there are more NESs in VP8. A second NES (NES2) is located within residues 95 to 123 (156). This sequence is resistant to the CRM1 inhibitor and does not contain hydrophobic residues (156). Thus, it uses another nuclear export pathway other than the CRM1-dependent pathway. NES2 is more effective than NES1 to transport a fusion protein to the cytoplasm (156). However, deletion of NES1 and NES2 does not inhibit the cytoplasmic transport of VP8 (156), so mechanisms and biological significances of VP8 transport are not fully understood.

VP8 interacts with many proteins to benefit BoHV-1 infection. Firstly, VP8 binds with DNA damage binding protein-1 (DDB1), an element of the Cul4A-DDB1 E3 ubiquitin ligase complex, resulting in monoubiquitination of VP8 (157). Secondly, VP8 associates with signal transducer and activator of transcription 1 (STAT1), a critical protein in the interferon (IFN)-signaling pathway. VP8 prevent the entry of STAT1 into the nucleus to interrupt the IFN responses (158). Thirdly, VP8 interacts with CK2 and US3 to obtain phosphorylation (15). Additionally, in context of BoHV-1-infection VP8 has RNA-binding activity (121, 159).

1.2.4 Glycoproteins of alphaherpesviruses and BoHV-1

Alphaherpesviruses are enveloped by a lipid bilayer and glycoproteins that facilitate viral attachment, penetration, and spread. Glycoprotein D is essential for HHV-1 to attach to host cells by binding with cellular receptors (160). A number of cellular receptors for gD have been identified, including nectin-1 and -2 (161), herpesvirus entry mediator (HVEM, or HveA) (160), and 3-O sulfated heparan sulfate (3-*O* HS) (162). Glycoprotein D is not conserved among all alphaherpesviruses. For example, HHV-3 lacks a gD and its gH-gL complex engages cellular receptors (163). HHV-1 gC also binds to heparan sulphate to facilitate virus attachment (164). Entry of HHV-1 is mainly mediated through gB, gH, and gL (165). In the HHV-1 envelope gB forms a homotrimer, and gH and gL form a heterodimer (166). After the virus attaches to a host cell, the gB complex goes through conformational changes leading to insertion of its fusion loops into the host cell lipid bilayer. This triggers merging of the virus envelope and cell membrane (166). The conformational change of the gB complex is triggered and regulated by the gH-gL complex (165). Other HHV-1 glycoproteins, such as gK (167) and gM (168), show activity of mediating membrane fusion, suggesting their roles in virus entry.

In addition to facilitating virus attachment and entry, glycoproteins of alphaherpesviruses play important roles in virus maturation and cell-to-cell spread. During early stages of HHV-1 infection, gM localizes in the nuclear membrane and may play a role in the nuclear egress of virus capsids by its membrane fusion activity (169). Glycoprotein M directs gN from the endoplasmic reticulum (ER) to the Golgi apparatus by interacting with gN, while gN has no impact on the localization of gM (169). The interaction of gM and gN is also found during EHV-1 infection (84). At a late phase of HHV-1 infection, gK interacts with U_L20 in the TGN (170) to facilitate the egress of virus through promoting virus to transport towards the cell membrane (171). This activity of gK to promote virus transport is in line with the fact that gK is essential for efficient spread of HHV-1 in corneal epithelium and trigeminal ganglia in a mouse model (172). During the egress of HHV-1, gD and the gE-gI heterodimeric complex are important for efficient secondary envelopment (173). However, deletion of gD, gE or gI of SuHV-1 does not significantly impair the secondary envelopment (173).

BoHV-1 glycoproteins contributing to attachment are gB, gC, and gD (126). gB forms a protein complex consisting an uncleaved subunit with a mass of 130 kDa, two cleaved subunits with masses of 74 kDa and 55 kDa proteins, respectively. These two cleaved polypeptides are linked by disulfide bonds (174). Blocking the cleavage site of gB reduces the plaque size of BoHV-1, suggesting that gB cleavage contributes to cell-to-cell spread of BoHV-1 (175). The 74-kDa subunit of gB binds with heparin sulfate on the cell surface to facilitate viral entry (77). BoHV-1 additionally uses gC to mediate the initial interaction of BoHV-1 with host cells by interacting with a heparin-like moiety on the cell surface (176). The 91-kDa mature product of gC forms a homodimer in BoHV-1-infected cells (174). gC is not essential for BoHV-1 to enter into host cells, although viral replication is drastically reduced in the absence of gC (126). gD, an essential protein for BoHV-1 infection, mediates viral attachment and entry (126, 177). gB and gD cause membrane fusion in transiently transfected cells, supporting their activities of mediating viral entry (126, 178). Additionally, intramuscular immunization with gB or gD induces high levels of neutralizing antibodies and protects cattle from BoHV-1 challenge (179, 180).

Two non-essential BoHV-1 glycoproteins, gE and gI, form a complex soon after their expression (181) and they remain as heterodimer when they are incorporated in the virion of

BoHV-1 (79). gE is essential for the viral incorporation of gI, whilst gI is not required for the packaging of gE (79). gI ensures the proper maturation of gE (181). Deleting both proteins reduces the size of viral plaques, indicating they are important for the cell-to-cell spread of BoHV-1 (79). However, they may not be related to viral attachment and penetration (79). The virulence of BoHV-1 with gE-deletion is greatly reduced and the reactivation from latent infection is repressed, making the gE-deleted mutant suitable to be a marker vaccine virus (182).

gG of BoHV-1 is a secreted glycoprotein that binds to a wide range of chemokines, and thus blocks chemokine activity by preventing them from binding to receptors (183). gG is involved in maintaining the junctional adherence among BoHV-1-infected cells, which is important for cell-to-cell spread of virus (81, 184). This protein may also be an anti-apoptotic viral factor during BoHV-1 infection (185). Additionally, gG-deleted virus has greatly reduced virulence, and gG has the potential to be used as a selective marker in live vaccine (182).

gH is required for the entry of BoHV-1 into host cells (186). gH needs to form functional heterodimers with gL to be properly processed and transported in BoHV-1-infected cells (83). The gH-gL complex facilitates the penetration of BoHV-1 (82) through mediating membrane fusion between the viral envelope and cell membrane (187, 188).

Several other glycoproteins are also identified in BoHV-1, making different contributions to virus infection. Glycoprotein K, forming a complex with U_L20 in infected cells, plays an indispensable role in BoHV-1 infection (189). Glycoprotein M interacts with gN through a disulfide bond resulting in a heterodimer in BoHV-1-infected cells (84), suggesting a conserved function with the HHV-1 gM-gN complex (169).

1.3 Protein phosphorylation and kinase proteins

1.3.1 Introduction of protein phosphorylation

Phosphorylation is a universal protein modification in eukaryotic cells that takes place through an acute and reversible reaction (190). The reaction is catalyzed by protein kinases, resulting in covalent addition of a phosphoryl group to the side chain of a specific residue in a substrate protein (190). Removing a phosphoryl group is called protein dephosphorylation which is catalyzed by protein phosphatases (191). In eukaryotes, most of the phosphorylation occurs on serine and threonine, and occasionally on tyrosine. These amino acids have a

nucleophilic (hydroxyl) group that attacks the gamma phosphate group of ATP, resulting in transfer of the phosphoryl group from the donor to the side chain of this amino acid (190). The reaction is facilitated by metal ions (192). The addition of one or multiple phosphoryl groups to a protein alters the conformation and electric charge of the protein, resulting in changes in protein function.

Protein phosphorylation plays an important regulatory role in protein function (190). It transforms extracellular and intracellular signals into metabolic patterns in almost every aspect of the cell life cycle because of its specifically controlled mechanisms and flexible combinations. It is estimated that 3-4% of the genes in eukaryotes encode protein kinases (193).

1.3.2 Casein kinase 2 (CK2) and CK2-specific inhibitors

CK2 is a constitutively active kinase. Because it lacks an inactive state, its activity is not under regulation of any second messenger (194). Generally, the holoenzyme of CK2 is composed of two catalytic subunits (α subunit and α' subunit) and two regulatory subunits (β subunit), forming a tetramer ($\alpha\alpha'\beta_2$, $\alpha_2\beta_2$, or $\alpha'_2\beta_2$) (195). The CK2 tetramer has a butterfly-like shape with a β_2 dimer in the center and one α subunit on both sides. The C-terminal tails of the β-subunits mediate the β-β and the α-β contacts, making the symmetric holoenzyme a strong complex that does not spontaneously dissociate in aqueous solutions (195). Different from most of the cellular kinases that require dramatic conformational changes to become activated, the catalytic subunits of CK2 have a rigid structure which limits the conformational change and underpins its constitutive activity (196). The two catalytic subunits catalyze phosphorylation of substrates and their activity is either increases or decreased by the presence of regulatory subunits (196, 197).

CK2 is ubiquitous in mammalian cells. It is expressed in almost all organs of mouse embryos (198) and is present in nearly every subcellular compartment (199). CK2 has different functions according to its subcellular localization. It shifts between the cytoplasm and the nucleus during the different stages of the cell cycle. For example, CK2α subunit is predominantly cytoplasmic during the synthesis (S) phase, but more nuclear in the Gap 1 (G1) phase, suggesting a regulatory role of CK2 in cell division (200). In the mitochondria, CK2 activity is primarily in the intermembrane space involving cell death signalling (201, 202). The

ER-associated CK2 is responsible for signal transductions, such as ER-stress signaling (203), cell-survival signaling (204), and ER-to-Golgi protein transport (205). In microtubules, CK2 regulates cytoskeletal rearrangement (206). CK2 also associates with centrosomes contributing to the growth of microtubules (207). At the stage of embryonic development the plasma membrane-associated CK2 might be related to embryonic and postnatal development (208).

CK2 is a pleiotropic protein kinase. It phosphorylates over 350 substrates, regulating almost every aspect of cell metabolism (209, 210). The number of substrates keeps increasing every year. CK2 is largely recognized as a S/T protein kinase, but increasing evidence shows that it occasionally modifies tyrosine residues (211). CK2 phosphorylation does not indiscriminately take place on any hydroxyl amino acid residue, but occurs in certain sequence/structural contexts. The amino acid residues flanking the phosphorylated residues are important in determining the binding of the kinase to a substrate (210). The recognition motif of CK2 has been summarized as (E/D/X)-(S/T/Y)-(D/E/X')-(E/D/X)-(E/D)-(E/D/X), in which X represents any residue except basic residues, and X' represents any residue but basic residues and proline (210). However, the above motif is not strictly necessary for CK2-mediated phosphorylation. In some cases it also recognizes a minimizal motif, (S/T/Y)-X-X-(E/D), with acidic residues located downstream of the phosphorylation amino acid (209, 212).

Tethered tetrabromobenzene molecules are cell-permeable inhibits that inhibit CK2 activity by selectively occupying the hydrophobic area of an ATP-binding pocket (213). A compound named 4,5,6,7-tetrabromobenzotriazole (TBB) has remarkable inhibition towards CK2, with a half maximal inhibitory concentration (IC_{50}) of 0.50 μM (213, 214). However, TBB also displays significant inhibition towards several other kinases, including dual-specificity Tyr phosphorylation-regulated kinase 1A (DYRK1α), phosphorylase kinase (PhK), glycogen synthase kinase 3β (GSK3β), and cyclin-dependent kinase 2 (CDK2), with IC_{50} values of 0.19, 8.70, 11.20 and 15.60 μM, respectively (213-215). Another compound derived from TBB, called 2-dimethylamino-4,5,6,7-tetrabromo-1*H*-benzimidazole (DMAT), has improved ability to inhibit CK2 in comparison with TBB (213). Its IC_{50} value is 0.14 μM. (213, 215). They share the feature of a brominated benzene ring that is important for occupying the ATP-binding pocket of CK2, but have different side chains (213). However, an obvious defect of DMAT is that it inhibits DYRK1α (IC_{50} = 0.12 μM) more efficiently than CK2 (213). A further improved

inhibitor is tetrabromocinnamic acid (TBCA), which is generated by replacing the five-atom triazole ring of TBB with a polar side chain (213). This compound not only causes enhanced inhibition, but also has better specificity towards CK2 (IC_{50} = 0.10 μM). Amongst the common cellular kinases, it has no comparable effect on DYRK1α. The inhibitory activity against SKG and GSK3β is 12-fold less than that against CK2 (213).

1.3.3 BoHV-1 kinase US3

US3 is a serine/threonine (S/T) protein kinase. The catalytic loop and ATP binding regions of US3 are conserved among the members of the *alphaherpesvirinae.* In BoHV-1, it is encoded by the *us3* gene in the U_S region of the viral genome (216). SuHV-1 expresses two isoforms of US3, a short isoform US3a and a long isoform US3b (217). Although US3 is not essential for virus infection, it plays important roles through its kinase activity in several important events during infection (218).

A common function of US3 is that it rearranges cytoskeleton proteins through its kinase activity, causing cells to round up and to form filamentous protrusions (219-222). The pathway has been described in SuHV-1-infected cells. US3 phosphorylates p21-activated kinase 2 (PAK2) (223), which subsequently phosphorylates Ras homolog protein family member A (RhoA) (4). Phosphorylated RhoA mediates the dephosphorylation of cofilin. Without phosphorylation, cofilin is unable to maintain actin stress fibers (221, 224), causing damage to the integrity of the plasma membrane (4, 223). The damaged membrane facilitates virus entry (221) and cell-to-cell spreading (3, 4).

By sensing the early events of virus infection, host cells trigger the apoptosis signaling pathway to restrict the viral replication (225). Herpesviruses express many proteins to counteract apoptosis of host cells. Anti-apoptotic activity of US3 has been observed in HHV-1 (226), SuHV-1 (217, 227) and BoHV-5 (220), but is less obvious in BoHV-1 (216). US3 of HHV-1 has significant importance in the survival of neurons (99). The expression of US3 in trigeminal ganglion (TG) neurons causes the cells to be more resistant towards apoptotic stimulation than other primary cell types (100, 101). The anti-apoptotic signaling pathway is activated by US3 in the TG cells of SuHV-1-infected pigs even before the onset of symptoms of infection (100). Similarly, during HHV-1 infection, US3 restrains the neuronal apoptosis in a mouse model (102).

US3 is associated with controlling neurovirulence and maintaining latency infection (99, 102) rather than directly contributing to viral lytic infection. This is confirmed by a finding that inhibition of apoptosis does not restore the titer of US3-deleted HHV-1 during lytic infection (228).

In addition to phosphorylating cellular proteins, US3 also has a broad range of viral protein substrates. In HHV-1, US3 phosphorylates gB (229), VP13/14 (142) and VP11/12 (230) to regulate their expression levels and/or incorporation efficiency. US3 of BoHV-1 phosphorylates VP22 (118) and VP8 (15). This activity of BoHV-1 US3 is abolished by mutating two conserved residues K^{195} and K^{282}, in the catalytic loop and ATP-binding pocket regions, which are critical for the kinase activity of BoHV-1 US3 (15).

Over all, it was determined in the previous studies that BoHV-1 replication is severely impaired when VP8 is depleted (64), and that VP8 is phosphorylated by US3 and CK2 (15). Of particular interest is whether phosphorylation contributes to the function of VP8 in BoHV-1 replication. Previous analysis proposed several potential consensus sequences in VP8 for US3 and CK2 (15). However, because of the sophistication of protein phosphorylation, identification of functional motifs in VP8 relies on experimental confirmation. The first objective of this research is to identify US3- and CK2-dependent phosphorylation residues in VP8. Moreover, US3 is a viral kinase, whereas CK2 is a cellular kinase; and they are localized differently in BoHV-1-infected cells (15), indicating that they may have different effects on the function of VP8. Thus the second objective is to identify the impacts of US3- and CK2-mediated VP8 phosphorylation in the life cycle of BoHV-1. Furthermore, VP8 is mostly localized in the nucleus of BoHV-1-infected cells, and it is capable of shuttling between the nucleus and cytoplasm (25, 154, 155). The third objective is to understand the impact of phosphorylation in the cellular translocation of VP8 during BoHV-1 infection. Over all, this research characterizes the phosphorylation-regulated functions and cellular translocation of VP8 in the life cycle of BoHV-1.

CHAPTER 2

2 LINKER BETWEEN CHAPTER 1 AND CHAPTER 3

Nuclear domain 10 (ND10) is a cell nuclear structure containing many anti-viral proteins, including promyelocytic leukaemia (PML), speckled protein 100 (SP100), alpha thalassemia/ mental retardation syndrome X-linked protein (ATRX), and death domain-associated protein 6 (DAXX) (104, 231-233). Herpesvirus infection significantly changes and disperses the cellular foci (234). An increasing amount of research demonstrates that the structure and the dynamics of ND10s are gradually changed during herpesvirus infection, and that tegument proteins as well as immediate early proteins play important roles in redistributing and degrading ND10 components. The current knowledge on how herpesvirus proteins counteracting ND10 is reviewed in the next chapter. VP8 is abundantly released from the incoming BoHV-1 virus into host cells, and thus it has the potential to target ND10, like other herpesvirus tegument proteins, such as U_L35 and pp71 of HHV-5 (104, 235-237). This review provides background knowledge for studying the interplay between VP8 and ND10 proteins.

CHAPTER 3

3 HERPESVIRUS TEGUMENT AND IMMEDIATE EARLY PROTEINS ARE PIONEERS IN THE BATTLE BETWEEN VIRAL INFECTION AND NUCLEAR DOMAIN TEN-RELATED HOST DEFENSE

Kuan Zhang [1,3] and Sylvia van Drunen Littel-van den Hurk [1,2 *]

[1]VIDO-Intervac, University of Saskatchewan, Saskatoon, SK, S7N 5E3, Canada.
[2]Microbiology & Immunology, University of Saskatchewan, Saskatoon, SK, S7N 5E3, Canada.
[3]Vaccinology & Immunotherapeutics, University of Saskatchewan, Saskatoon, SK, S7N 5E3, Canada.

Running title: Herpesviruses Use Tegument and Immediate Early Proteins to Counteract ND10

Key words: nuclear domain 10, herpesvirus, tegument protein, immediate early protein

Corresponding author*:
Dr. Sylvia van Drunen Littel-van den Hurk;
Vaccine and Infectious Diseases Organization
University of Saskatchewan,
120 Veterinary Road,
Saskatoon, SK, S7N 5E3, Canada;
Telephone: 1 + (306) 966-1559;
Fax: 1 + (306) 966-7478.

The information in this chapter was previously published:
Kuan Zhang, and Sylvia van Drunen Littel - van den Hurk. Herpesvirus Tegument and Immediate Early Proteins are Pioneers in the Battle between Viral Infection and Nuclear Domain 10-related Host Defense. Virus Research, 2017. 238: p. 40-8.

3.1 Abstract

The sophisticated anti-viral functions of nuclear domain 10 (ND10) are revealed by identifying the role of each component and the countermeasures applied by viruses. Several ND10 proteins suppress herpesviruses at initial and early phases of infection. Herpesviruses need to antagonize these anti-viral proteins to start a productive infection. In this review the recently identified similarities and differences among the strategies adopted by the three subfamilies of herpesviruses are discussed, highlighting that one of the significant purposes of incorporating tegument proteins into the viral particles might be to counteract ND10 proteins immediately after the viral genome enters the host nucleus. Once the infection progresses, a sufficient amount of immediate early proteins is expressed to disperse and hydrolyze ND10 proteins, accelerating the development of infection.

3.2 Highlights

- The three herpesvirus subfamilies have tegument proteins that counteract the nuclear domain 10-related repression of the viral genome.
- Each type of herpesvirus discussed in this review contains at least one immediate early protein to disrupt ND10, and their mechanisms of action are not exactly the same.
- Nuclear domain 10 targets pre-replication sites of herpesviruses by recognizing specific factors required for viral DNA replication, but not the incoming viral genome.

3.3 Introduction

Nuclear domain 10 (ND10) contains intrinsic and innate immune factors that respond to herpesvirus infections. The composition and existence of ND10 frequently change in response to several important events during herpesvirus infection. To overcome the ND10-mediated antiviral defences, the three major herpesvirus subfamilies use similar, yet distinct, strategies to reform and disrupt ND10 at very early stages of infection. The goal of this review is to discuss recent research on the strategies used by each subfamily of herpesviruses. Overall, they share some similarities, as is summarized in Figure 3.2. First, the incoming tegument proteins interrupt intrinsic antiviral responses before the onset of viral gene expression. To break the cellular suppression of the viral input genome, tegument proteins are released into the cells together with

viral DNA, so that they can produce a favorable condition for the viral genome as soon as they enter host cells. A common target for tegument proteins is the cellular protein complex formed by alpha thalassemia/mental retardation syndrome X-linked protein (ATRX) with death domain-associated protein 6 (DAXX) (236, 238, 239). Meanwhile, other ND10 components may also be targeted (240). ATRX primarily is a physical mediator for the association of tegument proteins with DAXX, while DAXX is the target to be degraded (104, 241). The ultimate purpose of disrupting the ATRX-DAXX complex might be activation of immediate early gene expression (103, 104, 241, 242). Secondly, the immediate early proteins target ND10 to manipulate interferon (IFN)-stimulated proteins, such as promyelocytic leukemia protein (PML) and speckled protein of 100 kDa (SP100). The expression of these viral proteins is increased by tegument protein-meditated DAXX degradation (103, 104, 242). The specific approaches used by immediate early proteins vary between different herpesviruses. ICP0 of human herpesvirus 1 (HHV-1) degrades all isoforms of PML through its E3-ligase activity (243). IE1 of human herpesvirus 5 (HHV-5) (244), BZLF1 of human herpesvirus 4 (HHV-4) (245), and ICP0 homologues in bovine herpesvirus type 1 (BoHV-1) (246) and equine herpesvirus type 1 (EHV-1) (246) tend to reduce SUMOylated PML. ICP27 of human herpesvirus 2 (HHV-2) alters the splicing of PML pre-mRNA to switch the PML isoforms so that cells predominantly produce virus-friendly PML isoforms instead of antiviral isoforms (247). Eventually, in the presence of immediate early proteins herpesviruses are less vulnerable to IFN-stimulated repression (105).

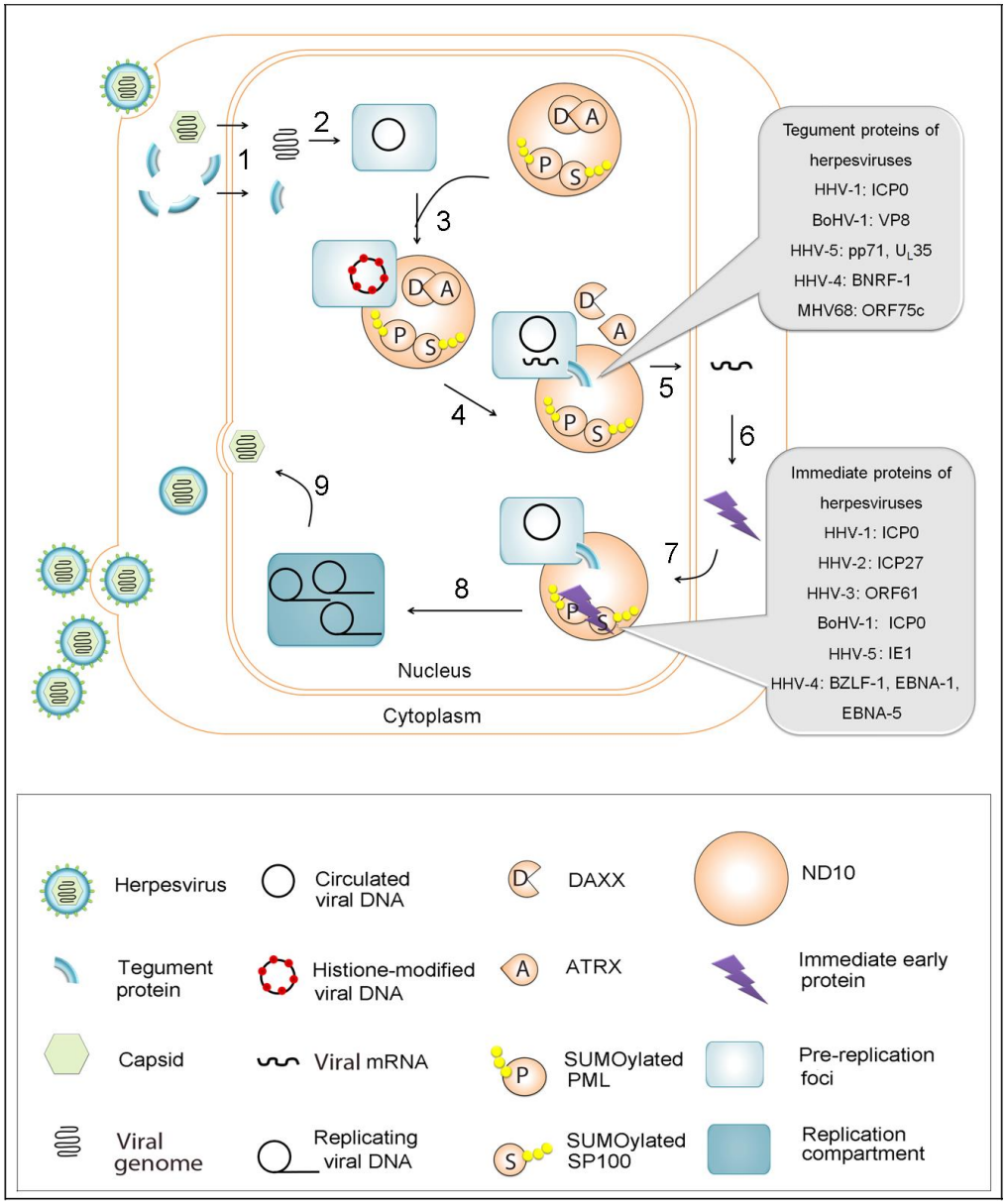

Figure 3.2 Model of herpesviruses counteracting nuclear domain 10 (ND10).

1. The viral genome and tegument proteins are released into the cell nucleus. 2. Viral DNA is circularized and recruited to the pre-replication foci. 3. ND10 is recruited towards pre-replication foci. The ATRX-DAXX complex mediates deposition of histone proteins on the viral genome. 4. Viral tegument proteins degrade PML and/or dissociate the ATRX-DAXX complex from ND10 to allow the transcription of viral mRNA. Tegument proteins that have such functions are listed. 5. Viral mRNA is transported to the cell cytoplasm. 6. Immediate early proteins are expressed. 7. Immediate early proteins are translocated into the nucleus to target PML and/or SP100. Immediate early proteins that have such functions are listed. 8. When ND10 is disrupted viral DNA replication is facilitated forming a replication compartment. 9. Viral capsid with the genome is ready to egress from the nucleus.

3.4 Introduction of nuclear domain 10 (ND10)

ND10s, also called promyelocytic leukemia nuclear bodies (PML-NBs), are nuclear matrix–associated domains with a punctate structure. They were originally described in acute promyelocytic leukemia (APL) patients. In the APL patients the *retinoic acid receptor-α (RARα)* gene and the *pml* gene are fused by chromosome translocation and express PML/RARα fusion protein causing changes in the size and number of ND10s (248, 249). The ND10 structures are characterized by the presence of several constitutive and transient protein components. The structural proteins are relatively stable in the foci, with constant and rapid self-renewal (250), while the transient proteins only appear in the foci under certain conditions depending on the protein function (251). PML is one of the major proteins localized in this structure; thus, the ND10s appear as multiple nuclear speckles by immunostaining with anti-PML antibody (252). They are present in almost all mammalian cells, and the number varies from 1 to over 30, depending on the cell type and condition (252). The dynamic changes in ND10 protein content reflect the active function of these nuclear foci. They have been found to play a pivotal role in a wide range of important cellular events, including cell–cycle control (253), programmed cell death (254) and genome transcription (255). Based on studies of the regulatory function of PML in DNA replication, it appears that ND10 is involved in intrinsic and innate defenses against virus infection (105).

3.4.1 Promyelocytic leukemia protein (PML)

PML, a member of the tripartite motif-containing protein (TRIM) family, is also known as TRIM 19, and essential for the formation of ND10 (256). It is an IFN-stimulated protein (105) and involved in regulating a broad array of ND10-related cellular events. A single copy of the human *pml* gene generates at least 12 isoforms (UniProtKB-P29590) by alternative splicing post-translation. They share the same N-terminus, encompassing a zinc-really interesting new gene (RING) finger domain, B box-1, B box-2 and coiled-coil region (257). Each isoform contains a unique C-terminal sequence, exhibiting different characteristics (257). For example, PML isoforms 1-5 are nuclear proteins involved in gene transcription regulation and chromatin remodeling (258), and PML-2 specifically promotes the formation of nuclear lipid droplets (259).

The function of PML protein depends on the consensus motifs and post-translational modifications. A nuclear localization signal (NLS) is contained in most PML isoforms to perform nuclear functions such as regulation of transcription and innate immune responses (257). These activities also require the region for DNA-binding, ubiquitin protein ligase-binding, and RING-finger (260). The coiled-coil region contributes to the heterodimerization and homodimerization, which are important for assembly of ND10 and protein recruitment (261). Several SUMOylation motifs are distributed in the PML sequence, and the association with SUMO-1/2 is essential for dimerization, maintaining protein stability, and controlling activity (262).

3.4.2 Speckled protein of 100 kDa (SP100)

SP100 is one of the major constituents of ND10. Many factors contribute to the assembly of SP100 in the ND10 foci. First, the association of SP100 with ND10 is stabilized by PML, and inversely, PML is protected by SP100 from hydrolysis (263). Secondly, covalent SUMO-1 modification is essential for SP100 to localize in ND10 (264). Finally, SP100 has self-aggregation properties that may enhance its accumulation in the ND10 foci (265). SP100 regulates cellular gene activity and tumorigenesis by recruiting heterochromatin protein 1 (HP1) (266). As an IFN-induced protein, SP100 is an important factor in the innate immune response, mediating IFN-stimulated repression of immediate early proteins of HHV-1 (232).

Four major alternatively spliced variants of SP100 have been studied, namely SP100-A, SP100-B, SP100-C, and SP100-HMG (267). When they are analyzed independently in the mammalian cell nucleus, these four isoforms display distinct localization patterns, suggesting that they have common as well as specific functions (232). The protein sequence of SP100-A contains a SUMO-1-binding motif, HP1-binding motifs and a half-site reaction (HSR) motif essential for dimerization (267). Because of the SUMOylation and acidic sequence, SP100-A shows a slower electrophoretic mobility than the calculated mass (54 kDa) would predict (264, 266). Most of the SP100-A sequence (477 amino acid residues) is present in SP100-B, SP100-C, and SP100-HMG, but the last three isoforms also share a SAND (named after Sp100, AIRE-1, NucP41/75, DEAF-1) domain (267), which has DNA-binding activity and plays a role in regulation of chromatin-dependent transcription (268, 269). SP100-C contains a plant

homeodomain (PHD) (267), which has the potential to bind to non-methylated histone protein to activate gene expression (270). SP100-HMG contains a unique high-mobility group (HMG) domain (267), involved in DNA-binding (271).

3.4.3 Alpha thalassemia/mental retardation syndrome X-linked protein (ATRX) and death domain-associated protein 6 (DAXX)

ATRX is a member of the chromatin remodeling protein family (272), which modulates histone deposition (273) and genomic DNA methylation (274). These activities contribute to the regulatory role of ATRX in cell cycle control and gene expression. By altering phosphorylation status, ATRX shuttles between the nuclear matrix-associated ND10 and the chromatin in a cell-cycle dependent manner (253). In addition, ATRX plays a protective role by controlling aberrant gene transcription and tumorigenesis depending on a PHD motif and an ATPase/helicase domain (253). Mutation of ATRX is strongly correlated to the development of several cancers (272, 275-277). Deletion of ATRX accelerates tumour cell replication (272), which is partially due to overexpression of anti-apoptotic factor P53 as a result of loss of ATRX (277). Moreover, ATRX restricts the genomes of many viruses in the host cells (104, 238, 239).

DAXX is a histone chaperone that is essential for histone H3.3 deposition covering the whole genome in mice (273). This activity requires association with ATRX. By recognizing chromatin modifications, the ATRX-DAXX complex selectively localizes to certain regions of the heterochromatin, providing an essential condition for H3.3 deposition (273). In the meantime, the ATRX-Dnmt3-Dnmt3L (ADD) domain of ATRX (278) interacts with the histone tail of H3.3 which is trimethylated at lysine 9 (H3K9me3) to maintain the protein on the heterochromatin (273). Reversely, disrupting either component of the ATRX-DAXX complex causes H3K9me3 to disappear from the heterochromatin (273). Overall, the ATRX-DAXX complex plays an important role in regulating cellular gene expression by supressing transcription. Disruption of the complex causes aberrant transcription (273) and tumor progression (275). It has been suggested that in clinical practice the punctated appearance of DAXX and ATRX in the cell nucleus should be incorporated into the pathologic evaluation of neuroendocrine and neuroblastoma tumors (279, 280), as the ATRX-DAXX complex is frequently disrupted when cells become cancerous (275).

3.5 ND10 and herpesvirus

3.5.1 ND10 and alphaherpesvirus infection

3.5.1.1 Tegument and immediate early proteins are important for alphaherpesviruses to confront ND10

It has been well recognized that ICP0 of HHV-1 disrupts ND10 by degrading a major protein, PML, in the structure (281). Recently ORF61, a homologous protein of ICP0 in human herpesvirus 3 (HHV-3), was also found to disperse PML-foci, through SUMO-interacting motifs (282). The impact of ICP0 on ND10 appears at very early phases of HHV-1 infection. Since ICP0 is incorporated into the viral tegument by associating with HHV-1 capsids (283), the ICP0 from the incoming virus is released into the host cell immediately after viral entry and has the potential to target ND10. According to evidence presented by several groups, the pre-existing ND10s are dispersed at the initial stages of infection (284, 285). Since it is difficult to separate input and *de novo* synthesized ICP0 at this stage of infection, further studies are needed to determine the contribution of input ICP0 to the disruption of ND10.

Other tegument proteins might directly or indirectly facilitate the disruption of ND10. ICP4 is a minor tegument and immediate early protein in HHV-1 (286). At the early stage of infection, ICP4 plays a role in mediating the interaction between ND10 and pre-replication foci by associating with DAXX (287), and it is contained in the pre-replication foci (288). The input ICP4 protein potentially has a similar activity, being involved in ND10 remodeling at a pre-immediate early stage of infection, before protein synthesis. In BoHV-1 the *ul47* gene product is a major tegument protein, named VP8 (289). Transfected VP8 recruits PML to form PML-aggregates in the nucleus (290). Since PML foci are not completely dispersed in cells solely expressing VP8 (290), VP8 may assist in remodeling PML foci at initial stages of infection before ND10 is disrupted by ICP0. It is not known whether such an activity of the *ul47* gene product is conserved in other alphaherpesviruses.

3.5.1.2 ND10 is related to cellular repression of the viral genome

Soon after the pre-existing ND10s are dispersed, a small group of ND10s re-appears in the cell nucleus, in association with HHV-1 pre-replication foci, which are the initiation sites for viral DNA replication during the early phase of infection (284). By this time, the *de novo*

synthesis of immediate early proteins has started, and ICP4 foci can be experimentally detected (284). The re-appearance of ND10 in the pre-replication foci is very transient and takes place before the formation of replication compartments (284), suggesting a regulatory role of ND10 in initiation of viral DNA replication. The re-appeared ND10s are formed by recruitment of diffused components towards the pre-replication foci, and possibly only include PML-isoforms that are resistant to ICP0 (284). Thus, they are different from the pre-existing ND10.

It is unlikely that pre-replication foci form in ND10, but the ND10 components have the potential to migrate towards pre-replication foci. This is confirmed by the observation that, in the absence of ICP0, pre-existing PML foci are able to move towards the pre-replication foci and to merge with them (284, 285). In the presence of ICP0, PML foci associate with the pre-replication foci merely for a very short period of time, and soon disappear. In the meantime, pre-replication foci are gradually replaced by larger globular nuclear domains, called replication compartments, where HHV-1 DNA replication takes place (284). Several ND10 components, except for a subpopulation of PML isoforms, remain in the replication compartments when ICP0 is not present (284, 291). Certain isoforms of PML are missing (291) and they have different morphologic appearances in comparison to that in the cellular pre-existing ND10s (292). A subpopulation of HHV-1-infected cells contain a type of cellular foci that partially share protein components with the pre-replication foci, for example U_L29 (293). However, these foci do not contain PML, but are related to cellular DNA synthesis instead of virus replication (293), so they are functionally different from pre-replication sites and need to be considered in a different context.

3.5.1.3 Recruitment of ND10 towards pre-replication sites

The aggregation of ND10 towards pre-replication foci is more likely a cellular behavior rather than a viral response, because the ND10 components resist viral infection (294). PML at the pre-replication sites represses HHV-1 gene expression at the initial stages of infection (294). DAXX might indirectly contribute to the association between the ND10 complex and the pre-replication foci (287).

Although PML is recruited to repress the initiation of viral infection, viral gene transcription does not necessarily have to take place to attract PML (294). PML is recruited by

recognizing certain viral elements within the pre-replication sites (287, 291). The pre-replication sites contain the viral genomes and viral proteins that regulate viral gene expression and replication, including single-strand binding protein U_L29, heterotrimeric helicase-primase complex (U_L5, U_L8, and U_L52), origin binding protein U_L9, and DNA polymerase U_L30 (295). The presence of U_L30 is essential for recruitment of PML to the pre-replication focus; however, U_L30 does not need to be active (291). This is also in agreement with the fact that the PML recruitment at the pre-replication site is independent from the actual event of viral gene transcription (294). Several other factors are related to ND10 deposition to the pre-replication focus, such as exposure of a short viral gene replication origin (Ori_S), and viral gene transcription proteins (ICP4 and ICP27) (287).

3.5.1.4 The development of replication compartments is facilitated by disruption of ND10

DNA replication compartments develop from pre-replication sites, which are often marked by ICP4 for study purposes (288). ND10 is found in the vicinity of the pre-replication sites, which are composed of factors promoting viral replication, such as DNA polymerase and origin binding protein (284, 288). ICP0 disrupts ND10 to ensure optimal DNA replication by promoting pre-replication sites to develop into replication compartments. However, the number of pre-replication sites is usually higher than that of the replication compartments, because not all but only several pre-replication sites are able to enlarge to globular structures, while the rest are abolished (288). When ICP0 is present, the pre-replication sites have a significantly higher chance to become replication compartments than in the absence of ICP0 (288) as ICP0 eliminates the restriction factors by disrupting ND10. ICP4 foci without ICP0 are less likely to become replication compartments because of the restriction from ND10. ICP0 targets the anti-viral ND10 as opposed to directly being involved in pre-replication events. The sub-nuclear localization of ICP0 is in agreement with it targeting ND10 instead of pre-replication sites as ICP0 precisely co-localizes with ND10 and not with pre-replication sites (288).

ICP0 of HHV-1 damages ND10 by mediating PML dissociation and degradation, thus promoting viral gene replication and expression (296). The C-terminal domain of ICP0 associates with the ND10 structure, and the RING finger is the active domain for redistribution of PML (243). The redistributed PML is degraded by the E3 ubiquitin ligase activity of ICP0

through a ubiquitin-dependent proteasome pathway (296). In addition, herpesvirus-associated ubiquitin-specific protease (HAUSP) (296) and ubiquitin-conjugating enzyme H5a (UbcH5a) (297) have been found to contribute to the ICP0-mediated degradation of PML. The methods of PML degradation by ICP0 vary between different alphaherpesviruses. In BoHV-1 and EHV-1, ICP0 proteins reduce SUMO-modified PML-1/2 without affecting the un-modified PML-1/2 (246). Therefore, ICP0 of BoHV-1 and EHV-1 have not been found to disperse ND10 foci in the cell nucleus (246, 298).

In addition to being a target for degradation by ICP0, PML might also attract ND10-degrading proteins to disperse SP100. It is known that IFN treatment enlarges SP100 foci and causes reformation of SP100 foci even when PML is knocked down in human epithelial type 2 (Hep-2) cells (105). However, in the context of IFN treatment, ICP0-induced dispersal of SP100 foci is delayed in the PML-null cells in comparison with wild-type cells (105), possibly because ICP0 has a lower chance to access SP100 foci when PML is not present (105).

It is a topic of debate whether ICP0 directly contributes to the degradation of SP100. In one study focused on individual isoforms of SP100, transient expression of ICP0 was found not to degrade SP100-A, SP100-B, SP100-C, or SP100-HMG (232). Similarly, homologues of ICP0 in BoHV-1 and EHV-1 do not reduce the SP100-A protein levels (246). However, this is not consistent with the statements from several other publications that ICP0 degrades SP100 through the proteasome pathway (297, 299, 300). A convincing conclusion is that during HHV-1 infection, the SP100 protein level is drastically reduced, and SP100 foci are dispersed (297, 299). It is possible that ICP0 mediates the dispersion of SP100 through degrading PML and that SP100 is degraded through an ubiquitin-dependent pathway. This contention is based on the following evidence. First, PML, the essential factor to maintain SP100 in ND10 (301), is degraded by ICP0 through the proteasome pathway (243, 302). A proteasome inhibitor, MG132, protects the SP100 from degradation during infection (299), perhaps because treatment with the proteasome inhibitor protects PML from degradation, which subsequently preserves SP100 from displacement. Secondly, UbcH5a is involved in the degradation of SP100 (297), suggesting that it is an ubiquitin-dependent protein degradation, which is sensitive to MG132. It is possible that the dissociation of SP100 in ICP0-expressing cells (300) is the result of ICP0-induced PML degradation, and the mechanism of SP100 degradation requires further investigation.

3.5.1.5 ND10 restricts viral DNA activity, not only at early stages of infection

The impact of ND10 on viral infection may last till the time when replication compartment develops, because some ND10 protein components appear in replication compartments in the absence of ICP0 (303). To avoid ICP0-induced disruption of ND10, replication compartments were established by transfecting essential elements of HHV-1 DNA synthesis (303). This is based on the theory that DNA synthesis initiates at one of three viral origins of the HHV-1 genome, including one copy of Ori_L (long) and two copies of Ori_S (short) (65). It also requires seven essential replication proteins, namely heterotrimeric helicase primase complex (U_L5, U_L8 and U_L52), a DNA polymerase (U_L30), a DNA polymerase accessory subunit (U_L42), origin-binding protein (U_L9), and a single-strand DNA-binding protein (U_L29) (303). Co-transfection of plasmids containing these essential replication proteins and HHV-1 replication origin creates replication compartments in the cell nucleus (303). PML-foci are closely associated with the edges of these artificially introduced replication compartments (303), suggesting that this protein may have an impact throughout the later phases of viral DNA replication.

ND10 proteins associate with HHV-1 replication compartments to restrict DNA replication later during HHV-1 infection (304). This was studied in context of deletion of ICP0 from the HHV-1 genome (304). The punctated appearance of ND10 is not disrupted in ICP0-null virus-infected cells and stably remains adjacent to the parental viral genome (304). The formation of replication compartments starts from the viral DNA sites and they gradually grow into globular structures, accompanied by ND10 foci (304). With the growth of the compartments, the major components of ND10 form different patterns within the compartments (292). The medium-sized compartments contain PML and SP100 as punctated foci (292). Subsequently, the large-sized compartments contain thread-structured PML and SP100 (292). DAXX recruitment is less significant in the large compartments than in the medium ones (292). Cellular repression of the genome of ICP0-null virus is decreased when PML is depleted, demonstrating that PML aggregation to the viral genome is a cellular antiviral response (294, 305).

Remodeling of ND10 is closely associated with the behavior of the HHV-1 genome in trigeminal ganglion neurons during the establishment of latent infection (306, 307). This is reflected by the appearance of the viral genome and PML in neurons. During latency, HHV-1

genomes are stored within the nucleus of ganglion neurons with punctated appearance (306). Each cell contains a single focus or multiple foci of viral genomes because of the heterogeneity of the viral genome during latency infection (306). The single genome focus in the neural nucleus is more frequently covered with a PML shell and co-localized with ATRX and DAXX, whereas the multiple genome foci are less likely to be associated with PML, DAXX, and ATRX (306). If the genome is associated with the above ND10 proteins, active transcription of latency-associated transcript (LAT), which is the only gene highly expressed during latency, is less likely to occur; this agrees with the fact that LAT expression occurs more significantly within the multiple foci. These reports suggest that ND10 plays a major role in the control of latency (306, 308).

3.5.1.6 ND10 is a mediator of the interferon-induced antiviral response

Convincing data have been reported to support the involvement of PML in the IFN-stimulated antiviral defence. PML has been shown to suppress HHV-1 infection when ICP0 is removed (309) or a low level of input virus is applied to the cells (105). IFN-α and -γ reduce the production of ΔICP0-HHV-1 in PML-containing wild-type cells more effectively than in $PML^{-/-}$ cells (309). $PML^{-/-}$ cells produce more HHV-1 than wild-type cells do when cells are infected with low PFU of virus (105). However, HHV-1 replicates equally well in both types of cells when given high PFU of virus (105), demonstrating that the restriction by PML can be easily eliminated by a high amount of input virus, which contains sufficient viral proteins to counteract PML (105). Together with the fact that PML is an IFN-stimulated protein (310-312), it has been concluded that PML is a downstream responder of the IFN-stimulated antiviral pathway.

SP100 is another ND10-resident IFN-stimulated protein. The sensitivity to IFN treatment of individual SP100 isoforms varies depending on the cell type. For example, IFN-β more favorably stimulates SP100-A in Hep-2 and human embryonic kidney (HEK-293) cells (232), while SP100-C is more significantly enhanced by IFN-β than other isoforms in Stemgent BJ human fibroblasts (BJ) cells (263). SP100-B, -C, and -HMG effectively suppress immediate early protein expression, and IFN-β enhances the repression (232). Furthermore, nuclear DNA helicase II (NDHII) is recruited to ND10 and associates with SP100 to regulate IFN-α-stimulated

gene transcription (313). This provides evidence that ND10 is a gene-transcription regulating site stimulated by IFN.

3.5.2 ND10 and betaherpesvirus infection

3.5.2.1 ND10 restricts human herpesvirus 5 (HHV-5) infection

HHV-5, a betaherpesvirus that establishes latent infection in monocytes, is usually asymptomatic in healthy humans, but can be life-threatening in immunocompromised individuals (314, 315). During initial phases of HHV-5 infection, ND10 associates with pre-replication sites to downregulate viral DNA replication and transcription, in a similar manner as during HHV-1 infection. First, PML- and SP100-containing foci become closely adjacent to pre-replication sites (316, 317), which contain six DNA replication core proteins including DNA polymerase U_L54, processivity factor U_L44, primase subunit U_L70, primase-associated factor U_L102, DNA helicase subunit U_L105, and single-strand DNA binding protein U_L57 (316). Subsequently, some of these foci gradually expand to globular replication compartments (316). The purpose of PML/SP100-foci aggregation near the pre-replication sites is to prevent them from developing into replication compartments (318). The antiviral function of ND10 is also supported by the fact that when ND10 is dispersed from pre-replication sites by a viral immediate early protein, IE1, the virus achieves better infection (234, 316, 317, 319).

3.5.2.2 Immediate early protein of HHV-5 disrupts ND10

An immediate early protein of HHV-5, IE1, disrupts the structure of ND10 by redistributing PML (316, 318), which is a restriction factor for HHV-5 infection (318). Shortly afterwards, IE1 diffusely distributes in the nucleus (234, 319). Without IE1, HHV-5 fails to disrupt ND10, and consequently shows delayed formation of a replication compartment and slow progression of infection (316, 318). Instead of causing significant degradation of the total protein level of PML, IE1 tends to attack SUMO-1-modified PML by degrading (244) or de-SUMOylating (320) PML. Specifically, the residue Leucine^{174} in the globular core domain of IE1 (IE1CORE) is essential for this activity (321). Direct interaction between the two proteins requires an acidic domain near the C-terminus of IE1 (231, 319), which targets the coiled-coil region of PML (322). Moreover, the RING finger domain of PML also contributes to the

interaction (231, 322). The structural interaction indicates that IE1 dissociates PML by occupying or deforming the critical structure for ND10-binding, which are the RING finger domain and the coiled-coil region on the N-terminus (231), leading to blocking of oligomerization and protein complex formation of PML (231). This results in the dissociation of ND10 from pre-replication sites (231).

Another immediate early protein, IE2, is involved in activating gene transcription by directly interacting with the parental viral genome (323). IE2-containing foci are frequently adjacent to ND10 (234, 316, 317, 319). However, a direct association between the viral genome and PML has not been reported, indicating that ND10 might be recruited towards pre-replication sites by recognizing a related protein instead of viral DNA.

3.5.2.3 Tegument proteins of HHV-5 target antiviral components in ND10

In addition to PML (233, 318, 324) and SP100 (324, 325), DAXX (233, 325) and ATRX (104) suppress initiation of viral gene expression, resulting in delayed or less productive HHV-5 infection. In eukaryotic cells, newly synthesized histones are rapidly deposited onto the cellular DNA immediately behind the replication fork to restrain aberrant replication or transcription (326). In this context, the viral DNA would be quickly wrapped by histones. DAXX interacts with histone deacetylases (HDAC) which tighten histones on DNA to suppress immediate early gene transcription (242). Since there is lack of evidence indicating direct association between DAXX and viral DNA, DAXX and HDAC may bind to the immediate early gene promoter through some unidentified complex (242). The DAXX-binding protein, ATRX (274), contains a zinc-finger domain implicated in DNA binding activity (327); thus, ATRX is a potential mediator between DAXX and the viral genome. The ATRX–DAXX complex represses viral immediate early gene transcription by modifying the acetylation of histone proteins (104, 242). In this scenario, PML and SP100 may play a role in repressing immediate early gene expression partially through maintaining the ND10 structure, which contains ATRX and DAXX.

Before the *de novo* synthesis of viral proteins, HHV-5 releases tegument proteins to counteract the ATRX-DAXX complex within ND10. Pp71(U_L82), a tegument protein encoded by the *ul48* gene, disrupts the ATRX-DAXX complex from ND10 (104) to activate immediate early gene expression (103). Immediately after infection, pp71 is released from virions and

delivered into the nucleus, appearing as punctated foci that colocalize with ND10s (328), where it breaks the interaction between ATRX and DAXX by associating with the coiled-coil domain of DAXX (329). This association may compete for the binding area with ATRX or directly interfere with the ATRX-binding domain on DAXX, making it an essential factor to disrupt the ATRX-DAXX interaction (104). Without the interaction with ATRX, DAXX becomes vulnerable to degradation mediated by pp71 through an ubiquitin-independent (239), proteasome-dependent pathway (242), leading to increased immediate early gene expression (242, 329). During HHV-5 infection, the strategy of removing DAXX is more predominant than degradation of PML and SP100 (242). At about 2 hpi the DAXX level is significantly reduced (242), while the PML and SP100 levels show a slight reduction (242, 320).

Several other tegument proteins have been found to collaboratively regulate the function of pp71, such as U_L35 and U_L35a (235, 236), although pp71 is sufficient to induce DAXX degradation (104). U_L35 is a late protein that is incorporated into mature virus as a minor tegument protein, and U_L35a is a viral protein expressed from early to late phases of infection and does not appear in the mature virus (235). U_L35 interacts with pp71 and collaboratively activates immediate early gene transcription (237). Together with the observation that U_L35 is able to independently remodel the ND10, and strongly co-localizes with the remodeled ND10 structures (235, 236), this indicates that U_L35 may facilitate pp71-mediated DAXX-ATRX disruption. However, U_L35a negatively regulates this process because it prevents U_L35 from remodeling ND10 and directs pp71 to the cytoplasm (236).

3.5.3 ND10 and gammaherpesvirus infection

3.5.3.1 ND10 counteracts human herpesvirus 4 (HHV-4) infection

ND10 plays a significant role in the pathogenesis of HHV-4, which is a gammaherpesvirus that establishes latency in B lymphocytes and causes immortalization of B cells (330), as well as epithelial cells (331). First, during primary infection ND10 may repress the origin of DNA replication (332) and immediate early gene expression (333). In the cell nucleus ND10 is juxtaposed to HHV-4 replication compartments that are created by transfection with plasmid carrying the viral origin of lytic replication (332). This physical interaction also provides access for PML and SP100 of ND10 to supress immediate early gene expression (333, 334).

Secondly, the reactivation of HHV-4 from latency is suppressed by ND10 (112, 335). To counteract the multiple types of repression caused by ND10, HHV-4 uses tegument proteins (241) and immediate early proteins (245) that specifically target the ATRX-DAXX complex, PML and SP100. Because these cellular proteins are important cell-death modulators, disturbing their function may contribute to the immortalization of infected cells.

3.5.3.2 HHV-4 uses tegument and immediate early proteins to neutralize ND10

DAXX and ATRX are transcription repressors that form heterodimers and are implicated in repressing transcription of viral genomes by reprograming histone proteins (273). BNRF-1, the major tegument protein of HHV-4, is delivered to the nucleus to subvert these antiviral factors. After dissociating from the virus, BNRF-1 closely associates with ND10 by interacting with DAXX (241), forming a stable quaternary complex with DAXX, Histone H3.3, and H4 (238). In the meantime, BNRF-1 disrupts the bond between DAXX and ATRX by dispersing ATRX (241), ending the repression of viral immediate early gene expression (241), and also contributing to immortalization of host B cells (238). The high amount of BNRF-1 in the infectious virions (336) is consistent with the important role of breaking cellular repression at the initial stages of infection.

With the help of BNRF-1, immediate early proteins of HHV-4 are efficiently expressed (241), and some of them, such as BZLF-1, EBNA-1 and EBNA-5 (EBNA-LD), target ND10-associated proteins through different mechanisms. BZLF-1 disrupts ND10 by reducing SUMO-1 modified PML (245). This viral protein may competitively inhibit PML SUMOylation by consuming limited amounts of SUMO-1(245). EBNA-1 degrades PML through the proteasome pathway (337). HAUSP is attracted to ND10 by EBNA-1 and contributes to PML degradation (337). In the meantime, CK2 is recruited to ND10 by EBNA-1, thereby enhancing phosphorylation of PML, which benefits polyubiquitination and degradation of PML (338). EBNA-5 associates with ND10 to target SP100 (333, 339). At early phases of infection, EBNA-5 is homogenously distributed throughout the nucleus and, soon after, is associated with ND10 (340) by interacting with SP100 (333), which leads to dispersal of SP100 (339). Tegument protein-induced ND10 disruption has also been observed during infection with murine

herpesvirus 68 (MHV68). This virus expresses ORF75c, a homologous protein of BNRF-1, to degrade PML protein and disrupt ND10 (240).

3.6 Conclusions

The intrinsic immune responses mediated by ND10 components are likely to constrain the initiation of herpesvirus infection. The three herpesvirus subfamilies have adopted unique strategies to disrupt the ND10. Tegument proteins released from input viruses could be the earliest viral factors disrupting ND10 proteins at a pre-immediate early phase. A betaherpesvirus, HHV-5, is so far the best described virus in this context, using its tegument proteins, pp71 and U_L35, to disrupt the ATRX-DAXX complex, which results in ATRX dispersion and DAXX degradation (104, 237, 239, 329). Pp71 plays an essential role, whereas U_L35 is a facilitator (236, 237). A major tegument protein of HHV-4, BNRF-1, has a similar function as pp71. It disperses the ATRX-DAXX complex by disrupting the interaction between ATRX and DAXX (241). This example indicates that gammaherpesviruses also express tegument proteins to interrupt the ATRX-DAXX complex. An example in alphaherpesviruses is a major tegument protein of BoHV-1, VP8 (*ul47* gene product), which relocates PML foci (290), raising the possibility that alphaherpesviruses may also use tegument proteins to target ND10 components. The pattern of PML foci redistributed by VP8 (290) is morphologically similar to that induced by U_L35 of HHV-5 (236, 237), and both do not eliminate ND10; hence, another protein in BoHV-1 may have the ability to disrupt the ATRX-DAXX complex. Some tegument components vary between BoHV-1 and HHV-1 in several aspects. First, the *ul47* gene product is a major tegument protein in BoHV-1, but a minor tegument protein in HHV-1 (14, 289). Secondly, ICP0 protein has been found in HHV-1 virions (286), but not in BoHV-1 virions (68). Thus, the specific activities of viral proteins to counteract ND10 components may not be absolutely conserved in alphaherpesviruses.

When a herpesvirus infection enters the immediate early phase, ND10 foci are completely disrupted. This has been confirmed for HHV-1 (341), HHV-3 (282), HHV-5 (318), and HHV-4 (112). Immediate early proteins play critical roles at this stage and can be classified into three groups by their activities. The first group constitutes the proteins that target PML. ICP0 of HHV-1 degrades all identified PML isoforms through the proteasomal pathway (341).

Others disrupt SUMOylated PML isoforms, including ICP0 of BoHV-1 (246, 298), ICP0 of EHV-1 (246), IE1 of HHV-5 (317-319, 342), and BENA-1 and BZLF-1 of HHV-4 (245, 343). The second group targets SP100, for example, EBNA-5 of HHV-4 (333, 339). The third group includes immediate early proteins ICP27 of HHV-2, which alters splicing and thereby switches PML isoforms (247), and IE2 of HHV-5 (317) and ICP4 of HHV-1 (287), which indirectly impact ND10, but do not degrade PML. Overall, the three subfamilies of herpesviruses have unique gene products to abolish ND10 proteins that restrict viral infection.

3.7 Acknowledgments

Research in the authors' laboratory is supported by funding from the Canadian Institutes of Health Research (CIHR), the National Science and Engineering Research Council (NSERC), the Krembil Foundation, the Alberta Livestock and Meat Agency (ALMA), and the Saskatchewan Agriculture Development Fund (ADF). This is VIDO manuscript number 797.

3.8 Conflict of interest statement

The authors declare no conflict of interest.

CHAPTER 4

4 HYPOTHESIS AND OBJECTIVES

4.1 Rationale and hypothesis

VP8 is indispensable for BoHV-1 to infect cattle, and deletion of VP8 causes drastic reduction of virus replication in tissue culture (64). The importance of VP8 is also reflected by the abundant incorporation into mature virus (14), implicating that VP8 is needed at the initial stages of BoHV-1 infection. In addition, VP8 is extensively phosphorylated in BoHV-1 infected cells (25). This raised the possibility that phosphorylation might be involved in regulating the function of VP8. We propose that CK2 and US3 may contribute differently to modulate the phosphorylation status and the biological characteristics of VP8, resulting in distinctive impacts on the function of VP8 during BoHV-1 infection.

Containing NLSs and NESs, VP8 has the potential to localize inside and outside a cell nucleus. The cellular localization of VP8 is under strict regulation, possibly through altering phosphorylation status. Understanding of the phosphorylation and translocation of VP8 in BoHV-1 infected cells might uncover unknown regulatory mechanisms of BoHV-1 infection. Thereby, we hypothesize that the nuclear and cytoplasmic localization of VP8 is regulated by CK2- and/or US3-mediated phosphorylation and that VP8 has different roles at different subcellular location of BoHV-1 infected cells.

4.2 Objectives

- Characterize the phosphorylation pattern of VP8 mediated by CK2 and US3 and identify VP8 residues that are essential for the two kinases.
- Study the function of phosphorylated VP8 mediated by CK2 and US3 in the life cycle of BoHV-1.
- Examine the impact of CK2- and/or US3-dependent phosphorylation on the cellular localization of VP8, and verify the roles of VP8 at different subcellular locations within BoHV-1-infected cells.

CHAPTER 5

5 REGULATION AND FUNCTION OF PHOSPHORYLATION ON VP8, THE MAJOR TEGUMENT PROTEIN OF BOVINE HERPESVIRUS-1

Kuan Zhang [1,3], Sharmin Afroz [1,3], Robert Brownlie [1], Marlene Snider [1],
Sylvia van Drunen Littel-van den Hurk [1,2 *]

[1]VIDO-Intervac, University of Saskatchewan, Saskatoon, SK, S7N 5E3, Canada.
[2]Microbiology & Immunology, University of Saskatchewan, Saskatoon, SK, S7N 5E3, Canada.
[3]Vaccinology & Immunotherapeutics, University of Saskatchewan, Saskatoon, SK, S7N 5E3, Canada.

Key words: BoHV-1, VP8, phosphorylation, PML
Running title: Regulation and Function of BoHV-1 VP8 Phosphorylation

Corresponding author*:
Dr. Sylvia van Drunen Littel-van den Hurk;
Vaccine and Infectious Diseases Organization
University of Saskatchewan,
120 Veterinary Road,
Saskatoon, SK, S7N 5E3, Canada;
Telephone: 1 + (306) 966-1559;
Fax: 1 + (306) 966-7478.

The information in this chapter was previously published:

Kuan Zhang, Sharmin Afroz, Robert Brownlie, Marlene Snider and Sylvia van Drunen Littel - van den Hurk., Regulation and function of phosphorylation on VP8, the major tegument protein of bovine herpesvirus-1. Journal of Virology, 2015. 89(8): p. 4598-611.

5.1 Abstract

The major tegument protein of bovine herpesvirus-1 (BoHV-1), VP8, is essential for viral replication in cattle. VP8 is phosphorylated *in vitro* by casein kinase 2 (CK2) and BoHV-1 unique short protein 3 (US3). In this study VP8 was found to be phosphorylated in both transfected and infected cells, but was detected as a non-phosphorylated form in mature virions. This suggests that phosphorylation of VP8 is strictly controlled during different stages of the viral life cycle. The regulation and function of VP8 phosphorylation by US3 and CK2 were further analyzed. An *in vitro* kinase assay, site-directed mutagenesis, and liquid chromatography-mass spectrometry were used to identify the active sites for US3 and CK2. The two kinases phosphorylate VP8 at different sites, resulting in distinct phosphopeptide patterns. S^{16} is firstly phosphorylated by US3 and it subsequently triggers phosphorylation at S^{32}. CK2 has multiple active sites, among which T^{107} appears to be a preferred residue. Additionally, CK2 consensus motifs in the N-terminus of VP8 are essential for the phosphorylation. Based on these results, a non-phosphorylated VP8 mutant was constructed, and used for further studies. In transfected cells phosphorylation was not required for nuclear localization of VP8. Phosphorylated VP8 appeared to recruit promyelocytic leukemia (PML) protein, and to remodel the distribution of PML in the nucleus; however, PML protein did not show an association with non-phosphorylated VP8. This suggests that VP8 plays a role in resisting PML-related host antiviral defenses by redistributing PML protein, and that this function depends on the phosphorylation of VP8.

5.2 Importance

The progression of VP8 phosphorylation over time and its function in BoHV-1 replication have not been characterized. This study demonstrates that activation of S^{16} initiates further phosphorylation at S^{32} by US3. Additionally, VP8 is phosphorylated by CK2 at several residues, with T^{107} having the highest level of phosphorylation. Evidence for a difference in phosphorylation status of VP8 in host cells and mature virus is presented for the first time. The phosphorylation was found to be a critical modification, which enables VP8 to attract and to redistribute PML protein in the nucleus. This might promote viral replication through interference with PML-mediated antiviral defense. This study provides new insights into the

regulation of VP8 phosphorylation and suggests a novel, phosphorylation-dependent function for VP8 in the life cycle of BoHV-1, which is important in view of the fact that VP8 is essential for viral replication *in vivo*.

5.3 Introduction

Bovine herpesvirus-1 (BoHV-1) is a herpesvirus belonging to the subfamily *alphaherpesviridae* and one of the most common pathogens in cattle. The major clinical symptoms caused by BoHV-1 are infectious bovine rhinotracheitis, conjunctivitis, vulvovaginitis and balanoposthitis. The virus particle is composed of a capsid containing the double-stranded DNA genome, which is surrounded by a tegument layer and an envelope containing viral glycoproteins. The tegument layer is a stable macromolecular structure formed by tegument proteins, which provide critical functions, such as regulation of transcription (344), kinase functions (142) and virus assembly (345).

Viral protein 8 (VP8), a phosphoprotein encoded by the *ul47* gene (289), is the most abundant tegument protein in BoHV-1. VP8 plays an indispensable role in BoHV-1 replication in host animals. A BoHV-1 mutant defective in expression of VP8 cannot establish a productive infection in cattle and poorly replicates in tissue culture (64). Herpesvirus tegument proteins can be post-translationally modified in several ways (14, 346), and based on the studies with human herpesvirus-1 (HHV-1) (345-347), it is conceivable that phosphorylation regulates the function of tegument proteins in BoHV-1. The HHV-1 tegument protein VP22 is phosphorylated in infected cells, which promotes expression and packaging of ICP0 (345); the VP22 itself is only packaged into mature virus particles after dephosphorylation (348). In BoHV-1, however, phosphorylation of VP22 is required prior to its incorporation into virions (71). The phosphorylation of HHV-1 VP13/14, a VP8 homologue, initiates dissociation of the structural components of the tegument (346).

Phosphorylation, in addition to potentiating functions, may also play a role in altering the cellular localization of target proteins. For example, HHV-1 VP22 has the capacity to perform nuclear-cytoplasmic shuttling during infection, and the non-phosphorylated form localizes to the cytoplasm while the phosphorylated form localizes to the nucleus (348, 349). BoHV-1 VP8 has been found to shuttle between the nucleus and cytoplasm, and this is mediated by two nuclear

localization signals (NLS) and one nuclear exportation signal (NES) (154, 155). However, the impact of phosphorylation on the cellular localization of VP8 is not known.

Promyelocytic leukemia (PML) protein is one of the components of PML nuclear bodies, also known as nuclear domain 10 (ND10). The PML protein contributes to the cellular defense by repressing viral lytic gene expression through modifying the viral genome (350), and thereby plays a key role in reducing herpesvirus replication (305). However, herpesviruses have developed a defence system against the PML-mediated anti-viral response. This is supported by evidence that when ICP0 is mutated, HHV-1 replication is reduced by failing to disrupt PML bodies (351). Further studies demonstrated that viral proteins disrupt PML bodies by interfering with the SUMOylation of PML protein (352). Some tegument proteins also remodel the PML protein. For example, human cytomegalovirus (HCMV) tegument protein U_L35 forms nuclear bodies that subsequently recruit PML protein (236).

According to previous *in vitro* studies, VP8 is phosphorylated by at least two kinases, the unique short protein 3 (US3), a BoHV-1 kinase, and casein kinase 2 (CK2), a cellular kinase (15). The VP8 open reading frame translates 741 amino acids, and 9.2% of them are serines and threonines, most of which are within consensus motifs for CK2 and US3. To better understand the role of VP8 phosphorylation during BoHV-1 infection, we investigated the phosphorylation events of VP8 at different viral life stages, and identified the active sites for US3 and CK2. We also showed that VP8 altered the distribution of PML protein in a phosphorylation-dependent manner.

5.4 Materials and methods

5.4.1 Cells and virus.

Madin Darby bovine kidney (MDBK) cells, African green monkey fibroblast-like (COS-7) cells, and primary fetal bovine testis (FBT) cells were cultured in Eagle's Minimum Essential Medium (MEM, Gibco, Life Technologies, Burlington, ON, Canada) supplemented with 10% fetal bovine serum (FBS, Gibco). Production of BoHV-1 strain 108 and Cooper were carried out in MDBK cells as previously described (25). Briefly, virus infections were accomplished by rocking 150 cm^2 85-90% confluent cell monolayers with BoHV-1 in 10 ml MEM at 37°C, which was replaced after 1 h with 10 ml MEM supplemented with 2% FBS, followed by further

incubation at 37°C. The virus titer was determined by plaque titration in 24-well plates overlayed with 8% low melting agarose (25).

5.4.2 Antibodies and chemical reagents.

Monoclonal anti-VP8 antibody, polyclonal anti-VP8 antibody (25) and polyclonal anti-US3 antibody (118) have been generated previously. Polyclonal anti-CK2*α* (Abcam, Toronto, ON, Canada), monoclonal anti-FLAG (Sigma-Aldrich, St. Louis, MO, USA), polyclonal anti-nucleolin (Abcam) and polyclonal anti-PML (Santa Cruz Biotech, Dallas, TX, USA) antibodies are all commercial products. IRDye® 680RD goat anti-rabbit IgG and IRDye® 800CW goat anti-mouse IgG were purchased from LI-COR Biosciences (Lincoln, NE, USA). Alexa® 488-conjugated goat anti-mouse IgG and Alexa® 633-conjugated goat anti-rabbit IgG were purchased from Life Technologies. The inhibitors SNS032 and AT7517 are products from Tocris Bioscience (Bristol, BS, USA) and Selleckchem (Houston, TX, USA). Phos-tag™ Acrylamide AAL-107 was purchased from Wako Pure Chemical Industries (Richmond, VA, USA).

5.4.3 Plasmid construction.

The *ul47* gene (GenBank accession no. AY530215.1) was cloned into the pFLAG-CMV-2 expression vector (Sigma-Aldrich), as previously described (15). The YFP ORF was cloned into pFLAG-CMV-2 to give pFLAG-YFP. VP8 mutations and deletions were constructed by PCR amplification using primers designed to create either mutations or deletions after ligation of PCR fragments back into the constructs. All primers were synthesized by Life Technologie (Table 5.1). PCR amplifications were carried out with Q5® Hot Start High-Fidelity DNA Polymerase (NEB, Ipswich, MA, USA) according to the manufacturer's instructions. Briefly, a 50 µl PCR reaction was carried out with 1 ng template, 1 µM primer pair, 200 µM dNTPs and 2 U DNA polymerase. The PCR-amplification products were purified with a PCR purification kit (Qiagen, Germantown, MA, USA) and treated with *Dpn*I (NEB). DH-5α competent cells were transformed with the DNA fragments ligated with T4 DNA ligase (NEB) and plated on selective LB agar plates. Plasmid purification was carried out following the Qiagen mini prep protocol. The selected positive mutants were confirmed by DNA sequencing performed by the NRC-Plant Biotechnology Institute (Saskatoon, SK, Canada).

Table 5.1 Primer list for plasmid construction using PCR (5' to 3'end)

Sample	Forward Primer	Reverse Primer
S16A	GCCGGAACGTACCGCACGCAC	GCGGCGCGGGCGGCGCTCAG
S32A	GCCCTGCTGGACGCCCTGCG	CCGCCGGGCAGAGGGGCGCTGG
S65A	GCCAGTGAGGACGAGAACGTGTATGATTAC	GTCCTCGTCCGGGGGCCGCTG
S66A	ACCGCTGAGGACGAGAACGTGTATGATTAC	GTCCTCGTCCGGGGGCCGCTG
S79A	GCCAGCGACAGCGCCGACGACTATG	ATCGCCGTCGATGTAATCATACACGTTCTC
S80A	AGCGCCGACAGCGCCGACGACTATG	ATCGCCGTCGATGTAATCATACACGTTCTC
S82A	GCCGCCGACGACTATGATAGCGATTATTTTACTGC	GTCGCTGCTATCGCCGTCGATG
T92A	TTGCTGCTAACCGCGGCCCCAATCAC	AATAATCGCTATCATAGTCGTCGGCGCTG
T107A	ACCCGAGCGCGCCCCGGAAG	GGTGCGTCTGCGTCCATAGCATCGCC
D65-110	GCCGACGACTATGATAGCGATTATTT	ATCATAGTCGTCGGCGCTGTC
D65-125	GCCGACGACTATGATAGCGATTATTT	CGTCAAGTAGTCTTGCGGGGCAC
D16-32	CTGCTGGACGCCCTGCGCGCTGCGGAC	GCGGCGCGGGCGGCGCTCAGG
D79-92	GCTAACCGCGGCCCCAATCAC	ATCGCCGTCGATGTAATCATACACGTTCTC
D65-82	GCCGACGACTATGATAGCGATTATTT	GTCCTCGTCCGGGGGCCGCTGGAAG
D88-110	CCCGAGCGCGCCCCGGAAGG	ATCATAGTCGTCGGCGCTGTC
D65-92	GCCCACCTGCGCGCCATCGAG	ATCGCCGTCGATGTAATCATACACGTTCTC
VP8 121-742	GCGGTAGATCTGATTCAAGACTACTTGACGGCCCACCTG	GGCAGTGAGCGCAACGCAATTAATG
VP8 219-742	CGGTAGATCTGATTGAGCGGCTGTCGGAAGGG	GGCAGTGAGCGCAACGCAATTAATG
VP8 343-742	CGGTAGATCTGATTGGCGGCATGTACGTGGGCGCCCCTGAG	GGCAGTGAGCGCAACGCAATTAATG
VP8 538-742	GCGGTAGATCTGATTGCGGCGGCCTTCCGCGAAGTG	GGCAGTGAGCGCAACGCAATTAATG
VP8 1-120	GAATCTAGAGCCACCATGGACTACAAAGACGATGAC	GAGCTCGAGTCAGCCGTGATTGGGGCCGCGGTTAG
VP8 1-125	GAATCTAGAGCCACCATGGACTACAAAGACGATGAC	GAGCTCGAGTCACGTCAAGTAGTCTTGCGGGGCAC
VP8 1-258	GAATCTAGAGCCACCATGGACTACAAAGACGATGAC	GAGCTCGAGTCACTCCCCCGCAGCCGCAGCG

5.4.4 Immunoprecipitation

BoHV-1-infected MDBK cells and plasmid-transfected COS-7 cells were pretreated with L-methionine-free or phosphate-free DMEM (Life Technologies) for 3 h prior to incubation with [^{35}S]-methionine or [^{32}P]-orthophosphate (Perkin Elmer, Woodbridge, ON, Canada). Cell lysates were pre-cleared with Protein G Sepharose (GE Healthcare, Burnaby, BC, Canada), and then incubated with anti-VP8 monoclonal antibody and Protein G Sepharose overnight at 4°C. The Protein G Sepharose was washed three times with wash buffer (50 mM Tris/HCl, 150 mM NaCl, pH 7.4) and boiled for 5 min with SDS-PAGE sample buffer. The samples were separated by SDS-PAGE in 10% gels. The gels were subsequently dried and exposed to Imaging Screen-K for visualization on a Molecular Imager FX (Bio-Rad, Mississauga, ON, Canada).

5.4.5 Protein purification and in vitro kinase assay

COS-7 cells in 6-well plates were transfected with plasmid (1.5 μg/well) using Lipofectamine and PLUS reagent (Life Technologies). Cell lysates were collected at 48 h post transfection (hpt). Twenty μl of anti-FLAG M2 affinity gel (Sigma-Aldrich) or anti-HA agarose (Pierce, Rockford, IL, USA) was washed according to the manufacturer's instructions and incubated with 200 μl of the appropriate lysate overnight at 4°C. The beads were washed five times with 1 ml wash buffer (50 mM Tris/HCl, 150 mM NaCl, pH 7.4). FLAG-VP8 (wild type, mutations and deletions) was eluted with 3×FLAG® tag peptide (Sigma-Aldrich) according to the manufacturer's instructions. The proteins were stored at -80°C until use.

Kinase assays were performed following a procedure described previously (15) with a few optimized steps. Briefly, a 25 μl reaction consisting of 0.3 mCi of [γ-^{32}P] ATP (Perkin Elmer), 1 μg of substrate protein, 0.5 ng of CK2 (EMD Millipore, Burlington, ON, Canada) or 5 μl of US3-HA on anti-HA agarose, and 6.25 μl of 4 × reaction buffer (80 mM HEPES pH 7.6, 0.6 M NaCl, 0.4 mM EDTA, 20 mM DTT, 0.4% Triton X-100) was incubated at 30°C for 10 min. The reaction was stopped by boiling with SDS-PAGE sample buffer for 5 min, and then the proteins were separated by SDS-PAGE in a 10% gel. The gels were dried and exposed to Imaging Screen for visualization on a Molecular Imager FX.

5.4.6 Co-immunoprecipitation and Western Blotting

Whole-cell extracts were prepared by suspension of cell pellets in RIPA buffer (50 mM Tris-HCl pH 8.0, 150 mM NaCl, 1% NP-40, 1% deoxycholate, 0.1% SDS) supplemented with protease inhibitor cocktail (Sigma-Aldrich) or phosphatase inhibitor cocktail (EMD Millipore). The cell lysates were clarified by centrifugation at 13,000 × g for 10 min at 4°C. Anti-FLAG M2 affinity gel or anti-HA agarose was incubated with cell lysate (20 µl resin per 400 µl) overnight at 4°C and washed three times with 1 ml wash buffer (150 mM NaCl, 50 mM Tris/HCl, pH 7.4). Proteins were eluted by boiling in SDS-PAGE sample buffer for 5 min. In each experiment, 20 µl of each sample was subjected to SDS-PAGE in a 10% gel, and then the proteins were transferred to nitrocellulose membranes and incubated with the appropriate antibodies. After washing, the membranes were further incubated with IRDye® 600RD/800CW-conjugated secondary antibodies at a 1:20,000 dilution and scanned with an Odyssey® CLx Infrared Imaging System (LI-COR Biosciences).

5.4.7 Liquid chromatography–mass spectrometry (LC-MS)

FLAG-VP8 protein on anti-FLAG M2 affinity gel was treated with λ-protein phosphatase (NEB) at 30°C for 30 min, and then eluted with 3 × FLAG peptide. The dephosphorylated VP8 was rephosphorylated with the appropriate kinases in the *in vitro* kinase assays, and subsequently subjected to SDS-PAGE. The gels were stained with Coomassie Brilliant Blue (CBB) R250 in 40% methanol, 10% acetic acid. Protein bands of interest were prepared and submitted to the University of Victoria Genome British Columbia Proteomics Centre (Victoria, BC, Canada) to analyze the tryptic peptide molecular masses by LC-MS. Briefly, gel slices were manually cut into 1 mm^3 pieces and transferred to a Genomics Solutions ProGest perforated digestion tray. The gel pieces were de-stained (50/45/5 v/v methanol/water/acetic acid) prior to reduction (10 mM dithiothreitol, Sigma-Aldrich) and alkylation (100 mM iodoacetamide, Sigma-Aldrich). Modified sequencing grade porcine trypsin solution (20 ng/µL, Promega, Madison, WI, USA) was added to the gel slices at an enzyme/protein ratio of 1:50. Protein was then digested for 5 h at 37°C prior to collection of tryptic digests and acid extraction of the gel slices (50/40/10 v/v acetonitrile/water/formic acid). The peptide mixtures were separated by on-line reverse phase chromatography using a Thermo Scientific EASY-nLC 1000 system. The chromatography

system was coupled on-line with an Orbitrap Fusion Tribrid mass spectrometer (Thermo Fisher Scientific, Waltham, MA, USA) equipped with a Nanospray Flex NG source (Thermo Fisher Scientific).

5.4.8 Immunofluorescence staining

COS-7 cells, cultured on Permanox 2-well chamber slides (Thermo Fisher Scientific), were transfected with 1.5 μg DNA per well using Lipofectamine and PLUS reagent for 3 h. After incubation for 20 h, the cells were washed three times with PBS, fixed with 4% paraformaldehyde for 20 min and then washed three times with PBS. Subsequently, the cells were permeabilized with 0.1% Triton X-100 in PBS for 20 min, washed with PBS, and then incubated with 1% normal goat serum (Gibco) in PBS for 2 h at room temperature. The cells were incubated with primary antibodies at the appropriate dilutions for 2 h at room temperature, followed by washing with PBS and incubation with Alexa Fluor®-conjugated antibodies (Life Technologies) at a 1:500 dilution for 1 h at room temperature. Finally, the cells were incubated with DAPI (4',6-Diamidino-2-Phenylindole, Dihydrochloride; 0.5 μg/ml; Life Technologies) at 37°C for 10 min. Slides were washed with PBS followed by de-ionized water, and then air-dried and mounted using ProLong Gold Antifade Reagent (Life Technologies) prior to examination on a Zeiss LSM410 confocal microscope equipped with external argon ion 488/633/461 nm laser.

5.4.9 Precision-cut lung slices (PCLS) preparation

An ovine lung was perfused with 1.5% low gelling temperature agarose (Sigma) in RPMI (Roswell Park Memorial Institute) medium prior to sectioning. 220-250 μm sections were obtained by a Krumdieck Tissue Slicer (TSE Systems, MO, USA). They were washed in 3 changes of RPMI medium with antimycotic, baytil, clotriazole and kanamycin, and then incubated overnight at 37°C. The sections were infected with 10^6 PFU of BoHV-1 Cooper strain for 24 h. The slides were analyzed by immunofluorescence staining using polyclonal anti-VP8 antibody and goat anti-rabbit Alexa Fluor®-conjugated antibodies (Life Technologies) as described above.

5.5 Results

5.5.1 VP8 is phosphorylated in BoHV- infected cells but not in virions

VP8 has been identified as a 97 kDa phosphorylated tegument protein expressed during the later stage of BoHV-1 infection. By using [^{35}S]-methionine or [^{32}P]-orthophosphate to label the proteins, we confirmed VP8 to be extensively phosphorylated in BoHV-1-infected MDBK cells. The phosphate was completely removed by λ-phosphatase treatment (Figure 5.1A). The *in vitro* dephosphorylation was confirmed by LC-MS, as no phosphopeptide was detected in the λ-phosphatase-treated VP8 (data not shown).

The VP8 phosphorylation status differed at different stages of infection. By using a Phos-tag™ acrylamide gel (353) followed by Western Blotting we showed that VP8 from transfected COS-7 cells and BoHV-1 infected MDBK cells migrates more slowly than VP8 from purified virus or a λ-phosphatase-treated protein sample (Figure 5.1B, upper panel). Phosphorylated protein associates with the phos-tag, which specifically binds phosphorylated ions, resulting in a greater molecular weight of phosphorylated protein than non-phosphorylated protein (353). As a result, the higher bands in the Phos-tag™ acrylamide gel represent phosphorylated VP8, and the lower bands are non-phosphorylated VP8. All samples had the same molecular weight in standard polyacrylamide gels (Figure 5.1B, lower panel). This suggests that VP8 differs phosphoisoforms during the life cycle of BoHV-1.

5.5.2 Identification of US3 phosphorylation sites in VP8

Previously we identified US3 as one of the kinases responsible for phosphorylation of VP8 in *in vitro* kinase assays (15). Interaction between VP8 and US3 was confirmed by co-immunoprecipitation. US3-HA was pulled down by FLAG-VP8 in co-transfected COS-7 cells, while FLAG-VP8 was pulled down by US3-HA (Figure 5.2A, left panel). There was no interaction between US3-HA and the anti-FLAG beads when FLAG-VP8 was not present or between the FLAG-VP8 and the anti-HA beads when US3-HA was not present. pFLAG-YFP was used as a control plasmid. As shown in Figure 5.2A (right panel), there was no interaction between FLAG-YFP and US3-HA in co-transfected COS-7 cells.

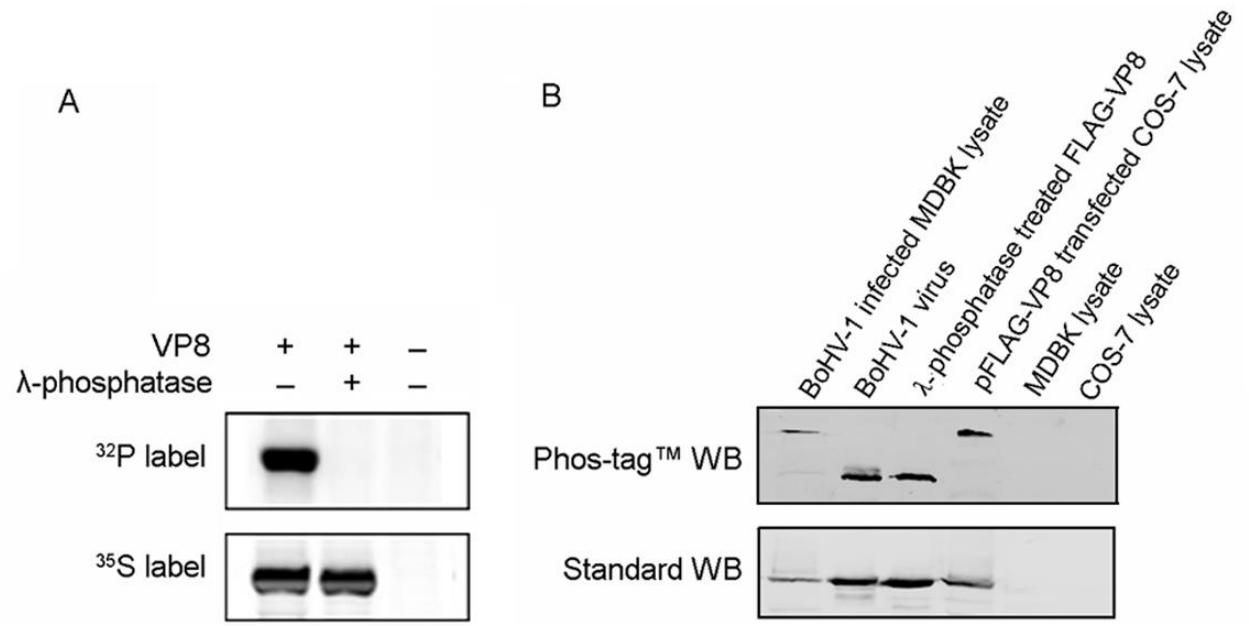

Figure 5.1 VP8 is phosphorylated in transfected and BoHV-1-infected cells, but is not phosphorylated in virions.

(A) [^{32}P]-orthophosphate- or [^{35}S]-methionine-labeled MDBK cells were infected with BoHV-1 at a MOI of 10. Cell lysates were collected at 18 hours post infection (hpi), and subsequently used for VP8 purification by incubation with anti-VP8 monoclonal antibody and Protein G Sepharose. A duplicate sample was treated with λ-phosphatase for 1 h at 30°C. The samples were separated by SDS-PAGE and exposed to Imaging Screen K. (B) BoHV-1 infected MDBK cell lysate, purified virus lysate, λ-phosphatase dephosphorylated FLAG-VP8, and pFLAG-VP8 transfected COS-7 cell lysate were analyzed in both Phos-tag™ and standard polyacrylamide gels followed by Western Blotting. MDBK and COS-7 cell lysates were used as controls. A polyclonal anti-VP8 antibody and IRDye® 800CW goat anti-mouse IgG were used to detect VP8. The upper panel shows migration of VP8 in the gel supplied with Phos-tag acrylamide, and the lower panel represents VP8 in a standard gel.

The phosphorylation of VP8 by US3 was further studied *in vivo* in pFLAG-VP8 and pUS3-HA co-transfected, [^{32}P]-orthophosphate-treated COS-7 cells. Phosphorylated VP8 was detected as early as 3 h post labelling, and the phosphorylation increased in a time-dependent manner (Figure 5.2B). At each time point, the intensity of phosphorylation was stronger in the presence of US3 than without US3 (Figure 5.2B). The *in vitro* kinase assay confirmed that VP8 is a substrate of US3 (Figure 5.2C). VP8 was intensely phosphorylated by wild-type US3, but not by the four US3 mutants, in which the two critical active sites for US3, K^{195} or K^{282}, located in the catalytic loop and in the ATP-binding pocket, were mutated (118). These results indicate that US3 phosphorylates VP8 *in vitro* and *in vivo*.

To identify the active sites for US3 on VP8, single site mutations were introduced into the potential target residues on VP8. Through aligning the VP8 sequence with a published minimal consensus sequence for US3 (118) four potential motifs (RRS^{16}GTYR, RRS^{32}LL, RRS^{173}LR and RRVT^{632}VR) have been identified. The serine and threonine within these motifs were replaced with alanine using site-directed mutagenesis. The six VP8 mutants were subsequently analyzed in the *in vitro* kinase assay in the presence of the CK2 inhibitor TBCA, which showed that mutating S^{16} with an A (S16A) completely blocked phosphorylation by US3. Mutating S^{16} and T^{18} (S16A, T18A) had the same impact. However, other mutations had no obvious effect on US3 phosphorylation (Figure 5.2D). As observed previously, US3 performed auto-phosphorylation.

To further identify the US3 phosphorylation sites on VP8, purified VP8 phosphorylated by US3 was digested with trypsin and scanned by LC-MS. This method allowed the unambiguous assignment of a phosphorylation site on a phosphopeptide, RS^{32}LLDALR (Table 5.2). This phosphopeptide was identified in 2 spectra, presenting the frequency of detection of this peptide, with a confidence greater than 95%, indicating a positive match. A non-phosphorylated peptide with the same sequence was detected in the λ-phosphatase-treated sample. Six spectra were identified with the highest confidence of 92%, indicating that the phosphoryl group on the S^{32} was removed by the phosphatase. However, due to the frequent presence of arginine in the VP8 sequence, especially within the US3 phosphorylation motifs, the tryptic LC-MS only covered 61% of VP8, and the S^{16} could not be identified.

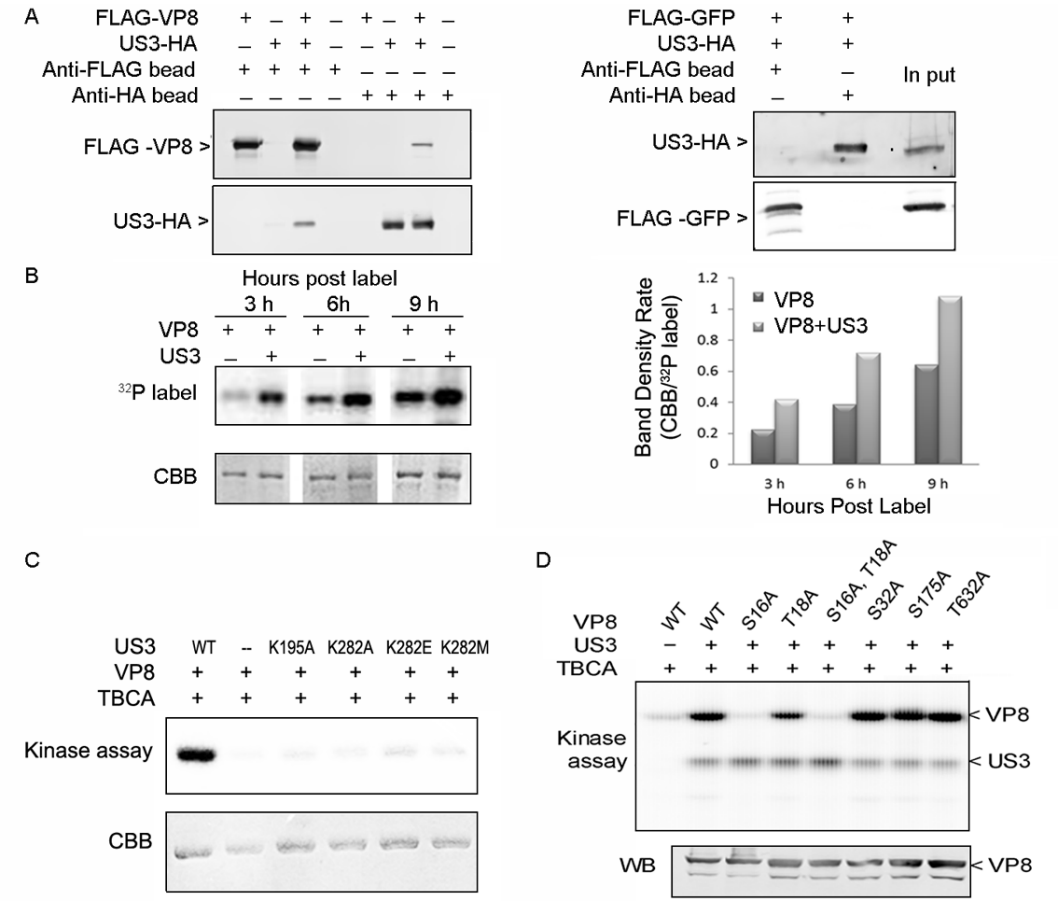

Figure 5.2 VP8 is a substrate for US3, and S[16] is a critical residue for the phosphorylation.

(A) FLAG-VP8 interacts with US3-HA. COS-7 cells were co-transfected with pFLAG-VP8 and pUS3-HA. Cell lysates were collected at 48 hpt. Protein was purified by incubating cell lysate with anti-FLAG beads or anti-HA beads for 12 h at 4°C, and was analyzed by Western Blotting. pFLAG-YFP was used as a negative control for co-immunoprecipitation. FLAG-VP8, US3-HA, and FLAG-YFP were detected by monoclonal anti-VP8 antibody, polyclonal anti-US3 antibody and monoclonal anti-FLAG antibody, followed by IRDye® 680RD goat anti-rabbit IgG or IRDye® 800CW goat anti-mouse IgG, respectively. (B) The presence of US3 increases phosphorylation of VP8 *in vivo*. COS-7 cells co-transfected with pFLAG-VP8 and pUS3-HA or transfected with pFLAG-VP8 were labeled with [^{32}P]-orthophosphate at 12 hpt. After a subsequent 3, 6 and 9 h incubation, FLAG-VP8 was purified from the cell lysate by anti-FLAG beads. The samples were separated by SDS-PAGE, exposed to Imaging Screen K and stained with CBB. Band densities were scanned by the Quantity One program (CBB/^{32}P labeled band). (C) VP8 is phosphorylated by wild-type US3 but not by US3 mutants. VP8 and US3 (wild type or mutants) were analyzed by *in vitro* kinase assays with [λ-^{32}P] ATP. TBCA was used to inhibit cellular kinases carried over by anti-FLAG beads and anti-HA beads during the protein purification process. Proteins were separated by SDS-PAGE and exposed to Imaging Screen K. (D) VP8 mutants were generated by substituting the serine/threonines with alanines. The VP8 mutants were analyzed by the *in vitro* kinase assay. Protein expression was confirmed by Western Blotting with monoclonal anti-VP8 antibody and IRDye® 800CW goat anti-mouse IgG.

5.5.3 VP8 is phosphorylated by CK2

Previously, we identified CK2 as a kinase phosphorylating VP8 *in vitro* (15). To confirm this and explore a potential role of other kinases, different kinase inhibitors were used to block VP8 phosphorylation. The phosphorylation was reduced by TBCA in a concentration-dependent manner, but not by other two kinase inhibitors, SNS032 and AT7519 (Figure 5.3A). TBCA, SNS032 and AT7519 specifically inhibit the activity of CK2, cyclin-dependent kinases (CDK) and glycogen synthase kinase-3 beta (GSK-3β), respectively. To test the impact of TBCA on the phosphorylation of VP8 *in vivo*, pFLAG-VP8 transfected COS-7 cells were pre-treated with TBCA at 80 μM for 3 h and then labeled with [^{32}P]-orthophosphate for 3, 6 or 9 h in the presence of TBCA. The phosphorylation was reduced in the TBCA-treated samples compared with the ones not treated with TBCA (Figure 5.3B). The phosphorylation of VP8 by CK2 was confirmed by subjecting CK2 and VP8 to the *in vitro* kinase assay (Figure 5.3C). The result showed that VP8 was phosphorylated in the presence of CK2 and that CK2 performed auto-phosphorylation.

The interaction between CK2 and VP8 was confirmed by co-immunoprecipitation. The 45 kDa CK2α subunit was pulled down by FLAG-VP8 in pFLAG-VP8 transfected COS-7 cell lysate, while the CK2α subunit was not pulled down by anti-FLAG beads in non-transfected or pFLAG-YFP-transfected cell lysate (Figure 5.3D).

5.5.4 CK2 phosphorylates VP8 at multiple residues

To identify the phosphorylation sites for CK2, a series of truncated VP8 proteins was constructed and analyzed in the *in vitro* kinase assay. The constructs without residues 1-120 (VP8 121-741, VP8 219-741, VP8 343-741 and VP8 538-741) were not phosphorylated by CK2, while the truncations containing the residues 1-120 (VP8 1-120, VP8 1-125 and VP8 1-258) were phosphorylated by CK2 (Figure 5.4A). These results imply a critical role of residues 1-120 in phosphorylation. There are five consensus sequences matching a published CK2 motif within residues 1-120, which were named CK2 motif 1 (CM1) to CK2 motif 5 (CM5) (Figure 5.4B). Single site mutations of the S/T within these motifs reduced the phosphorylation to different degrees, but did not achieve complete inhibition (Figure 5.4C). Shorter deletions in VP8 were constructed to determine the involvement of these CMs (Figure 5.4D). Deleting CM1 did not have an obvious impact; however, deleting CM2 to CM5 completely blocked phosphorylation,

and deleting CM2 and CM3, or CM3 and CM4 almost eliminated the phosphorylation. These results suggest that CM2, CM3, and CM4 play an important role in CK2-dependent phosphorylation. Indeed, deleting CM2, CM3 and CM4 (residues 65-92) eliminated the phosphorylation and mutating the S/T within these areas dramatically attenuated the phosphorylation, demonstrating that they all contribute to VP8 phosphorylation. Mutating the S/T in the CM2, CM3, CM4 and CM5 all at once achieved complete inhibition (Figure 5.4D). The above results reveal that CM2 to CM5 are critical for the phosphorylation of VP8 by CK2. To determine whether deleting CM2, CM3 and CM4 affects the interaction between the kinase and substrate, co-immunoprecipitation of VP8 D65-92 and CK2 was performed. This showed that CK2α was pulled down with VP8 D65-92 (Figure 5.4E), indicating that VP8 with CM2, CM3 and CM4 deleted still associated with CK2, but was not phosphorylated. Thus, removal of any of these motifs had no effect in preventing formation of the kinase-substrate complex.

CK2-treated VP8 was analyzed by tryptic LC-MS, which detects any modification of a peptide by calculating the mass of the modification. A list of phosphopeptides was identified in the CK2 (3.3 ng/μl) treated sample; specifically, peptide GPNGHAGDT^{107}DAPPER was detected in 20 spectra with a confidence higher than 95% (Table 5.3). These results indicated that five residues (T^{107}, S^{137}, S^{221}, S^{240} and S^{679}) were phosphoreceptors, among which the T^{107} had the highest level of phosphorylation. However, in the sample treated with lower concentration of CK2 ($\leqslant$ 3.3 pg/μl) two phosphopeptides containing residues T^{107} and S^{137} were detected, while the peptides containing S^{221}, S^{240} and S^{679} were non-phosphorylated.

Table 5.2 Peptides identified by liquid chromatography–mass spectrometry (LC-MS) in the US3-phosphorylated VP8.

Identified Peptide	Sample Treatment	Phosphorylated		Non-phosphorylated	
		Prob. (%)	Ident.	Prob. (%)	Ident.
RS[32]LLDALR	VP8 with US3	98	2	98	12
	VP8 without US3	0	0	92	6

Note: "Prob." indicates the highest probability score; and "Ident." indicates the identification of events.

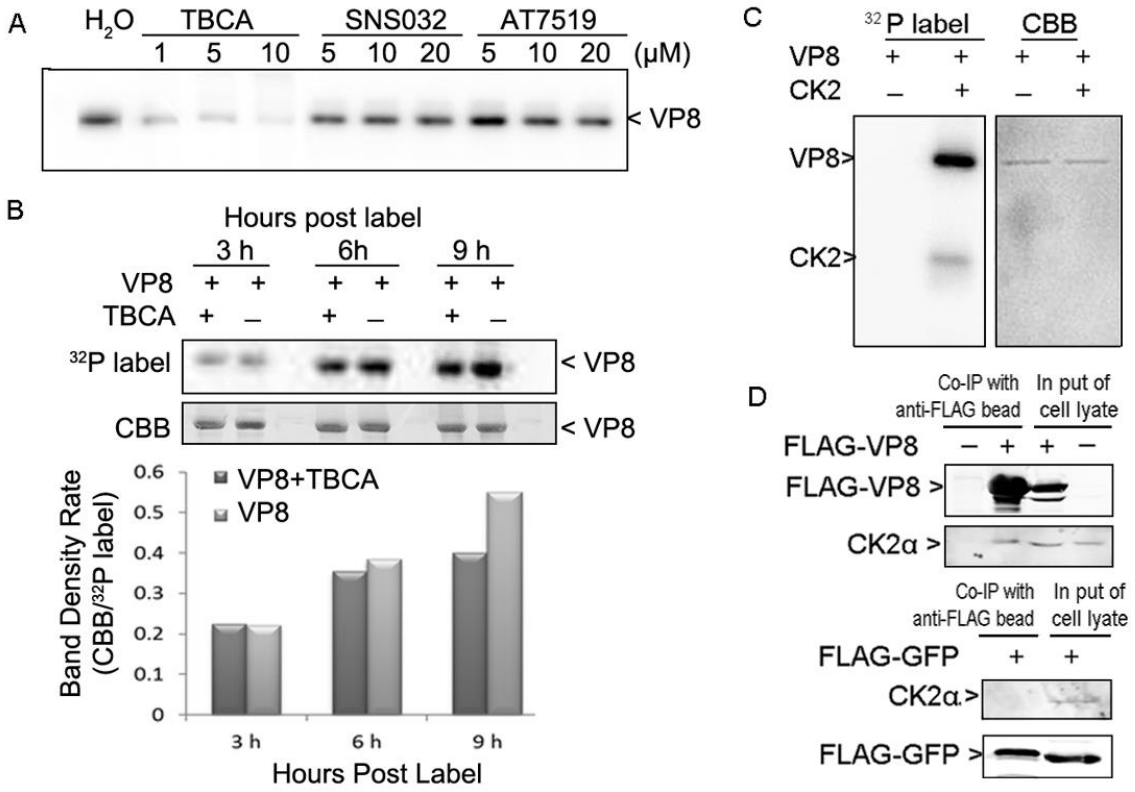

Figure 5.3 VP8 is a substrate for CK2, and interacts with CK2.

(A) A series of VP8 truncations was constructed as listed. The solid bar indicates the VP8 portion and the broken line indicates the deleted portion. The truncated proteins were purified from transfected COS-7 cell lysate and applied to *in vitro* kinase assays with CK2. Truncated proteins deleted in residues 1-120 and greater (VP8 121-741, VP8 219-741 and VP8 343-741) were not phosphorylated, while those truncated at the carboxyl end beyond residue 120 (VP8 1-120, VP8 1-125 and VP8 1-258) were phosphorylated by CK2 (upper panel). Protein expression is demonstrated by Western Blotting using anti-FLAG antibody (lower panel). (B) Five CK2 consensus motifs (CM1-CM5) found within residues 1-127 by aligning the VP8 sequence with a published CK2 motif, T/S-X_n-E/D ($n \geqslant 0$). The bar symbolizes the VP8 sequence with 741 amino acids, and residues 1-127 are highlighted. (C) Single-site mutations of VP8 by substituting S/T with an A within the identified CMs were analyzed by the *in vitro* kinase assays with CK2. Replacing S^{66}, S^{88} or T^{107} greatly reduced VP8 phosphorylation. The protein loading is shown by Western Blotting. The band density was scanned and analyzed by Quantity One. (D) Analyses of the truncations and mutants of VP8 in *in vitro* kinase assays. VP8 deletions, D, and multiple site mutations, M, were constructed according to Figure 5.4B. Purified proteins were applied to the *in vitro* kinase assays with CK2. The protein loading is shown by Western Blotting using monoclonal anti-FLAG antibody and IRDye® 800CW goat anti-mouse IgG. (E) Interaction of FLAG-VP8 D65-92, which has CM2, 3, 4 deleted, with CK2 in the transfected COS-7 cells. pFLAG-VP8 and pFLAG-CMV2 were used as positive and negative controls, respectively. The transfected COS-7 cell lysate was collected at 48 hpt, and analyzed by co-immunoprecipitation. VP8 and CK2 were detected by polyclonal anti-VP8 antibody and polyclonal anti-CK2α antibody followed by IRDye® 680RD goat anti-rabbit IgG.

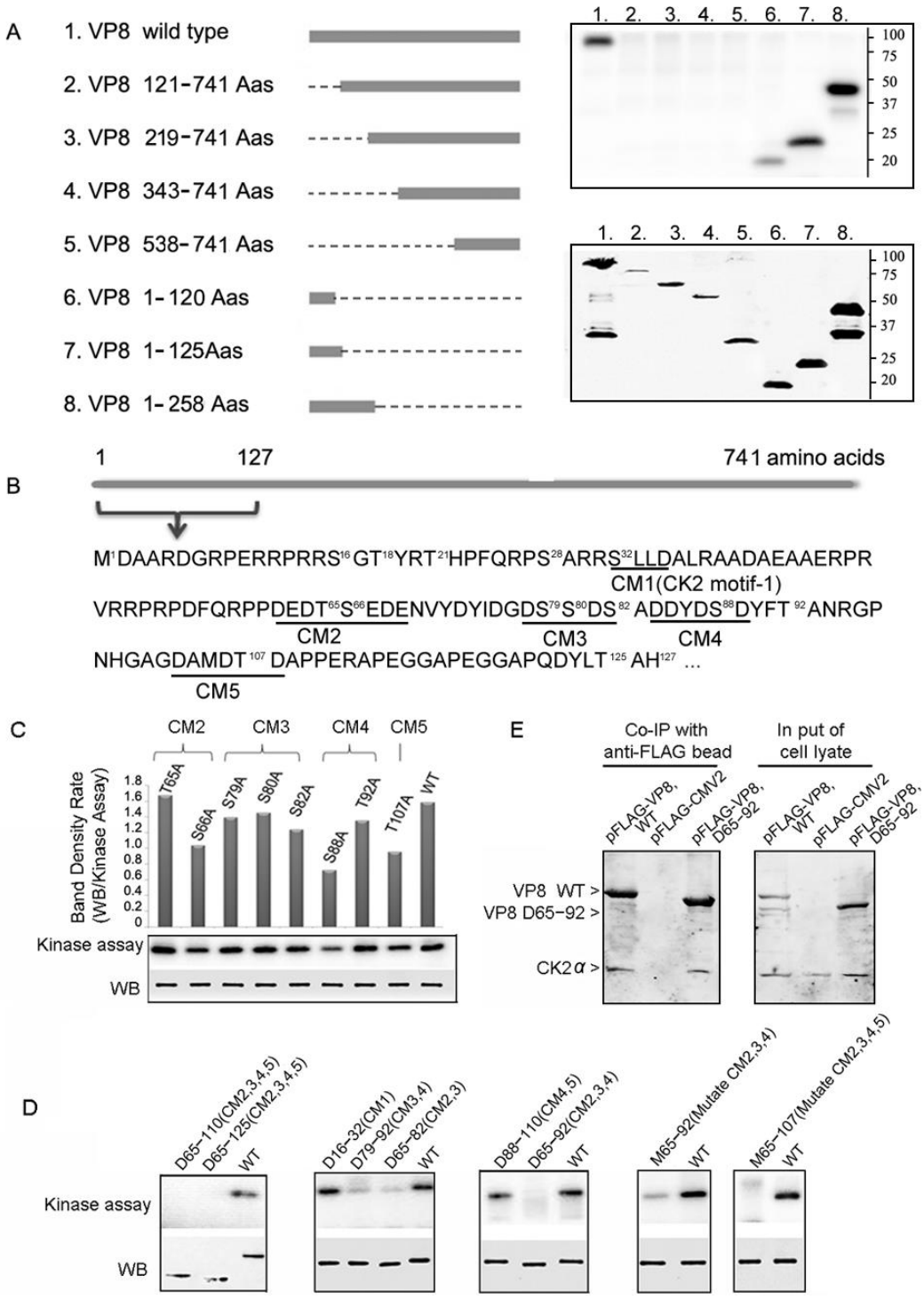

Figure 5.4 Identification of the critical residues on VP8 for phosphorylation by CK2.

(A) A series of VP8 truncations was constructed as listed. The solid bar indicates the VP8 portion and the broken line indicates the deleted portion. The truncated proteins were purified from transfected COS-7 cell lysate and applied to *in vitro* kinase assays with CK2. Truncated proteins deleted in residues 1-120 and greater (VP8 121-741, VP8 219-741 and VP8 343-741)

were not phosphorylated, while those truncated at the carboxyl end beyond residue 120 (VP8 1-120, VP8 1-125 and VP8 1-258) were phosphorylated by CK2 (upper panel). Protein expression is demonstrated by Western Blotting using anti-FLAG antibody (lower panel). (B) Five CK2 consensus motifs (CM1-CM5) found within residues 1-127 by aligning the VP8 sequence with a published CK2 motif, T/S-X_n-E/D ($n \geqslant 0$). The bar symbolizes the VP8 sequence with 741 amino acids, and residues 1-127 are highlighted. (C) Single-site mutations of VP8 by substituting S/T with an A within the identified CMs were analyzed by the *in vitro* kinase assays with CK2. Replacing S^{66}, S^{88} or T^{107} greatly reduced VP8 phosphorylation. The protein loading is shown by Western Blotting. The band density was scanned and analyzed by Quantity One. (D) Analyses of the truncations and mutants of VP8 in *in vitro* kinase assays. VP8 deletions, D, and multiple site mutations, M, were constructed according to Figure 5.4B. Purified proteins were applied to the *in vitro* kinase assays with CK2. The protein loading is shown by Western Blotting using monoclonal anti-FLAG antibody and IRDye® 800CW goat anti-mouse IgG. (E) Interaction of FLAG-VP8 D65-92, which has CM2, 3, 4 deleted, with CK2 in the transfected COS-7 cells. pFLAG-VP8 and pFLAG-CMV2 were used as positive and negative controls, respectively. The transfected COS-7 cell lysate was collected at 48 hpt, and analyzed by co-immunoprecipitation. VP8 and CK2 were detected by polyclonal anti-VP8 antibody and polyclonal anti-CK2*α* antibody followed by IRDye® 680RD goat anti-rabbit IgG.

Table 5.3 Peptides identified by liquid chromatography–mass spectrometry (LC-MS) in the CK2-phosphorylated VP8.

CK2 Concentration	Site	Identified Peptide	Phosphorylated		Non-phosphorylated	
			Prob. (%)	Ident.	Prob. (%)	Ident.
3.3 ng/μl	T^{107}	GPNGHAGDT^{107}DAPPER	100	20	100	64
		GPNGHAGDT^{107}DAPPERAPEGGAPQDYLTAHLR	81	1	100	31
	S^{137}	AIEALPES^{137}APHR	100	6	100	37
	S^{221}	LS^{221}EGPPLLNMEAAAAAAGER	98	1	100	136
		DERLS^{221}EGPPLLNMEAAAAAAGER	100	3	--	0
	S^{240}	S^{240}VVEELFTYAPAQPQVEVPLPR	99	2	100	78
	S^{679}	LRPVAS^{679}PPLAGK	100	2	100	14
⩽3.3 pg/μl	T^{107}	GPNGHAGDT^{107}DAPPER	100	2	100	35
		GPNGHAGDT^{107}DAPPERAPEGGAPQDYLTAHLR	--	0	100	18
	S^{137}	AIEALPES^{137}APHR	95	2	100	22
	S^{221}	LS^{221}EGPPLLNMEAAAAAAGER	--	0	100	154
		DERLS^{221}EGPPLLNMEAAAAAAGER	--	0	100	5
	S^{240}	S^{240}VVEELFTYAPAQPQVEVPLPR	--	0	100	70
	S^{679}	LRPVAS^{679}PPLAGK	--	0	100	29

Note: "Prob." indicates the highest probability score; and "Ident." indicates the identification of events

5.5.5 Phosphorylation of VP8 contributes to BoHV-1 replication

Based on the above results, a mutant VP8 (Mut-VP8), with all the critical phosphorylation sites for US3 (S^{16}) and CK2 (T^{65}, S^{66}, S^{79}, S^{80}, S^{82}, S^{88} and T^{107}) substituted by alanines, was constructed and analyzed in *in vitro* kinase assays. The Mut-VP8 was not phosphorylated by either CK2 or US3, while these two kinases phosphorylated the WT-VP8 as was expected (Figure 5.5A).

To study the impact of VP8 phosphorylation on virus replication, we analyzed the replication of a *ul47* gene-deleted mutant (BoHV-1-ΔU_L47), constructed previously (64), in WT-VP8 and Mut-VP8 expressing cells. FBT cells were infected with BoHV-1-ΔU_L47, and then transfected with pFLAG-WT-VP8, pFLAG-Mut-VP8 or pFLAG-YFP. At 36 hpi, the virus titer from the pFLAG-WT-VP8 transfected cells was higher than that from the pFLAG-Mut-VP8 transfected cells, while the pFLAG-YFP transfected cells showed the lowest titer (Figure 5.5B). This indicated that BoHV-1-ΔU_L47 replicated better in the WT-VP8 expressing cells than in the Mut-VP8 expressing cells.

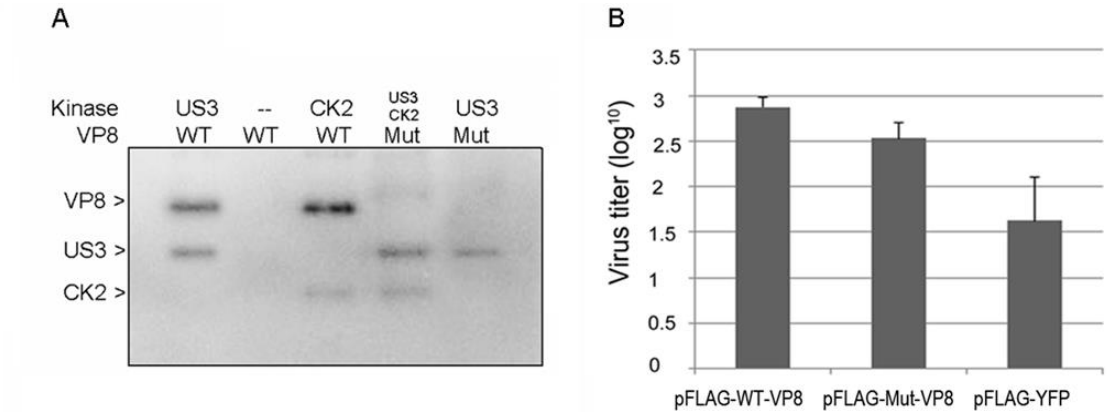

Figure 5.5 WT-VP8 benefits virus replication more than Mut-VP8, which is not phosphorylated by CK2 and US3.

(A) Confirmation of non-phosphorylated Mut-VP8 in the *in vitro* kinase assay. A Mut-VP8, which had all the critical phosphorylation sites for US3 (S^{16}) and for CK2 (T^{65}, S^{66}, S^{79}, S^{80}, S^{82}, S^{88} and T^{107}) substituted by alanines, was constructed and analyzed in kinase assays with CK2 and US3. (B) BHV1-ΔU_L47 replication in WT-VP8 expressing cells and in Mut-VP8 expressing cells. FBT cells were infected with BHV1-ΔU_L47 at a MOI of 0.3. At 4 hpi, cells were transfected with pFLAG-WT-VP8 or pFLAG-Mut-VP8. A control sample was transfected with pFLAG-YFP. Viruses were collected at 36 hpi, and titrated on MDBK cells.

5.5.6 Phosphorylation alters the intracellular localization of VP8 and PML protein

To determine whether phosphorylation of VP8 influences its subcellular localization, as has been found for other proteins, the localization of WT-VP8 and Mut-VP8 was examined by immunofluorescence in transfected COS-7 cells. WT-VP8 displayed nuclear localization (Figure 5.6A), which was consistent with previous results (155). Furthermore, the transfected cells developed circular bodies in the nucleus with WT-VP8 being strongly labeled on these circular bodies. The size of these nuclear bodies extended in a time-dependent manner. At 12 h they were visible as small dots in the nucleus and at later time points they became larger (Figure 5.6A, upper panel). In contrast, the Mut-VP8 was evenly distributed throughout the nucleus, and was not accumulated to the nuclear bodies (Figure 5.6A, lower panel). Double-staining using anti-nucleolin antibody and anti-VP8 antibody confirmed that these bodies were different from the nucleolus (data not shown). A similar pattern was observed in BoHV-1 infected lung tissue (Figure 5.6B). Some cells in the infected tissue developed circular areas not stained with either DAPI or anti-VP8 antibody. A certain amount of VP8 accumulated to the edge of the circular areas.

To gain insight into the identity of these nuclear bodies, the transfected cells were stained with both anti-PML and anti-VP8 antibodies. While the PML bodies were evenly distributed as round dots or speckles in the nucleus of non-transfected cells, WT-VP8 altered the distribution of PML protein by recruiting it to the edge of the circles (Figure 5.7). As is indicated by white arrow heads, PML aggregated to the nuclear bodies, where WT-VP8 was concentrated. Eventually, a large cluster of PML protein was formed around the VP8 bodies. The formation of nuclear bodies and accumulation of VP8 might happen independently of PML; instead, the nuclear bodies might recruit PML protein through interactions between VP8 and PML protein or other PML body components. This is supported by the observation that not all VP8 nuclear bodies were associated with PML protein; especially at 6 hpt several PML bodies were distinct from the newly developed VP8 nuclear bodies. This observation suggests that the PML accumulation happened after the VP8 nuclear body development. Figure 5.8 demonstrates the PML protein in the Mut-VP8 transfected COS-7 cells. Mut-VP8 did not accumulate to the nuclear bodies, and PML had the same distribution in the transfected cells as in the control cells. No co-localization was detected between Mut-VP8 and PML surrounding the nuclear bodies.

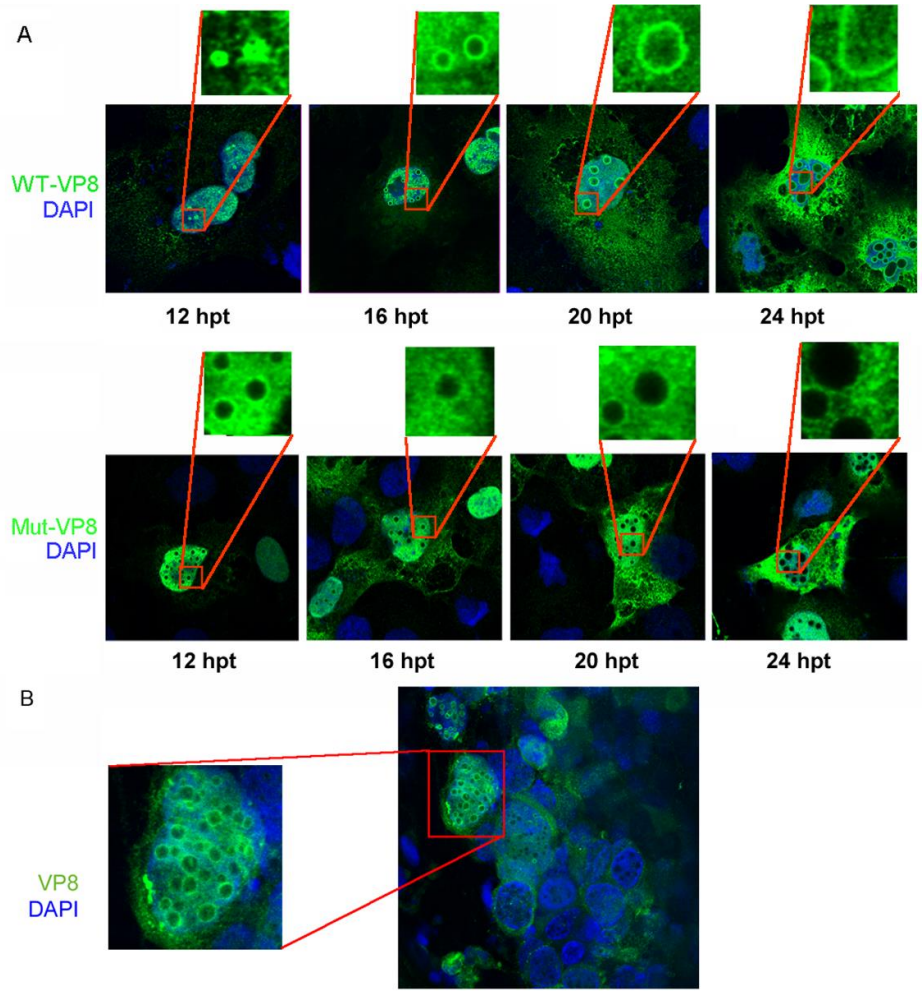

Figure 5.6 The cellular localization of WT-VP8 and Mut-VP8.

(A) Localization and different patterns of WT-VP8 and Mut-VP8 in the nucleus. WT-VP8 and Mut-VP8 were expressed in COS-7 cells. VP8 was detected with polyclonal anti-VP8 antibody and Alexa-488 conjugated goat anti-rabbit IgG. DNA was labeled with DAPI. The cells were observed with a Zeiss LSM410 confocal microscope. (B) Localization of VP8 in BoHV-1 infected lung tissue slices. 220-250 μm lung tissue sections infected with 10^6 PFU of BoHV-1 for 24 h. VP8 was detected with polyclonal anti-VP8 antibody and Alexa-488 conjugated goat anti-rabbit IgG. DNA was labeled with DAPI. The slides were observed with a Zeiss LSM410 confocal microscope.

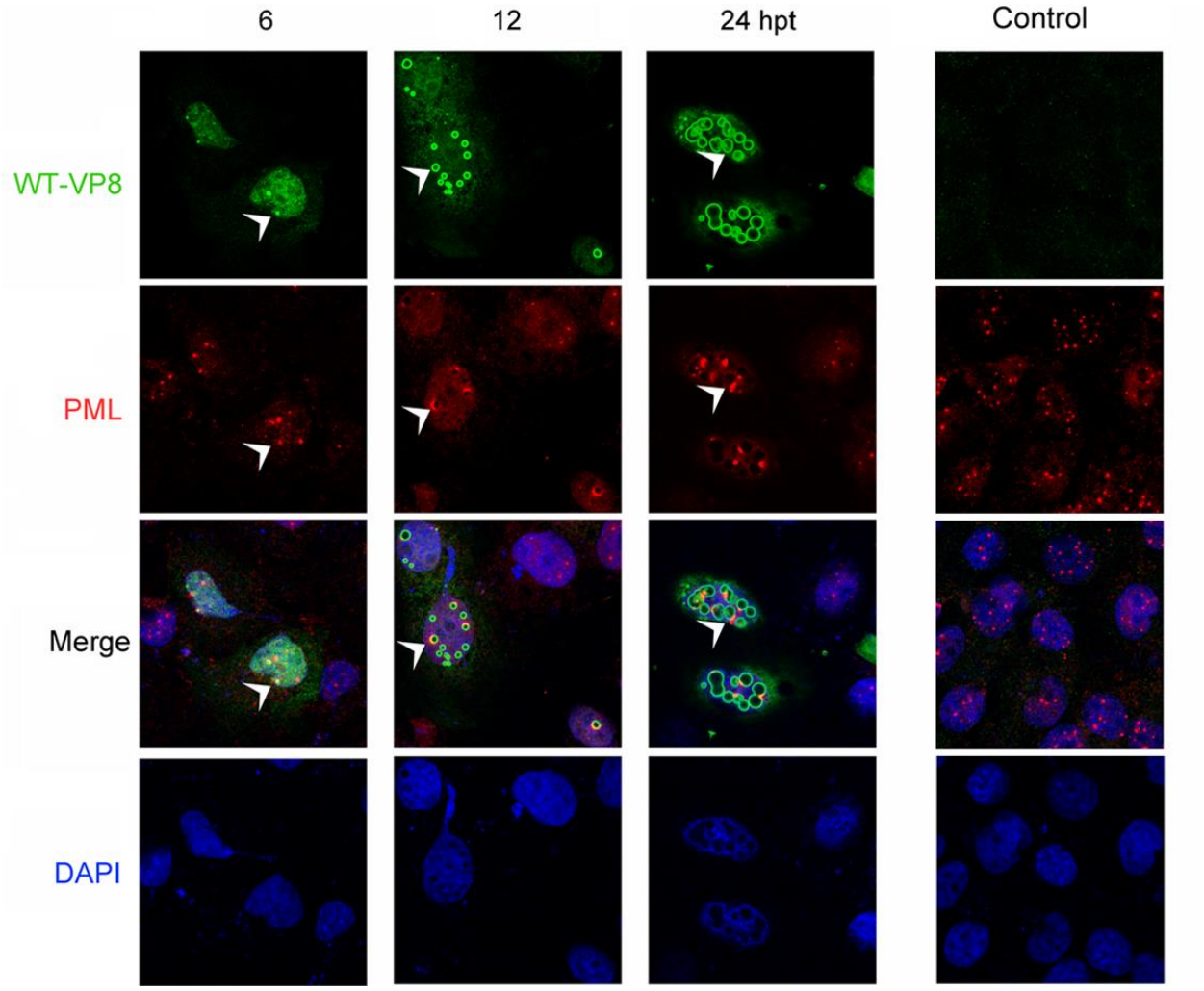

Figure 5.7 Promyelocytic leukemia (PML) protein accumulation to nuclear bodies and co-localization with WT-VP8.

(A) pFLAG-VP8 was transfected into COS-7 cells. FLAG-WT-VP8 was detected with monoclonal anti-FLAG antibody and Alexa-488-conjugated goat anti-mouse IgG, and PML with polyclonal anti-PML antibody and Alexa-633 conjugated goat anti-rabbit IgG. DNA was labeled with DAPI. The cells were observed with a Zeiss LSM410 confocal microscope. The white arrow head indicates that at 6 hpt PML protein is recruited to the edge of nuclear bodies, where WT-VP8 accumulates, and that at 24 hpt nuclear PML accumulates to the bodies resulting in protein clusters.

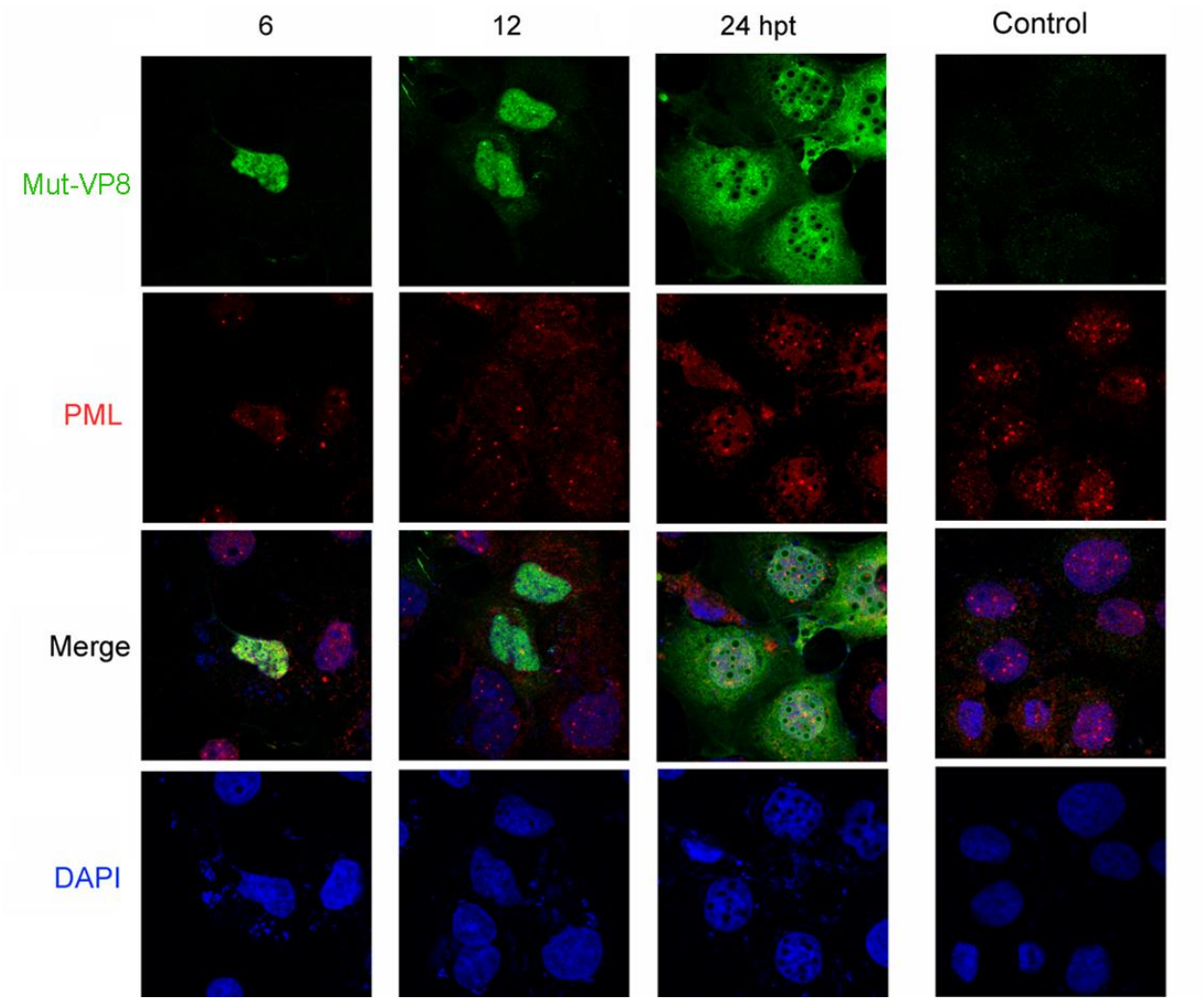

Figure 5.8 The distribution of PML protein is not affected by Mut-VP8.

pFLAG-Mut-VP8 was transfected into COS-7 cells. FLAG-Mut-VP8 was detected with monoclonal anti-FLAG antibody and Alexa-488 conjugated goat anti-mouse IgG, and PML with polyclonal anti-PML antibody and Alexa-633 conjugated goat anti-rabbit IgG. DNA was labeled with DAPI. The cells were observed a Zeiss LSM410 confocal microscope.

5.6 Discussion

VP8 is a known phosphoprotein and substrate for US3 and CK2 in an *in vitro* kinase assay (15). Based on this information, the objective of this study was to identify the specific residues of VP8 which are modified by the US3 and CK2 kinases, as well as a possible function of VP8 phosphorylation. This is the first evidence for a difference in phosphorylation status of VP8 in host cells and mature virus, and for phosphorylation being a critical modification for VP8 to recruit PML protein. We confirmed phosphorylation of VP8 by US3 and CK2 both *in vitro* and *in vivo*, and specified the active phosphorylation sites though site-directed mutagenesis and LC-MS. Phosphorylated, but not non-phosphorylated, VP8 tended to accumulate PML protein, which plays a role as an anti-viral protein (352).

Although VP8 contains four consensus sequences for US3, only mutation of S^{16} prevented VP8 phosphorylation by US3 (Figure 5.2D), demonstrating that the S^{16} is an essential residue for US3. It is not the only phosphoreceptor on VP8 because a phosphopeptide containing S^{32} was identified by LC-MS (Table 5.2). However, this site plays no decisive role in the phosphorylation at other sites, since mutating S^{32} did not result in reduced protein phosphorylation (Figure 5.2D). Both S^{16} and S^{32} are potential modified residues by US3 and they are within the US3-dependent consensus motif, R_n-X-S/T-Y-Y ($n \geqslant 2$; X is any residue; Y cannot not be aspartate, glutamate or proline) (15). The phosphorylation of S^{16} might complete the kinase recognition motif for the neighboring residue S^{32} to be phosphorylated, resulting in a sequential phosphorylation cascade. We propose that US3 phosphorylates VP8 on S^{16} and that this triggers additional phosphorylation on S^{32}. This contention is based on a previously described model, called primary phosphorylation, which proposes that the introduction of a phosphoryl group to a favorable site causes changes in the overall protein confirmation so that an otherwise unfavorable site is active for subsequent phosphorylation (354). Many other sequential phosphorylation examples have been described. For instance, a study of hepatitis C virus showed that there is a sequential and ordered cascade of phosphorylation events on the NS5A protein (355), where phosphorylation at S^{238} would trigger phosphorylation at S^{235}. Similarly, the regulatory phosphorylation of eukaryotic Elongation Factor 2 (eEF2) at S^{595} by CDK2 directly stimulates phosphorylation on T^{56} by eEF2 kinase (356). Reversely, phosphorylation of a primary site may down-regulate the further phosphorylation on other sites. For example,

extracellular signal-regulated protein kinase (ERK) phosphorylates mitogen-activated protein kinase kinase 1 (MEK1) on T^{292}, and this in turn blocks additional S^{298} phosphorylation (357).

Phosphorylation of VP8 by CK2 was confirmed by applying pure, active CK2 protein and VP8 to the *in vitro* kinase assay. TBCA, a relatively new CK2 inhibitor, with better specificity and less cellular toxicity than DMAT (2-Dimethylamino-4,5,6,7-tetrabromo-1H-benzimidazole) (213), inhibited the phosphorylation of VP8 in tissue culture. This is in agreement with our previous observation that DMAT (15) blocks phosphorylation of VP8. CK2 is constitutively expressed and active in COS-7 cells so TBCA was used to inhibit the CK2 activity. The reduction of VP8 phosphorylation in the TBCA-treated cells demonstrated that VP8 is phosphorylated by CK2 *in vivo*. Although no evidence has been reported that HHV-1 VP13/14 is phosphorylated by CK2, the phosphorylation on this tegument protein might be mediated by cellular kinases, including CK2. This is supported by the observation that VP13/14 is phosphorylated in cells infected with a HHV-1 US3-dead mutant; furthermore, two potential consensus motifs for CK2 on VP13/14 have been reported (15). It has also been found that in certain circumstances hUS3 shares a similar amino acid content with PKA (358) and Akt (359), suggesting that these kinases may play a role in VP13/14 phosphorylation.

Generally, CK2 modifies multiple residues with in one substrate, and overall about 75% of the phosphorylated sequences match the CK2 motif, S/T-X-X-D/E (360). Within the VP8 sequence ten threonines and nineteen serines match the motif. To identify the active sites for VP8, we started by analyzing shorter forms of VP8. VP8 fragments without the C-terminal residues 1-120 were found not to be phosphorylated by CK2 (Figure 5.4A), which has two possible reasons. The residues 1-120 maintain the protein structure for phosphorylation; alternatively, all the active sites are within this area. The fragments that encompass the residues 1-120 were phosphorylated, but the 1-258 fragment was more strongly labeled than the shorter ones, indicating the existence of active sites outside residues 1-120 (Figure 5.4A). There are five consensus sequences (Figure 5.4B) for CK2 within this area. Although the LC-MS did not detect any phosphopeptide that contains CM2, CM3, or CM4, these motifs appeared to be critical to maintain the catalytic domains without disrupting the formation of the kinase-substrate complex (Figure 5.4D).

Two phosphopeptides containing the CM5 were detected by the LC-MS (Table 5.3) suggesting T^{107} is a phosphoreceptor. However, it is not the only active site for CK2, since mutating this residue only reduced the phosphorylation to a certain level (Figure 5.3C). Four additional phosphorylated sites (S^{137}, S^{221}, S^{240} and S^{679}) were detected by tryptic LC-MS (Table. 3.3). Among these sites, the T^{107} had the most abundant phosphorylation event, 3-10 times higher than that of the other sites. This demonstrates that the T^{107} is the preferred phosphorylation site for CK2. Moreover, the S^{221}, S^{240} and S^{679} tended to be phosphorylated only in high concentration (3.3 ng/μl) of CK2, while a low concentration ($\leqslant$ 3.3 pg/μl) of kinase only phosphorylated T^{107} and S^{137}.

The mutagenesis results allowed us to generate a mutant VP8 (Mut-VP8) that is not phosphorylated by US3 or CK2 (Figure 5.5A). This enabled an investigation of the function of VP8 phosphorylation. Although phosphorylation by CK2 altered the subcellular localization of SV40 T-antigen (361), phosphorylation of VP8 had no obvious impact on its nuclear import. Both phosphorylated and non-phosphorylated VP8 were localized in the nucleus. In addition, the CM5, which contains a CK2 phosphorylation site, did not alter the nuclear import function of the VP8-NLS ($R^{11}RPRR^{15}$), as fusion proteins NLS-GFP and NLS-CM5-GFP had similar distribution patterns in the transfected COS-7 cells (data not shown). These results suggest that the phosphorylation does not change the nuclear localization of VP8. In contrast, phosphorylation by US3 on HHV-1 VP13/14 is needed for the NLS-mediated nuclear localization of VP13/14. VP13/14 contains a phospho-site for US3 at S^{77}, which is close to the NLS. Phosphorylation at S^{77} by HHV-1 US3 is essential for the nuclear localization of VP13/14, as mutating S^{77} to an A results in accumulation of this protein to the nuclear rim (142).

The expression of VP8 generated DAPI-stain negative nuclear bodies in COS-7 cells and WT-VP8 accumulated around these bodies (Figure 5.6A). A similar pattern was found in certain cells of infected lung tissue (Figure 5.6B), indicating a potential role of these non-stained areas in the pathology and mechanism of virus-host interaction during BoHV-1 infection. Concomitantly, PML protein was gradually attracted to the edge of the nuclear bodies, resulting in co-localization with WT-VP8 (Figure 5.7). Others observed that PML bodies suppress virus replication in HHV-1 infection. To survive in spite of the suppression, HHV-1 uses a regulatory protein ICP0 to degrade the PML bodies. This is supported by the finding that PML bodies

perform stronger suppression against HHV-1 infection in absence of the ICP0 protein (305). With respect to BoHV-1 infection, it is possible that VP8 plays a role in counteracting the PML-mediated cellular antiviral process. This is in agreement with our previous observation that BoHV-1 replication is dramatically reduced in the absence of VP8 (64).

The co-localization of WT-VP8 and PML protein in transfected cells suggests that VP8 might exert its effects on PML by remodeling PML bodies. This is in contrast with the results of another study on HCMV demonstrating that the formation of nuclear bodies and the recruitment of PML is enhanced by U_L82 (237) through increasing the efficiency of U_L35 nuclear body formation (236). However, other cellular proteins may be involved in the formation of VP8 nuclear bodies and remodeling of PML. We investigated the impact of phosphorylation of VP8 on its ability to recruit PML. A non-phosphorylated VP8 (Mut-VP8) did not attract PML protein, although circular areas unstained by either DAPI or anti-VP8 antibody were observed (Figure 5.8). As a result, the phosphorylation is a critical modification for VP8 to accumulate to nuclear bodies, as well as in subsequent remodeling of PML. It is possible that phosphorylation of VP8 may perform a potential role in protecting BoHV-1 from the PML-mediated antiviral defense. This contention is also supported by evidence that BoHV-1-ΔU_L47 replicated better in WT-VP8 transfected cells than in Mut-VP8 transfected cells. While deletion of VP8 reduces the virus titer by over 100-fold (64), this was partially amended by transiently expressing WT-VP8 and Mut-VP8, confirming the importance of VP8 in BoHV-1 replication. The fact that WT-VP8 increased the titer more than Mut-VP8 suggested that the phosphorylation of VP8 contributes to the virus replication.

The changing phosphorylation status of VP8 during the different stages of viral infection suggests a regulatory role for this modification. Phosphorylation of the incoming VP8 might be an immediate event in BoHV-1 infection. It has been found that phosphorylation of VP13/14, a homologue of VP8 in HHV-1, occurs between virion penetration of the cell and the onset of viral protein synthesis (346). Our results showed that VP8 was extensively phosphorylated in BoHV-1 infected cells. CK2 likely phosphorylates VP8 after viral entry and during VP8 transport through the cell, as this kinase is ubiquitous throughout the cell, including the plasma membrane, cytoplasm and nucleus (199). The virion-associated VP8 might capture the cellular kinase, and

the subsequent phosphorylation may help VP8 release, as was found for HHV-1 in that VP13/14 phosphorylation improves its dissociation from virions (346).

After release, the virion-associated VP8 has been shown to move to the nucleus as early as 2 h after infection (25), and this transport is mediated by the NLS independent of phosphorylation. The viral kinase US3 is synthesized later and is localized in the nucleus, where it can associate with VP8 (15). This indicates that the phosphorylation by US3 may affect a nuclear function of VP8, but not the tegument dissociation stage. This hypothesis is supported by a previous finding in HHV-1 that deletion of the viral kinase U_L13 had no effect on VP13/14 release in an *in vitro* assay (346).

In summary, this study demonstrates that phosphorylation is a critical modification for VP8 accumulation to nuclear bodies and recruitment of PML, which is important for the cellular antiviral defense. This function of VP8 appears to depend on its phosphorylation status. At least two kinases target VP8. The phosphorylation by US3 is likely a cascade process, in which the activation of S^{16} triggers further phosphorylation at S^{32}. CK2 phosphorylates VP8 on at least five active sites, among which T^{107} is the preferred residue.

5.7 Acknowledgements

The authors would like to thank Laura Latimer's kind assistance with immunoprecipitation experiments. This research was supported by a grant 90887-2010 RGPIN from the Natural Sciences and Engineering Research Council of Canada. The author Kuan Zhang was supported by a scholarship from the China Scholarship Council. This is VIDO manuscript number 727.

CHAPTER 6

6 LINKER BETWEEN CHAPTER 5 AND CHAPTER 7

In chapter 5, we determined the amino acids in VP8 that are responsible for phosphorylation through CK2 and US3. By knowing the essential residues for VP8 phosphorylation, we generated a mutant VP8 with the essential residues substituted with alanines. This mutant VP8 was validated in an *in vitro* kinase assay and in transiently transfected cells. It was not phosphorylated by CK2 and US3. The non-phosphorylated VP8 had a reduced capacity to rescue the production of BoHV-1-ΔU_L47 in tissue culture in comparison to wild-type VP8, suggesting a beneficial role of VP8 phosphorylation in BoHV-1 replication. Additionally, VP8 may benefit BoHV-1 replication by redistributing PML protein.

In chapter 7, we tested the impact of VP8 phosphorylation in virus replication in the context of BoHV-1 infection. A recombinant BoHV-1 encompassing non-phosphorylated VP8 was generated based on the findings in chapter 5. A comparison of the life cycles of the mutant and wild-type viruses revealed functions of VP8 phosphorylation during BoHV-1 infection.

CHAPTER 7

7 PHOSPHORYLATION OF BOVINE HERPESVIRUS-1 VP8 PLAYS A ROLE IN VIRAL DNA ENCAPSIDATION AND IS ESSENTIAL FOR ITS CYTOPLASMIC LOCALIZATION AND OPTIMAL VIRION INCORPORATION

Kuan Zhang [1,2], Robert Brownlie [1], Marlene Snider [1] and Sylvia van Drunen Littel - van den Hurk [1,3,*]

[1]VIDO-InterVac, University of Saskatchewan, Saskatoon, SK, S7N 5E3, Canada.
[2]Vaccinology & Immunotherapeutics, University of Saskatchewan, Saskatoon, SK, S7N 5E5, Canada. [3]Microbiology & Immunology, University of Saskatchewan, Saskatoon, SK, S7N 5E5, Canada.

Running title: Impact of VP8 Phosphorylation on the BoHV-1 Life cycle

Corresponding author*:
Dr. Sylvia van Drunen Littel-van den Hurk;
VIDO-InterVac University of Saskatchewan,
120 Veterinary Road,
Saskatoon, SK, S7N 5E3, Canada;
Telephone: 1 + (306) 966-1559;
Fax: 1 + (306) 966-7478.

The information in this chapter was previously published:

Kuan Zhang, Robert Brownlie, Marlene Snider and Sylvia van Drunen Littel - van den Hurk., Phosphorylation of Bovine Herpesvirus-1 VP8 Plays a Role in Viral DNA Encapsidation and Is Essential for Its Cytoplasmic Localization and Optimal Virion Incorporation. Journal of Virology, 2016. 90(9): p. 4427-40.

7.1 Abstract

VP8 is a major tegument protein of bovine herpesvirus-1 (BoHV-1) and is essential for viral replication in cattle. This protein obtains phosphorylation after transcription through cellular casein kinase 2 (CK2) and a viral kinase US3. In this study, a virus containing a mutated VP8, which is not phosphorylated by CK2 and US3 (BoHV-1-YmVP8), was constructed by homologous recombination in mammalian cells. When BoHV-1-YmVP8-infected cells were observed by electron transmission microscopy, blocking phosphorylation of VP8 was found to impair viral DNA encapsidation, resulting in release of incomplete viral particles to the extracellular environment. Consequently, less infectious virus was produced by the mutant virus, when compared with wild-type (WT) virus. A comparison of mutant and WT-VP8 by confocal microscopy revealed that mutant VP8 is nuclear throughout infection, while WT-VP8 is nuclear early during infection and associated with the Golgi at later stages. This together with the observation that mutant VP8 is present in virions, albeit in lower amounts, suggests that the incorporation of VP8 may occur at two stages. The first takes place without the need for phosphorylation and before or during nuclear egress of capsids, whereas the second occurs in the Golgi apparatus and requires phosphorylation of VP8. The results indicate that phosphorylated VP8 plays a role in viral DNA encapsidation and in the secondary virion incorporation of VP8. To perform these functions, the cellular localization of VP8 is regulated through phosphorylation.

7.2 Importance

In this study phosphorylation of VP8 was shown to have a function in BoHV-1 replication. A virus containing a mutated VP8 that is not phosphorylated by CK2 and US3 (BoHV-1-YmVP8) produced lower amounts of infectious virions in comparison with wild-type (WT) virus. The maturation and egress of WT and mutant BoHV-1 was studied showing a process similar to that reported for other alphaherpesviruses. Interestingly, lack of phosphorylation of VP8 by CK2 and US3 resulted in reduced incorporation of viral DNA into capsids during mutant BoHV-1 infection, as well as lower numbers of extracellular virions. Furthermore, mutant VP8 remained nuclear throughout infection in contrast to WT VP8, which is nuclear at early stages and Golgi-associated late during infection. This correlates to lower

amounts of mutant VP8 in virions and suggests for the first time that VP8 may be assembled into the virions at two stages, the latter being dependent on phosphorylation.

7.3 Introduction

Bovine herpesvirus-1 (BoHV-1), a member of the *alphaherpesviridae*, causes infectious bovine rhinotracheitis (IBR) in cattle, as well as conjunctivitis, vulvovaginitis and balanoposthitis. The herpesvirus particle is composed of a capsid containing the double-stranded DNA genome, which is surrounded by a tegument layer and an envelope containing viral glycoproteins (32). During the herpesvirus life cycle, genome synthesis, capsid assembly, DNA incorporation (362) and primary tegumentation (363) occur in the nucleus of infected cells. Subsequently, nucleocapsids leave the nucleus by budding through the nuclear membrane via an envelopment-de-envelopment pathway (364). Capsids acquire tegument proteins, envelope proteins and glycoproteins in the cytoplasm, and finally egress via the cellular secretory pathway (147). During the maturation process, viral components are sequentially incorporated into viral particles in a strictly controlled manner.

Tegument proteins have various functions, including regulation of transcription (344), kinase functions (142) and virus assembly (345). The BoHV-1 *ul47* gene product (289), VP8, is a 97 kDa tegument protein, which is indispensable for viral replication in host animals (64). While VP8 is the most abundant viral protein (25), the mechanism of incorporation of VP8 into virions is unknown. The cellular localization of VP8 changes at different stages of infection, indicating various roles of this protein during the virus life cycle. Navigated by a N-terminal nuclear localization signal (NLS) (154, 155), virion-derived VP8 is targeted to the nucleus immediately upon BoHV-1 infection (25, 154). At late stages of infection, VP8 accumulates in the cytoplasm (25), but no cytoplasmic function has been identified for VP8. In transfected cells VP8 is mainly restricted to the nucleus, and the nuclear VP8 appears to remodel the promyelocytic leukaemia nuclear body (PML-NB) (290), which is a suppressor of human herpesvirus 1 (HHV-1) replication (305). VP8 also has the capacity to interact with intron-less mRNAs of BoHV-1 (159).

In BoHV-1-infected cells VP8 is highly expressed and extensively phosphorylated. Phosphorylation is an important post-translational modification for VP8 to maintain PML-

remodeling capacity; however, it does not directly affect the nuclear localization of VP8 (290). This is in contrast to other proteins where phosphorylation changes their cellular localization. For example, VP22 of HHV-1 has the capacity to perform nuclear-cytoplasmic shuttling during infection, and the non-phosphorylated form localizes to the cytoplasm while the phosphorylated form localizes to the nucleus (348, 349). VP8 is mainly phosphorylated by a viral protein, US3, and a cellular protein, casein kinase 2 (CK2), through distinct target residues (15, 290). By site-specific mutagenesis of BoHV-1 VP8, serine 16 was identified to be essential for phosphorylation by US3, and seven residues (threonine 65, serine 66, serine 79, serine 80, serine 82, serine 88 and threonine 107) were critical for phosphorylation by CK2 (290).

Phosphorylation on BoHV-1 proteins has been reported to correlate with viral replication and protein incorporation. Blocking tyrosine phosphorylation of glycoprotein E (gE), an envelope protein, reduces viral replication (365). Removing tyrosine phosphorylation of VP22 decreases the amount of VP22 incorporated into virions (71). However, how phosphorylation benefits viral replication and determines the protein incorporation is not clear. The presence of VP8 in the cytoplasm and the nucleus indicates that this protein has different functions corresponding to the cellular localization. These functions might be related to the extensive phosphorylation of VP8, mediated by serine/threonine kinases CK2 and US3. This is also supported by a previous result that US3 associates with nuclear VP8 but not with cytoplasmic VP8 (15).

To study the role of VP8 phosphorylation in BoHV-1 replication, we constructed a recombinant BoHV-1, containing a mutant VP8 that is not phosphorylated by CK2 or US3. This mutant virus showed reduced DNA encapsidation and virus production. Furthermore, VP8 was found to be nuclear at early stages and Golgi-associated late during infection, while mutant VP8 remained nuclear throughout infection, which indicates that the localization of VP8 to the Golgi requires phosphorylation. Furthermore, as mutant VP8 was incorporated into virions, but in lower amounts, this suggests that VP8 may be incorporated into virions at two stages during BoHV-1 infection.

7.4 Materials and Methods

7.4.1 Cells and virus

Madin Darby bovine kidney (MDBK) cells and primary fetal bovine testis (FBT) cells were cultured in Eagle's Minimum Essential Medium (MEM, Gibco, Life Technologies, Burlington, ON, Canada) supplemented with 10% fetal bovine serum (FBS, Gibco). Production of all viral stocks was carried out in MDBK cells as previously described (25). Briefly, virus infections were accomplished by rocking 150 cm^2 85-90% confluent cell monolayers with BoHV-1 in 10 ml MEM at 37°C, which was replaced after 1 h with 10 ml MEM supplemented with 2% FBS, followed by further incubation at 37°C. The virus titer was determined by plaque titration in 24-well plates overlayed with 8% low-melting agarose in MEM (25, 64).

7.4.2 Antibodies

Monoclonal antibodies specific for gB, gC, and gD (78), and polyclonal antibodies specific for VP8 (25), VP22 (118), VP5 (64) and US3 (118) were raised as described previously. Monoclonal anti-Golgi 58K protein antibody was purchased from Sigma-Aldrich (St. Louis, MO, USA). IRDye® 680RD goat anti-rabbit IgG and IRDye® 800CW goat anti-mouse IgG were purchased from Li-Cor Biosciences (Lincoln, NE, USA). Alexa®488-conjugated goat anti-mouse IgG and Alexa®633-conjugated goat anti-rabbit IgG were purchased from Life Technologies.

7.4.3 Construction of recombinant viruses

Recombinant viruses were constructed by homologous recombination between WT strain 108 (9) viral DNA and recombinant PCR products within FBT cells. U_L47 was mutated (mU_L47) so as to remove all essential phosphorylation sites within VP8 by replacing serine 16, threonine 65, serine 66, serine 79, serine 80, serine 82, serine 88 and threonine 107 with alanine (13). Briefly, plasmids with YFP (yellow fluorescent protein) fused in frame with both U_L47 and mU_L47 together with flanking regions of homology, were constructed and used to generate DNA fragments (Figure 7.1A). A DNA fragment encoding YFP was PCR-amplified from pEYFP-N1 using primers 5'-CGAGCTC*AAGCTT*CGAATTCTGCAGTC-3', and 5'-GAA*AGATCT*CGCTT GTACAGCTCG TCCATGCC-3', cut with *HindIII* and *BglII*, and cloned into pFLAG-VP8 and

pFLAG-Mut-VP8 (290) similarly cut, giving pYFP-U_L47 and pYFP-mU_L47. The recognition sequences for restriction enzymes designed in primers are underlined. The 5' homology region was amplified from BoHV-1 DNA by PCR using primers 5'-GAA*GGTACC*GCTGGCCTTTGC GCATATGTACG-3', and 5'-GAA*ACCGGT*GCG TCTA AGGGCGCCTAGAA-3', and inserted into pYFP-U_L47 and pYFP-mU_L47 after digestion with *Kpn*I and *Age*I, resulting in pU_L48-YFP-U_L47 and pU_L48-YFP-mU_L47. For transfection, DNA fragments were generated by PCR using the primers 5'-CGTGTTCGTTTCGCTGTACT ATGC-3' and 5'-CAGTAAATCAGGGAGCCC ATTGAG-3'; these fragments contained about 950 bp of homologous DNA for recombination on either side of the YFP and mutagenized U_L47.

To introduce the YFP-mU_L47 into the viral genome (Figure 7.1B), 2 μg of PCR fragment was co-transfected with 1 μg of wild-type BoHV-1(WT BoHV-1) genomic DNA into FBT cells with Lipofectamine and PLUS reagent (Life Technologies). YFP-positive plaques were plaque purified several times to eliminate contamination from wild-type virus. The resulting virus (BoHV-1-YmVP8) encompasses an YFP-tagged mutant VP8. The same procedure was performed to introduce the YFP-U_L47 into the viral genome, resulted a virus (BoHV-1-YVP8) expressing YFP-tagged WT-VP8.

To produce a revertant virus with wild-type (WT) U_L47, homologous DNA fragments containing 921 bp of DNA upstream of the *ul47* gene and 1,308 bp from the starting codon of the *ul47* ORF were PCR-amplified from the WT BoHV-1 genome by using the primers 5'-CGTGTTCGTTTCGCTGTACTATGC-3' and 5'-CAGTAAATCAGGGAGCCCATTGAG-3'. Two μg of this DNA was co-transfected with 1 μg of genomic DNA of BoHV-1-YmVP8 into FBT cells as described above. YFP-negative plaques were plaque purified several times to eliminate contamination from mutant virus. In the revertant virus (BoHV-1-RVP8) genome, the WT *ul47* ORF was repaired.

The PCR, restriction digestions, and ligations were carried out with Q5® Hot Start High-Fidelity DNA Polymerase (NEB, Ipswich, MA, USA), restriction enzymes (NEB) and T4 DNA ligase (NEB). The DNA sequencing was performed by the NRC-Plant Biotechnology Institute (Saskatoon, SK, Canada).

7.4.4 Immunoprecipitation

MDBK cells were pretreated with phosphate-free Dulbecco's modified Eagle's medium (DMEM; Life Technologies) for 3 h prior to virus infection and subsequent incubation with [^{32}P]-orthophosphate (Perkin Elmer, Woodbridge, ON, Canada). Cell lysates were pre-cleared with Protein G-Sepharose (GE Healthcare, Burnaby, BC, Canada), and then incubated with anti-VP8 polyclonal antibody and Protein G-Sepharose overnight at 4°C. The Protein G-Sepharose was washed three times with wash buffer (50 mM Tris-HCl, 150 mM NaCl, pH 7.4) and boiled for 5 min with SDS-PAGE sample buffer. The samples were separated in SDS-PAGE gels. The gels were subsequently dried and exposed to Imaging Screen-K for visualization on a Molecular Imager FX (Bio-Rad, Mississauga, ON, Canada). ProtoBlue Safe (National Diagnostics, Atlanta, GA, USA) was used to stain gels.

7.4.5 Western Blotting

Whole-cell extracts were prepared by suspension of cell pellets in radioimmunoprecipitation assay (RIPA) buffer (50 mM Tris-HCl pH 8.0, 150 mM NaCl, 1% NP-40, 1% deoxycholate, 0.1% SDS) supplemented with protease inhibitor cocktail (Sigma-Aldrich) and phosphatase inhibitor cocktail (EMD Millipore). The cell lysates, clarified by centrifugation at 13,000 × g for 10 min at 4°C, were boiled in SDS-PAGE sample buffer for 5 min. After separation by SDS-PAGE the proteins were transferred to nitrocellulose membranes and incubated with the appropriate antibodies. The membranes were washed and incubated with IRDye 600RD/800CW-conjugated secondary antibodies at a 1:20,000 dilution and scanned with an Odyssey® CLx Infrared Imaging System (Li-Cor Biosciences).

Densitometry was used to quantify the proteins in the SDS-PAGE gels and Western blots. Capsid protein VP5 was used to normalize the amount of input viruses. The Relative Quantity (RQ) of each protein was calculated by dividing the density of the viral protein of interest (D_{int}) by the density of VP5 (D_{VP5}) in the same lane. The Relative Difference of the protein of interest (RD) was used to illustrate the changes in quantity of that protein between the recombinant viruses (sample) and wild-type virus (WT). These calculations are presented as the following equation:

$$RD = \frac{RQ_{sample}}{RQ_{WT}} \times 100\%, \quad RQ = \frac{D_{int}}{D_{VP5}}$$

7.4.6 Confocal microscopy

MDBK cells, cultured on Permanox 2-well chamber slides (Thermo Fisher Scientific, Waltham, MA, USA), were infected with viruses or mock-infected. At indicated time points, the cells were washed three times with PBS (136.9 mM NaCl, 2.7 mM KCl, 7.0 mM Na_3PO_4, and 0.9 mM Na_3PO_4, pH 7.4), and fixed with 4% paraformaldehyde for 20 min, followed by three washes with PBS. Subsequently, the cells were permeabilized with 0.1% Triton X-100 in PBS for 20 min, washed with PBS, and then incubated with 1% normal goat serum (Gibco) in PBS for 30 min at room temperature. The cells were incubated with primary antibodies at the appropriate dilutions for 2 h at room temperature, followed by washing with PBS and incubation with Alexa Fluor®-conjugated antibodies (Life Technologies) at a 1:500 dilution for 1 h at room temperature. Finally, slides were mounted with ProLong Gold Antifade Mountant with DAPI (Life Technologies) prior to examination with a Leica SP5 confocal microscope (Leica Microsystems CMS GmbH, Mannheim, Germany) equipped with external argon ion 488/633/461 nm laser.

7.4.7 Transmission electron microscopy

MDBK cells in T75 flasks were infected with viruses at a MOI of 1. At 15 hpi, the cells were harvested with trypsin and washed in cold PBS. The cells were pelleted at 500 × g for 10 min at 4°C. The cell pellets were fixed with 2.5% glutaraldehyde in PBS for 4 h and post-fixed with 1% osmium tetraoxide for 4 h. After washing with PBS for 30 min, the fixed samples were dehydrated in graded concentrated ethanol (50, 70, 90, and 100%) and polymerized with propylene oxide for 1 h. Subsequently, the pellets were embedded in Epon 812, followed by polymerization for 3 days at 60°C. Ultrathin sections with a thickness of 50-70 nm prepared by a Reichert-Jung Ultracut E Ultramicrotome (Reichert-Jung, Vienna, Austria) were mounted on 200-mesh carbon-coated grids, and post-stained with 2% uranyl acetate for 10 min and 1% lead citrate for 40 min. After washing with water and air drying, the specimens were observed with a

Philips CM10 transmission electron microscope (Philips Electron Optics, Eindhoven, Netherlands).

7.4.8 Virus purification

MDBK cells cultured in T150 flasks were infected with BoHV-1, BoHV-1-YVP8 or BoHV-1-YmVP8 at a MOI of 1. The medium was harvested when over 90% of the cells showed cytopathic effect, and centrifuged at 3,000 × g for 30 min at 4°C to remove cell debris. The viruses were pelleted by centrifugation at 25,000 rpm for 2 h at 4°C in a Beckman Coulter SW 32 Ti Rotor (Beckman Coulter Inc., Atlanta, GA, USA). The virus pellets were resuspended in a small volume of TNE buffer (50 mm Tris-HCl, pH 7.4, 100 mm NaCl, and 0.1 mm EDTA) overnight. The virus suspensions were loaded on top of a 10-60% potassium sodium tartrate gradient in TNE buffer, and centrifuged at 25,000 rpm for 2 h at 4°C in a Beckman Coulter SW 41 Ti rotor.

7.4.9 Statistical analysis

Data were analyzed by using Microsoft Excel 2010. Standard deviation was calculated based on the entire population of each group, and shown as vertical error bars. Two-tailed t test was used to determine the statistical differences between two groups. Differences were considered statistically significant if $0.01 < P \leq 0.05$, and statistically highly significant if $P \leq 0.01$.

7.5 Results

7.5.1 Construction of recombinant BoHV-1 viruses

To study the impact of phosphorylation of VP8 during BoHV-1 infection, we constructed a virus expressing mutant VP8 (Mut-VP8) in which all essential phosphorylation sites for CK2 and US3 were removed by point mutations. YFP N-terminally fused to VP8 and Mut-VP8 served as a selection marker. Integration of DNA was confirmed by PCR (Figure 7.1C) and DNA sequencing. The PCR fragments were sequenced and found to be identical to the WT sequence of U_L47 in the case of YFP-U_L47 and R-U_L47 (revertant U_L47), and to the mutated sequence in the case of YFP-mU_L47. VP8 proteins from infected cell lysates were analyzed by Western

Blotting. YVP8 (YFP-VP8) and YmVP8 (YFP-mutant VP8) are about 27.5 kDa larger than WT-VP8 and RVP8 (revertant VP8), which correlates to the apparent molecular mass of YFP (Figure 7.1D).

7.5.2 Blocking phosphorylation of VP8 impairs the production of BoHV-1

The phosphorylation status of WT-VP8, YVP8, YmVP8, and RVP8 in infected cells was investigated by immunoprecipitation. [^{32}P]-orthophosphate-labeled VP8 proteins were purified from infected MDBK cells, and equal amounts were loaded onto SDS-PAGE gels (Figure 7.2A). WT-VP8 was phosphorylated in the infected cells, and YVP8 had a similar phosphorylation level as WT-VP8. However, YmVP8 showed a highly significant reduction in phosphorylation. Phosphorylation was restored in RVP8 to a similar level as that of WT-VP8 and YVP8.

Production of WT BoHV-1, BoHV-1-YVP8, BoHV-1-YmVP8, and BoHV-1-RVP8 was analyzed by titrating the viruses from the combined supernatants and cells (Figure 7.2B). The titer of BoHV-1-YmVP8 was significantly lower than that of WT BoHV-1. The titers were restored to WT levels by repairing VP8 in BoHV-1-RVP8, and the BoHV-1-YVP8 titer was equal to that of WT BoHV-1. To verify the intracellular and extracellular production of the mutant virus, viruses from the cells and supernatants were collected separately every 5 h (up to 30 hpi) and subjected to one-step growth analysis (Figure 7.2C-F). The intracellular WT BoHV-1 titer rapidly increased from 5 hpi (10 PFU/ml) to 15 hpi ($10^{5.4}$ PFU/ml), indicating a major replication stage during this time period. Subsequently, a moderate increase in titer was observed from 15 hpi ($10^{5.4}$ PFU/ml) to 25 hpi ($10^{6.0}$ PFU/ml), followed by a slight decrease during the next 5 h (from $10^{6.0}$ to $10^{5.8}$ PFU/ml). Concomitantly, the extracellular virus titer increased substantially between 10 hpi ($10^{4.6}$ PFU/ml) and 20 hpi ($10^{8.0}$ PFU/ml) (Figure 7.2C). This suggests that major egress takes place from 10 to 20 hpi. BoHV-1-YVP8 had a similar growth pattern to WT BoHV-1 (Figure 7.2D). In contrast, the intracellular BoHV-1-YmVP8 titer increased constantly and slowly from 5 hpi ($10^{0.8}$ PFU/ml) to 30 hpi ($10^{3.6}$ PFU/ml), and the extracellular virus titer increased concurrently from 5 hpi ($10^{2.6}$ PFU/ml) to 30 hpi ($10^{4.6}$ PFU/ml) (Figure 7.2E). Repair of the phosphorylation residues on VP8 brought the virus growth curve to a similar pattern as observed with WT BoHV-1 (Figure 7.2F).

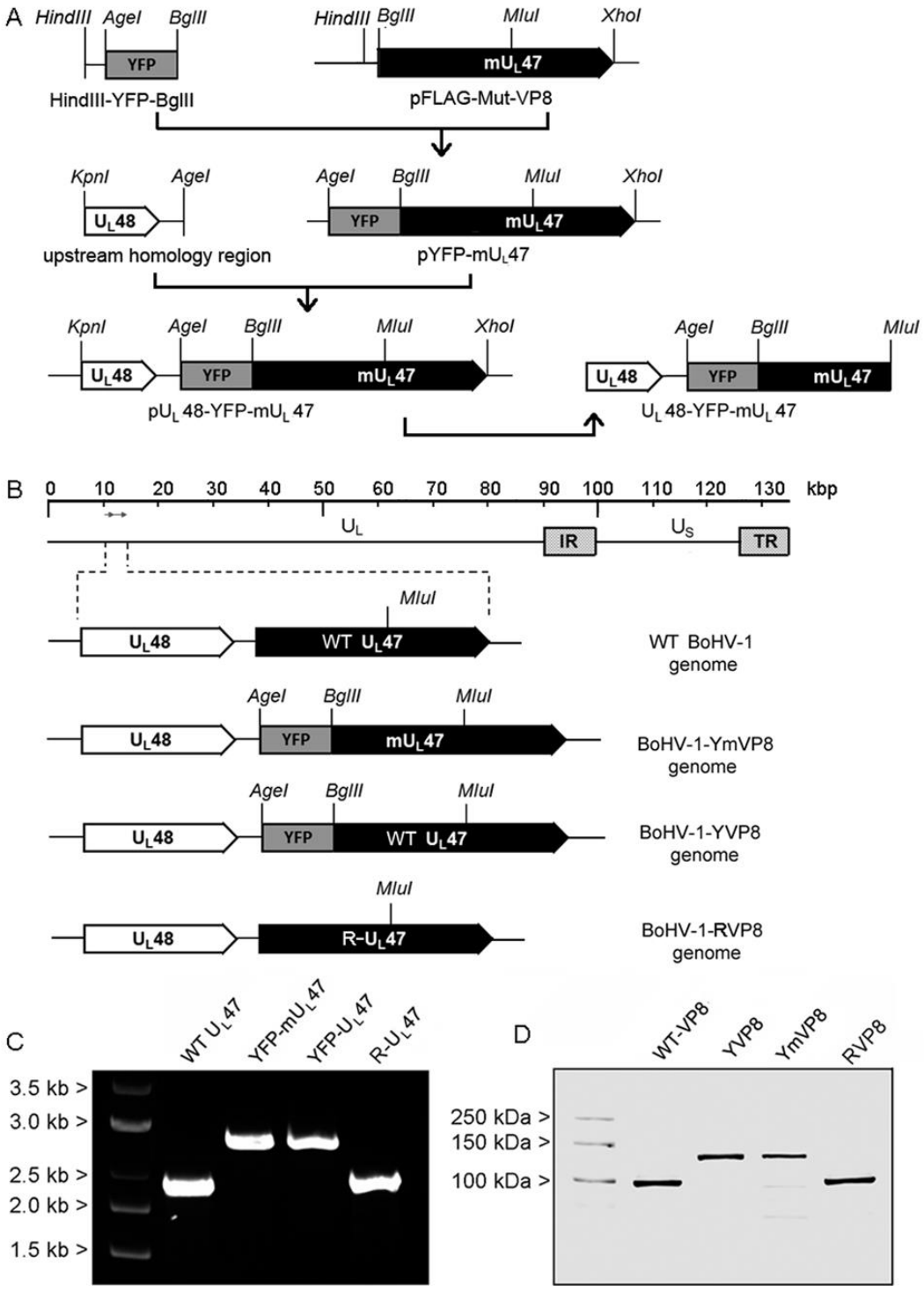

Figure 7.1 Schematic representations of DNA constructs and the genome of recombinant viruses.

(A) Development of DNA fragments for homologous recombination. The locations of restriction sites are indicated on each construct. (B) The genomes of the recombinant viruses. The BoHV-1 genome consists of a unique long (U_L) region and a unique short (Us) region, bracketed by

inverted-repeat sequences (IR and TR). The ORFs of *ul48*, and *ul47* are highlighted. (C) PCR analysis of the viral genomes. Purified genomic DNA of WT BoHV-1, BoHV-1-YVP8, BoHV-1-YmVP8, and BoHV-1-RVP8 were used as PCR template. PCR products covering from about 1 kbp upstream flanking sequence of *ul47* to the *MluI* restriction site of the *ul47* gene were amplified using primers 5'-CGTGTTCGTTTCGCTGTACTATGC-3' and 5'-CAGTAAATCAG GGAGCCCATTGAG-3'. PCR products were separated in a 1% agarose gel with a DNA marker. (D) Western Blotting of VP8 proteins. MDBK cells were infected with WT BoHV-1, BoHV-1-YVP8, BoHV-1-YmVP8, or BoHV-1-RVP8 at a MOI of 1 for 20 h. Whole protein extracts from cell lysates were analyzed by Western Blotting using polyclonal anti-VP8 antibody and IRDye 600RD-conjugated secondary antibody. Molecular weight markers are shown in the left margin.

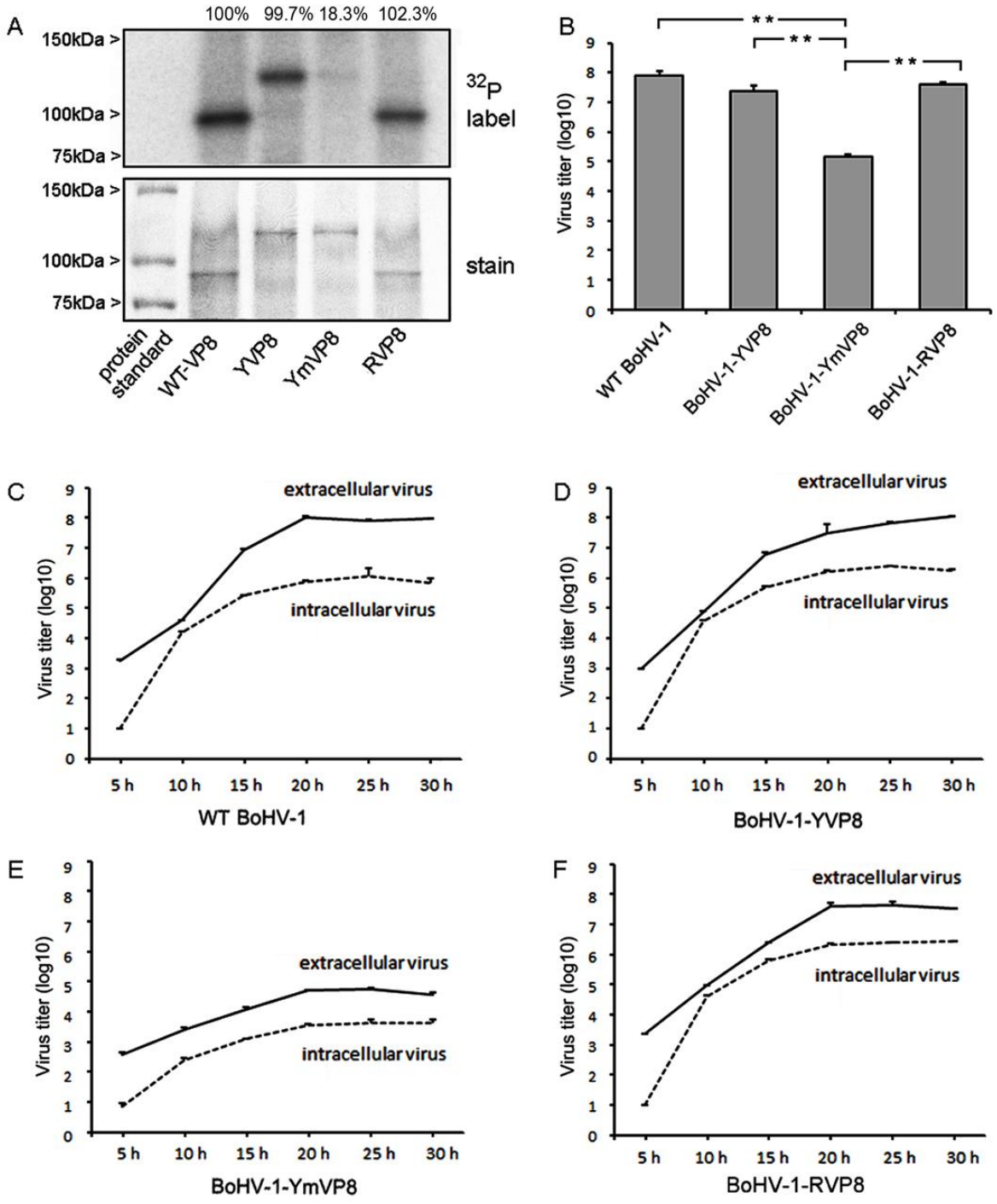

Figure 7.2 Phosphorylation status of VP8 and growth characteristics of viruses in MDBK cells.

(A) Analysis of VP8 proteins by immunoprecipitation. MDBK cells were infected with WT BoHV-1, BoHV-1-YVP8, BoHV-1-YmVP8, and BoHV-1-RVP8 at a MOI of 1 and labeled with [^{32}P]-orthophosphate. Cell lysates were collected at 20 hpi, and used for VP8 purification by incubation with anti-VP8 polyclonal antibody and Protein G Sepharose. The samples were separated by SDS-PAGE and exposed to Imaging Screen K (upper panel). The gels were stained

with ProtoBlue Safe to indicate the amount of protein loading (lower panel). The relative differences of each sample against WT-VP8 are shown as numbers on the top line. (B) Titration of viruses. MDBK cells were infected with viruses at a MOI of 1. The supernatant and cells were collected at 24 hpi. Viruses from infected cells and supernatants were quantified by plaque titration on MDBK cell monolayers. The data were analyzed with Two-tailed t test. The statistical significance of the difference between the values is shown as "*", indicating $0.01 < P \leq 0.05$; and "**", indicating $P \leq 0.01$. (C-F) Single-step growth curves of viruses. MDBK cells were infected with viruses at a MOI of 1, and cell culture medium and cells were harvested separately at the indicated time points. The titer of infectious virus progeny in each sample was determined by plaque assay on MDBK cells.

7.5.3 Phosphorylation affects the incorporation and the cellular localization of VP8 during infection

Deletion of VP8 impairs the incorporation of gB, gD, VP22, and especially gC, into BoHV-1 (64). To determine whether phosphorylation of VP8 plays a role in incorporation of major glycoproteins or tegument proteins, whole protein extracts from purified virions were analyzed by SDS-PAGE (Figure 7.3A) and Western Blotting (Figure 7.3B). After densitometry, the normalized values for the BoHV-1-YVP8 and BoHV-1-YmVP8 proteins were compared to the corresponding values for the WT virus. The overall profiles of the three viruses were similar, with the exception that the incorporation of YmVP8 was lower than that of WT-VP8 and YVP8, and that the molecular weight of YVP8 and YmVP8 was about 27.5 kDa higher (Figure 7.3A) than that of VP8. The packaging of VP8 into BoHV-1-YVP8 and BoHV-1-YmVP8 virions was reduced by 10% and 65%, respectively. There were no obvious changes in glycoprotein (gB, gC, and gD), and tegument protein (VP22 and US3) amounts when analyzed by Western Blotting. The value of gC from BoHV-1-YmVP8 was compared to that of BoHV-1-YVP8, because gC (91 kDa) was partially masked by VP8 (97 kDa) in the WT BoHV-1 lane. The densities of YVP8 and YmVP8 were 21% and 70% lower than that of WT-VP8 (Figure 7.3B), respectively, indicating that the reduced packaging of VP8 may be due to a block in phosphorylation.

The localization of VP8 in infected MDBK cells was observed by confocal microscopy (Figure 7.4A). WT-VP8 first appeared in the cytoplasm at 2 hpi. At 4 hpi, the majority of WT-VP8 localized in the nucleus, and the level of nuclear VP8 slightly decreased during the following 4 h. In contrast, the cytoplasmic VP8 population increased slowly before 4 hpi, and increased relatively quickly from 6 to 8 hpi, and ultimately exceeded the nuclear population. A similar trend in YFP-VP8 distribution was found in BoHV-1-YVP8-infected cells (Figure 7.4B). In BoHV-1-YmVP8-infected cells, the non-phosphorylated Mut-VP8 first appeared in the cytoplasm at 2 hpi. Nuclear Mut-VP8 started to increase from 2 to 8 hpi, while the cytoplasmic level remained the same (Figure 7.4B). Similar results with respect to the distribution of VP8 proteins were found in infected embryonic bovine tracheal (EBTr) cells (data not shown). To track the location of VP8 in the cytoplasm, infected cells were labeled with monoclonal anti-58k protein antibody, which is used as a marker of the Golgi apparatus (366). In WT BoHV-1 and BoHV-1-YVP8 infected cells, VP8 accumulated to the cytoplasm and localized to the Golgi

network, while YmVP8 did not localize to the cytoplasm or Golgi apparatus of BoHV-1-YmVP8 infected cells (Figure 7.5).

To examine whether Golgi-association of VP8 resulted from translocation of virus particles, capsid protein VP5 was labeled with polyclonal anti-VP5 antibody in infected MDBK cells. In WT BoHV-1 infected cells, the VP5 signal was mostly in the nucleus and did not associate with cytoplasmic VP8, indicating that the majority of cytoplasmic VP8 was not virus-associated (Figure 7.6). The distribution of VP5 was not different between WT BoHV-1 and BoHV-1-YmVP8 infected cells. YmVP8 showed a punctate pattern, but VP5 did not, indicating that the speckled YmVP8 was not virus-associated.

7.5.4 Phosphorylation of VP8 benefits the viral DNA content

To further study the effects of VP8 phosphorylation, the BoHV-1 life cycle was studied by transmission electron microscopy. Figure 7.7 demonstrates the life cycle of WT BoHV-1 from empty nucleocapsids to cytoplasmic enveloped particles. Capsid formation and DNA encapsidation took place in the nucleus (Figure 7.7A-B). The nuclear capsids exited from the nucleus to the cytoplasm by budding through the two leaflets of the nuclear membrane. First, these nucleocapsids were in intimate contact with the inner nuclear membrane, while the membrane bent inward to enclose the capsid (Figure 7.7B), resulting in a primary-enveloped virus in the perinuclear space (Figure 7.7C). These capsids were surrounded by a smooth envelope. Capsids were released from the perinuclear space by fusion of the primary envelope with the outer nuclear membrane (Figure 7.7D), so that the viral particles lost the primary envelope (Figure 7.7E) and became free naked capsids in the cytoplasm (Figure 7.7F). The cytoplasmic capsids migrated towards to the Golgi area (Figure 7.7G) and obtained the secondary envelope by being wrapped with Golgi membrane (Figure 7.7H-I). Viral capsids were surrounded by a thick layer of electron-dense material in the Golgi apparatus and the Golgi-derived envelope was contained visible surface projections, when compared with the perinuclear envelope (Figure 7.7H-J). BoHV-1-YVP8 infected cells were also observed by transmission electron microscopy, and the virus exhibited the same maturation as WT virus (data not shown).

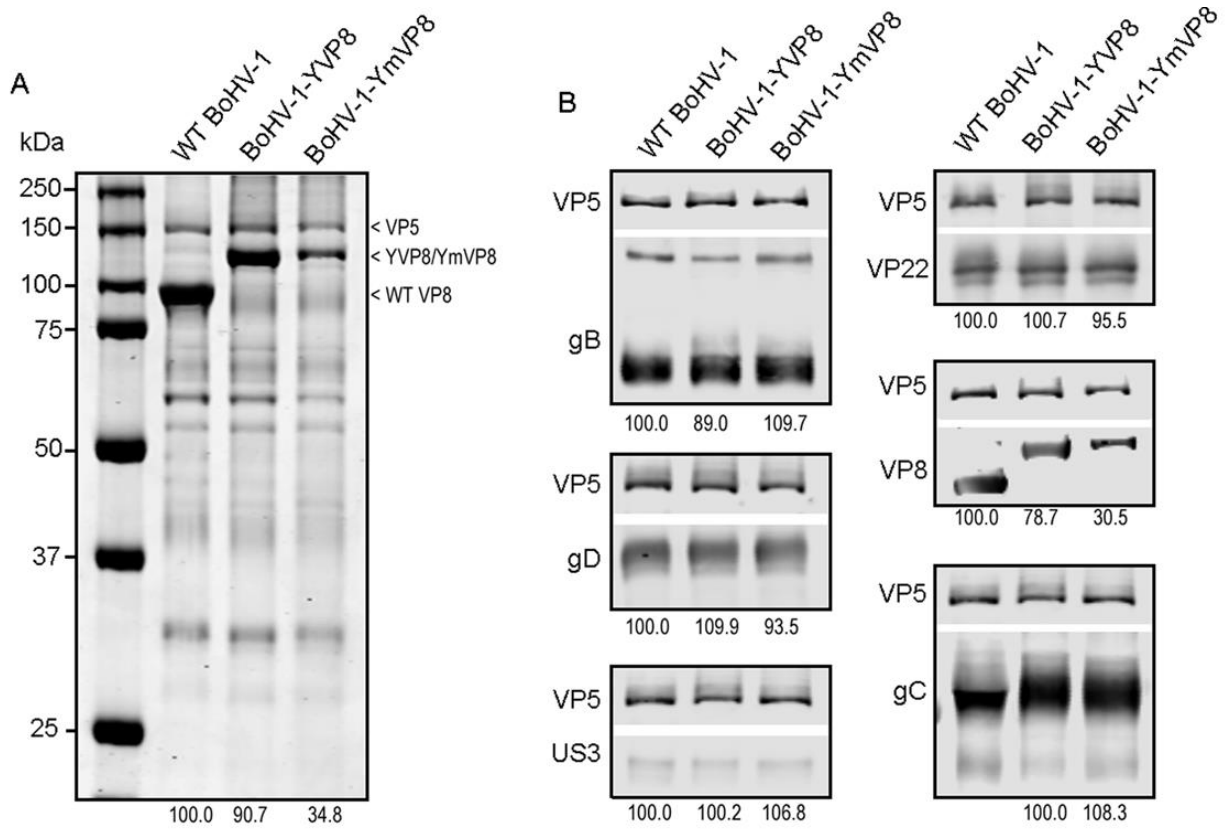

Figure 7.3 Influence of blocking VP8 phosphorylation on virion composition.

(A) Solubilized proteins of purified extracellular virions of BoHV-1, BoHV-1-YVP8 and BoHV-1-YmVP8 were analyzed by SDS-PAGE and the proteins were stained with ProtoBlue Safe. The densities of VP5 and VP8 were analyzed by densitometry. The percentages of YVP8 and YmVP8 in comparison to WT-VP8 are indicated below each sample. (B) Western Blotting of viral proteins. Solubilized proteins of purified extracellular WT BoHV-1, BoHV-1-YVP8 and BoHV-1-YmVP8 virions were analyzed by Western Blotting. The proteins were detected with polyclonal anti-VP5, VP22, VP8 and US3 antibodies, monoclonal anti-gB, gC, gD antibodies, followed by IRDye® 680RD goat anti-rabbit IgG and IRDye® 800CW goat anti-mouse IgG. Each tested protein was simultaneously run with VP5, shown in the top panel of each group. Blots were analyzed by densitometry.

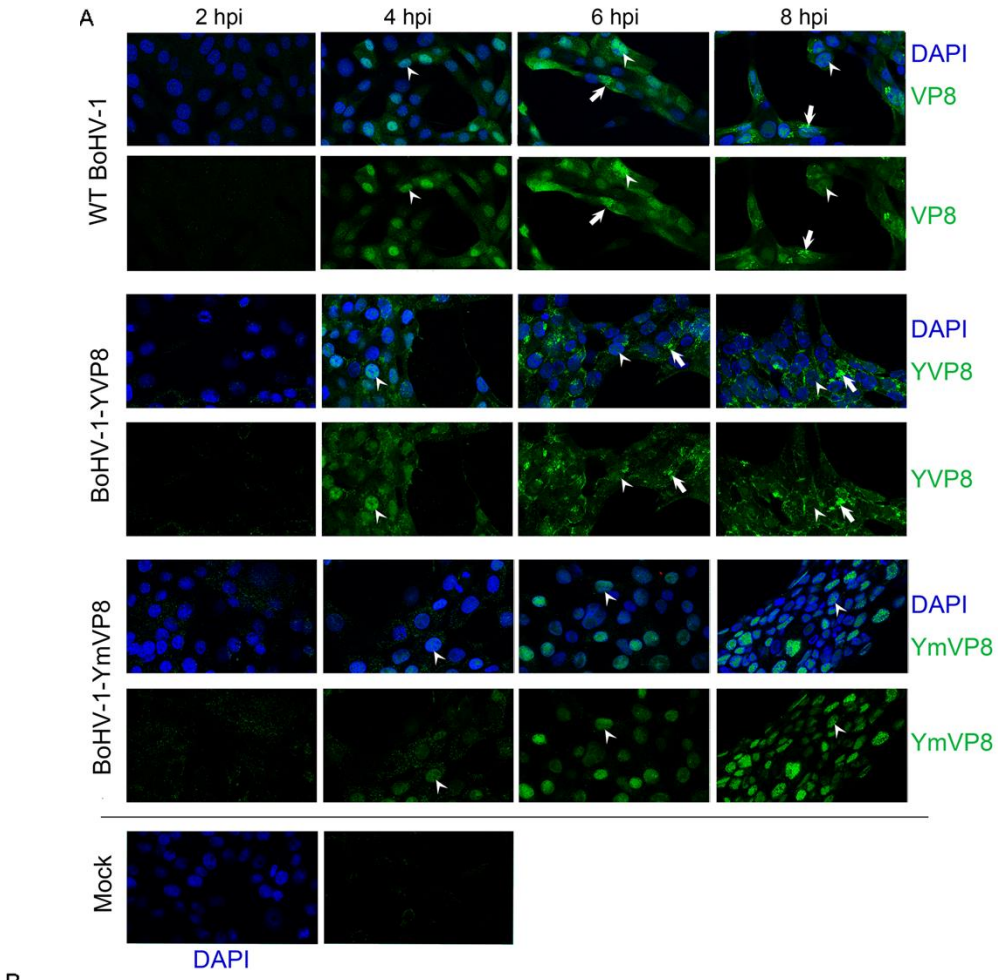
A
2 hpi
4 hpi
6 hpi
8 hpi
WT BoHV-1
DAPI
VP8
VP8
BoHV-1-YVP8
DAPI
YVP8
YVP8
BoHV-1-YmVP8
DAPI
YmVP8
YmVP8
Mock
DAPI

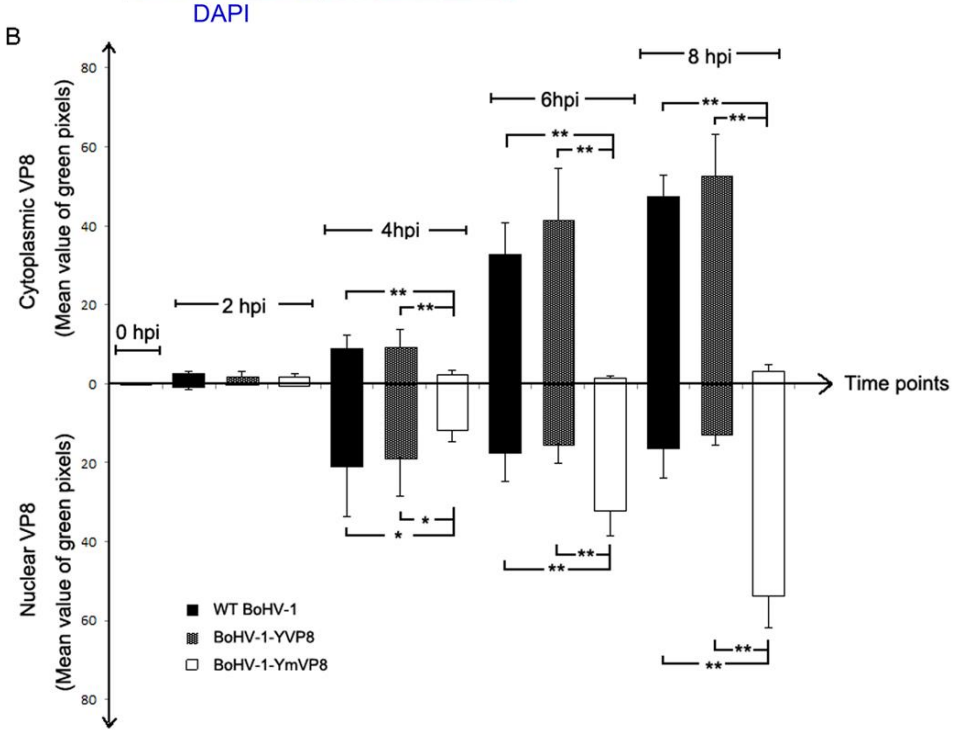
B
Cytoplasmic VP8
(Mean value of green pixels)
Nuclear VP8
(Mean value of green pixels)
0 hpi
2 hpi
4hpi
6hpi
8 hpi
Time points
WT BoHV-1
BoHV-1-YVP8
BoHV-1-YmVP8

Figure 7.4 Localization of VP8 proteins in infected MDBK cells.

MDBK cell monolayers were infected with WT BoHV-1, BoHV-1-YVP8 or BoHV-1-YmVP8 at a MOI of 5, and processed for immunofluorescence staining every 2 h until 8 hpi. (A) VP8 was labeled with polyclonal anti-VP8 antibody and Alexa 488-conjugated antibody. DNA was labeled with DAPI. Arrow heads indicate nuclear VP8 and arrows indicate cytoplasmic VP8. (B) The cell images of each time point were analyzed with a biological image processing program, Fiji (367). The average green value within a selected area in a picture was calculated by the program. At each time point, the cytoplasm and the nucleus of ten cells were selected and analyzed. The mean values are shown in the figure. The data were analyzed with Two-tailed t test. The statistical significance of the difference between the values is shown as "*", indicating $0.01 < P \leq 0.05$; and "**", indicating $P \leq 0.01$.

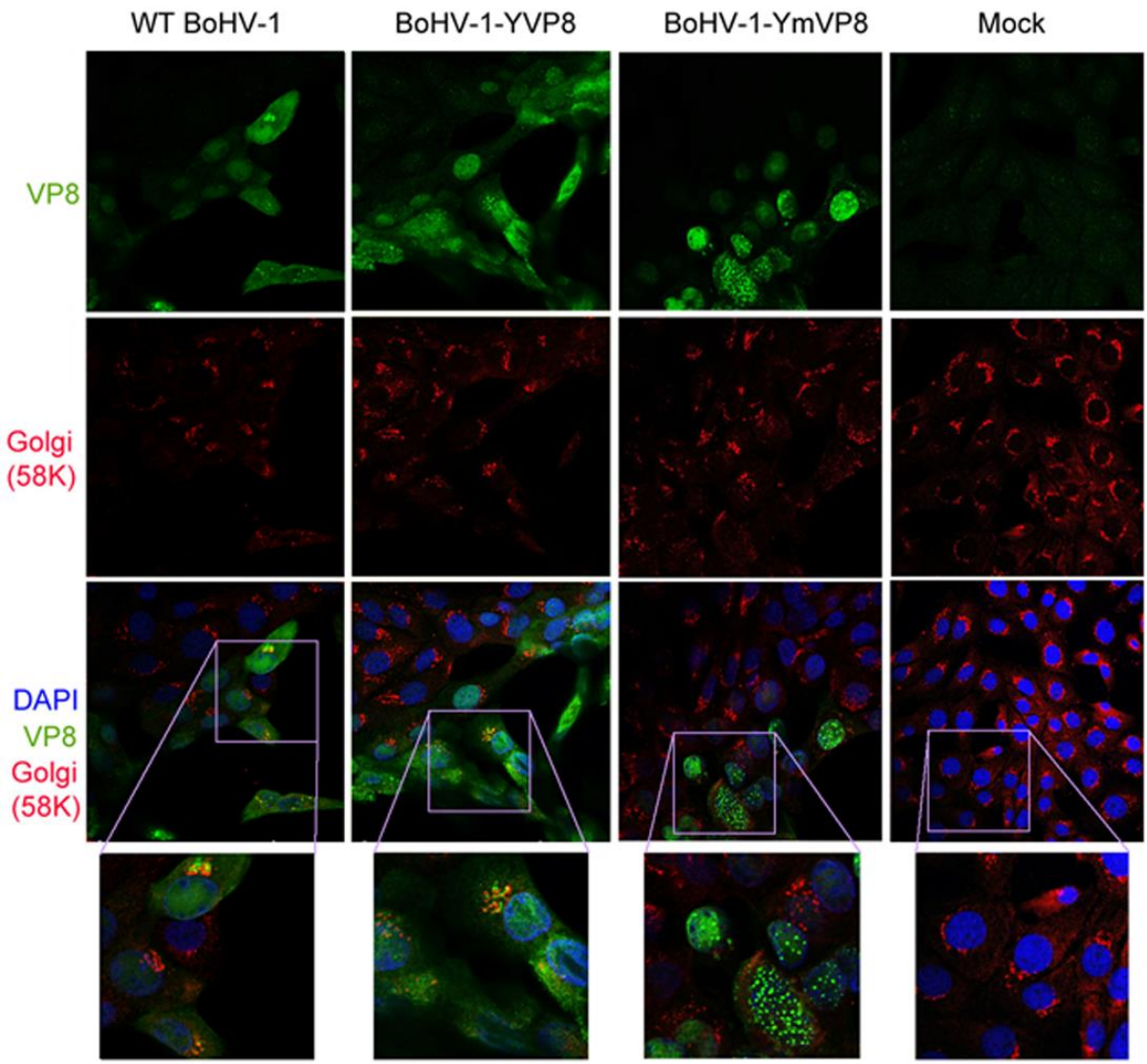

Figure 7.5 Co-localization of cytoplasmic VP8 with the Golgi-apparatus.

MDBK cell monolayers were infected with WT BoHV-1, BoHV-1-YVP8 or BoHV-1-YmVP8 at a MOI of 0.001 until plaques were well-developed. WT-VP8 was labeled with monoclonal anti-VP8 antibody and Alexa 488-conjugated antibody. The Golgi-apparatus was identified with polyclonal anti-58k protein antibody and Alexa 633-conjugated antibody. The DNA was labeled with DAPI. The cells were observed under a Leica SP5 confocal microscope. The selected areas were enlarged in the bottom panel.

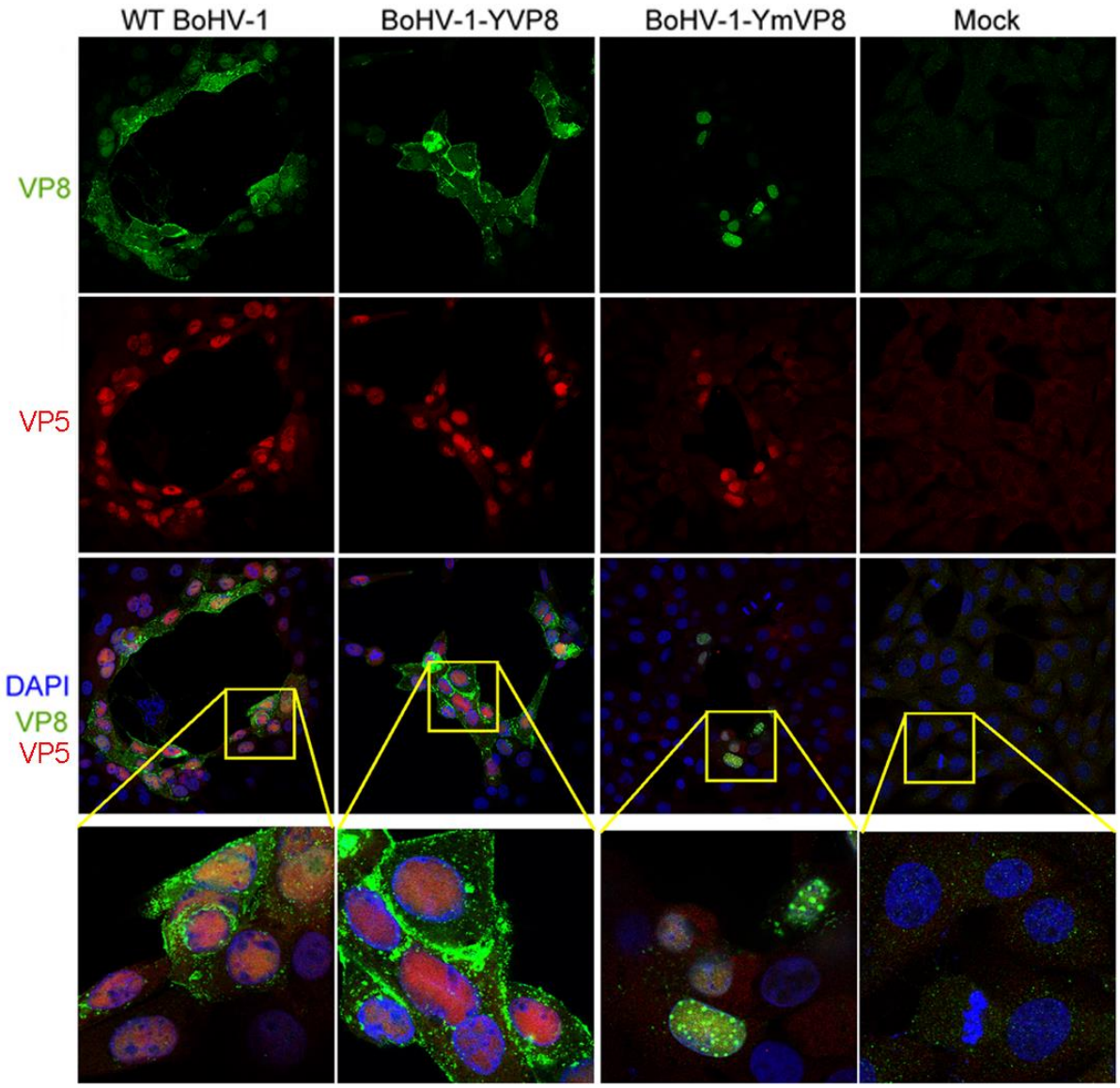

Figure 7.6 Co-immunostaining of VP8 and VP5.

MDBK cell monolayers were infected with WT BoHV-1, BoHV-1-YVP8 or BoHV-1-YmVP8 at a MOI of 0.001 until plaques were well-developed. WT-VP8 was labeled with monoclonal anti-VP8 antibody and Alexa 488-conjugated antibody. VP5 was identified with polyclonal anti-VP5 antibody and Alexa 633-conjugated antibody. DNA was labeled with DAPI. The cells were observed under a Leica SP5 confocal microscope. The selected areas were enlarged in the bottom panel.

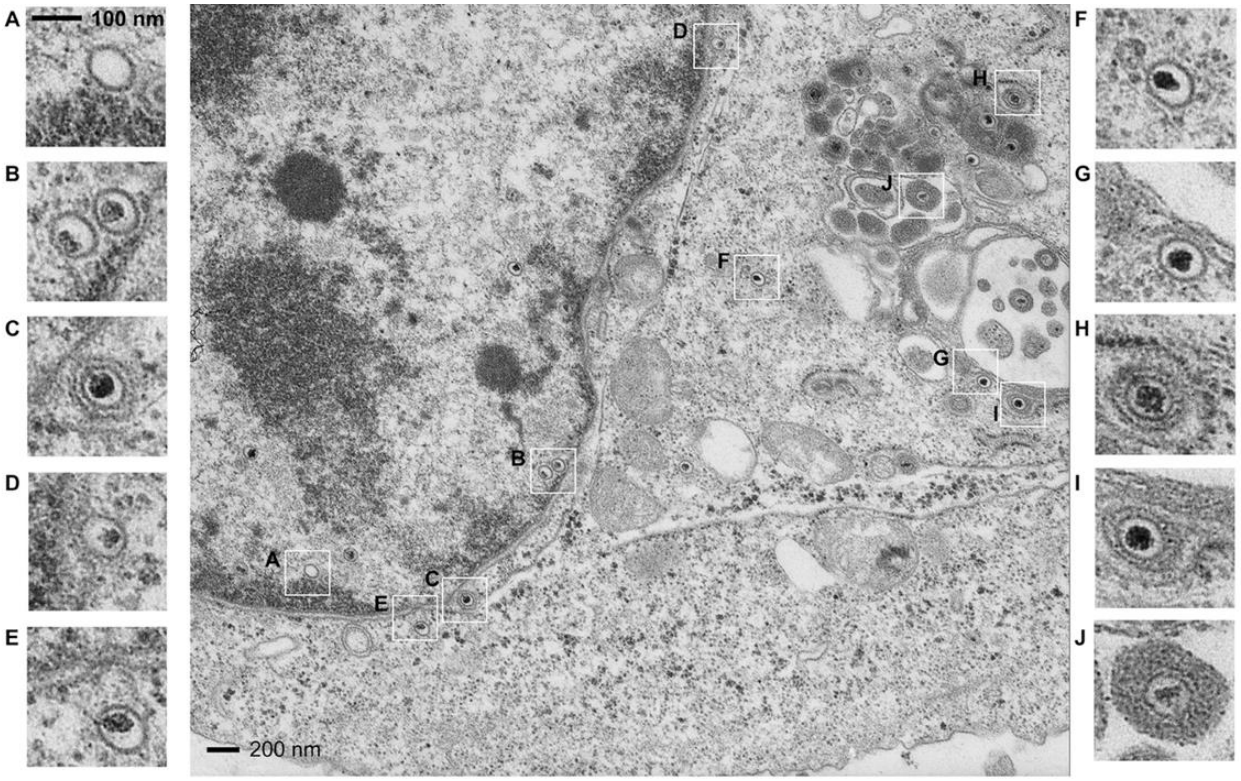

Figure 7.7 Transmission electron microscopy of cells infected with WT BoHV-1.

MDBK cells infected with WT BoHV-1 at a MOI of 1 were collected and processed at 15 hpi and observed with a Philips CM10 transmission electron microscope. The selected areas from the picture in the middle (Bar = 200 nm) were enlarged and displayed on the right and left sides (Bar = 100 nm).

When compared with WT BoHV-1 (Figure 7.8A) and BoHV-1-YVP8 (Figure 7.8B) nuclear capsids, which mostly contained DNA cores at 15 hpi, BoHV-1-YmVP8 infected cells had more empty nucleocapsids present in the nucleus (Figure 7.8C). Five views were captured in the nucleus of cells infected with WT BoHV-1, BoHV-1-YFP or BoHV-1-YmVP8. The numbers of capsids with and without DNA core were counted in each view. Over 80% of the WT BoHV-1 and BoHV-1-YVP8 nucleocapsids had DNA incorporated, while less than 30% of the BoHV-1-YmVP8 nucleocapsids had DNA cores (Figure 7.8D). These results suggest that phosphorylated VP8 might play a role in promoting production or encapsidation of viral DNA.

7.5.5 Phosphorylation on VP8 does not affect virus particle release from the nucleus

In BoHV-1-YmVP8 infected cells, both empty capsids (Figure 7.9A-D) and DNA-containing capsids (Figure 7.9F-I) egressed from the nucleus through the envelopment-de-envelopment pathway. Empty nucleocapsids migrated towards the inner nuclear membrane (Figure 7.9A), which subsequently enclosed the capsids, forming a primary envelope surrounding the empty capsids. The particles were presented as two-layer halos in the perinuclear space (Figure 7.9A, B). DNA-free capsids (Figure 7.9C, D) and DNA-containing capsids (Figure 7.9E, H, I) were found in the cytoplasm. Figure 9H shows that DNA-containing capsids were captured by the Golgi structure in the cytoplasm for further maturation and eventual release out of the cells (Figure 7.9J). There was no apparent evidence for blockage of empty capsid egress from the nucleus in BoHV-1-YmVP8 infected cells.

The amount of extracellular virus of WT BoHV-1, BoHV-1-YVP8 and BoHV-1-YmVP8 is presented in Figure 7.10. In agreement with the viral growth characteristics (Figure 7.2B), BoHV-1-YmVP8 -infected cells were surrounded by apparently smaller amounts of extracellular virions when compared to cells infected with WT BoHV-1 or BoHV-1-YVP8 (Figure 7.10A). Five views of extracellular virus of WT BoHV-1, BoHV-1-YVP8 and BoHV-1-YmVP8 were captured and the numbers of mature virus particles were counted. The numbers of released WT BoHV-1 virions and BoHV-1-YVP8 virions were significantly higher than those of BoHV-1-YmVP8 (Figure 7.10B). The ultrastructure of the three viruses did not have any obvious difference (data not shown).

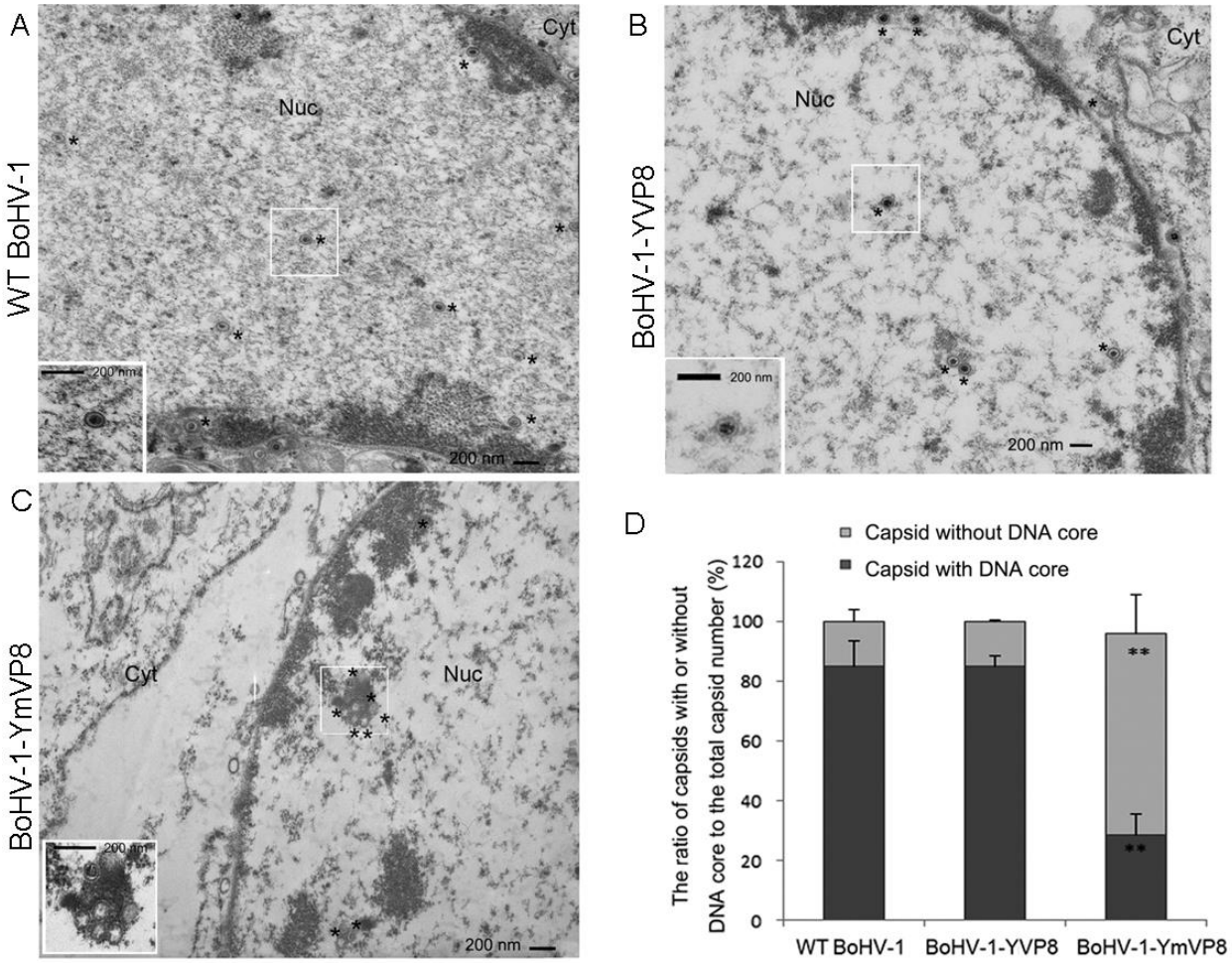

Figure 7.8 Analysis of the impact of blocking phosphorylation of VP8 on viral DNA content.

(A-C) MDBK cells infected with WT BoHV-1, BoHV-1-YVP8, or BoHV-1-YmVP8 at a MOI of 1 were collected and processed at 15 hpi and observed with a Philips CM10 transmission electron microscope. The location of nuclear capsids was marked with a "*". "Cyt" indicates cytoplasmic area, and "Nuc" indicates nuclear area. The selected area from each picture was enlarged and displayed in the left-bottom corner (Bar = 200 nm). (D) The numbers of capsids were counted from five views of the nuclear areas infected with WT BoHV-1, BoHV-1-YVP8, or BoHV-1-YmVP8. The data were analyzed with Two-tailed t test. The statistical significance of the difference between the values is shown as "**", $P \leq 0.01$.

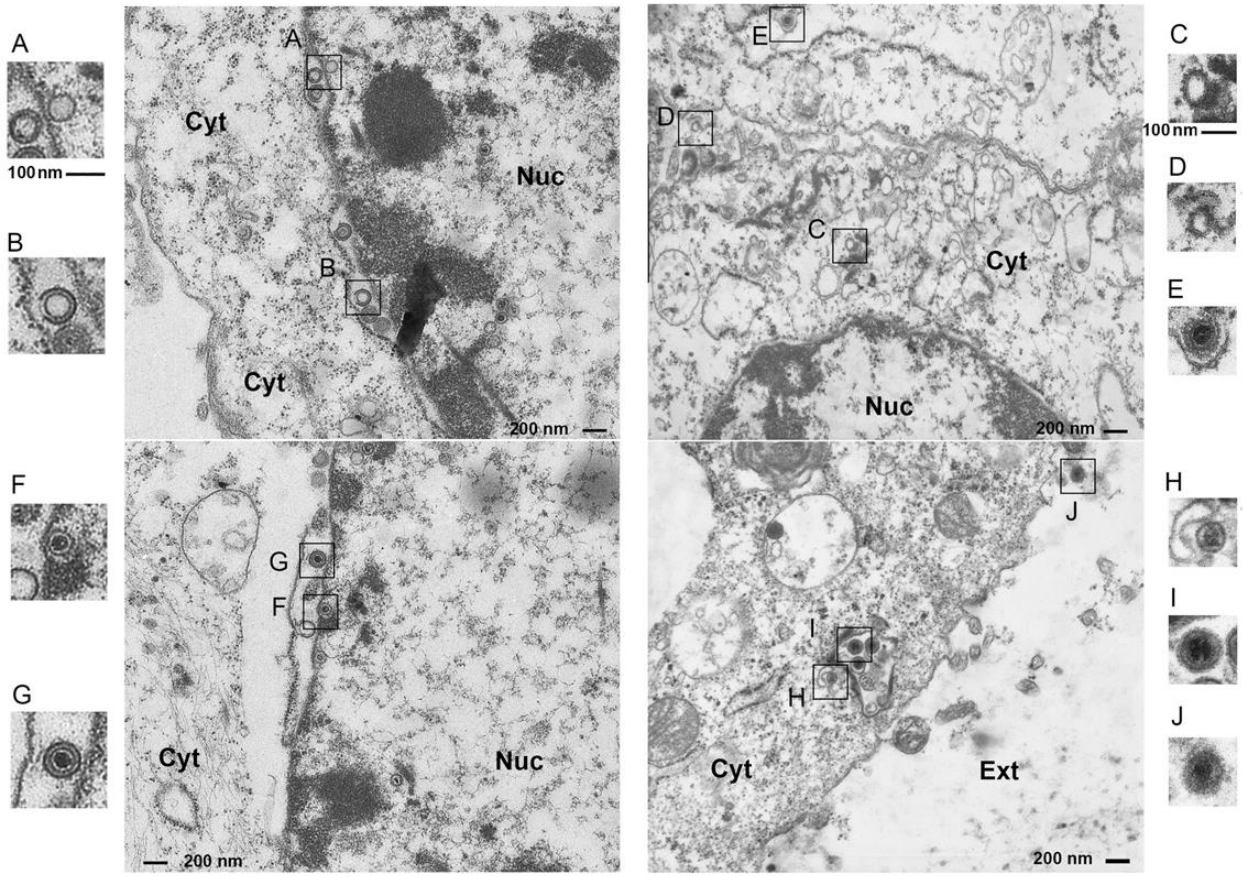

Figure 7.9 Transmission electron microscopy of cells infected with BoHV-1-YmVP8.

MDBK cells infected with BoHV-1-YmVP8 at a MOI of 1 were collected and processed at 15 hpi and observed with a Philips CM10 transmission electron microscope. The selected areas from the picture in the middle (Bar = 200 nm) were enlarged and displayed on the right and left sides (Bar = 100 nm). "Cyt", "Nuc", and "Ext" indicate cytoplasmic area, nucleus area and extracellular area, respectively.

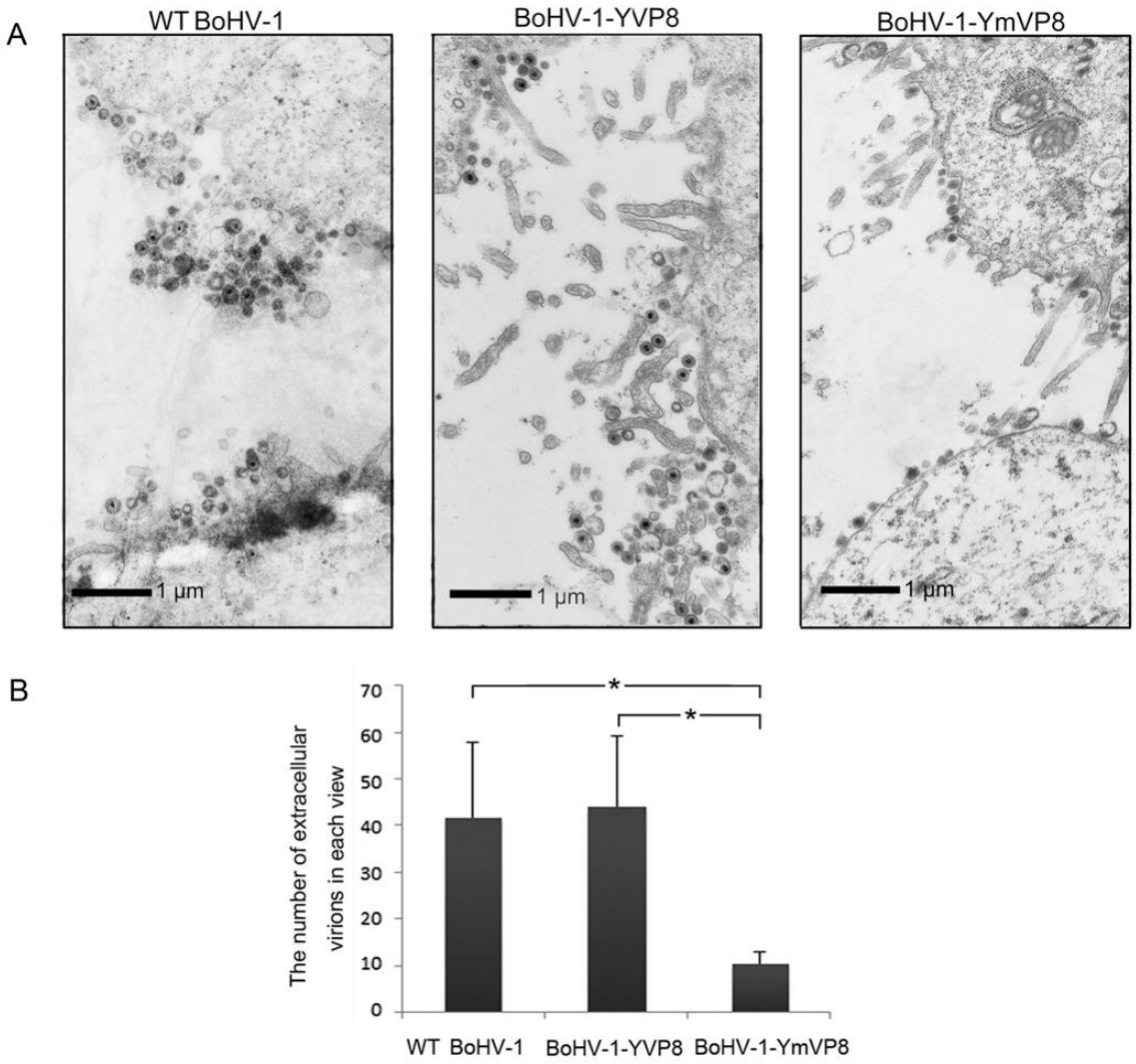

Figure 7.10 Analysis of extracellular viruses.

(A) MDBK cells infected with WT BoHV-1, BoHV-1-YVP8, or BoHV-1-YmVP8 at a MOI of 1 were collected and processed at 15 hpi, and observed with a Philips CM10 transmission electron microscope. The extracellular viral particles are displayed (Bar = 1 μm). (B) The numbers of viral particles were counted from five views of extracellular areas of each treatment. The data were analyzed with Two-tailed t test. The statistical significance of the difference between the values is shown as "*", $0.01 < P \leq 0.05$.

To further confirm the presence of empty virions in BoHV-1-YmVP8 infected cells, viral particles released to the cell culture medium were collected and separated in a sodium potassium tartrate density gradient (Figure 7.11). WT BoHV-1 and BoHV-1-YVP8 consisted of a single virus band located at 40%-50% of the density gradient, while BoHV-1-YmVP8 had two visible bands. The lower band had the same density as that in wild-type virus. These bands contained mature virions with DNA cores (Figure 7.11A, B and D). The upper band of BoHV-1-YmVP8 contained incomplete virions without DNA cores or with partial genomes (Figure 7.11C), which thus had a lower density than the complete virions. The band with complete WT BoHV-1 virions was thicker and brighter than that of BoHV-1-YmVP8. These data are consistent with the results shown in Figure 7.2 and Figure 7.10 that demonstrated lower virus production by BoHV-1-YmVP8.

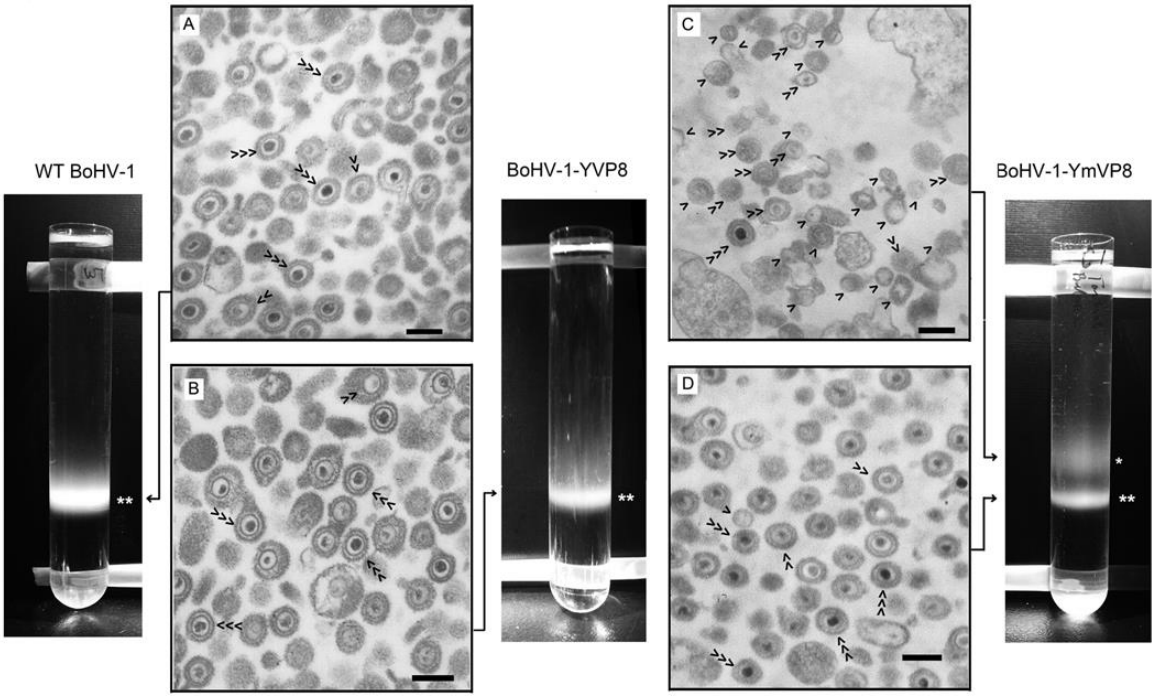

Figure 7.11 Gradient sedimentation analysis and TEM observation of extracellular viruses.

Extracellular viral particles were loaded onto 10-60% potassium sodium tartrate gradients in TNE buffer, and sedimented by centrifugation at 25,000 rpm for 2 h at 4°C in a SW41 rotor. The virus bands were visualized by passing a light beam from the top through the tartrate gradient in a dark environment. "**" indicates a band containing complete viruses with higher density, and "*" indicates a band containing incomplete viruses with lower density. (A-D) The virus bands were aspired and observed by TEM. ">" indicates a virion without a DNA core, ">>" indicates a virion with an incomplete DNA core, and ">>>"indicates a virion with a complete DNA core (Bar = 200 nm).

7.6 Discussion

To characterize the function of phosphorylation on VP8 and eventually the impact on the life cycle of BoHV-1, a recombinant BoHV-1 virus expressing mutant VP8 was constructed. The mutant VP8, which has been previously studied *in vitro* (290) outside the context of infection, is not phosphorylated by CK2 or US3 as amino acid residues at the essential sites for the kinases have been substituted with alanines. The results showed that blocking phosphorylation on VP8 leads to reduced virus production (Figure 7.2B). Accordingly, a lower number of complete BoHV-1-YmVP8 virus particles was found adjacent to infected cells when compared to WT BoHV-1 (Figure 7.10). According to the results of the single-step growth curve, this reduction may have at least two reasons. Firstly, the replication of the VP8-mutant virus was impaired when compared to that of wild-type virus. From 5 to 15 hpi, intracellular BoHV-1-YmVP8 virions increased 163 fold (from $10^{0.8}$ PFU/ml to $10^{3.1}$ PFU/ml), whereas intracellular WT BoHV-1 virus experienced a more rapid amplification, about 26,700 fold (from 10 PFU/ml to $10^{5.4}$ PFU/ml). As a result, during this period the amount of extracellular BoHV-1-YmVP8 was lower in comparison to extracellular WT BoHV-1. Secondly, the mature mutant virus was less efficiently released from the host cells than the wild-type virus. From 10 to 25 hpi, extracellular WT virus showed a rapid increase of ~2,000 fold (from $10^{4.6}$ PFU/ml to $10^{7.9}$ PFU/ml), which was associated with a slower increase in intracellular virus. In contrast the extracellular mutant virus increased about 20-fold (from $10^{3.4}$ PFU/ml to $10^{4.8}$ PFU/ml) (Figure 7.2C, E). Repairing phosphorylation on VP8 (Figure 7.2A) restored the virus titer (Figure 7.2B) and growth property (Figure 7.2F), suggesting the attenuated virus growth in BoHV-1-YmVP8 was due to diminished phosphorylation on VP8.

The ultrastructural study of virus-infected cells revealed a potential function of phosphorylated VP8 in BoHV-1 maturation. The maturation process of WT BoHV-1 from the nucleus to the cytoplasm is displayed in Figure 7.7. Capsid formation and DNA incorporation occurred in the nucleus. Nuclear capsids traveled through the nuclear membrane via an envelopment-de-envelopment process, and obtained most of the tegument and envelope in the cytoplasm. This maturation and egress model is in agreement with the one described previously for other herpesviruses, such as HHV-1 (133), human cytomegalovirus (HCMV) (368) and pseudorabies virus (PRV) (364). In the nucleus of BoHV-1-YmVP8-infected cells, most capsids

did not contain a DNA core, indicating that phosphorylated VP8 may promote viral DNA production or packaging into capsids; however, this is not an absolute requirement as a certain number of DNA-containing particles were found in the nucleus, cytoplasm and extracellular environment. Encapsidation of herpesvirus DNA involves cooperation of many viral proteins that cleave viral DNA and introduce the cleaved DNA into capsids (369). The *ul25* gene product of HHV-1 encompasses a capsid-binding domain, through which the protein targets to capsids and propels DNA into the capsid (94). Viral structural proteins L1 and L2 of PRV are required for assembly of viral DNA into capsids (370). For BoHV-1, phosphorylated VP8 appeared to be a contributing factor for DNA replication or encapsidation. DNA incorporation was not critical for nuclear egress of capsids, and neither was phosphorylation of VP8, because empty capsids were present in the perinuclear space and cytoplasm. In BoHV-1-YmVP8-infected cells, empty capsids merged with the inner nuclear membrane and obtained a primary envelope similar to DNA-containing capsids. Ultimately, the DNA-free particles were released to the extracellular environment, resulting in an additional lower-density virus band in a potassium tartrate gradient (Figure 7.11).

The inefficient incorporation of mutant VP8 into the virion indicates that optimal VP8 packaging requires phosphorylation and that this may have an impact on virion maturation and release. This also suggests that VP8 may be incorporated at two stages, the first occurring in the nucleus and the second one taking place in the cytoplasm. The YmVP8 from the mutant virus was mainly localized to the nucleus during the infection (Figure 7.4), indicating that the virion-associated YmVP8 was incorporated prior to or during nuclear egress, and that phosphorylation by CK2 and US3 is not required for the primary incorporation of VP8. This conclusion is also supported by data from a previous study using VP8-specific immunogold staining that showed accumulation of VP8 protein around the nuclear capsids as well as along the outer nuclear membrane (25). The addition of certain tegument components of herpesviruses to capsids prior to or during nuclear egress is referred to as primary tegumentation (371). In HHV-1, U_L36, U_L37, ICP0 and ICP4 have been identified as primary tegument proteins that are present on the capsids before they get to the cytoplasm (371). The *ul31* and *ul34* gene products of PRV are incorporated in the primary enveloped capsids and eventually dissociate from the capsids during the later

process (372). US3 of PRV is another primary tegument protein which, however, does not dissociate from the viral particle during de-envelopment (373).

Both viral particles (Figure 7.7) and WT-VP8 protein (Figure 7.5) accumulated to the Golgi area during the late stages of infection indicating that the Golgi apparatus is a major site for VP8 incorporation. Previous evidence that immunogold particle-labeled VP8 localized to the Golgi area (25) also supports these results. The secondary incorporation of VP8 requires this protein to be phosphorylated by CK2 and/or US3, as without CK2- and/or US3-mediated phosphorylation it did not associate with the Golgi (Figure 7.5). It is less likely that the Golgi-associated VP8 is the result of viral particle transport, as the cytoplasmic localization of VP8 was independent from VP5 protein, a major component of viral capsids (Figure 7.6).

That VP8 localizes in the cytoplasm and associates with the Golgi only during infection, but remains mainly in the nucleus in VP8-transfected cells (290), suggests that VP8 needs the presence of other viral components for direction to the Golgi. Blocking phosphorylation on VP8 inhibited the protein from targeting the Golgi, which likely resulted in disruption of the secondary incorporation of VP8, and ultimately reduced infectious virus production. In contrast, tegument protein VP13/14, a gene product of HHV-1 U_L47 and a homologue of VP8, assembles mainly in the nucleus. The majority of VP13/14 localizes in the nucleus during all infection stages, and it forms punctate patterns in the late stages. The relative cytoplasmic intensity of VP13/14 is very low in comparison to the nuclear intensity, which may result from viral particle migration (374).

In summary, this study demonstrates that blocking phosphorylation of VP8 may have a negative impact on viral DNA encapsidation and reduce the viral replication efficiency. Phosphorylation was found to be essential for the cytoplasmic incorporation of VP8 into virions, but not for primary packaging of VP8 in the nucleus. Ultimately, the impairment in cytoplasmic maturation of the virus reduced the efficiency of viral release.

7.7 Acknowledgements

The authors would like to thank Dr. Guosheng Liu's kind assistance with TEM experiments. This research was supported by a grant 90887-2010 RGPIN from the Natural

Sciences and Engineering Research Council of Canada. The author Kuan Zhang was supported by a scholarship from the China Scholarship Council. This is VIDO manuscript number 753.

CHAPTER 8

8 LINKER BETWEEN CHAPTER 7 AND CHAPTER 9

Nuclear-to-cytoplasmic shuttling of VP8 has been observed in several previous studies (25, 72, 154). In BoHV-1-infected cells, VP8 was initially localized in the nucleus and then appeared in the Golgi apparatus. Results in chapter 7 suggest that the cellular localization of VP8 may be correlated to the protein function at different phases of BoHV-1 infection. Phosphorylated VP8 promoted the viral DNA encapsidation in the nucleus. Afterwards, VP8 moved from the nucleus to the Golgi where VP8 was incorporated into BoHV-1 virus. The virion-contained VP8 may benefit the infection at a pre-immediate early stage. In the next chapter, we describe a phosphorylation-based regulatory mechanism that controls the nuclear export of VP8 in BoHV-1 infected cells. We investigated the impact of US3 and CK2 in VP8 translocation, respectively. The results suggested that the US3-mediated phosphorylation activates the nuclear export of VP8, but that CK2 does not affect the nuclear localization of VP8.

CHAPTER 9

9 NUCLEAR EXPORT OF VP8, A TEGUMENT PROTEIN OF BOVINE HERPESVIRUS-1, IS MEDIATED BY US3 KINASE AND FOLLOWED BY ACCUMULATION IN THE CIS-GOLGI APPARATUS ALLOWING THE PROTEIN INCORPORATION INTO VIRIONS

Kuan Zhang [1,2], Tara Donovan [1], Robert Brownlie [1], Marlene Snider [1], and Sylvia van Drunen Littel - van den Hurk [1,3,*]

[1]VIDO-InterVac, University of Saskatchewan, Saskatoon, SK, S7N 5E3, Canada.
[2]Vaccinology & Immunotherapeutics, University of Saskatchewan, Saskatoon, SK, S7N 5E5, Canada. [3]Microbiology & Immunology, University of Saskatchewan, Saskatoon, SK, S7N 5E5, Canada.

Running title: Nuclear-to-Golgi translocation of VP8 is activated by US3-mediated phosphorylation during BoHV-1 infection

Corresponding author*:
Dr. Sylvia van Drunen Littel-van den Hurk;
VIDO-InterVac University of Saskatchewan,
120 Veterinary Road,
Saskatoon, SK, S7N 5E3, Canada;
Telephone: 1 + (306) 966-1559;
Fax: 1 + (306) 966-7478.

The information in this chapter is to be published.
Kuan Zhang, Tara Donovan, Robert Brownlie, Marlene Snider and Sylvia van Drunen Littel - van den Hurk. Nuclear export of bovine herpesvirus-1 VP8 is mediated by US3 kinase and followed by accumulation in the *cis*-Golgi apparatus allowing incorporation into virions.

9.1 Abstract

Bovine herpesvirus-1 (BoHV-1) infects bovine species to cause respiratory infections, genital disorders and abortions. VP8 is the most abundant tegument protein of BoHV-1 and is critical for virus replication in cattle. In this study the cellular translocation of VP8 was found to be regulated by a phosphorylation-based mechanism during BoHV-1 infection. Early during infection VP8 was translocated to the nucleus. Subsequently, presumably after completion of its role in the nucleus, VP8 localized to the cytoplasm and accumulated to the Golgi apparatus. During the VP8 translocation process, phosphorylation by the viral kinase US3 played a critical role in mediating the nuclear export of VP8. When US3 was deleted, or the essential US3-phosphorylation site in VP8 was mutated, VP8 remained in the nucleus. Examination of the amino acid sequence of VP8 supported a potential role of US3-mediated phosphorylation in regulating the nuclear localization signals (NLSs) and nuclear export signals (NESs) of VP8. The US3-mediated phosphorylation sites (S^{16} and S^{32}) are close to the NLSs ($P^{11}RPRR^{15}$ and $R^{48}PRVRRPRP^{54}$), supporting the contention that the NLSs might be disguised and deactivated by phosphorylation at these two residues. However, the nuclear export signals (NESs) are not close to the US3-targeted motifs and their functions appeared to be not abolished by the phosphorylation, such that they were capable of translocating VP8 into the cytoplasm. The cytoplasmic VP8 migrated to the *cis*-Golgi apparatus, but not to the *trans*-Golgi network (TGN), suggesting that VP8 is in the Golgi to be incorporated into the virions.

9.2 Importance

NLSs and NESs are important elements directing VP8 to the desired locations in the virus-infected cell. In this study a critical regulator was found that switches the nuclear and cytoplasmic localization of VP8 in BoHV-1 infected cells. BoHV-1 used viral kinase US3 to regulate the activity of the NLSs in VP8. Once US3 was expressed, phosphorylated VP8 egressed from the nucleus and subsequently accumulated in the *cis*-Golgi apparatus, presumably to be incorporated into virions. In addition, we propose that the Golgi localization of VP8 is stimulated by other viral factors.

9.3 Introduction

Bovine herpesvirus-1 (BoHV-1) is a member of the *alphaherpesviridae*, and predominantly infects cattle. It causes infectious bovine rhinotracheitis, pustular vulvovaginitis and balanoposthitis (28). This virus may also cause abortions in host animals during pregnancy (47). BoHV-1 contains a double-stranded DNA genome of 135 kilo base pairs (kbp) enclosed in a capsid shell which is about 125 nm in diameter (69). Outside the capsid is a tegument protein layer surrounded by a lipid envelope and glycoproteins (64). VP8 is the major component of the tegument layer and is essential for BoHV-1 to infect host animals (25). It is a late protein expressed by the *ul47* gene, which is conserved in the *alphaherpesviridae* (289). In human herpesvirus 1 (HHV-1) the *ul47* gene expresses a non-essential tegument protein, named VP13/14 (14).

VP8 is phosphorylated by the viral unique short protein 3 (US3) and the cellular casein kinase 2 (CK2) in BoHV-1-infected cells (15). Phosphorylation of VP8 is removed when the protein is incorporated into mature virions, indicating that the major role of phosphorylation might be regulating cellular functions of VP8 (290). US3 phosphorylates VP8 at residues S^{16} and S^{32} (290), and phosphorylation at S^{16} is essential for the subsequent phosphorylation at S^{32} (290). CK2 has multiple targets on VP8 with different preferences. Seven residues (T^{65}, S^{66}, S^{79}, S^{80}, S^{82}, S^{88}, and T^{107}) localized in the N-terminus of VP8 are critical for phosphorylation through CK2, T^{107} being most frequently phosphorylated (290).

The localization of VP8 with in a cell changes with the progression of BoHV-1 infection (25). Early during infection, VP8 is accumulated in the nucleus. Subsequently, VP8 accumulates in the Golgi apparatus in the cytoplasm at later stages of infection (375). Two arginine-rich nuclear localization signals (NLSs), P^{11}RPRR^{15} and R^{48}PRVRRPRP^{54}, contribute to the nuclear localization of VP8 (72, 154). At least two nuclear export signals (NESs) have been described in VP8. One of them depends on the chromosomal maintenance 1 (CRM1)-signal pathway and the other one is CRM1-independent (156). It has been suggested that they are not the only NESs in VP8 because mutating both NESs does not completely block VP8 translocation from one nucleus to another within the same cell generated by interspecies heterokaryons (155, 156). In the BoHV-1 replication cycle the NLSs and NESs of VP8 might be regulated by a viral strategy to precisely navigate VP8 to a desired subcellular location.

Phosphorylation-regulated cellular localization of proteins has been reported for many proteins including eukaryotic and viral proteins. One example is that phosphorylation controls the cellular recycling of eIF6, a protein essential for separation of the 60S subunit from the 40S subunit, and trafficking from the cytoplasm to the nucleus (376). When phosphorylated through casein kinase 1 (CK1), eIF6 is translocated from the nucleus to the cytoplasm together with the 60S subunit (376). The cytoplasmic eIF6 is then dephosphorylated through calcineurin (376) and subsequently recycled to the nucleus (377). Phosphorylation also controls the sub-cellular localization of VP13/14 in HHV-1 (289). The nuclear localization of VP13/14 is mediated through a NLS and is regulated by US3 of HHV-1. US3-phosphorylated VP13/14 localizes in the nucleoplasm and in the nuclear membrane of HHV-1-infected cells. However, without phosphorylation, VP13/14 is predominantly in the nuclear membrane. This translocation of VP13/14 is correlated to stromal keratitis caused by HHV-1 in mice (142). VP8 of BoHV-1 has been described as a nuclear-cytoplasmic shuttling protein, leading to the hypothesis that cellular localization of VP8 might be regulated by US3- and/or CK2-mediated phosphorylation.

9.4 Materials and methods

9.4.1 Viruses and cell lines

Madin-Darby bovine kidney (MDBK) cells, human hepatoma (Huh-7) cells, African green monkey fibroblast-like (COS-7) cells, embryonic bovine tracheal (EBTr) cells, fetal bovine testis (FBT) cells, and Henrietta Lacks' immortal (Hela) cells were cultured in Eagle's minimum essential medium (MEM) (Gibco/Thermo Fisher Scientific, Waltham, MA, USA) supplemented with 10 mM of N-2-hydroxyethylpiperazine-N-2-ethane sulfonic acid (HEPES, Gibco), 1% non-essential amino acids (Gibco), and 10% fetal bovine serum (FBS, Gibco).

US3-deleted virus (ΔUS3-BoHV-1) and US3-revertant virus (RUS3-BoHV-1) were generated from the Cooper strain (24). A virus expressing YFP-VP8, BoHV-1-YVP8, was made from the 108 strain (25). Production of all viral stocks was carried out in MDBK cells as previously described (290). Briefly, virus infections were accomplished by incubating 85-90% confluent cell monolayers in 150 cm^2 flacks with 10 ml diluted virus at 37°C, which was replaced with 15 ml of MEM with 2% FBS at 1 hpi. Viruses were collected when cytopathic effect was well developed. The virus titers were determined by plaque titration on MDBK cells

in 24-well plates overlaid with 8% UltraPure low-melting-point agarose (Invitrogen/Thermo Fisher Scientific) in MEM.

9.4.2 Generation of US3-deleted BoHV-1 (ΔUS3-BoHV-1) and US3-revertant BoHV-1 (RUS3-BoHV-1)

The viral genome of ΔUS3-BoHV-1 in a bacterial artificial chromosome (BAC) system was developed through homologous recombinations in *E. coli* DH10B cells (24) (Donovan et al. manuscript in preparation) between a plasmid pCooper BAC and a recombinant DNA fragment that contains a kanamycin resistance cassette flanking an upstream region and a downstream region of the *us3* gene. The homologous recombination system also contains a pML300 plasmid that carries the lambda-red recombinant genes driven by a recombinase-sensitive promotor. Recombination in DH10B cells was stimulated with rhamnose and clones containing pΔUS3-BoHV-1 BAC were selected with proper antibiotics.

To generate a US3-revertant BoHV-1 (RUS3-BoHV-1) the *en passant* mutagenesis strategy, a two-step marker-less red recombination system, was adopted. A linear transgene fragment was used for the recombination with pΔUS3-BoHV-1 BAC. This transgene fragment encompassed a central cassette containing an *I-SceI* recognition site and a zeocin selective marker. The centre cassette was flanked by the front half of the *us3* gene, which was deleted in ΔUS3-BoHV-1, and the rear half of the *us3* gene. These flanking regions contained 300 bp of identical sequences for the second-step recombination. On each distant end of the transgene fragment, it contained the upstream and downstream regions of the *us3* gene for the first-step recombination. The first-step recombination system took place in DH10B cells harboring pΔUS3-BoHV-1 BAC, the transgene fragment, and pML300. The second-step recombination was performed in the *E.coli* strain GS1783, expressing an inducible *I-SceI* enzyme and lambda-red enzymes. By stimulating the expression of *I-SceI* enzyme followed by activating the lambda-red recombination, the *I-SceI* site and the zeocin selective marker were removed, resulting in BAC clones containing pRUS3-BoHV-1. Viruses were rescued by transfecting pΔUS3-BoHV-1 and pRUS3-BoHV-1 into fetal bovine testis (FBT) cells, respectively.

9.4.3 Antibodies and plasmids

The antibodies used were monoclonal antibodies specific for VP8 (1G4 2G2) (25), FLAG (Sigma-Aldrich), and formimidoyltransferase cyclodeaminase (FTCD) (Sigma-Aldrich), and polyclonal antibodies specific for VP8 (25), US3 (118), golgin subfamily B member 1 (GOLGB1) (Sigma-Aldrich), and *trans*-Golgi network integral membrane protein 2 (TGOLN2) (Thermo Fisher Scientific). Alexa 488-conjugated goat anti-mouse IgG and Alexa 633-conjugated goat anti-rabbit IgG (Thermo Fisher Scientific) were used for immunofluorescent staining. IRDye® 680RD goat anti-rabbit IgG and IRDye® 800CW goat anti-mouse IgG (Li-Cor Biosciences, Lincoln, NE, USA) were used for Western Blotting.

Plasmids pFLAG-VP8 and pUS3-HA were previously generated by amplification from the cDNA of the BoHV-1 108 strain (15). Plasmids pFLAG-VP8-S16A and pFLAG-VP8-M65-017 were modified from pFLAG-VP8 by site-directed mutagenesis (290).

9.4.4 Immunofluorescent staining and quantification

Tissue cultures were prepared in permanox chamber slides (Thermo Fisher Scientific). After washing with phosphate-buffered saline (PBS) (136.9 mM NaCl, 2.7 mM KCl, 7.0 mM Na_3PO_4, and 0.9 mM Na_3PO_4, pH 7.4) the cultures were fixed with 4% paraformaldehyde for 20 min and again washed with PBS. The fixed cells were permeabilized with 0.1% Triton X-100 in PBS for 30 min, washed with PBS, and blocked with 1% normal goat serum (Gibco) for 30 min. To identify the proteins of interest, the cells were incubated with primary antibodies for 2 h, and then with secondary antibodies for 1 h. Cells were washed three times with PBS following each antibody incubation. All incubations and washes were performed at room temperature. To stain the nucleus the slides were incubated with DAPI (4,6-diamidino-2-phenylindole, 0.5 µg/ml) for 10 min at 37°C. To identify lipids, cells were stained with Nile red (10 µg/mL). To identify *trans*-Golgi, cells were treated with brefeldin A (BFA, 5 µg/ml, Biolegend, San Diego, CA, USA) or DMSO (0.1%). Finally, the slides were mounted with ProLong Gold Antifade Mountant (Thermo Fisher Scientific) prior to examination with a Leica SP5 confocal microscope (Leica Microsystems CMS GmbH, Mannheim, Hesse, Germany).

Three-color images were generated by sequential scanning using 488 nm, 633 nm, and 461 nm lasers. A computer program Leica Application Suite X (Leica Microsystems CMS

GmbH) was used to process the images and to calculate the relative quantification of fluorescent intensities according to the manufacturer's manual. After making selections of the nuclear and cytoplasmic areas, the mean intensity of each channel within the defined area was quantified by the software, shown as procedure defined unit (PDU). The generated data were used for statistical analysis.

9.4.5 Western Blotting

Cell pellets were lysed in radioimmunoprecipitation assay (RIPA) buffer (50 mM Tris-HCl pH 8.0, 150 mM NaCl, 1% NP-40, 1% deoxycholate, 0.1% SDS) supplemented with protease inhibitor cocktail (Sigma-Aldrich). The cell lysates were clarified by centrifugation at 13,000 × g for 10 min at 4°C. The clarified lysates were boiled in SDS-PAGE sample buffer for 5 min. Proteins were separated by using SDS-PAGE. After separation, they were transferred to nitrocellulose membranes and incubated with primary antibodies. The membranes were then washed and incubated with IRDye® 600RD/800CW-conjugated secondary antibodies (Li-Cor Biosciences, Lincoln, NE, USA). The resulting membranes were scanned with an Odyssey® CLx Infrared Imaging System (Li-Cor Biosciences).

9.4.6 Transmission electron microscopy

MDBK cells were infected with viruses at a MOI of 1. At 15 hpi, the cells were harvested with trypsin and washed in cold PBS. The procedure for transmission electron microscopy has been previously described (375). Briefly, after centrifugation at 500 ×g for 10 min at 4°C, cells were fixed with 2.5% glutaraldehyde and then with 1% osmium tetraoxide. The fixed samples were dehydrated with graded concentrated ethanol and polymerized with propylene oxide. After dehydration, the pellets were embed using Epon 812. Ultrathin sections of 50-70 nm in thickness were prepared by a Reichert-Jung Ultracut E Ultramicrotome (Reichert-Jung, Vienna, Austria) and were mounted on 200-mesh carbon-coated grids. The sections were post-stained with 2% uranyl acetate and 1% lead citrate. The specimens were observed with a Philips CM10 transmission electron microscope (Philips Electron Optics, Eindhoven, North-Brabant, Netherlands).

9.4.7 Statistical analysis

Data were analyzed with Microsoft Excel 2010. Standard deviations were calculated based on the entire population of each group and are shown as error bars. A two-tailed student's t-Test with two-sample unequal variances was used to determine the statistical differences between two independent populations. If $0.01 < P$ values ≤ 0.05 differences between two populations were considered statistically significant; if P values ≤ 0.01 differences were considered statistically highly significant.

9.5 Results

9.5.1 Nuclear VP8 is transported to the cytoplasm during the late phase of infection

VP8 has been found to accumulate in the Golgi apparatus in BoHV-1 infected cells late during infection (375). This raised the question whether the previously synthesized nuclear VP8 or the newly synthesized cytoplasmic VP8 was accumulated in the Golgi. To determine the source of Golgi-localized VP8, wild-type VP8 with two different tags (FLAG-VP8 and YFP-VP8) was expressed in EBTr cells, a bovine cell line that is susceptible to BoHV-1 infection and to transient transfection. FLAG-VP8 was first expressed by transient transfection. After 24 h, the transfected cells were mock-infected or infected with BoHV-1-YVP8 to express YFP-VP8. Transiently expressed FLAG-VP8 localized in the nucleus of mock-infected cells, which did not express YFP-VP8, from 28 hpt to 43 hpt (Figure 9.1). In comparison, when the transfected cells were infected with BoHV-1-YVP8, YFP-VP8 appeared in the nucleus and colocalized with FLAG-VP8 at 4 hpi (Figure 9.1). At 11 hpi YFP-VP8 appeared in the nuclear periphery of the cytoplasm, while nuclear YFP-VP8 was reduced. At 19 hpi most of the YFP-VP8 accumulated in the perinuclear region of the cytoplasm, while nuclear YFP-VP8 was greatly reduced. Within the time frame of infection, transfected FLAG-VP8 was translocated from the nucleus to the cytoplasm in a fashion identical to that of YFP-VP8, providing evidenc that nuclear VP8 is transported to the Golgi during the infection.

In transfected EBTr cells, nuclear VP8 accumulated around ring-shaped sub-nuclear structures (Figure 9.1). These VP8-induced sub-nuclear rings also appeared in VP8-transfected COS-7 cells. To identify these sub-nuclear structures, VP8-transfected COS-7 cells were stained with Nile red (Figure 9.2), a compound that is commonly used for the detection of intracellular

neutral lipids (378, 379). The interior of the round structures was stained with Nile red, indicating they were nuclear lipid droplets (LDs). The LDs appeared at 7 hpt with FLAG-VP8, and they gradually grew into larger nuclear LDs at 24 hpt. However, the non-transfected COS-7 cells did not have LDs. Huh-7 cells that naturally contain LDs (380) were used to indicate the efficacy of lipid-staining by Nile red. Numerous LDs of different sizes were observed in the cytoplasm of Huh-7 cells. These results indicate that the expression of VP8 caused the nuclear LD formation in transfected cells, and VP8 accumulated around the LDs, forming ring-shaped structures.

9.5.2 US3 is critical for the cytoplasmic translocation of VP8 during the late stage of BoHV-1 infection

To examine the impact of US3 on the cellular localization of VP8, MDBK cells, bovine cells that are susceptible to BoHV-1 infection, were infected with wild-type BoHV-1 (Cooper and 108), ΔUS3-BoHV-1 (Cooper), and RUS3-BoHV-1 (Cooper). The localization of VP8 was observed at 4 and 8 hpi. At 4 hpi VP8 and US3 appeared in the nuclei of cells infected with wild-type viruses and revertant virus. ΔUS3-BoHV-1 infected cells expressed VP8 but not US3, and VP8 was also in the nucleus (Figure 9.3A). There was no noticeable difference between the four viruses in the nuclear localization of VP8 early during infection. In wild-type virus-infected cells VP8 was translocated to the cytoplasm at 8 hpi, leaving US3 in the nucleus. The two strains of wild-type viruses and the revertant virus showed comparable patterns of VP8 localization, and the expression of US3 was increased in these cells. However, in ΔUS3-BoHV-1-infected cells the majority of VP8 was in the nucleus with punctate appearance, and US3 was not detected (Figure 9.3B). VP8 and US3 were not observed in mock-infected cells (Figure 9.3C). The protein expression by the four viruses was confirmed by Western Blotting, showing that US3 was expressed by all viruses except ΔUS3-BoHV-1, and that VP8 was expressed by all viruses. US3 of the Cooper strain migrated slightly faster than US3 of the 108 strain (Figure 9.3D). These results implicate that US3 activates the nuclear export of VP8 in infected cells at a later stage of infection.

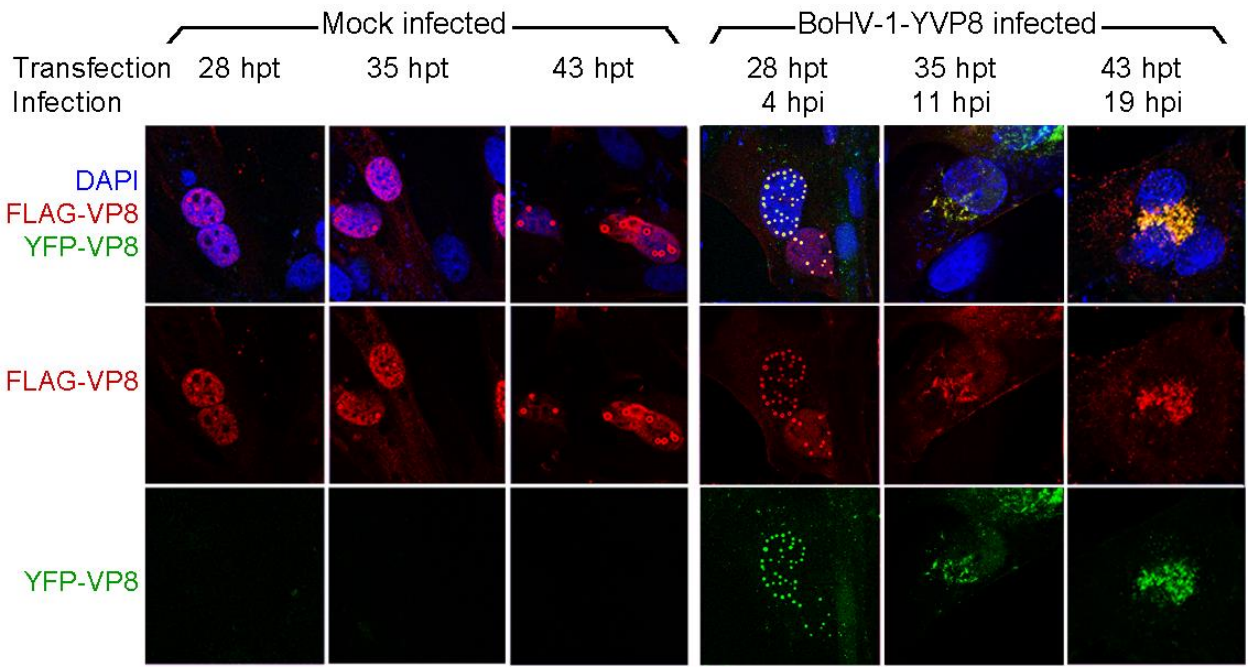

Figure 9.1 Translocation of VP8 from the nucleus to the cytoplasm in BoHV-1-YVP8-infected cells.

EBTr cells transfected with pFLAG-VP8 were cultured for 24 h before infection. The FLAG-VP8-expressing cells were then mock-infected or infected with BoHV-1-YVP8 at a MOI of 5. Cells were fixed at indicated time points for immunofluorescent staining. FLAG-VP8 was detected with monoclonal anti-FLAG antibody followed by Alexa 633-conjugated secondary antibody. YFP-VP8 was tracked through the YFP label. The cell nucleus was shown by DAPI staining.

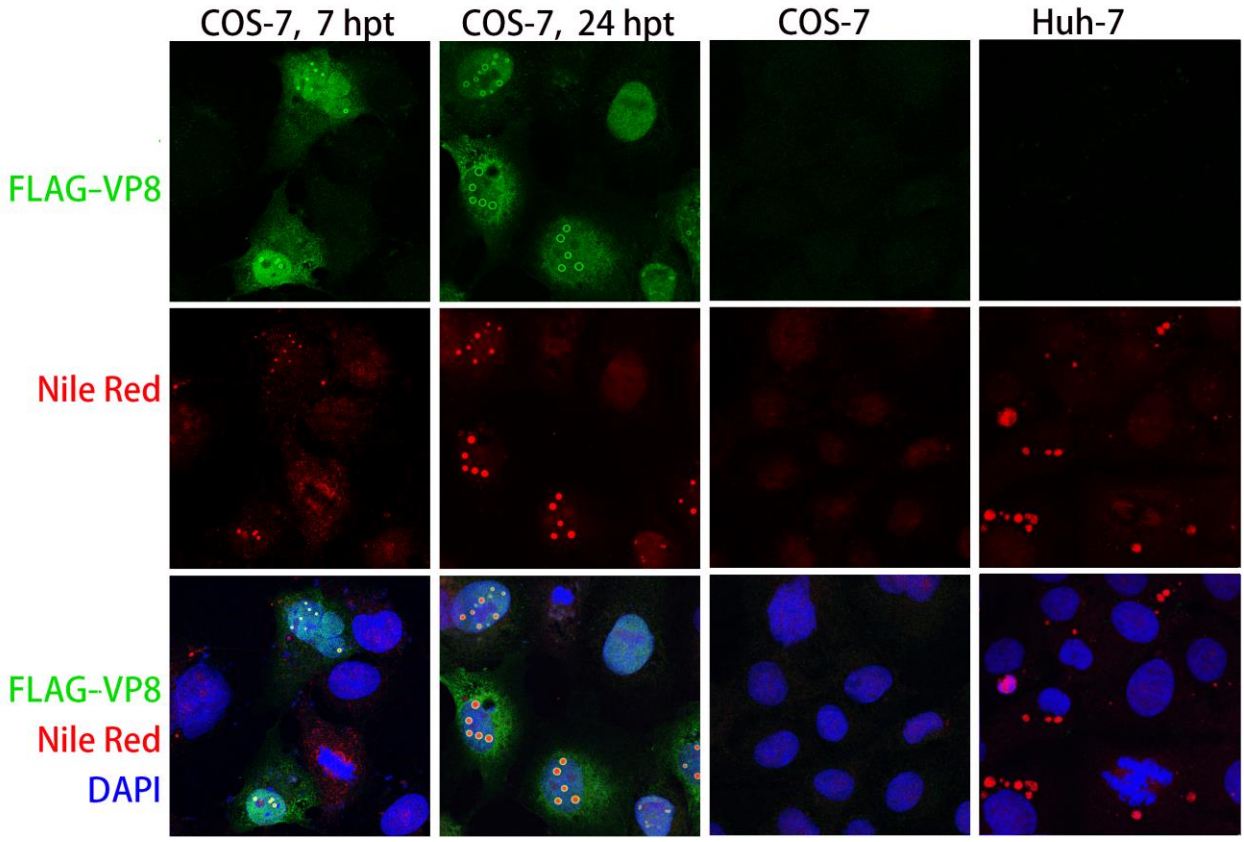

Figure 9.2 Accumulation of VP8 around nuclear lipid droplets (LDs) in transfected cells.

COS-7 cells were transfected with pFLAG-VP8 and fixed at 7 and 24 hpt. Control groups included the non-transfected COS-7 and Huh-7 cells. VP8 was detected with VP8 specific monoclonal antibody followed by Alexa 488-conjugated secondary antibody. Cells were stained with Nile red and DAPI.

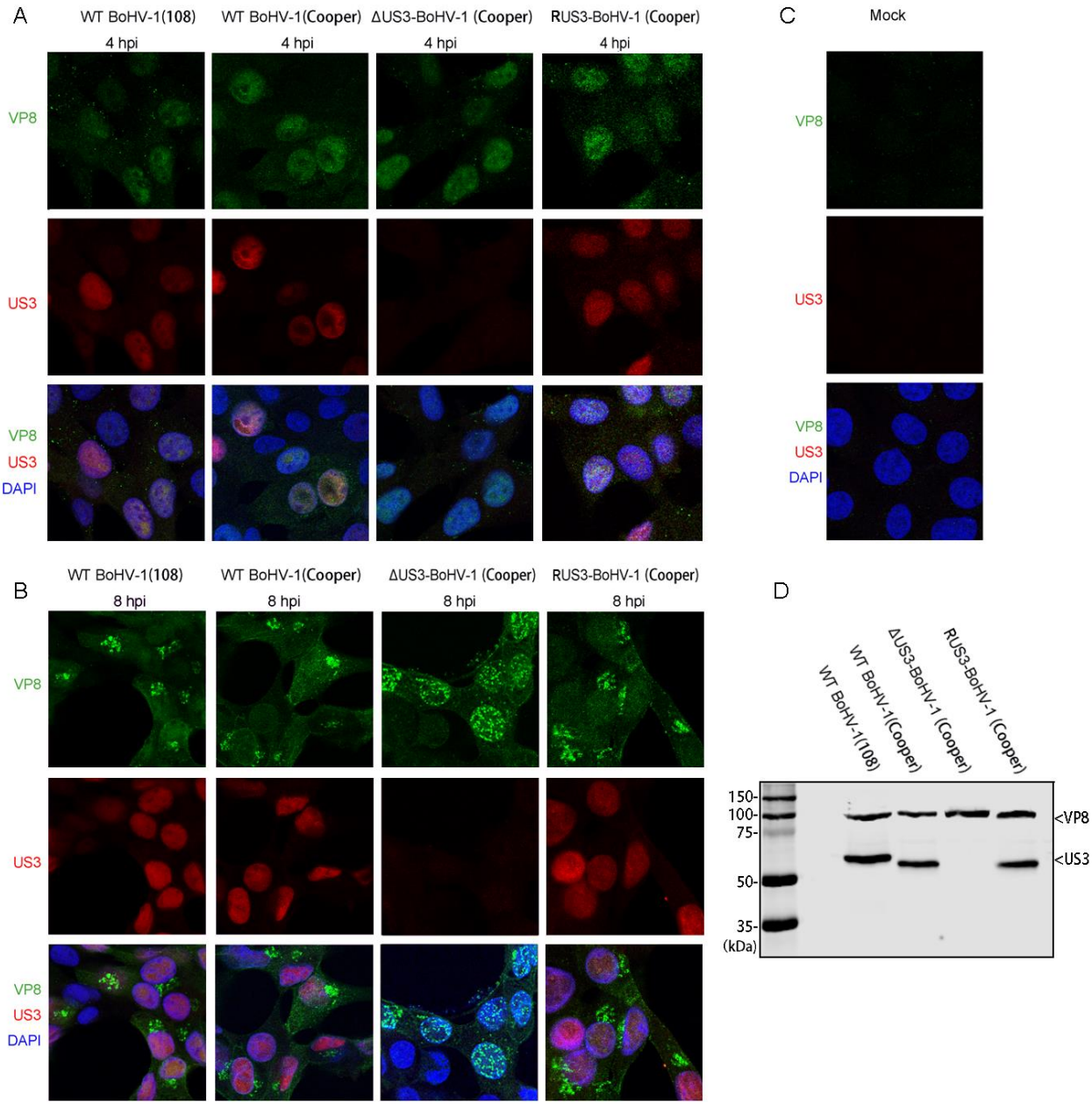

Figure 9.3 Cytoplasmic localization of VP8 at a late stage of BoHV-1 infection requires US3.

(A-C) MDBK cells were infected with indicated viruses at a MOI of 5 or mock-infected. Cells were processed for immunofluorescent staining at 4 and 8 hpi. VP8 was detected with monoclonal anti-VP8 antibody followed by Alexa 488-conjugated secondary antibody. US3 was identified with polyclonal anti-US3 antibody followed by Alexa 633-conjugated secondary antibody. The cell nucleus was indicated by DAPI staining. (D) Virus-infected MDBK cell lysates were analysed by Western Blotting. VP8 and US3 were detected with mouse anti-VP8 and rabbit anti-US3 antibodies, respectively.

9.5.3 Phosphorylation by US3 activates the nuclear export of VP8

Since US3 was required for the cytoplasmic transport of VP8, it was possible that the kinase activity of US3 regulates translocation of VP8. To confirm this, the impact of US3 on the cellular translocation of wild-type VP8 and a mutated VP8 (VP8-S16A) was compared in transfected cells (Figure 9.4). Previously we reported that US3-mediated phosphorylation in VP8-S16A is abolished by substituting the essential residue S^{16} with an A (290). In the absence of US3, wild-type VP8 and VP8-S16A were localized in the nucleus (Figure 9.4A, panel 1 and 3). When US3 was expressed, wild-type VP8 was distributed throughout the cell, whereas VP8-S16A was localized in the nucleus (Figure 9.4A panels 2 and 4), demonstrating that phosphorylation by US3 is critical for the nuclear export of VP8.

The relative quantities of cytoplasmic and nuclear VP8 were measured based on the intensity of green fluorescence pixels within the confocal microscopy pictures of above cells. Wild-type VP8 in the cytoplasm was significantly increased in US3-expressing cells when compared with cells without US3 (Figure 9.4B). When the phosphorylation site of VP8 was mutated, US3 was not capable of increasing the quantity of cytoplasmic VP8 (Figure 9.4B). These results implicated a critical role of phosphorylation by US3 in the transport of VP8 to the cytoplasm.

In US3 and wild-type VP8 co-transfected cells, VP8 was dispersed in the cytoplasm (Figure 9.4A), which was different from the juxtanuclear aggregation of VP8 shown at the late phase of BoHV-1 infection (Figure 9.3B). This observation suggests that the Golgi-accumulation of VP8 is due to a second transport following nuclear export of VP8, and not dependent on US3-mediated phosphorylation. The cytoplasmic VP8 might require an unidentified viral protein or stimulus to target the Golgi.

To demonstrate that the nuclear export of VP8 might be enhanced with increasing amounts of US3, FLAG-VP8 was first transfected into EBTr cells and US3-HA was subsequently transfected at different time points into the cells expressing FLAG-VP8. At 0 hpt, before transfection with US3-HA, the average readout at the 633 nm channel was 6.9 PDU, thus this level was considered as the baseline for US3 expression. The fluorescent pixels below this baseline were considered as background signals. The results show that from 0 hpt to 15 hpt with pUS3-HA, the intensity of nuclear US3 increased to about 130 PDU. With the increase of US3,

cytoplasmic VP8 gradually increased from 20 DPU to 120 DPU, while the intensity of nuclear VP8 did not significantly change (Figure 9.5), confirming that US3 activated cytoplasmic transport of VP8.

9.5.4 NLSs and US3 phosphorylation sites of VP8 are adjacent and conserved

In the amino acid sequences of VP8 from strains 108 and Cooper, NLSs (155, 156) and US3-phosphorylated residues (290) were closely localized in the extreme N-terminus of VP8 (Figure 9.6). NLS1 was immediately followed by a phosphorylated residue S^{16}. In between of NLS1 and NLS2 is the second phosphorylation site at S^{32}. Together with the results that phosphorylation by US3 activated cytoplasmic localization of VP8 (Figure 9.4 and 9.5), this suggests that US3-mediated phosphorylation might interfere with the activity of the NLSs. Moreover, multi-way protein alignment showed that the two US3 phosphorylation residues and NLS2 were conserved among two strains of BoHV-1 viruses. NLS1 was partially conserved with two-amino-acid variation in the Cooper strain comparing with the strain 108. This indicates that phosphorylation-regulated activity of the NLS might be conserved among these strains.

9.5.5 Phosphorylation by CK2 does not alter the nuclear localization of VP8

In addition to US3, VP8 is also phosphorylated by CK2 (290). To determine whether phosphorylation by CK2 regulates the nuclear localization of VP8, the cellular localization of VP8-M65-107, which was not phosphorylated by CK2 (290), was compared with that of wild-type VP8 in EBTr cells (Figure 9.7). Previously, VP8-M65-107 was modified from wild-type VP8 by introducing site-directed mutations at critical residues (T^{65}, S^{66}, S^{79}, S^{80}, S^{82}, S^{88}, and T^{107}) for CK2-mediated phosphorylation (290). Wild-type VP8 and VP8-M65-107 localized in the nucleus of transfected cells (Figure 9.7), implicating that blocking CK2-mediated phosphorylation did not change the nuclear localization of VP8.

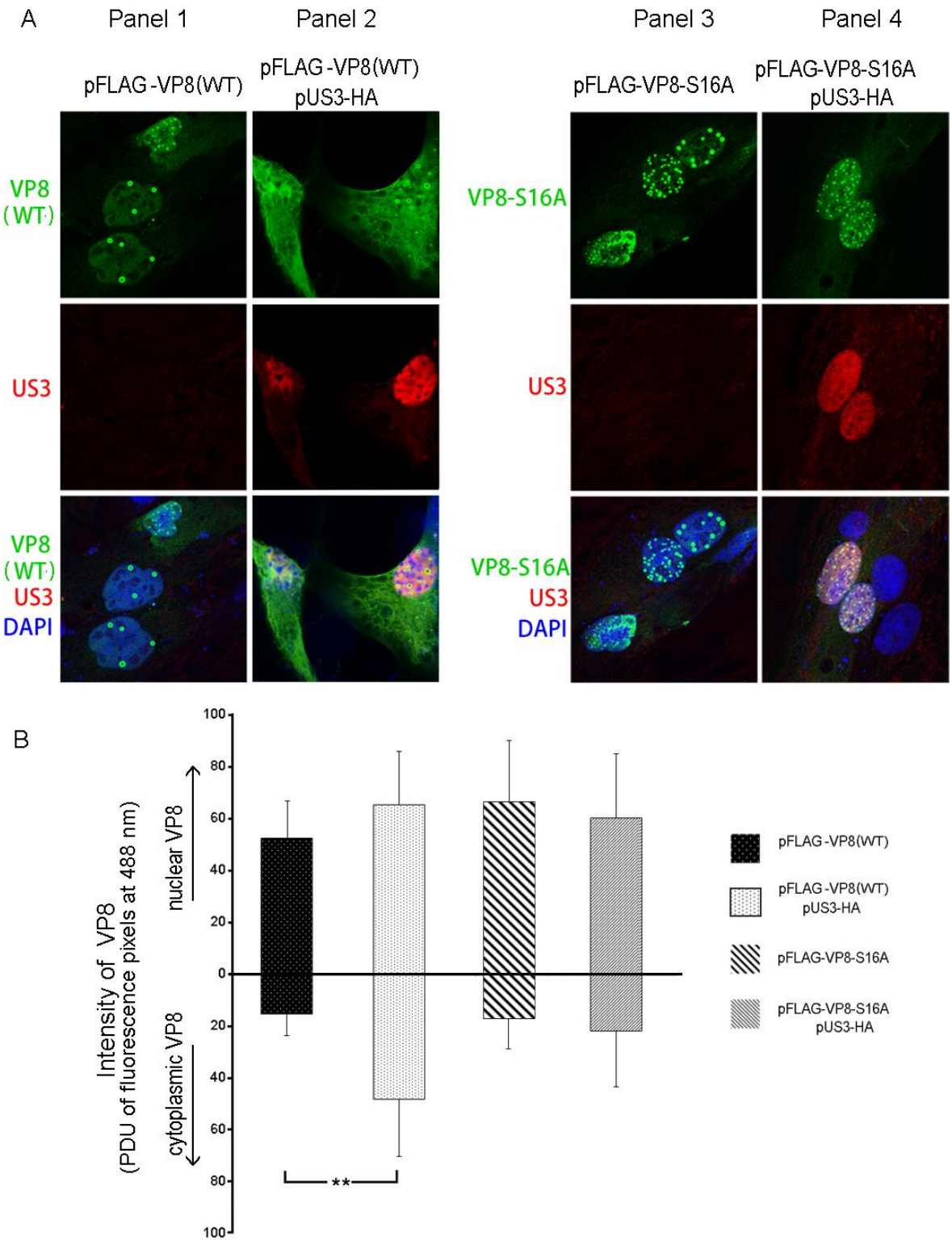

Figure 9.4 US3-mediated phosphorylation promotes the cytoplasmic localization of VP8.

(A) EBTr cells were transfected with different (combinations of) plasmids. Cells in panel 1 were transfected with pFLAG-VP8. Cells in panel 2 were co-transfected with pFLAG-VP8 and pUS3-HA. Cells in panel 3 were transfected with pFLAG-VP8-S16A. Cells in panel 4 were co-transfected with pFLAG-VP8-S16A and pUS3-HA. VP8 was identified with monoclonal anti-VP8 antibody followed by Alexa 488-conjugated secondary antibody, and US3 was identified with polyclonal anti-US3 antibody followed by Alexa 633-conjugated secondary antibody. (B) Relative quantification of the cytoplasmic and the nuclear VP8. Software Leica Application Suite X (version 3.0.2) was used to analyze confocal pictures. The intensity of VP8 was represented as the fluorescence pixels at a wavelength of 488 nm. The mean values of PDU are shown in the bar graphs. Error bars represent the standard deviations. The statistical significance is shown as follows: **, $P \leq 0.01$.

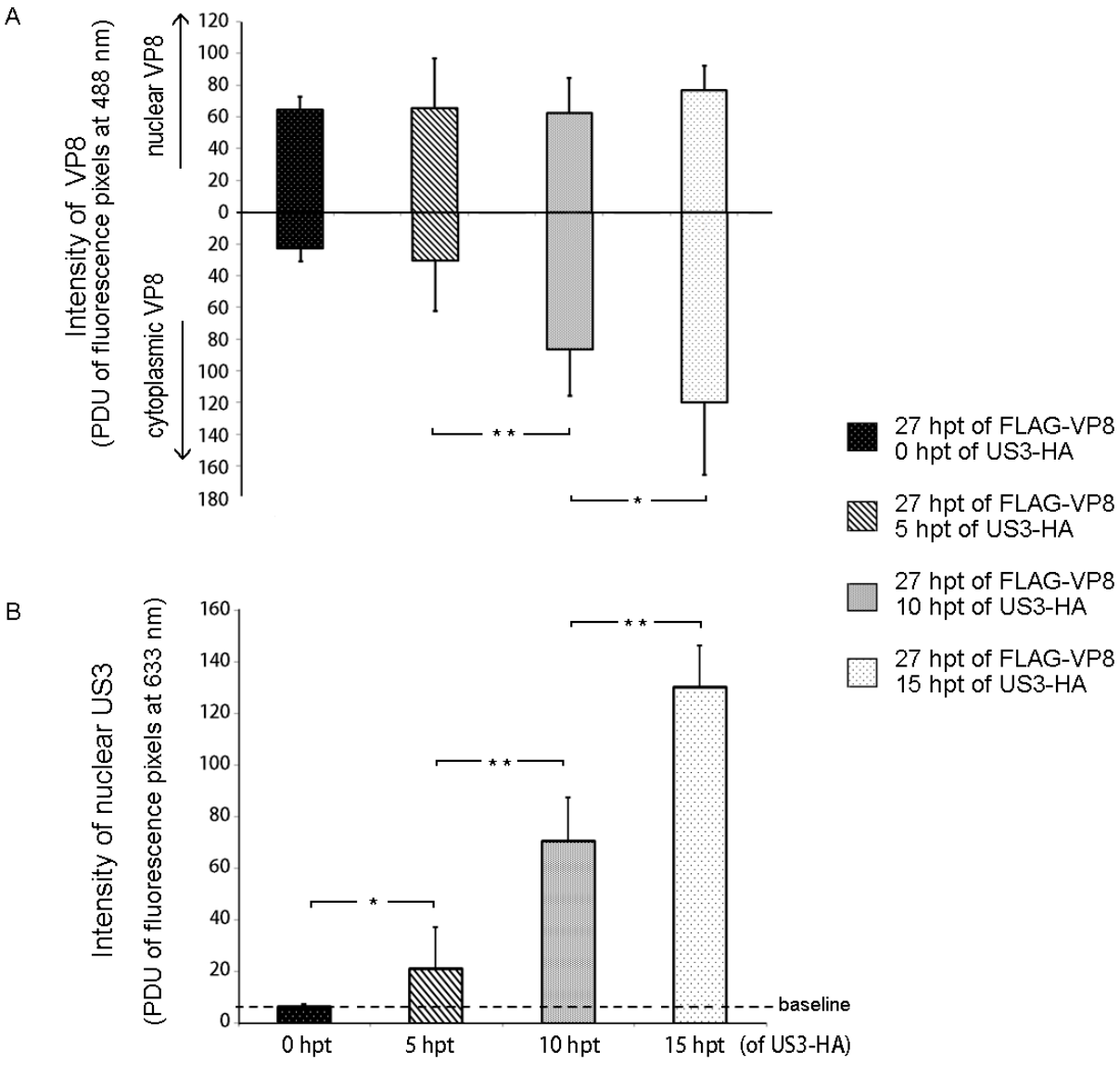

Figure 9.5 The amount of cytoplasmic FLAG-VP8 increases with the expression level of US3-HA.

(A) The intensities of cytoplasmic and nuclear VP8. EBTr cells were transfected with pFLAG-VP8 and incubated for 12 h. This allowed VP8 to be expressed and localized to the nucleus. Subsequently, cells were transfected with pUS3-HA at 12 hpi, 17 hpi, or 22 hpi after transfection with pFLAG-VP8. All samples were fixed at 27 h for immunofluorescent staining, and the cell images were analyzed with software Leica Application Suite X for protein quantification. Intensity of fluorescence pixels at wavelength of 488 nm was captured to indicate the quantity of VP8. The mean values of PDU are shown in the bar graphs. Error bars represent the standard deviations (B) The intensity of US3 in the nucleus. Intensity of fluorescence pixels at a wavelength of 633 nm was captured to indicate the quantity of US3. The statistical significance is shown as follows: *, $0.01 < P \leq 0.05$; **, $P \leq 0.01$.

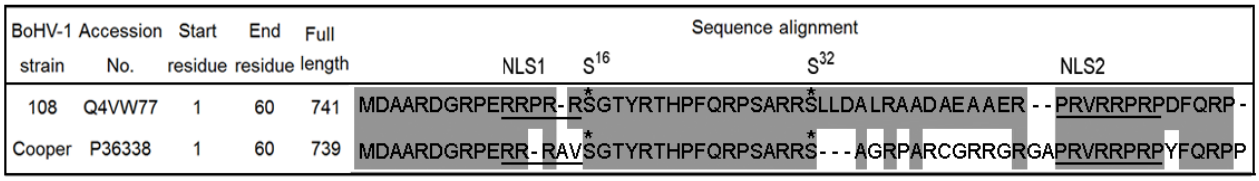

Figure 9.6 Nuclear localization signals (NLSs) and US3-phosphorylated residues in partial sequences of VP8.

Protein sequences of VP8 from strains 108 and Cooper were obtained from a protein bank, UniProKB (http://www.uniprot.org/). NLS1 and NLS2 are underlined. US3-phosphorylated residues are labeled with "*". Multi-way protein alignment was performed using a program, Clone Manager (381). Gray color indicates conserved regions and white color indicates mutations or deletions.

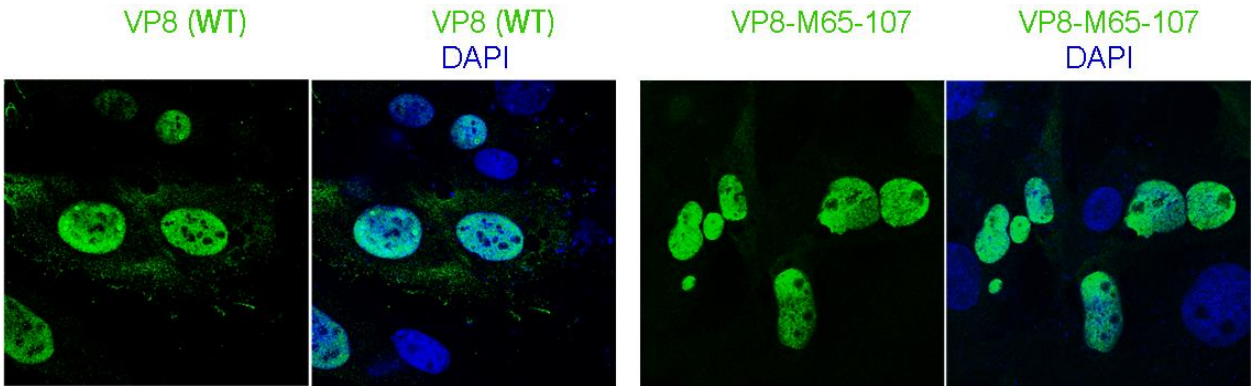

Figure 9.7 Phosphorylation through CK2 does not change the nuclear localization of VP8.

EBTr cells transfected with pFLAG-VP8 or pFLAG-VP8-M65-107 were fixed for immunofluorescent staining. VP8 proteins were labeled with polyclonal anti-VP8 antibody followed by Alexa 488-conjugated secondary antibody. The cell nucleus was stained with DAPI.

9.5.6 Nuclear export of VP8 is sensitive to leptomycin B (LMB)

To determine whether the nuclear export of VP8 during BoHV-1 infection is dependent on CRM1, a CRM1-specific inhibitor, leptomycin B (LMB), was used to treat BoHV-1 infected MDBK cells. Wild-type BoHV-1 infected cells were cultured with or without LMB (Figure 9.8). At 4 hpi VP8 was in the nucleus, while at 6 hpi the distribution of VP8 was different between the two treatments. VP8 formed perinuclear aggregates in the cell cytoplasm without LMB. In contrast, in LMB-treated cells VP8 remained in the nucleus and did not accumulate in the cytoplasm. When cells were cultured till 8 hpi without LMB the majority of the cells showed cytoplasmic accumulation of VP8, whereas cells with LMB displayed occasional cytoplasmic accumulation of VP8. These results showed that the nuclear export of VP8 was delayed by the CRM1-specific inhibitor, but not completely inhibited.

9.5.7 VP8 is co-localized with cis-Golgi cisternae proteins

The location of the Golgi cisternae was determined with antibodies specific for with two Golgi proteins, FTCD and GOLGB1. FTCD has been found to associate with the Golgi membranes of the *cis*- and medial-cisternae (382-384), and is involved in the conversion of L-histidine to L-glutamate (384, 385). GOLGB1 is a transmembrane Golgi protein (386) that mainly associates to the Golgi apparatus (387) with preference to the *cis*-Golgi (388). In mock-infected MDBK cells, FTCD and GOLBG1 showed almost identical localization in the Golgi area (Figure 9.9, top panel). This was consistent with previous findings that both proteins were in the *cis*-cisternae and the stacks of the Golgi (382-384, 387, 388). Thus, GOLGB1 was used as a marker protein to indicate the *cis*-Golgi and the Golgi stacks in BoHV-1 infected MDBK cells (Figure 9.9, lower panels). At 6 h 40 min post infection, VP8 appeared in the cytoplasm but most VP8 was localized in areas different from GOLGB1. At 7 h 20 min post infection, the majority of VP8 was co-localized with GOLGB1 in the cytoplasm. The co-localization of VP8 and GOLGB1 persisted till 8 h of infection.

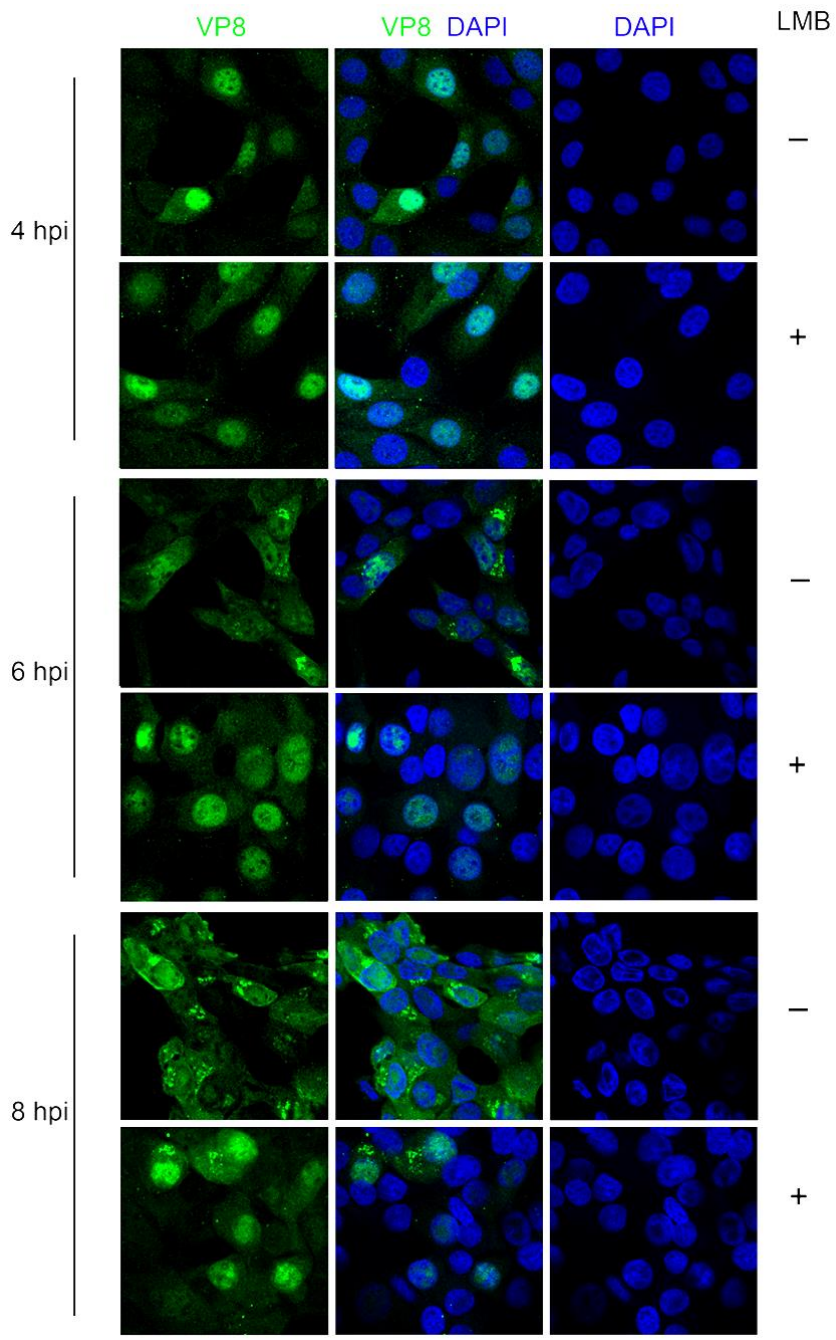

Figure 9.8 The nuclear export of VP8 is sensitive to leptomycin B (LMB). MDBK cells were infected with BoHV-1.

Culture medium supplemented with or without LMB (20 nM) was applied to cells at 1 hpi. Medium with or without LMB was renewed every 2 h. Cells were fixed at 4, 6, and 8 hpi, and stained with monoclonal anti-VP8 antibody followed by Alexa 488-conjugated secondary antibody. The cell nuclei were indicated by DAPI staining.

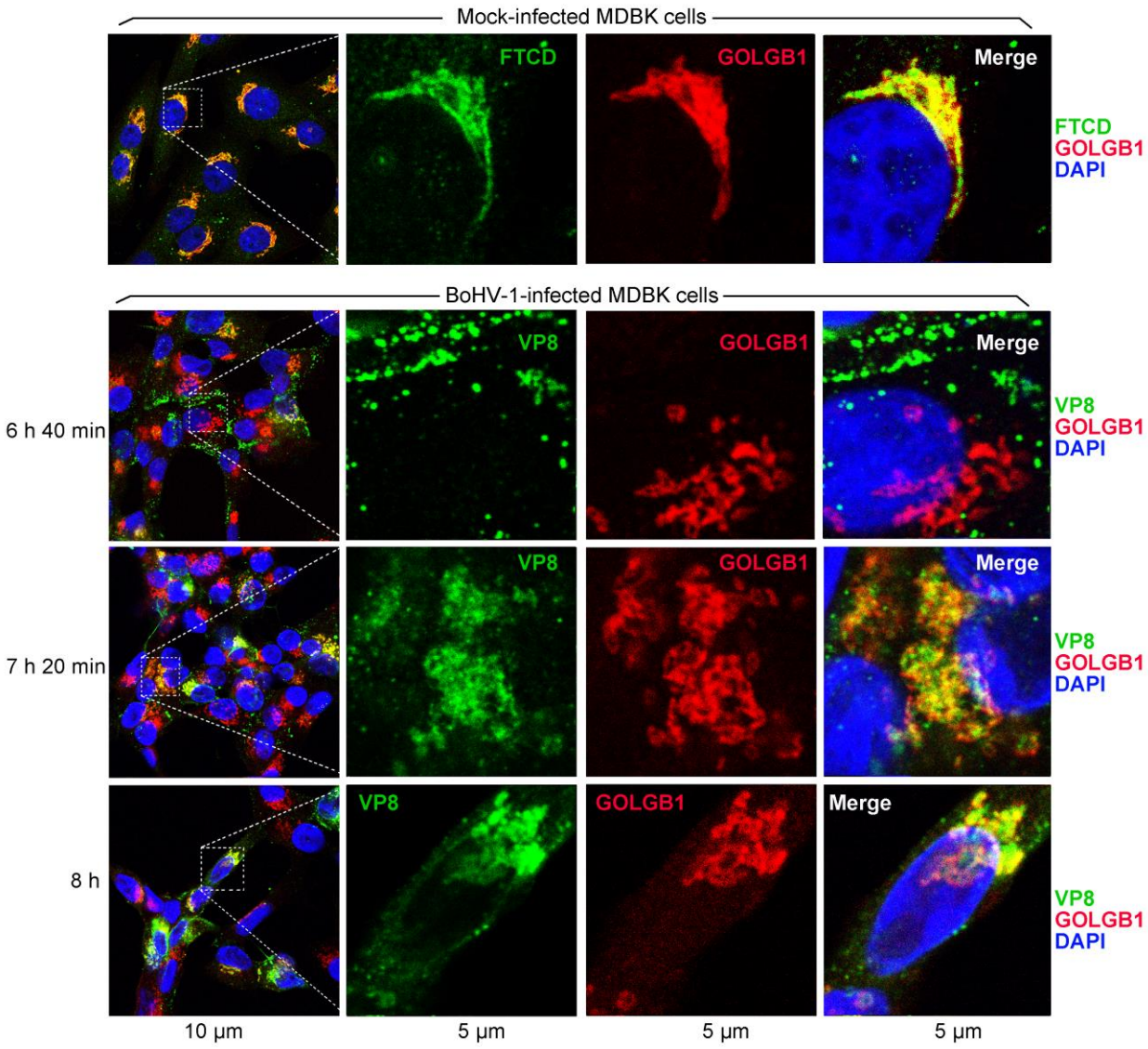

Figure 9.9 Co-localization of VP8 and a cis-Golgi protein.

MDBK cells mock-infected or infected with wild-type BoHV-1 (108 strain) were fixed for immunofluorescent staining. Mock-infected cells shown in the top panel were identified with mouse anti-FTCD and rabbit anti-GOLGB1 antibodies. BoHV-1-infected cells in the lower three panels were identified with mouse anti-VP8 and rabbit anti-GOLGB1 antibodies. Secondary antibodies were Alexa 488-conjugated goat anti-mouse IgG and Alexa 633-conjugated goat anti-rabbit IgG. The cell nucleus was stained with DAPI. The cells were observed under a confocal microscope. Selected areas of the pictures in the first row were zoomed in and shown on the right side.

During BoHV-1 infection, the Golgi apparatus went through obvious morphological changes. The *cis*-Golgi and the Golgi stacks illustrated with GOLGB1 were reshaped as capsule-like structures. VP8 gradually accumulated towards these structures. However, in mock-infected cells, the Golgi structures labeled with FTCD and GOLGB1 were multilayer sheets closely adjacent to the cell nucleus (Figure 9.9).

9.5.8 VP8 is not in the trans-Golgi network

To determine whether VP8 was associated with the *trans*-Golgi network (TGN), BFA was used to distinguish the TGN from the *cis*- and medial-Golgi. It is known that BFA causes redistribution of membranes and proteins of the Golgi cisternae, while the TGN responds differently to this compound (389-391). To confirm this effect, FTCD and GOLGB1 were used to demonstrate the Golgi cisternae, including the *cis*-Golgi network. TGOLN2, a protein that associates with the TGN to participate in the transport between the TGN and the cell surface (392), was used to indicate the TGN. The experiment was performed in Hela cells, a commonly used human cell line, because the antibody against TGOLN2 is of human origin and does not cross interact with bovine lines. In non-treated Hela cells, FTCD and TGOLN2 formed clear juxtanuclear aggregates (Figure 9.10). In BFA-treated cells, FTCD was scattered at 2 h of treatment, whereas TGOLN2 aggregations were reshaped but not dispersed. With BFA the TGOLN2 aggregates persisted till 8 h post treatment. Moreover, in cells that were co-stained with antibodies against FTCD and GOLGB1, the two *cis*-Golgi proteins were scattered by BFA at 2 h, confirming that the *cis*- and medial-Golgi but not the TGN was redistributed by BFA.

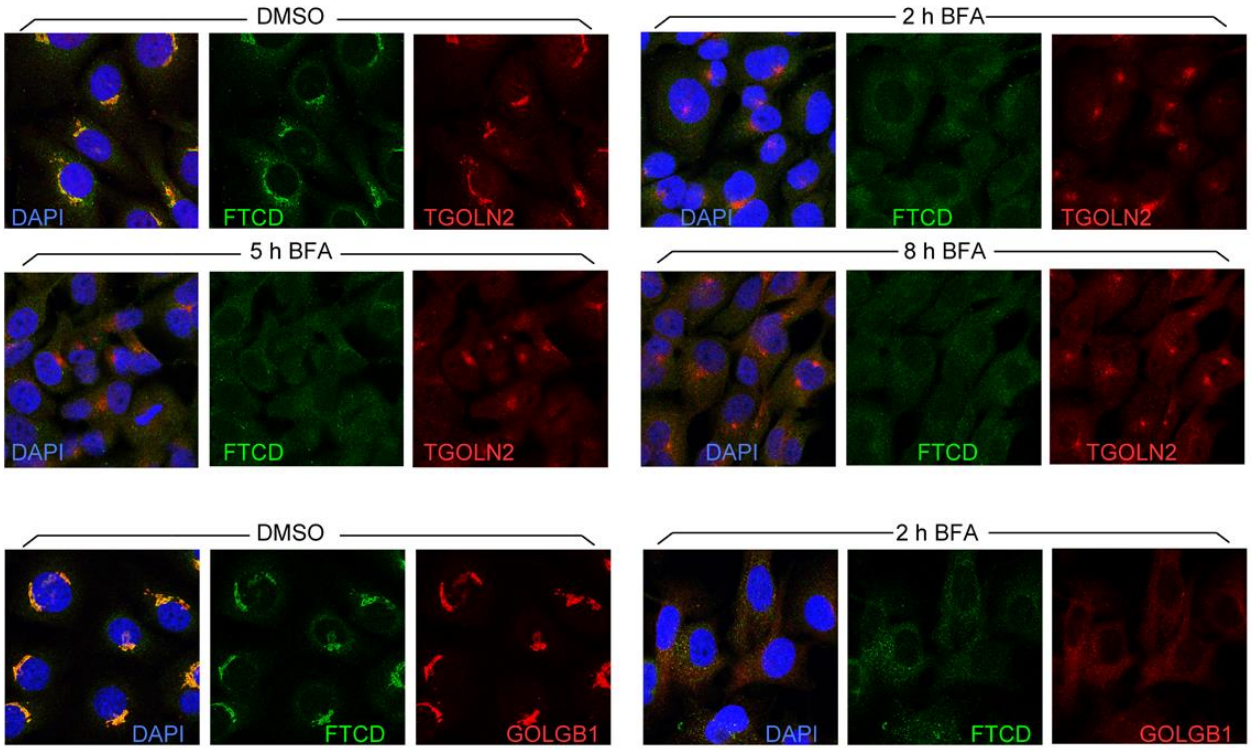

Figure 9.10 Brefeldin A (BFA) disperses the cis-Golgi proteins but not the trans-Golgi network (TGN) protein.

Hela cells were treated with BFA or DMSO. The BFA was renewed every 2 h. *Cis*-Golgi proteins FTCD and GOLGB1 were detected with mouse anti-FTCD and rabbit anti-GOLGB1 antibodies. TGN protein TGOLN2 was detected with rabbit anti-TGOLN2 antibody. Alexa 488-conjugated goat anti-mouse IgG and Alexa 633-conjugated goat anti-rabbit IgG were used as secondary antibodies. The cellular DNA was stained with DAPI.

BoHV-1-infected cells were treated with BFA to determine its impact on VP8 distribution. MDBK cells were infected with BoHV-1 followed by BFA treatment at 1 hpi. In the presence of BFA, nuclear VP8 appeared at 4 hpi. From 4 to 8 hpi the infected cells contained increasing amounts of cytoplasmic and nuclear VP8 with diffused distribution (Figure 9.11A). In the DMSO-treated cells, cytoplasmic VP8 gradually accumulated in the juxtanuclear areas from 6 to 8 hpi. The cytoplasmic distribution of VP8 in DMSO-treated cells was profoundly different from that of VP8 in BFA-treated cells. A comparable impact of BFA on the Golgi-localization of VP8 was observed in EBTr cells (data not shown). To observe the dispersal of Golgi-localized VP8, MDBK cells infected with BoHV-1-YVP8 were treated with BFA at 7 hpi when VP8 accumulated in the Golgi apparatus. The cells were observed with life-cell imaging confocal microscopy at 7 hpi for 30 min. Five minutes after BFA was applied, the amount of Golgi-localized YFP-VP8 started to decrease. The cytoplasmic VP8 aggregates were dispersed within 30 min of BFA treatment.

9.5.9 BoHV-1 virions are wrapped with electron-dense material within vesicles near the Golgi stacks

The Golgi apparatus of BoHV-1-infected MDBK cells were observed with transmission electron microscopy. At 15 hpi, numerous viral capsids were accumulated near the Golgi stacks (Figure 9.12A, B). Many were enclosed within vesicles. The capsids inside the vesicles were coated with a thick electron-dense layer, but the capsids outside the vesicles did not have this layer. Figure 9.12C shows that the membrane of a virus-containing vesicle was connected to the membrane of the Golgi cisternae, indicating that the Golgi apparatus might develop these vesicles to envelop virus. This is in agreement with the observations in Figure 9.9 that the Golgi was enlarged in BoHV-1 infected cells.

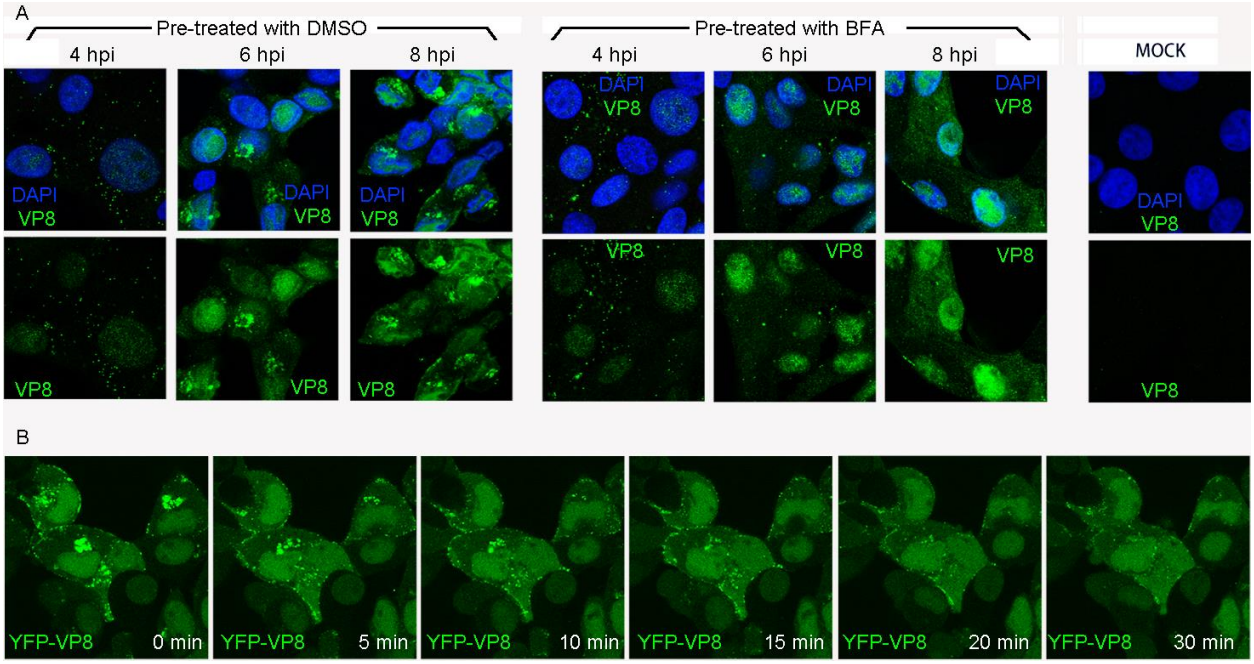

Figure 9.11 The Golgi accumulation of VP8 is sensitive to brefeldin A (BFA).

(A) MDBK cells infected with BoHV-1 were treated with BFA or DMSO at 1 hpi. Cells were fixed and stained with monoclonal anti-VP8 antibody followed by Alexa 488-conjugated secondary antibody. The cell nuclei were stained with DAPI. (B) MDBK cells infected with BoHV-1-YVP8 were treated with BFA at 7 hpi. The imaging of life cells showing YFP-VP8 was performed from 7 hpi for 30 min.

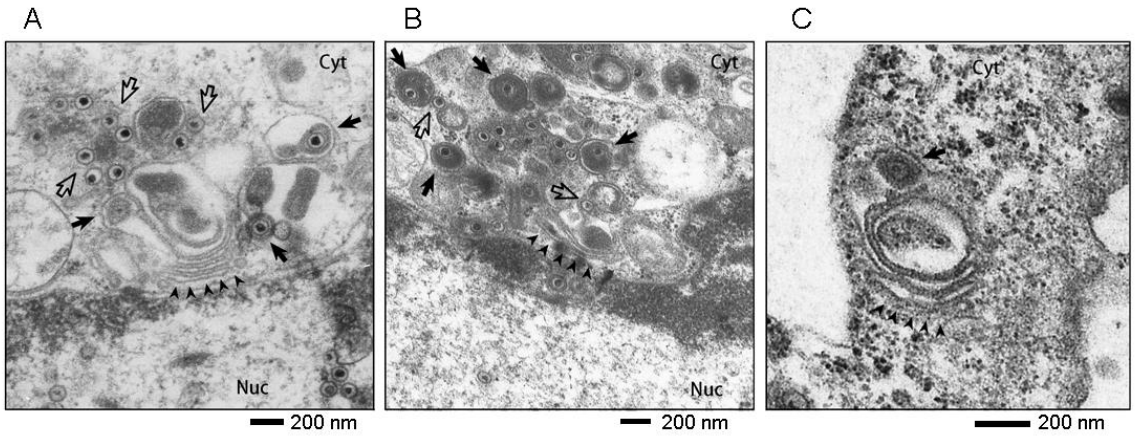

Figure 9.12 Transmission electron microscopy of BoHV-1-infected cells.

(A, B) BoHV-1 viral particles are located near the Golgi apparatus. (C) A viral particle is enveloped by membrane extended from the Golgi apparatus. MDBK cells infected with BoHV-1 (108 strain) at a MOI of 1 were harvested at 15 hpi, and observed with a Philips CM10 transmission electron microscope (Bar = 200 nm). Solid black arrow heads indicate the Golgi stacks; Solid black arrows indicate capsids wrapped with electron-dense materials and membranes. Hollow arrows indicate unwrapped capsids.

9.6 Discussion

In this study US3-mediated phosphorylation was found to activate the nuclear export of VP8 during BoHV-1 infection, suggesting that the modification status of VP8 is altered when it moves from the nucleus to the cytoplasm and, ultimately, from the Golgi into the mature virus. VP8 contains two functional NLSs on the extreme N-terminus (72) leading the protein to translocate into the nucleus early during infection. The cellular kinase CK2 is universally expressed in almost every subcellular structure; therefore, it might be available to phosphorylate VP8 inside or outside of the nucleus. However, the nuclear localization of VP8 did not require and was not affected by CK2-mediated phosphorylation (Figure 9.7). This implicates that early during infection, VP8 is effectively transported into the nucleus to promote early events of virus replication, for instance viral DNA encapsidation (375), and to redistribute ND10 (290). To perform these nuclear functions VP8 requires phosphorylation (375). Additionally, the nuclear VP8 appears to cause abnormal lipid metabolism in cells. Nuclear LDs were formed in VP8-transfected EBTr cells and COS-7 cells (Figures 9.1 and 7.2). This ability was unique to VP8 because nuclear LDs were not found in US3-transfected and YFP-transfected cells (data not shown). This indicates VP8 may alter the lipid metabolism of host cells to supply lipid for viral replication. Such peculiar lipid accumulation has been reported in human herpesvirus-8 (HHV-8) -infected cells during the lytic phase of infection (393). HHV-8 infection increases the cellular triglycerides that are stored in the cytoplasmic LDs. This has been suggested to be related to the abnormal viral requirements for lipids (393). During BoHV-1 infection, VP8 may change the cellular lipid metabolism.

Nuclear VP8 is transported to the cytoplasm at later stages of infection (Figure 9.1). The results of Figures 9.3 and 7.4 implicate that US3-mediated phosphorylation activates the nuclear export of VP8, as the majority of VP8 was in the nucleus of transfected cells if US3 was not expressed. Cytoplasmic VP8 gradually increased with the progression of US3 expression. However, the intensity of nuclear VP8 did not decrease with the increase of cytoplasmic VP8 (Figures 9.4B and 9.5). The reason might be that VP8 was constantly synthesized and imported into the nuclei of transfected cells.

During BoHV-1 infection, a regulatory system might exist to balance the activities of NLSs and NESs at the right time. Early during infection, VP8 is transported into the nucleus

suggesting that the NLSs are active and possibly are more efficient than the NESs. To move to and remain in the cytoplasm later during infection, VP8 would need to have inactive NLSs or NESs that are more effective than the NLSs. Since US3-mediated phosphorylation is essential for the cytoplasmic localization of VP8, US3 appears to be involved in regulating the balance between NLSs and NESs. Evidence supporting this is found in the amino acid sequence of VP8. US3-phosphorylated residues (S^{16} and S^{32}) and the NLSs ($P^{11}RPRR^{15}$, and $R^{48}PRVRRPRP^{54}$) are closely located in the same region of VP8 (Figure 9.6). Thus, the NLSs might be active to guide VP8 into the nucleus when VP8 is not phosphorylated by US3 at early times of infection. When the nuclear VP8 is phosphorylated by US3 the addition of phosphoryl groups on S^{16} and S^{32} may mask the binding activity of the NLSs, resulting in VP8 leaving the nucleus. In addition to inactivation of the NLSs, the nuclear export of VP8 also requires functional NESs. The NESs of VP8 might be constantly active and not impaired by US3-mediated phosphorylation. This would be in agreement with previous findings that VP8 within a transfected cell nucleus is transported to the non-transfected nucleus in an interspecies cell fusion assay (155, 156). When US3 is expressed in a cell, the NLSs are inactivated and the function of the NESs possibly will become predominant, leading to the nuclear export of VP8. The possibility remains that, in properly folded VP8, NESs could be affected or activated by US3-mediated phosphorylation. Because of the lack of a tertiary structure of VP8 it is difficult to have direct evidence. However, previous research has found that VP8 is exported from one nucleus and enters another in a fused cell in the absence of US3 (155), indicating the activity of VP8 NESs may not require US3. In addition, VP8 with NLSs deletion localizes in the cytoplasm (144, 155), supporting that inactivating NLSs by deleting the motifs or by masking the sequence through phosphorylation may result in VP8 localizing in the cytoplasm.

There are variations in the sequences of VP8 amongst different strains (Figure 9.6) and the electrophoretic mobility of US3 of the Cooper strain was higher than that of the 108 strain (Figure 9.3D). However, because the US3 target sites and NLS motifs in VP8 are conserved, this US3-regulated cellular localization of VP8 is likely to be conserved among the tested strains of BoHV-1. Consistently, the patterns of nuclear-cytoplasmic translocation of VP8 were identical in strains 108 and Cooper (Figure 9.3A and B).

When VP8 finishes its tasks in the nucleus, it is transported into the cytoplasm (Figure 9.1). This might be a recycling process of VP8 from the nucleus to the cytoplasm so as to effectively use the protein and/or allow virion incorporation. The types of NESs in VP8 have been explored in several studies. A leucine-rich peptide $L^{485}SAYLTLFVAL^{495}$ (NES1) of VP8 is a classic CRM1-dependent signal, the activity of which is sensitive to LMB (144, 155, 156). Another NES that is CRM1-independent exists in the region between residue 95 and 123 (NES2) (156). LMB treatment delayed nuclear export of this protein during BoHV-1 infection (Figure 9.8), which might be due to inhibition of NES1 by LMB. However, LMB did not completely block the cytoplasmic localization of VP8, which is consistent with the characteristic of NES2. During the late phase of infection, both NESs might be functional to ensure the nuclear export of VP8.

After leaving the nucleus, VP8 continues to the Golgi apparatus. The results from Figure 9.9 demonstrate that the cytoplasmic VP8 gradually migrated towards the Golgi and co-localized with *cis*-Golgi protein. Although the nuclear export of VP8 required US3-mediated phosphorylation, the subsequent Golgi-localization is not directly related to US3 (Figure 9.4). VP8 needs further modifications by or interactions with other viral factors in the cytoplasm to accumulate in the Golgi.

The Golgi apparatus is an important site for cytoplasmic maturation of herpesviruses. This organelle is composed of several continuous compartments, including *cis*-Golgi network (CGN), *cis*-, medial-, *trans*-cisternae, and TGN (394). They play different, yet related, roles in protein sorting, modification, transport, and secretion (395, 396). Therefore, determining the localization of VP8 in the Golgi compartments will reveal a potential function of the Golgi-localized VP8. We demonstrated co-localization of VP8 and *cis*-Golgi marker protein, proving that VP8 might be translocated to the *cis*-Golgi. We next tested whether VP8 was also localized in the TGN. BFA is a fungal antibiotic that causes rapid and dramatic disorganization of the cisternal Golgi in mammalian cells by redistributing the membrane and enzymes from the Golgi cisternae to the endoplasmic reticulum (ER) (389, 391). However, the response of TGN to BFA is dissimilar to that of the Golgi cisternae (391). This was confirmed in Hela cells in which the TGN protein TGOLN2 aggregated the juxtanuclear space when cultured with BFA, whereas the *cis*-Golgi protein FTCD was dispersed (Figure 9.10). BFA blocked the Golgi-localization of VP8

(Figure 9.11A) and disrupted the Golgi-localized VP8 (Figure 9.11B). A similar result was found in the cis-Golgi protein FTCD, but not in the TGN protein TGOLN2, indicating VP8 may be associated with the cisternal Golgi rather than the TGN.

Herpesvirus particles obtain their envelopes and are delivered towards the cell membrane through the TGN (397, 398). It is unlikely that VP8 is involved in the process of envelopment or viral egress. The major purpose of VP8 targeting to the Golgi apparatus might be packaging into virus to be released into newly infected cells to initiate the next viral life cycle. The electron microscopy results showed that many vesicles were formed near the Golgi stacks and some vesicle membrane was connected with Golgi stacks. Viral capsids were wrapped with electron-dense materials within these vesicles, possibly to obtain a tegument layer. Similarly, in the immunofluorescently stained cells the Golgi cisternae became small cystic structures containing VP8 during BoHV-1 infection (Figure 9.9). These findings support the hypothesis that VP8 is incorporated into BoHV-1 particles in these Golgi vesicles.

9.7 Acknowledgements

This research was supported by grant 90887-2010 RGPIN from the Natural Sciences and Engineering Research Council of Canada. The author Kuan Zhang was supported by a scholarship from the China Scholarship Council. The Cooper-strain BoHV-1-containing bacterial artificial chromosome (BAC) system and GS1783 cell line used in this system was a kind gift from Dr. Benedikt Kaufer in Berlin, Germany.

CHAPTER 10

10 GENERAL CONCLUSIONS AND DISCUSSION

10.1 General conclusions

Early during infection of BoHV-1, VP8 localizes in the cell nucleus and is phosphorylated by a cellular kinase CK2. CK2 phosphorylates VP8 at multiple residues, including T^{65}, S^{66}, S^{79}, S^{80}, S^{82}, S^{88}, T^{107}, S^{137}, S^{221}, S^{240}, and S^{679}. The N-terminal residues (T^{65}, S^{66}, S^{79}, S^{80}, S^{82}, S^{88}, T^{107}) are essential for VP8 phosphorylation mediated by CK2. This phosphorylation does not change the cellular localization of VP8. CK2-phosphorylated VP8 redistributes PML foci in VP8-transfected cells, suggesting a role of VP8 in PML-related antiviral defences. Moreover, CK2-phosphorylated VP8 promotes viral DNA encapsidation in BoHV-1-infected cell nucleus. However, blocking phosphorylation of VP8 does not abolish the egress of BoHV-1. BoHV-1-YmVP8 virions with and without DNA cores are released into extracellular environment. Before or during the nuclear egress of BoHV-1, the virus incorporates a small amount of VP8.

At late stages of BoHV-1 infection, nuclear VP8 is phosphorylated by US3 at two residues, S^{16} and S^{32}. Phosphorylation at S^{16} is essential for the subsequent phosphorylation at S^{32}. When nuclear VP8 is phosphorylated by US3, it is exported into the cytoplasm. Phosphorylation at S^{16} and S^{32} may inhibit the activity of NLSs, and thus affect the cellular localization of VP8. In the cytoplasm VP8 may be modified by or interact with other viral factors to accumulate in the *cis*-Golgi, but not in the TGN. VP8 is then abundantly incorporated into the virus in the Golgi apparatus. When the mature virus is released into the extracellular environment, VP8 that is incorporated on the virus is not phosphorylated, suggesting that a de-phosphorylation process takes place during and/or after the incorporation of VP8 into BoHV-1 virus. In addition, VP8 causes lipid accumulation in the nucleus of VP8-transfected cells, forming nuclear LDs, indicating that VP8 may alter cellular lipid metabolisms to supply lipid for viral replication.

10.2 General discussion

VP8 is in a phosphorylated form in BoHV-1-infected cells but not in BoHV-1 virions, implicating that phosphorylation regulates the functions of VP8 in infected cells and that a mechanism for dephosphorylating VP8 is needed. Having confirmed that VP8 is phosphorylated through a viral kinase US3 and a cellular kinase CK2 during BoHV-1 infection, we identified the critical residues for phosphorylation in VP8, aiming to block phosphorylation of VP8 and to identify the functional significance of this modification.

US3 and CK2 phosphorylate VP8 by recognizing distinct motifs (15). VP8 has two functional consensus sequences for US3 ($R^{14}RSGT^{18}$ and $R^{30}RSLL^{34}$). Phosphorylation at S^{16}, the primary target residue, is essential for the subsequent phosphorylation at S^{32}. Phosphorylation of VP8 mediated by CK2 is more complicated than by US3. CK2 phosphorylates multiple residues of VP8. A cluster of N-terminal motifs for CK2 is critical for phosphorylation at other sites in VP8. This suggests that CK2 may phosphorylate VP8 in a sequential manner. CK2 initially phosphorylates VP8 in the N-terminal region, and subsequently in the middle and the C-terminal regions. CK2 has different preferences towards the target residues, T^{107} being the most frequently phosphorylated site. Coordinated phosphorylation of multiple residues in a single protein is described in other kinases. For instance, phosphorylation of phospholamban (PLB) at S^{16} by PKA is obligatory to phosphorylation at T^{17} by calmodulin-dependent kinase 2 (CAMK2) (399). The conformational changes caused by primary phosphorylation are required for activating the subsequent phosphorylation (400). Such phosphorylation pattern might also apply to US3- and CK2-mediated phosphorylation in VP8.

VP8 is in the cell nucleus early during infection with BoHV-1. VP8 does not need to be phosphorylated to translocate into the nucleus. However, it requires phosphorylation to perform certain nuclear functions. Phosphorylated VP8 promotes the viral genome to be incorporated into capsids in the nucleus. When cells are infected with a mutant virus expressing non-phosphorylated VP8, viral DNA encapsidation is less efficient in comparison with wild-type virus. Although the non-phosphorylated VP8 also localizes in the nucleus, it has a reduced capacity to promote the packaging of the viral genome. A model for genome encapsidation has been suggested for HHV-1, which requires cleavage of the concatemeric replicated viral genome prior to incorporation into capsids (87, 88), and stabilization of the DNA-contained capsids to

retain the viral genome (7). Although the actual mechanism of cleaving the genome concatemer has yet to be described, some viral proteins has been found to play roles in this process. The alkaline nuclease U_L12 might be one of the enzymes that cleave the viral DNA concatemer, because an *in vitro* study has found that U_L12 digests HHV-1 DNA replication intermediates into heterogeneous fragments in size from 10 to 50 kb (87). U_L12 specifically targets the cleavage sites through recognizing special DNA structural modifications instead of particular sequences (87). Deleting U_L12 severely reduces the virus production of HHV-1(401). $U_L12.5$ is a capsid-associated nuclease translated from an internal start codon of the *ul12* gene (88). $U_L12.5$ may contribute to processing the viral genomes by its nuclease activity when they are incorporated into capsids (88). Although the actual role of $U_L12.5$ has yet to be identified, it cannot substitute the biochemical functions of U_L12, and vice versa (88). The cleaved viral DNA is inserted through a portal into a capsid shell (89). This insertion process requires collaboration between several viral proteins (6, 7, 90, 91) and recognition of two unique signal elements in the viral genome (85, 86). In order to retain the incorporated DNA, capsids are further stabilized by viral proteins U_L17 and U_L25 (7). It is possible that BoHV-1 uses a DNA encapsidation strategy similar to HHV-1 because some HHV-1 proteins are conserved in other alphaherpesviruses. For example, U_L12 has the similar nuclease activity in HHV-1 and HHV-5 (87). Capsid portal protein U_L6 and DNA stabilizing protein U_L25 are conserved between HHV-1 and BoHV-1 (68). More proteins contributing to DNA encapsidation are yet to be identified. The finding that VP8 is required for the optimal incorporation of the BoHV-1 genome suggests that the protein may play a role in the DNA encapsidation.

Nuclear localization of VP8 does not require the protein to be phosphorylated by CK2 or US3, and is not blocked by CK2-dependent phosphorylation, providing VP8 the opportunity to efficiently enter the cell nucleus. Nuclear VP8 modulates cellular factors presumably to create a suitable environment for BoHV-1 infection. Transfected VP8 disturbs the balance of cellular lipid metabolism, causing lipid to accumulate in the cell nucleus. It is known that infection with herpesvirus, such as HHV-5 and HHV-8, causes disorders of the cellular lipid metabolism (402, 403), (393, 404). The cellular cholesterol is significantly increased in HHV-5-infected cells when compared to mock-infected cells (402). Given the fact that virus delivery (405) and envelopment (402) are all dependent on cellular lipids, there is a high demand for lipid in productively

infected cells. VP8 causes lipid accumulation in host cells, presumably to supply lipid for viral production. When VP8 is accumulated in the nucleus of a transfected cell, LDs are gradually developed in the nucleus. VP8 intensely coats to the surface of the LDs forming bright ring-like structures. The development of nuclear LDs is not restricted by abolishing phosphorylation of VP8 indicating that the regulation of the lipid metabolism does not require phosphorylation.

Another cellular factor affected by VP8 is PML foci. PML of ND10s forms punctuated nuclear foci in a non-mitotic cell (250). The normal distributing pattern of PML is interrupted by phosphorylated VP8 in transiently transfected cells. Punctate PML foci are replaced with larger PML aggregates on the surface of LDs, where VP8 is accumulated. When BoHV-1 enters host cells, the virus releases many tegument proteins that are important for initiating viral replication. VP8 is dissociated from incoming viruses and has the potential to redistribute PML. Although VP8 does not directly degrade PML, it might interrupt the anti-viral function of PML by redistributing it. According to studies on adenovirus 5, viral protein E4ORF3 causes PML and SP100 foci to form strips that are separated from viral DNA replication compartments in order for the viral DNA to effectively replicate (406-408). This suggests that the antiviral function of ND10 can be affected by redistributing the protein components of ND10. In the initial stages of BoHV-1 infection, the incoming viral DNA might be restricted by ND10 in the nucleus, in a pattern similar to that of other alphaherpesviruses (306). Before degradation of SUMOylated PML by ICP0 synthesized at the immediate early stage (298), incoming VP8 might repress the antiviral activity of PML by redistributing PML. Evidence that the virus uses tegument proteins to interfere with ND10 antiviral functions has been described for HHV-5 infection. Tegument protein pp71 disrupts the ATRX-DAXX complex in ND10 to increase the expression of immediately early proteins (242, 329). This process is facilitated by another tegument protein U_L35 which redistributes ND10 (235, 236). Implicated by the fact that the pattern of PML redistributed by VP8 is similar to the pattern of ND10 formed by U_L35 (236), VP8 might perform a comparable function as U_L35 to interrupt ND10 at the initial stage of BoHV-1 infection.

At late stages of BoHV-1 infection, VP8 is transported from the nucleus to the cytoplasm (25, 154). Phosphorylation by US3 is necessary and sufficient to activate the nuclear export of VP8. When VP8 is co-expressed with US3 it appears in the cytoplasm; whilst when US3 is

deleted in BoHV-1 the nuclear VP8 is not transported in to the cytoplasm of cells infected with this virus. The nuclear export of VP8 is also abolished by mutating the essential residue (S^{16}) for US3-mediated phosphorylation, confirming that the nuclear export of VP8 requires the protein to be phosphorylated by US3.

The US3-regulated localization of VP8 is explained by the adjacent locations of US3-target residues and NLSs in the extreme N-terminus of VP8. Phosphorylation at S^{16} and S^{32} may inactivate the nearby NLSs by occupying the space for protein binding. When the NLSs are masked by the nearby phosphoryl groups, the effect of NESs might be revealed, and VP8 is consequently exported from the nucleus into the cytoplasm. It is less likely that NES is activated by US3 for at least two reasons. First, US3 motifs are not close to any of the identified NESs, and the NESs are independent of each other (155, 156). Second, NESs might be active when US3 is absent. Previous research on NESs in VP8 has been performed in transiently transfected cells that do not have US3 (155, 156). The results have shown that VP8 is able to be exported from one cell nucleus and subsequently enter into another cell nucleus (155, 156).

Protein phosphorylation not only inactivates the nuclear localization of a substrate. In some situations, phosphorylation works in an opposite way. For instance, in HHV-1 infection, US3 promotes the nuclear localization of VP13/14 by phosphorylating the protein (143). VP13/14 contains a NLS and thus it predominantly localizes in the nuclei of HHV-1-infected cells. US3-phosphorylated VP13/14 is mainly localized in the nucleoplasm, while the non-phosphorylated VP13/14 is mostly accumulated at the nuclear membrane (142). The reason might be that the NLS of VP13/14 is enhanced by phosphorylation at a nearby residue mediated through US3 (142).

US3 may not contribute to the nuclear function of VP8 because US3-phosphorylated VP8 is exported to the cytoplasm and is unavailable to regulate nuclear events. However, CK2 might play a key role in regulating the nuclear activities of VP8 since CK2 phosphorylation does not disturb the nuclear localization of VP8. As a universally distributed cellular kinase CK2 is available to phosphorylate VP8 without changing its cellular localization as soon as VP8 enters or is synthesized in a cell.

In the cytoplasm VP8 is accumulated in the Golgi apparatus. The Golgi accumulation of VP8 is not directly regulated by US3, supported by the findings that VP8 is not in the Golgi of

cells co-expressing US3 and VP8. However, it only takes place in the context of BoHV-1 infection, suggesting that a virus-related modification or protein interaction is required for cytoplasmic VP8 to target the Golgi apparatus. VP8 is mainly in the *cis*-Golgi and does not spread to the TGN. Given the fact that the TGN is resistant and the *cis*-Golgi is sensitive to a Golgi-redistributing drug, BFA (391), the response of Golgi-localized VP8 to BFA would reflect the localization of VP8 in the Golgi compartments. Golgi-localized VP8 was quickly dispersed by BFA, which is a common reaction of *cis*-Golgi proteins (391). VP8 is less likely to participate in viral envelopment and transport that mainly take places in the TGN. Instead, VP8 uses the *cis*-Golgi as the major site to be incorporated into progeny virus. When cytoplasmic translocation of VP8 is blocked by mutating phosphorylation sites VP8 is not able to localize to the Golgi, thus virus-incorporated VP8 is considerably reduced. The small amount of virus-associated VP8 implies that the incorporation of VP8 may also take place before or during the viral capsids egress from the nucleus. Packaging large amounts of VP8 into virions may have significance in remodeling PML during the next round of infection.

Overall, this research demonstrated that, in the life cycle of BoHV-1, VP8 performs several major functions that are correlated with its subcellular localization and are regulated by phosphorylation (Figure 10.1). During a productive infection of BoHV-1, a large amount of VP8 is synthesized in infected cells. The *de novo* synthesized VP8 enters the cell nucleus and is phosphorylated by CK2 during this time. In the nucleus, CK2-phosphorylated VP8 is involved in the incorporation of the viral genome into the capsids. The nuclear VP8 also alters the cellular lipid metabolism. Presumably when the majority of DNA encapsidation is completed, the nuclear VP8 is phosphorylated by US3, which subsequently triggers the nuclear-to-cytoplasmic transport of VP8. In the cytoplasm, with a thus far unidentified virus-induced modification or protein interaction, VP8 is accumulated into the *cis*-Golgi apparatus, where it is packaged into the viral particles that are also localized in the Golgi. There might be a de-phosphorylation process for VP8 because the virion VP8 is not phosphorylated. After incorporation into the progeny virus, VP8 leaves the host cell inside the virions when released from the cell. The virion VP8 will become incoming VP8 during subsequent infection, and has the potential to redistribute PML.

During viral infection, phosphorylation regulates biological functions of viral proteins through different dynamic patterns, and leads to diverse biological outcomes. Immediate protein

63 (IE63) of HHV-3 is predominantly localized in the nucleus during productive infection, and is in the cytoplasm during latency (409). The nuclear and cytoplasmic localization of IE63 is related to the balance between CDK1-dependent phosphorylation and CK1/CK2-dependent phosphorylation (409, 410). Blocking CK1/CK2-mediated phosphorylation induces more IE63 to localize in the cytoplasm (409, 411). However, abolishing CDK1-mediated phosphorylation increases the nuclear localization of IE63 (410). IE63 negatively regulates viral DNA replication during HHV-3 infection and it has been known that the contribution of IE63 to HHV-3 pathogenesis is dependent on the differentiated human cell types (412, 413). It might partially because the enzyme systems are different between those cell types. For example, IE63 is phosphorylated by CDK1, a universally expressed kinase, at T^{222} and S^{224} (410). The same residues are also phosphorylated by CDK5, a kinase that is only active in neural cells (410). Consequently, phosphorylation of IE63, contributed by different kinases in two types of cells, may lead to dissimilar biological impacts. Phosphorylation is important for many other herpesvirus proteins to regulate protein activity, including VP13/14 of HHV-1 which uses phosphorylation to regulate nuclear localization (142), U_L12 of HHV-1 which requires phosphorylation to obtain nuclease activity (414), and ORF57 of HHV-8 which needs phosphorylation to interact with heterogeneous nuclear ribonucleoprotein K (hnRNP K), a cellular protein involved in gene expression (415).

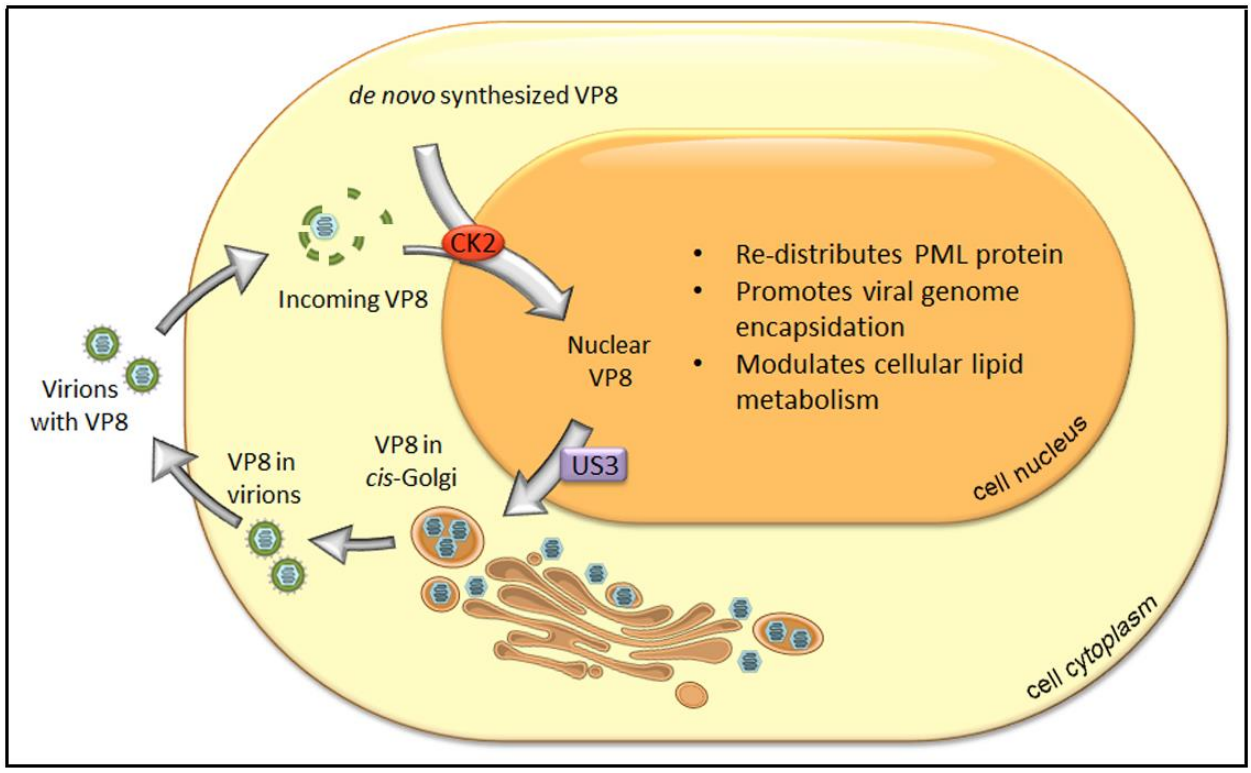

Figure 10.1 Summary of the translocation of VP8 during the infection of BoHV-1.

The nucleus, cytoplasm and Golgi apparatus of a host cell are illustrated. Gray arrows indicate the translocation directions of VP8. BoHV-1 virion enters the host cell and releases VP8 which is the incoming VP8. During the infection, VP8 is *de novo* synthesized and is translocated into the nucleus. When VP8 comes across the cellular kinase CK2 it becomes phosphorylated. The nuclear localization, and possibly the CK2-dependent phosphorylation, also happens to the incoming VP8. In the nucleus, VP8 is capable of redistributing PML, changing the cellular lipid metabolism, and promoting the viral DNA encapsidation. When nuclear VP8 is phosphorylated by a viral kinase US3 the nuclear-to-cytoplasmic translocation of VP8 is activated. In the cytoplasm, VP8 is accumulated in the *cis*-Golgi, where it is packaged into the progeny virus of BoHV-1. These viruses, with VP8 incorporated, are released into the extracellular environment when they are mature.

10.3 Future directions

In the nucleus of BoHV-1-infected cells, VP8 promotes viral DNA to incorporate into capsids, and it requires VP8 to be phosphorylated. Newly synthesized viral DNA and capsids require further processing prior to encapsidation (87, 88, 90). Disrupting any of the processing steps will reduce the efficacy of DNA encapsidation. Omitting VP8 phosphorylation increases empty nuclear capsids and reduces virus titer, indicating an important role of phosphorylated VP8 in viral DNA encapsidation. VP8 is possibly involved in cleaving the genome concatemer by promoting the activity of viral nucleases, or in modifying the viral capsids by interacting with capsids proteins. In future research, the impact of VP8 in the cleavage of viral DNA concatemer will be determined by observing the impact of VP8 on the efficacy of BoHV-1 nuclease. To identify the impact of VP8 in BoHV-1 capsids maturation, A, B, and C capsids will be analyzed with and without the presence of VP8.

CK2-phosphorylated VP8 redistributes PML foci in VP8-transfected cells. PML protein gradually accumulates to the surface of nuclear LD that is coated with VP8. However, non-phosphorylated VP8 does not cause such accumulation of PML protein. Several herpesvirus tegument proteins play important roles in disrupting or redistributing ND10 proteins. For example, in HHV-4-infected cells, ATRX-DAXX complex is disrupted by BNRF-1 (241). Pp71 of HHV-5 degrades DAXX (104). U_L35 of HHV-5 redistributes ND10 foci, containing PML, SP100, DAXX, and ATRX, in transfected cells, and enhances the activity of pp71 to degrade DAXX (104, 237). The unique PML pattern in VP8-transfected cells is similar to that in U_L35-transfected cells (235, 236). This supports the possibility that BoHV-1 VP8 contributes to disrupting ND10 components. Thus, future research may firstly focus on identifying the impact of VP8 in ND10 foci-contained proteins. PML could be directly redistributed by VP8, or be indirectly reorganized by another ND10 protein which directly contacts with VP8. Secondly, since VP8 is abundantly released into BoHV-1-infected cells at pre-immediate early phase, it is likely that incoming VP8 is involved in counteracting ND10. Identifying whether incoming VP8 molecules target ND10 foci will provide evidence for the role of incoming VP8 in neutralizing ND10-dependent anti-viral defences.

At late stage of BoHV-1 infection when VP8 is phosphorylated by US3, VP8 is translocated from the nucleus to the cytoplasm. Because US3-dependent phosphorylation

residues are near the NLSs of VP8, the activity of NLSs might be interfered with by phosphorylation. A tertiary structure of VP8 is needed to confirm this mechanism in the future. Moreover, US3 does not directly transport VP8 through the nuclear membrane, because US3 remains in the nucleus when VP8 is exported to the cytoplasm. This indicates that US3-phosphorylated VP8 may be subsequently involved in NES-dependent protein-protein interactions to transport through the nuclear membrane. Besides of the two known NESs of VP8, more NES has been suggested to exist in the protein (144, 155, 156). Future research might focus on identifying functional NESs of VP8 and NES-dependent signal pathways.

After exporting from the nucleus, VP8 is transported into the *cis*-Golgi apparatus in the cytoplasm of BoHV-1-infected cells. However, VP8 is scattered in the cytoplasm in VP8 and US3-cotransfected cells, indicating that other viral factors are involved in translocating cytoplasmic VP8 into the Golgi. Future study will identify the viral factors that mediate the Golgi-localization of VP8. A protein localizes to the Golgi apparatus either through Golgi localization signals (416) or though interacting with another Golgi-localized proteins (382). Thus, after identification of the viral factor that mediates the Golgi-localization of VP8, research will be set out to answer whether a Golgi localization signal of VP8 is activated by the factor or VP8 is transported to the Golgi by interacting with the factor.

A mutant BoHV-1 expressing non-phosphorylated VP8 has a reduced titer in comparison with wild-type virus, because VP8 needs US3- and CK2-mediated phosphorylation to change cellular localization and to perform proper functions. A previous finding shows that VP8-deleted virus does not replicate in cattle, and thus it is not suitable to be an attenuated vaccine candidate (64). As non-phosphorylated VP8 only omits phosphorylation-related functions, the mutant virus replicates better than ΔU_L47-BoHV-1 in tissue culture. This indicates that the replication capacity is partially restored in the mutant virus by expressing non-phosphorylated VP8. In future research, the replication capacity and the virulence of this mutant BoHV-1 will be tested in host animals. The virulence and replication capacity can be controlled by restoring some of the mutated phosphorylation residues in VP8 according to the needs of animal research. The mutant BoHV-1 will potentially contribute to vaccine development against BoHV-1 infection.

REFERENCES

1. **Jones C, Chowdhury S.** 2010. Bovine herpesvirus type 1 (BHV-1) is an important cofactor in the bovine respiratory disease complex. Vet Clin North Am Food Anim Pract **26:**303-321.
2. **Ellis JA.** 2009. Update on viral pathogenesis in BRD. Anim Health Res Rev **10:**149-153.
3. **Favoreel HW, Van Minnebruggen G, Adriaensen D, Nauwynck HJ.** 2005. Cytoskeletal rearrangements and cell extensions induced by the US3 kinase of an alphaherpesvirus are associated with enhanced spread. Proc Natl Acad Sci U S A **102:**8990-8995.
4. **Jacob T, Van den Broeke C, Van Waesberghe C, Van Troys L, Favoreel HW.** 2015. Pseudorabies virus US3 triggers RhoA phosphorylation to reorganize the actin cytoskeleton. J Gen Virol **96:**2328-2335.
5. **Mossman KL, Sherburne R, Lavery C, Duncan J, Smiley JR.** 2000. Evidence that herpes simplex virus VP16 is required for viral egress downstream of the initial envelopment event. J Virol **74:**6287-6299.
6. **Albright BS, Kosinski A, Szczepaniak R, Cook EA, Stow ND, Conway JF, Weller SK.** 2015. The putative herpes simplex virus 1 chaperone protein UL32 modulates disulfide bond formation during infection. J Virol **89:**443-453.
7. **Cockrell SK, Huffman JB, Toropova K, Conway JF, Homa FL.** 2011. Residues of the UL25 protein of herpes simplex virus that are required for its stable interaction with capsids. J Virol **85:**4875-4887.
8. **Ohta A, Yamauchi Y, Muto Y, Kimura H, Nishiyama Y.** 2011. Herpes simplex virus type 1 UL14 tegument protein regulates intracellular compartmentalization of major tegument protein VP16. Virol J **8:**365.
9. **Bigalke JM, Heuser T, Nicastro D, Heldwein EE.** 2014. Membrane deformation and scission by the HSV-1 nuclear egress complex. Nat Commun **5:**4131.
10. **Funk C, Ott M, Raschbichler V, Nagel CH, Binz A, Sodeik B, Bauerfeind R, Bailer SM.** 2015. The Herpes Simplex Virus Protein pUL31 Escorts Nucleocapsids to Sites of

Nuclear Egress, a Process Coordinated by Its N-Terminal Domain. PLoS Pathog **11:**e1004957.

11. **Bigalke JM, Heldwein EE.** 2015. Structural basis of membrane budding by the nuclear egress complex of herpesviruses. Embo j **34:**2921-2936.
12. **Mou F, Wills E, Baines JD.** 2009. Phosphorylation of the U(L)31 protein of herpes simplex virus 1 by the U(S)3-encoded kinase regulates localization of the nuclear envelopment complex and egress of nucleocapsids. J Virol **83:**5181-5191.
13. **Shindo K, Kato A, Koyanagi N, Sagara H, Arii J, Kawaguchi Y.** 2015. Characterization of a Herpes Simplex Virus 1 (HSV-1) Chimera in Which the Us3 Protein Kinase Gene Is Replaced with the HSV-2 Us3 Gene. J Virol **90:**457-473.
14. **Meredith DM, Lindsay JA, Halliburton IW, Whittaker GR.** 1991. Post-translational modification of the tegument proteins (VP13 and VP14) of herpes simplex virus type 1 by glycosylation and phosphorylation. J Gen Virol **72:**2771-2775.
15. **Labiuk SL, Babiuk LA, van Drunen Littel-van den Hurk S.** 2009. Major tegument protein VP8 of bovine herpesvirus 1 is phosphorylated by viral US3 and cellular CK2 protein kinases. J Gen Virol **90:**2829-2839.
16. **Steukers L, Vandekerckhove AP, Van den Broeck W, Glorieux S, Nauwynck HJ.** 2011. Comparative analysis of replication characteristics of BoHV-1 subtypes in bovine respiratory and genital mucosa explants: a phylogenetic enlightenment. Vet Res **42:**33-33.
17. **Wentink GH, van Oirschot JT, Verhoeff J.** 1993. Risk of infection with bovine herpes virus 1 (BHV1): a review. Vet Q **15:**30-33.
18. **Muylkens B, Thiry J, Kirten P, Schynts F, Thiry E.** 2007. Bovine herpesvirus 1 infection and infectious bovine rhinotracheitis. Vet Res **38:**181-209.
19. **Fulton RW, d'Offay JM, Dubovi EJ, Eberle R.** 2016. Bovine herpesvirus-1: Genetic diversity of field strains from cattle with respiratory disease, genital, fetal disease and systemic neonatal disease and their relationship to vaccine strains. Virus Res **223:**115-121.
20. **Xu F, Lee FK, Morrow RA, Sternberg MR, Luther KE, Dubin G, Markowitz LE.** 2007. Seroprevalence of herpes simplex virus type 1 in children in the United States. J Pediatrics **151:**374-377.

21. **Mertz GJ, Benedetti J, Ashley R, Selke SA, Corey L.** 1992. Risk factors for the sexual transmission of genital herpes. Annals of Internal Medicine **116:**197-202.
22. **Bernstein DI, Bellamy AR, Hook III EW, Levin MJ, Wald A, Ewell MG, Wolff PA, Deal CD, Heineman TC, Dubin G.** 2012. Epidemiology, clinical presentation, and antibody response to primary infection with herpes simplex virus type 1 and type 2 in young women. Clinical Infectious Diseases **56:**344-351.
23. **Jones C, Chowdhury S.** 2007. A review of the biology of bovine herpesvirus type 1 (BHV-1), its role as a cofactor in the bovine respiratory disease complex and development of improved vaccines. Animal Health Research Review **8:**187-205.
24. **Donovan T.** 2013. Functional characterization of the US3 serine/theronine kinase during BHV-1 infection. Master of Science. University of Saskatchewan.
25. **van Drunen Littel-van den Hurk S, Garzon S, van den Hurk JV, Babiuk LA, Tijssen P.** 1995. The role of the major tegument protein VP8 of bovine herpesvirus-1 in infection and immunity. Virology **206:**413-425.
26. **Greig AS, Bannister GL, Mitchell D, Barker CA.** 1958. Cultivation In Tissue Culture Of An Infectious Agent From Coital Exanthema Of Cattle. A Preliminary Report. Can J Comp Med Vet Sci **22:**119-122.
27. **van Oirschot JT.** 1995. Bovine herpesvirus 1 in semen of bulls and the risk of transmission: a brief review. Vet Q **17:**29-33.
28. **van Drunen Littel-van den Hurk S.** 2006. Rationale and perspectives on the success of vaccination against bovine herpesvirus-1. Vet Microbiol **113:**275-282.
29. **MADIN S.** 1956. Isolation of the Infectious Bovine Rhinotracheitis Virus. Science **124:**721-722.
30. **Castrucci G, Osburn BI, Frigeri F, Ferrari M, Salvatori D, Lo Dico M, Barreca F.** 2000. The use of immunomodulators in the control of infectious bovine rhinotracheitis. Comp Immunol Microbiol Infect Dis **23:**163-173.
31. **Taylor JD, Fulton RW, Lehenbauer TW, Step DL, Confer AW.** 2010. The epidemiology of bovine respiratory disease: What is the evidence for predisposing factors? The Canadian Veterinary J **51:**1095-1102.

32. **Levings RL, Roth JA.** 2013. Immunity to bovine herpesvirus 1: I. Viral lifecycle and innate immunity. Anim Health Res Rev **14:**88-102.
33. **Schroeder RJ, Moys MD.** 1954. An acute upper respiratory infection of dairy cattle. J Am Vet Med Assoc **125:**471-472.
34. **Straub OC.** 1991. BHV1 infections: relevance and spread in Europe. Comp Immunol Microbiol Infect Dis **14:**175-186.
35. **Pruvot M, Kutz S, van der Meer F, Musiani M, Barkema HW, Orsel K.** 2014. Pathogens at the livestock-wildlife interface in Western Alberta: does transmission route matter? Vet Res **45:**18.
36. **Tessaro SV, Deregt D, Dzus E, Rohner C, Smith K, Gaboury T.** 2005. Herpesvirus infection in woodland caribou in Alberta, Canada. J Wildl Dis **41:**803-805.
37. **Aslan ME, Azkur AK, Gazyagci S.** 2015. Epidemiology and genetic characterization of BVDV, BHV-1, BHV-4, BHV-5 and Brucella spp. infections in cattle in Turkey. J Vet Med Sci **77:**1371-1377.
38. **Verma AK, Kumar A, Sahzad, Reddy NC, Shende AN.** 2014. Seroprevalence of infectious bovine rhinotracheitis in dairy animals with reproductive disorders in Uttar Pradesh, India. Pak J Biol Sci **17:**720-724.
39. **Patil SS, Prajapati A, Hemadri D, Suresh KP, Desai GS, Reddy GB, Chandranaik BM, Ranganatha S, Rahman H.** 2016. Phylogenetic analysis of glycoprotein B gene sequences of bovine herpesvirus 1 isolates from India reveals the predominance of subtype 1.1. Vet World **9:**1364-1369.
40. **Han Z, Gao J, Li K, Shahzad M, Nabi F, Zhang D, Li J, Liu Z.** 2016. Prevalence of Circulating Antibodies to Bovine Herpesvirus 1 in Yaks (Bos grunniens) on the Qinghai-Tibetan Plateau, China. J Wildl Dis **52:**164-167.
41. **Raaperi K, Orro T, Viltrop A.** 2014. Epidemiology and control of bovine herpesvirus 1 infection in Europe. Vet J **201:**249-256.
42. **O'Neill R, Mooney J, Connaghan E, Furphy C, Graham D.** 2014. Patterns of detection of respiratory viruses in nasal swabs from calves in Ireland: a retrospective study. Vet Record **175:**351-351.

43. **Tuncer-Goktuna P, Alpay G, Oner EB, Yesilbag K.** 2016. The role of herpesviruses (BoHV-1 and BoHV-4) and pestiviruses (BVDV and BDV) in ruminant abortion cases in western Turkey. Trop Anim Health Prod **48:**1021-1027.
44. **Fulton RW.** 2009. Bovine respiratory disease research (1983-2009). Anim Health Res Rev **10:**131-139.
45. **Statham JM, Randall LV, Archer SC.** 2015. Reduction in daily milk yield associated with subclinical bovine herpesvirus 1 infection. Vet Rec **177:**339.
46. **Mahajan V, Banga HS, Deka D, Filia G, Gupta A.** 2013. Comparison of diagnostic tests for diagnosis of infectious bovine rhinotracheitis in natural cases of bovine abortion. J Comp Pathol **149:**391-401.
47. **Lucchese L, Benkirane A, Hakimi I, El Idrissi A, Natale A.** 2016. Seroprevalence study of the main causes of abortion in dairy cattle in Morocco. Vet Italiana **52:**13-19.
48. **Jones C, da Silva LF, Sinani D.** 2011. Regulation of the latency-reactivation cycle by products encoded by the bovine herpesvirus 1 (BHV-1) latency-related gene. J Neurovirol **17:**535-545.
49. **Mackenzie-Dyck S, Latimer L, Atanley E, Kovacs-Nolan J, Attah-Poku S, Babiuk LA, van Drunen Littel-van den Hurk S.** 2015. Immunogenicity of a bovine herpesvirus 1 glycoprotein D DNA vaccine complexed with bovine neutrophil beta-defensin 3. Clin Vaccine Immunol **22:**79-90.
50. **Lung O, Furukawa-Stoffer T, Burton Hughes K, Pasick J, King DP, Hodko D.** 2016. Multiplex RT-PCR and Automated Microarray for Detection of Eight Bovine Viruses. Transbound Emerg Dis doi:10.1111/tbed.12591.
51. **Hay KE, Morton JM, Clements AC, Mahony TJ, Barnes TS.** 2016. Associations between feedlot management practices and bovine respiratory disease in Australian feedlot cattle. Prev Vet Med **128:**23-32.
52. **Kaashoek MJ, Moerman A, Madic J, Weerdmeester K, Maris-Veldhuis M, Rijsewijk FA, van Oirschot JT.** 1995. An inactivated vaccine based on a glycoprotein E-negative strain of bovine herpesvirus 1 induces protective immunity and allows serological differentiation. Vaccine **13:**342-346.

53. **Ackermann M, Muller HK, Bruckner L, Kihm U.** 1990. Eradication of infectious bovine rhinotracheitis in Switzerland: review and prospects. Vet Microbiol **23:**365-370.
54. **Weiss M, Brum MCS, Anziliero D, Weiblen R, Flores EF.** 2015. A glycoprotein E gene-deleted bovine herpesvirus 1 as a candidate vaccine strain. Braz J Med Biol Res **48:**843-851.
55. **Strube W, Auer S, Block W, Heinen E, Kretzdorn D, Rodenbach C, Schmeer N.** 1996. A gE deleted infectious bovine rhinotracheitis marker vaccine for use in improved bovine herpesvirus 1 control programs. Vet Microbiol **53:**181-189.
56. **Lemaire M, Schynts F, Meyer G, Georgin JP, Baranowski E, Gabriel A, Ros C, Belak S, Thiry E.** 2001. Latency and reactivation of a glycoprotein E negative bovine herpesvirus type 1 vaccine: influence of virus load and effect of specific maternal antibodies. Vaccine **19:**4795-4804.
57. **Lemaire M, Schynts F, Meyer G, Thiry E.** 1999. Antibody response to glycoprotein E after bovine herpesvirus type 1 infection in passively immunised, glycoprotein E-negative calves. Vet Rec **144:**172-176.
58. **Davison AJ.** 2007. Human Herpesviruses: Biology, Therapy, and Immunoprophylaxis. Chapter2 Comparative analysis of the genomes. Cambridge University Press, UK.
59. **Carroll KC, Hobden JA, Miller S, Morse SA, Mietzner TA, Detrick B, Mitchell TG, McKerrow JH, Sakanari JA.** 2015. Herpesviruses, Jawetz, Melnick, & Adelberg's Medical Microbiology, 27e. McGraw-Hill Education, New York, NY.
60. **Engels M, Loepfe E, Wild P, Schraner E, Wyler R.** 1987. The genome of caprine herpesvirus 1: genome structure and relatedness to bovine herpesvirus 1. J Gen Virol **68 (Pt 7):**2019-2023.
61. **Schynts F, McVoy MA, Meurens F, Detry B, Epstein AL, Thiry E.** 2003. The structures of bovine herpesvirus 1 virion and concatemeric DNA: implications for cleavage and packaging of herpesvirus genomes. Virology **314:**326-335.
62. **Roizman B.** 2013. The herpesviruses. Springer Science & Business Media.
63. **Robinson KE, Meers J, Gravel JL, McCarthy FM, Mahony TJ.** 2008. The essential and non-essential genes of Bovine herpesvirus 1. J Gen Virol **89:**2851-2863.

64. **Lobanov VA, Maher-Sturgess SL, Snider MG, Lawman Z, Babiuk LA.** 2010. A UL47 gene deletion mutant of bovine herpesvirus type 1 exhibits impaired growth in cell culture and lack of virulence in cattle. J Virol **84:**445-458.

65. **Weller SK, Coen DM.** 2012. Herpes simplex viruses: mechanisms of DNA replication. Cold Spring Harb Perspect Biol **4:**a013011.

66. **Meyer G, Vlcek C, Paces V, O'Hara MK, Pastoret PP, Thiry E, Schwyzer M.** 1997. Sequence analysis of the bovine herpesvirus type 1 genes homologous to the DNA polymerase (UL30), the major DNA-binding protein (UL29) and ICP18.5 assembly protein (UL28) genes of herpes simplex virus. Arch Virol **142:**89-102.

67. **Chung YT, Hsu W.** 1996. Functional expression of the bovine herpesvirus 1 alkaline deoxyribonuclease (UL12) in Escherichia coli. Arch Virol **141:**2457-2464.

68. **Barber KA, Daugherty HC, Ander SE, Jefferson VA, Shack LA, Pechan T, Nanduri B, Meyer F.** 2017. Protein Composition of the Bovine Herpesvirus 1.1 Virion. Vet Sciences **4:**11.

69. **Haanes EJ, Thomsen DR, Martin S, Homa FL, Lowery DE.** 1995. The bovine herpesvirus 1 maturational proteinase and scaffold proteins can substitute for the homologous herpes simplex virus type 1 proteins in the formation of hybrid type B capsids. J Virol **69:**7375-7379.

70. **Frizzo da Silva L, Kook I, Doster A, Jones C.** 2013. Bovine Herpesvirus 1 Regulatory Proteins bICP0 and VP16 Are Readily Detected in Trigeminal Ganglionic Neurons Expressing the Glucocorticoid Receptor during the Early Stages of Reactivation from Latency. J Virol **87:**11214-11222.

71. **Ren X, Harms JS, Splitter GA.** 2001. Tyrosine phosphorylation of bovine herpesvirus 1 tegument protein VP22 correlates with the incorporation of VP22 into virions. J Virol **75:**9010-9017.

72. **Zheng C, Brownlie R, Babiuk LA, van Drunen Littel-van den Hurk S.** 2005. Characterization of the Nuclear Localization and Nuclear Export Signals of Bovine Herpesvirus 1 VP22. J Virol **79:**11864-11872.

73. **Lam N, Letchworth G.** 2004. A derivative of bovine herpesvirus 1 (BoHV-1) UL3.5 lacking the last forty amino acids inhibits replication of BoHV-1. Arch Virol **149:**2295-2306.

74. **Lam N, Letchworth GJ.** 2000. Bovine Herpesvirus 1 U(L)3.5 Interacts with Bovine Herpesvirus 1 α-Transinducing Factor. J Virol **74:**2876-2884.

75. **Desloges N, Simard C.** 2003. Implication of the product of the bovine herpesvirus type 1 UL25 gene in capsid assembly. J Gen Virol **84:**2485-2490.

76. **Raza S, Deng M, Shahin F, Yang K, Hu C, Chen Y, Chen H, Guo A.** 2016. A bovine herpesvirus 1 pUL51 deletion mutant shows impaired viral growth in vitro and reduced virulence in rabbits. Oncotarget **7:**12235-12253.

77. **Li Y, Liang X, van Drunen Littel-van den Hurk S, Attah-Poku S, Babiuk LA.** 1996. Glycoprotein Bb, the N-terminal subunit of bovine herpesvirus 1 gB, can bind to heparan sulfate on the surfaces of Madin-Darby bovine kidney cells. J Virol **70:**2032-2037.

78. **Li Y, van Drunen Littel-van den Hurk S, Babiuk LA, Liang X.** 1995. Characterization of cell-binding properties of bovine herpesvirus 1 glycoproteins B, C, and D: identification of a dual cell-binding function of gB. J Virol **69:**4758-4768.

79. **Yoshitake N, Xuan X, Otsuka H.** 1997. Identification and characterization of bovine herpesvirus-1 glycoproteins E and I. J Gen Virol **78 (Pt 6):**1399-1403.

80. **Baranowski E, Keil G, Lyaku J, Rijsewijk FA, van Oirschot JT, Pastoret PP, Thiry E.** 1996. Structural and functional analysis of bovine herpesvirus 1 minor glycoproteins. Vet Microbiol **53:**91-101.

81. **Nakamichi K, Matsumoto Y, Otsuka H.** 2002. Bovine herpesvirus 1 glycoprotein G is necessary for maintaining cell-to-cell junctional adherence among infected cells. Virology **294:**22-30.

82. **van Drunen Littel-van den Hurk S, Khattar S, Tikoo SK, Babiuk LA, Baranowski E, Plainchamp D, Thiry E.** 1996. Glycoprotein H (gII/gp108) and glycoprotein L form a functional complex which plays a role in penetration, but not in attachment, of bovine herpesvirus 1. J Gen Virol **77 (Pt 7):**1515-1520.

83. **Khattar SK, van Drunen Littel-van den Harke S, Attah-Poku SK, Babiuk LA, Tikoo SK.** 1996. Identification and characterization of a bovine herpesvirus-1 (BHV-1)

glycoprotein gL which is required for proper antigenicity, processing, and transport of BHV-1 glycoprotein gH. Virology **219:**66-76.

84. **Wu SX, Zhu XP, Letchworth GJ.** 1998. Bovine herpesvirus 1 glycoprotein M forms a disulfide-linked heterodimer with the U(L)49.5 protein. J Virol **72:**3029-3036.
85. **Hodge PD, Stow ND.** 2001. Effects of mutations within the herpes simplex virus type 1 DNA encapsidation signal on packaging efficiency. J Virol **75:**8977-8986.
86. **Stow ND, McMonagle EC, Davison AJ.** 1983. Fragments from both termini of the herpes simplex virus type 1 genome contain signals required for the encapsidation of viral DNA. Nucleic Acids Res **11:**8205-8220.
87. **Goldstein JN, Weller SK.** 1998. In vitro processing of herpes simplex virus type 1 DNA replication intermediates by the viral alkaline nuclease, UL12. J Virol **72:**8772-8781.
88. **Bronstein JC, Weller SK, Weber PC.** 1997. The product of the UL12.5 gene of herpes simplex virus type 1 is a capsid-associated nuclease. J Virol **71:**3039-3047.
89. **Newcomb WW, Juhas RM, Thomsen DR, Homa FL, Burch AD, Weller SK, Brown JC.** 2001. The UL6 gene product forms the portal for entry of DNA into the herpes simplex virus capsid. J Virol **75:**10923-10932.
90. **Albright BS, Nellissery J, Szczepaniak R, Weller SK.** 2011. Disulfide bond formation in the herpes simplex virus 1 UL6 protein is required for portal ring formation and genome encapsidation. J Virol **85:**8616-8624.
91. **Nellissery JK, Szczepaniak R, Lamberti C, Weller SK.** 2007. A putative leucine zipper within the herpes simplex virus type 1 UL6 protein is required for portal ring formation. J Virol **81:**8868-8877.
92. **Newcomb WW, Homa FL, Brown JC.** 2006. Herpes simplex virus capsid structure: DNA packaging protein UL25 is located on the external surface of the capsid near the vertices. J Virol **80:**6286-6294.
93. **Ogasawara M, Suzutani T, Yoshida I, Azuma M.** 2001. Role of the UL25 gene product in packaging DNA into the herpes simplex virus capsid: location of UL25 product in the capsid and demonstration that it binds DNA. J Virol **75:**1427-1436.
94. **Cockrell SK, Sanchez ME, Erazo A, Homa FL.** 2009. Role of the UL25 protein in herpes simplex virus DNA encapsidation. J Virol **83:**47-57.

95. **Lye MF, Wilkie AR, Filman DJ, Hogle JM, Coen DM.** 2017. Getting to and through the inner nuclear membrane during herpesvirus nuclear egress. Current Opinion in Cell Biology **46:**9-16.

96. **Bowman BR, Baker ML, Rixon FJ, Chiu W, Quiocho FA.** 2003. Structure of the herpesvirus major capsid protein. The EMBO Journal **22:**757-765.

97. **Heine JW, Honess RW, Cassai E, Roizman B.** 1974. Proteins specified by herpes simplex virus. XII. The virion polypeptides of type 1 strains. J Virol **14:**640-651.

98. **Smiley JR.** 2004. Herpes Simplex Virus Virion Host Shutoff Protein: Immune Evasion Mediated by a Viral RNase? J Virol **78:**1063-1068.

99. **Mori I.** 2012. Herpes simplex virus US3 protein kinase regulates host responses and determines neurovirulence. Microbiol Immunol **56:**351-355.

100. **Geenen K, Favoreel HW, Nauwynck HJ.** 2006. Cell type-specific resistance of trigeminal ganglion neurons towards apoptotic stimuli. Vet Microbiol **113:**223-229.

101. **Geenen K, Favoreel HW, Nauwynck HJ.** 2005. Higher resistance of porcine trigeminal ganglion neurons towards pseudorabies virus-induced cell death compared with other porcine cell types in vitro. J Gen Virol **86:**1251-1260.

102. **Mori I, Goshima F, Watanabe D, Ito H, Koide N, Yoshida T, Liu B, Kimura Y, Yokochi T, Nishiyama Y.** 2006. Herpes simplex virus US3 protein kinase regulates virus-induced apoptosis in olfactory and vomeronasal chemosensory neurons in vivo. Microbes Infect **8:**1806-1812.

103. **Bresnahan WA, Shenk TE.** 2000. UL82 virion protein activates expression of immediate early viral genes in human cytomegalovirus-infected cells. Proc Natl Acad Sci U S A **97:**14506-14511.

104. **Lukashchuk V, McFarlane S, Everett RD, Preston CM.** 2008. Human cytomegalovirus protein pp71 displaces the chromatin-associated factor ATRX from nuclear domain 10 at early stages of infection. J Virol **82:**12543-12554.

105. **Xu P, Mallon S, Roizman B.** 2016. PML plays both inimical and beneficial roles in HSV-1 replication. Proc Natl Acad Sci U S A **113:**E3022-3028.

106. **Krautwald M, Fuchs W, Klupp BG, Mettenleiter TC.** 2009. Translocation of incoming pseudorabies virus capsids to the cell nucleus is delayed in the absence of tegument protein pUL37. J Virol **83:**3389-3396.
107. **Hennig T, Abaitua F, O'Hare P.** 2014. Functional analysis of nuclear localization signals in VP1-2 homologues from all herpesvirus subfamilies. J Virol **88:**5391-5405.
108. **Kelly BJ, Fraefel C, Cunningham AL, Diefenbach RJ.** 2009. Functional roles of the tegument proteins of herpes simplex virus type 1. Virus Res **145:**173-186.
109. **Abaitua F, Daikoku T, Crump CM, Bolstad M, O'Hare P.** 2011. A single mutation responsible for temperature-sensitive entry and assembly defects in the VP1-2 protein of herpes simplex virus. J Virol **85:**2024-2036.
110. **Schipke J, Pohlmann A, Diestel R, Binz A, Rudolph K, Nagel CH, Bauerfeind R, Sodeik B.** 2012. The C terminus of the large tegument protein pUL36 contains multiple capsid binding sites that function differently during assembly and cell entry of herpes simplex virus. J Virol **86:**3682-3700.
111. **Lin AE, Greco TM, Döhner K, Sodeik B, Cristea IM.** 2013. A Proteomic Perspective of Inbuilt Viral Protein Regulation: pUL46 Tegument Protein is Targeted for Degradation by ICP0 during Herpes Simplex Virus Type 1 Infection. Molecular & Cellular Proteomics : MCP **12:**3237-3252.
112. **Sivachandran N, Wang X, Frappier L.** 2012. Functions of the Epstein-Barr virus EBNA1 protein in viral reactivation and lytic infection. J Virol **86:**6146-6158.
113. **Morrison EE, Wang YF, Meredith DM.** 1998. Phosphorylation of structural components promotes dissociation of the herpes simplex virus type 1 tegument. J Virol **72:**7108-7114.
114. **Elliott G, O'reilly D, O'hare P.** 1996. Phosphorylation of the herpes simplex virus type 1 tegument protein VP22. Virology **226:**140-145.
115. **Loomis JS, Courtney RJ, Wills JW.** 2006. Packaging determinants in the UL11 tegument protein of herpes simplex virus type 1. J Virol **80:**10534-10541.
116. **Kato A, Yamamoto M, Ohno T, Tanaka M, Sata T, Nishiyama Y, Kawaguchi Y.** 2006. Herpes simplex virus 1-encoded protein kinase UL13 phosphorylates viral Us3

protein kinase and regulates nuclear localization of viral envelopment factors UL34 and UL31. J Virol **80:**1476-1486.

117. **Cano-Monreal G, Tavis JE, Morrison LA.** 2008. Substrate Specificity of the Herpes Simplex Virus Type 2 UL13 Protein Kinase. Virology **374:**1-10.

118. **Labiuk SL, Lobanov V, Lawman Z, Snider M, Babiuk LA, van Drunen Littel-van den Hurk S.** 2010. Bovine herpesvirus-1 US3 protein kinase: critical residues and involvement in the phosphorylation of VP22. J Gen Virol **91:**1117-1126.

119. **Aggarwal A, Miranda-Saksena M, Boadle RA, Kelly BJ, Diefenbach RJ, Alam W, Cunningham AL.** 2012. Ultrastructural visualization of individual tegument protein dissociation during entry of herpes simplex virus 1 into human and rat dorsal root ganglion neurons. J Virol **86:**6123-6137.

120. **Triezenberg SJ, Kingsbury RC, McKnight SL.** 1988. Functional dissection of VP16, the trans-activator of herpes simplex virus immediate early gene expression. Genes Dev **2:**718-729.

121. **Donnelly M, Verhagen J, Elliott G.** 2007. RNA binding by the herpes simplex virus type 1 nucleocytoplasmic shuttling protein UL47 is mediated by an N-terminal arginine-rich domain that also functions as its nuclear localization signal. J Virol **81:**2283-2296.

122. **Dobrikova E, Shveygert M, Walters R, Gromeier M.** 2010. Herpes simplex virus proteins ICP27 and UL47 associate with polyadenylate-binding protein and control its subcellular distribution. J Virol **84:**270-279.

123. **Shu M, Taddeo B, Zhang W, Roizman B.** 2013. Selective degradation of mRNAs by the HSV host shutoff RNase is regulated by the UL47 tegument protein. Proc Natl Acad Sci U S A **110:**E1669-1675.

124. **Granzow H, Klupp BG, Mettenleiter TC.** 2005. Entry of pseudorabies virus: an immunogold-labeling study. J Virol **79:**3200-3205.

125. **Delboy MG, Nicola AV.** 2011. A pre-immediate-early role for tegument ICP0 in the proteasome-dependent entry of herpes simplex virus. J Virol **85:**5910-5918.

126. **Liang XP, Babiuk LA, van Drunen Littel-van den Hurk S, Fitzpatrick DR, Zamb TJ.** 1991. Bovine herpesvirus 1 attachment to permissive cells is mediated by its major glycoproteins gI, gIII, and gIV. J Virol **65:**1124-1132.

127. **Lyman MG, Enquist LW.** 2009. Herpesvirus Interactions with the Host Cytoskeleton. J Virol **83:**2058-2066.
128. **Jovasevic V, Liang L, Roizman B.** 2008. Proteolytic cleavage of VP1-2 is required for release of herpes simplex virus 1 DNA into the nucleus. J Virol **82:**3311-3319.
129. **Roberts AP, Abaitua F, O'Hare P, McNab D, Rixon FJ, Pasdeloup D.** 2009. Differing roles of inner tegument proteins pUL36 and pUL37 during entry of herpes simplex virus type 1. J Virol **83:**105-116.
130. **Pitts JD, Klabis J, Richards AL, Smith GA, Heldwein EE.** 2014. Crystal structure of the herpesvirus inner tegument protein UL37 supports its essential role in control of viral trafficking. J Virol **88:**5462-5473.
131. **Skepper J, Whiteley A, Browne H, Minson A.** 2001. Herpes simplex virus nucleocapsids mature to progeny virions by an envelopment→ deenvelopment→ reenvelopment pathway. J Virol **75:**5697-5702.
132. **Jin F, Ma K, Chen M, Zou M, Wu Y, Li F, Wang Y.** 2016. Pentagalloylglucose Blocks the Nuclear Transport and the Process of Nucleocapsid Egress to Inhibit HSV-1 Infection. Jpn J Infect Dis **69:**135-142.
133. **Guan Y, Guo L, Yang E, Liao Y, Liu L, Che Y, Zhang Y, Wang L, Wang J, Li Q.** 2014. HSV-1 nucleocapsid egress mediated by UL31 in association with UL34 is impeded by cellular transmembrane protein 140. Virology **464-465:**1-10.
134. **Liu Z, Kato A, Oyama M, Kozuka-Hata H, Arii J, Kawaguchi Y.** 2015. Role of Host Cell p32 in Herpes Simplex Virus 1 De-Envelopment during Viral Nuclear Egress. J Virol **89:**8982-8998.
135. **Maruzuru Y, Shindo K, Liu Z, Oyama M, Kozuka-Hata H, Arii J, Kato A, Kawaguchi Y.** 2014. Role of herpes simplex virus 1 immediate early protein ICP22 in viral nuclear egress. J Virol **88:**7445-7454.
136. **Mou F, Wills EG, Park R, Baines JD.** 2008. Effects of lamin A/C, lamin B1, and viral US3 kinase activity on viral infectivity, virion egress, and the targeting of herpes simplex virus U(L)34-encoded protein to the inner nuclear membrane. J Virol **82:**8094-8104.

137. **Leach NR, Roller RJ.** 2010. Significance of host cell kinases in herpes simplex virus type 1 egress and lamin-associated protein disassembly from the nuclear lamina. Virology **406:**127-137.

138. **Wu S, Pan S, Zhang L, Baines J, Roller R, Ames J, Yang M, Wang J, Chen D, Liu Y, Zhang C, Cao Y, He B.** 2016. Herpes Simplex Virus 1 Induces Phosphorylation and Reorganization of Lamin A/C through the gamma134.5 Protein That Facilitates Nuclear Egress. J Virol **90:**10414-10422.

139. **Wang Y, Yang Y, Wu S, Pan S, Zhou C, Ma Y, Ru Y, Dong S, He B, Zhang C, Cao Y.** 2014. p32 is a novel target for viral protein ICP34.5 of herpes simplex virus type 1 and facilitates viral nuclear egress. J Biol Chem **289:**35795-35805.

140. **Chen YM, Knipe DM.** 1996. A dominant mutant form of the herpes simplex virus ICP8 protein decreases viral late gene transcription. Virology **221:**281-290.

141. **Yura Y, Kusaka J, Tsujimoto H, Yoshioka Y, Yoshida H, Sato M.** 1997. Effects of protein tyrosine kinase inhibitors on the replication of herpes simplex virus and the phosphorylation of viral proteins. Intervirology **40:**7-14.

142. **Kato A, Liu Z, Minowa A, Imai T, Tanaka M, Sugimoto K, Nishiyama Y, Arii J, Kawaguchi Y.** 2011. Herpes simplex virus 1 protein kinase Us3 and major tegument protein UL47 reciprocally regulate their subcellular localization in infected cells. J Virol **85:**9599-9613.

143. **Donnelly M, Elliott G.** 2001. Nuclear localization and shuttling of herpes simplex virus tegument protein VP13/14. J Virol **75:**2566-2574.

144. **Williams P, Verhagen J, Elliott G.** 2008. Characterization of a CRM1-dependent nuclear export signal in the C terminus of herpes simplex virus type 1 tegument protein UL47. J Virol **82:**10946-10952.

145. **Wang L, Liu L, Che Y, Wang L, Jiang L, Dong C, Zhang Y, Li Q.** 2010. Egress of HSV-1 capsid requires the interaction of VP26 and a cellular tetraspanin membrane protein. Virol J **7:**156.

146. **Pasdeloup D, McElwee M, Beilstein F, Labetoulle M, Rixon FJ.** 2013. Herpesvirus tegument protein pUL37 interacts with dystonin/BPAG1 to promote capsid transport on microtubules during egress. J Virol **87:**2857-2867.

147. **Mingo RM, Han J, Newcomb WW, Brown JC.** 2012. Replication of herpes simplex virus: egress of progeny virus at specialized cell membrane sites. J Virol **86:**7084-7097.
148. **David AT, Saied A, Charles A, Subramanian R, Chouljenko VN, Kousoulas KG.** 2012. A herpes simplex virus 1 (McKrae) mutant lacking the glycoprotein K gene is unable to infect via neuronal axons and egress from neuronal cell bodies. MBio **3:**e00144-00112.
149. **Ren X, Harms JS, Splitter GA.** 2001. Bovine herpesvirus 1 tegument protein VP22 interacts with histones, and the carboxyl terminus of VP22 is required for nuclear localization. J Virol **75:**8251-8258.
150. **Lobanov VA, Babiuk LA, van Drunen Littel-van den Hurk S.** 2010. Intracellular trafficking of VP22 in bovine herpesvirus-1 infected cells. Virology **396:**189-202.
151. **Hinkley S, Ambagala APN, Jones CJ, Srikumaran S.** 2000. A vhs-like activity of bovine herpesvirus-1. Arch Virol **145:**2027-2046.
152. **Carpenter DE, Misra V.** 1991. The most abundant protein in bovine herpes 1 virions is a homologue of herpes simplex virus type 1 UL47. J Gen Virol **72 (Pt 12):**3077-3084.
153. **Kopp M, Klupp BG, Granzow H, Fuchs W, Mettenleiter TC.** 2002. Identification and characterization of the pseudorabies virus tegument proteins UL46 and UL47: role for UL47 in virion morphogenesis in the cytoplasm. J Virol **76:**8820-8833.
154. **Verhagen J, Hutchinson I, Elliott G.** 2006. Nucleocytoplasmic shuttling of bovine herpesvirus 1 UL47 protein in infected cells. J Virol **80:**1059-1063.
155. **Zheng C, Brownlie R, Babiuk LA, van Drunen Littel-van den Hurk S.** 2004. Characterization of nuclear localization and export signals of the major tegument protein VP8 of bovine herpesvirus-1. Virology **324:**327-339.
156. **Verhagen J, Donnelly M, Elliott G.** 2006. Characterization of a novel transferable CRM-1-independent nuclear export signal in a herpesvirus tegument protein that shuttles between the nucleus and cytoplasm. J Virol **80:**10021-10035.
157. **Vasilenko NL, Snider M, Labiuk SL, Lobanov VA, Babiuk LA, van Drunen Littel-van den Hurk S.** 2012. Bovine herpesvirus-1 VP8 interacts with DNA damage binding protein-1 (DDB1) and is monoubiquitinated during infection. Virus Res **167:**56-66.

158. **Afroz S, Brownlie R, Fodje M, van Drunen Littel-van den Hurk S.** 2016. VP8, the Major Tegument Protein of Bovine Herpesvirus 1, Interacts with Cellular STAT1 and Inhibits Interferon Beta Signaling. J Virol **90:**4889-4904.
159. **Islam A, Schulz S, Afroz S, Babiuk LA, van Drunen Littel-van den Hurk S.** 2015. Interaction of VP8 with mRNAs of bovine herpesvirus-1. Virus Res **197:**116-126.
160. **Connolly SA, Landsburg DJ, Carfi A, Wiley DC, Eisenberg RJ, Cohen GH.** 2002. Structure-based analysis of the herpes simplex virus glycoprotein D binding site present on herpesvirus entry mediator HveA (HVEM). J Virol **76:**10894-10904.
161. **Spear PG.** 2004. Herpes simplex virus: receptors and ligands for cell entry. Cell Microbiol **6:**401-410.
162. **Shukla D, Liu J, Blaiklock P, Shworak NW, Bai X, Esko JD, Cohen GH, Eisenberg RJ, Rosenberg RD, Spear PG.** 1999. A novel role for 3-O-sulfated heparan sulfate in herpes simplex virus 1 entry. Cell **99:**13-22.
163. **Oliver SL, Yang E, Arvin AM.** 2016. Varicella-Zoster Virus Glycoproteins: Entry, Replication, and Pathogenesis. Current Clinical Microbiology Reports **3:**204-215.
164. **Spear PG.** 2004. Herpes simplex virus: receptors and ligands for cell entry. Cell Microbiol **6:**401-410.
165. **Sathiyamoorthy K, Chen J, Longnecker R, Jardetzky TS.** 2017. The COMPLEXity in herpesvirus entry. Curr Opin Virol **24:**97-104.
166. **Lamers SL, Newman RM, Laeyendecker O, Tobian AA, Colgrove RC, Ray SC, Koelle DM, Cohen J, Knipe DM, Quinn TC.** 2015. Global Diversity within and between Human Herpesvirus 1 and 2 Glycoproteins. J Virol **89:**8206-8218.
167. **Melancon JM, Luna RE, Foster TP, Kousoulas KG.** 2005. Herpes simplex virus type 1 gK is required for gB-mediated virus-induced cell fusion, while neither gB and gK nor gB and UL20p function redundantly in virion de-envelopment. J Virol **79:**299-313.
168. **Kim I-J, Chouljenko VN, Walker JD, Kousoulas KG.** 2013. Herpes simplex virus 1 glycoprotein M and the membrane-associated protein UL11 are required for virus-induced cell fusion and efficient virus entry. J Virol **87:**8029-8037.
169. **El Kasmi I, Lippé R.** 2015. Herpes Simplex Virus 1 gN Partners with gM To Modulate the Viral Fusion Machinery. J Virol **89:**2313-2323.

170. **Foster TP, Melancon JM, Olivier TL, Kousoulas KG.** 2004. Herpes Simplex Virus Type 1 Glycoprotein K and the UL20 Protein Are Interdependent for Intracellular Trafficking and trans-Golgi Network Localization. J Virol **78:**13262-13277.

171. **Hutchinson L, Johnson DC.** 1995. Herpes simplex virus glycoprotein K promotes egress of virus particles. J Virol **69:**5401-5413.

172. **David AT, Baghian A, Foster TP, Chouljenko VN, Kousoulas KG.** 2008. The herpes simplex virus type 1 (HSV-1) glycoprotein K(gK) is essential for viral corneal spread and neuroinvasiveness. Curr Eye Res **33:**455-467.

173. **Farnsworth A, Goldsmith K, Johnson DC.** 2003. Herpes Simplex Virus Glycoproteins gD and gE/gI Serve Essential but Redundant Functions during Acquisition of the Virion Envelope in the Cytoplasm. J Virol **77:**8481-8494.

174. **van Drunen Littel-van den Hurk S, Babiuk LA.** 1986. Synthesis and processing of bovine herpesvirus 1 glycoproteins. J Virol **59:**401-410.

175. **Kopp A, Blewett E, Misra V, Mettenleiter TC.** 1994. Proteolytic cleavage of bovine herpesvirus 1 (BHV-1) glycoprotein gB is not necessary for its function in BHV-1 or pseudorabies virus. J Virol **68:**1667-1674.

176. **Okazaki K, Matsuzaki T, Sugahara Y, Okada J, Hasebe M, Iwamura Y, Ohnishi M, Kanno T, Shimizu M, Honda E, et al.** 1991. BHV-1 adsorption is mediated by the interaction of glycoprotein gIII with heparinlike moiety on the cell surface. Virology **181:**666-670.

177. **Fehler F, Herrmann JM, Saalmuller A, Mettenleiter TC, Keil GM.** 1992. Glycoprotein IV of bovine herpesvirus 1-expressing cell line complements and rescues a conditionally lethal viral mutant. J Virol **66:**831-839.

178. **Tikoo SK, Fitzpatrick DR, Babiuk LA, Zamb TJ.** 1990. Molecular cloning, sequencing, and expression of functional bovine herpesvirus 1 glycoprotein gIV in transfected bovine cells. J Virol **64:**5132-5142.

179. **van Drunen Littel-van den Hurk S, Gifford GA, Babiuk LA.** 1990. Epitope specificity of the protective immune response induced by individual bovine herpesvirus-1 glycoproteins. Vaccine **8:**358-368.

180. **Alves Dummer L, Pereira Leivas Leite F, van Drunen Littel-van den Hurk S.** 2014. Bovine herpesvirus glycoprotein D: a review of its structural characteristics and applications in vaccinology. Vet Res **45:**111.

181. **Whitbeck JC, Knapp AC, Enquist LW, Lawrence WC, Bello LJ.** 1996. Synthesis, processing, and oligomerization of bovine herpesvirus 1 gE and gI membrane proteins. J Virol **70:**7878-7884.

182. **Kaashoek MJ, Rijsewijk FA, Ruuls RC, Keil GM, Thiry E, Pastoret PP, Van Oirschot JT.** 1998. Virulence, immunogenicity and reactivation of bovine herpesvirus 1 mutants with a deletion in the gC, gG, gI, gE, or in both the gI and gE gene. Vaccine **16:**802-809.

183. **Bryant NA, Davis-Poynter N, Vanderplasschen A, Alcami A.** 2003. Glycoprotein G isoforms from some alphaherpesviruses function as broad-spectrum chemokine binding proteins. The EMBO journal **22:**833-846.

184. **Nakamichi K, Ohara K, Kuroki D, Otsuka H.** 2000. Bovine herpesvirus 1 glycoprotein G is required for viral growth by cell-to-cell infection. Virus Res **68:**175-181.

185. **Nakamichi K, Kuroki D, Matsumoto Y, Otsuka H.** 2001. Bovine herpesvirus 1 glycoprotein G is required for prevention of apoptosis and efficient viral growth in rabbit kidney cells. Virology **279:**488-498.

186. **Meyer G, Hanon E, Georlette D, Pastoret PP, Thiry E.** 1998. Bovine herpesvirus type 1 glycoprotein H is essential for penetration and propagation in cell culture. J Gen Virol **79 (Pt 8):**1983-1987.

187. **Baranowski E, Dubuisson J, Pastoret PP, Thiry E.** 1993. Identification of 108K, 93K, and 42K glycoproteins of bovine herpesvirus-1 by monoclonal antibodies. Arch Virol **133:**97-111.

188. **Fitzpatrick DR, Zamb TJ, Babiuk LA.** 1990. Expression of bovine herpesvirus type 1 glycoprotein gI in transfected bovine cells induces spontaneous cell fusion. J Gen Virol **71 (Pt 5):**1215-1219.

189. **Haque M, Stanfield B, Kousoulas KG.** 2016. Bovine herpesvirus type-1 glycoprotein K (gK) interacts with UL20 and is required for infectious virus production. Virololgy **499:**156-164.

190. **Bigeard J, Rayapuram N, Pflieger D, Hirt H.** 2014. Phosphorylation-dependent regulation of plant chromatin and chromatin-associated proteins. Proteomics **14:**2127-2140.

191. **C HSL, Liu K, Tan LP, Yao SQ.** 2012. Current chemical biology tools for studying protein phosphorylation and dephosphorylation. Chemistry **18:**28-39.

192. **Nubling G, Bader B, Levin J, Hildebrandt J, Kretzschmar H, Giese A.** 2012. Synergistic influence of phosphorylation and metal ions on tau oligomer formation and coaggregation with alpha-synuclein at the single molecule level. Mol Neurodegener **7:**35.

193. **Kostich M, English J, Madison V, Gheyas F, Wang L, Qiu P, Greene J, Laz TM.** 2002. Human members of the eukaryotic protein kinase family. Genome Biology **3:**research0043.0041-research0043.0012.

194. **Turowec JP, Duncan JS, French AC, Gyenis L, St Denis NA, Vilk G, Litchfield DW.** 2010. Protein kinase CK2 is a constitutively active enzyme that promotes cell survival: strategies to identify CK2 substrates and manipulate its activity in mammalian cells. Methods Enzymol **484:**471-493.

195. **Lolli G, Ranchio A, Battistutta R.** 2014. Active form of the protein kinase CK2 alpha2beta2 holoenzyme is a strong complex with symmetric architecture. ACS Chem Biol **9:**366-371.

196. **Gouron A, Milet A, Jamet H.** 2014. Conformational Flexibility of Human Casein Kinase Catalytic Subunit Explored by Metadynamics. Biophys J **106:**1134-1141.

197. **Buchou T, Vernet M, Blond O, Jensen HH, Pointu H, Olsen BB, Cochet C, Issinger OG, Boldyreff B.** 2003. Disruption of the regulatory beta subunit of protein kinase CK2 in mice leads to a cell-autonomous defect and early embryonic lethality. Mol Cell Biol **23:**908-915.

198. **Mestres P, Boldyreff B, Ebensperger C, Hameister H, Issinger OG.** 1994. Expression of casein kinase 2 during mouse embryogenesis. Acta Anat (Basel) **149:**13-20.

199. **Faust M, Montenarh M.** 2000. Subcellular localization of protein kinase CK2. A key to its function? Cell Tissue Res **301:**329-340.

200. **Homma MK, Homma Y.** 2008. Cell cycle and activation of CK2. Mol Cell Biochem **316:**49-55.

201. **Qaiser F, Trembley JH, Kren BT, Wu JJ, Naveed AK, Ahmed K.** 2014. Protein kinase CK2 inhibition induces cell death via early impact on mitochondrial function. J Cell Biochem **115:**2103-2115.

202. **Wang J, Feng C, He Y, Ding W, Sheng J, Arshad M, Zhang X, Li P.** 2015. Phosphorylation of apoptosis repressor with caspase recruitment domain by protein kinase CK2 contributes to chemotherapy resistance by inhibiting doxorubicin induced apoptosis. Oncotarget **6:**27700-27713.

203. **Intemann J, Saidu NE, Schwind L, Montenarh M.** 2014. ER stress signaling in ARPE-19 cells after inhibition of protein kinase CK2 by CX-4945. Cell Signal **26:**1567-1575.

204. **Manni S, Brancalion A, Mandato E, Tubi LQ, Colpo A, Pizzi M, Cappellesso R, Zaffino F, Di Maggio SA, Cabrelle A, Marino F, Zambello R, Trentin L, Adami F, Gurrieri C, Semenzato G, Piazza F.** 2013. Protein kinase CK2 inhibition down modulates the NF-kappaB and STAT3 survival pathways, enhances the cellular proteotoxic stress and synergistically boosts the cytotoxic effect of bortezomib on multiple myeloma and mantle cell lymphoma cells. PLoS One **8:**e75280.

205. **Koreishi M, Yu S, Oda M, Honjo Y, Satoh A.** 2013. CK2 phosphorylates Sec31 and regulates ER-To-Golgi trafficking. PLoS One **8:**e54382.

206. **Mattson-Hoss MK, Niitani Y, Gordon EA, Jun Y, Bardwell L, Tomishige M, Gross SP.** 2014. CK2 activates kinesin via induction of a conformational change. Proc Natl Acad Sci U S A **111:**7000-7005.

207. **Faust M, Gunther J, Morgenstern E, Montenarh M, Gotz C.** 2002. Specific localization of the catalytic subunits of protein kinase CK2 at the centrosomes. Cell Mol Life Sci **59:**2155-2164.

208. **Sarrouilhe D, Filhol O, Leroy D, Bonello G, Baudry M, Chambaz EM, Cochet C.** 1998. The tight association of protein kinase CK2 with plasma membranes is mediated by

a specific domain of its regulatory β-subunit. Biochimica et Biophysica Acta (BBA) - Molecular Cell Research **1403:**199-210.

209. **Meggio F, Pinna LA.** 2003. One-thousand-and-one substrates of protein kinase CK2? FASEB J **17:**349-368.

210. **Venerando A, Ruzzene M, Pinna LA.** 2014. Casein kinase: the triple meaning of a misnomer. Biochem J **460:**141-156.

211. **Bretana NA, Lu CT, Chiang CY, Su MG, Huang KY, Lee TY, Weng SL.** 2012. Identifying protein phosphorylation sites with kinase substrate specificity on human viruses. PLoS One **7:**e40694.

212. **Bian Y, Ye M, Wang C, Cheng K, Song C, Dong M, Pan Y, Qin H, Zou H.** 2013. Global screening of CK2 kinase substrates by an integrated phosphoproteomics workflow. Scientific reports **3:**3460.

213. **Pagano MA, Poletto G, Di Maira G, Cozza G, Ruzzene M, Sarno S, Bain J, Elliott M, Moro S, Zagotto G.** 2007. Tetrabromocinnamic acid (TBCA) and related compounds represent a new class of specific protein kinase CK2 inhibitors. Chembiochem **8:**129-139.

214. **Ryu S-Y, Kim S.** 2013. Evaluation of CK2 inhibitor (E)-3-(2, 3, 4, 5-tetrabromophenyl) acrylic acid (TBCA) in regulation of platelet function. European J pharmacology **720:**391-400.

215. **Pagano MA, Andrzejewska M, Ruzzene M, Sarno S, Cesaro L, Bain J, Elliott M, Meggio F, Kazimierczuk Z, Pinna LA.** 2004. Optimization of protein kinase CK2 inhibitors derived from 4, 5, 6, 7-tetrabromobenzimidazole. J Medi Chem **47:**6239-6247.

216. **Takashima Y, Tamura H, Xuan X, Otsuka H.** 1999. Identification of the US3 gene product of BHV-1 as a protein kinase and characterization of BHV-1 mutants of the US3 gene. Virus Res **59:**23-34.

217. **Geenen K, Favoreel HW, Olsen L, Enquist LW, Nauwynck HJ.** 2005. The pseudorabies virus US3 protein kinase possesses anti-apoptotic activity that protects cells from apoptosis during infection and after treatment with sorbitol or staurosporine. Virology **331:**144-150.

218. **Purves FC, Longnecker RM, Leader DP, Roizman B.** 1987. Herpes simplex virus 1 protein kinase is encoded by open reading frame US3 which is not essential for virus growth in cell culture. J Virol **61:**2896-2901.

219. **Proft A, Spiesschaert B, Izume S, Taferner S, Lehmann MJ, Azab W.** 2016. The Role of the Equine Herpesvirus Type 1 (EHV-1) US3-Encoded Protein Kinase in Actin Reorganization and Nuclear Egress. Viruses **8**.

220. **Ladelfa MF, Kotsias F, Del Medico Zajac MP, Van den Broeke C, Favoreel H, Romera SA, Calamante G.** 2011. Effect of the US3 protein of bovine herpesvirus 5 on the actin cytoskeleton and apoptosis. Vet Microbiol **153:**361-366.

221. **Jacob T, Van den Broeke C, Grauwet K, Baert K, Claessen C, De Pelsmaeker S, Van Waesberghe C, Favoreel HW.** 2015. Pseudorabies virus US3 leads to filamentous actin disassembly and contributes to viral genome delivery to the nucleus. Vet Microbiol **177:**379-385.

222. **Schumacher D, Tischer BK, Trapp S, Osterrieder N.** 2005. The protein encoded by the US3 orthologue of Marek's disease virus is required for efficient de-envelopment of perinuclear virions and involved in actin stress fiber breakdown. J Virol **79:**3987-3997.

223. **Jacob T, Van den Broeke C, van Troys M, Waterschoot D, Ampe C, Favoreel HW.** 2013. Alphaherpesviral US3 kinase induces cofilin dephosphorylation to reorganize the actin cytoskeleton. J Virol **87:**4121-4126.

224. **Van Minnebruggen G, Favoreel HW, Jacobs L, Nauwynck HJ.** 2003. Pseudorabies virus US3 protein kinase mediates actin stress fiber breakdown. J Virol **77:**9074-9080.

225. **Hagglund R, Munger J, Poon AP, Roizman B.** 2002. U(S)3 protein kinase of herpes simplex virus 1 blocks caspase 3 activation induced by the products of U(S)1.5 and U(L)13 genes and modulates expression of transduced U(S)1.5 open reading frame in a cell type-specific manner. J Virol **76:**743-754.

226. **Benetti L, Roizman B.** 2007. In transduced cells, the US3 protein kinase of herpes simplex virus 1 precludes activation and induction of apoptosis by transfected procaspase 3. J Virol **81:**10242-10248.

227. **Calton CM, Randall JA, Adkins MW, Banfield BW.** 2004. The pseudorabies virus serine/threonine kinase Us3 contains mitochondrial, nuclear and membrane localization signals. Virus Genes **29:**131-145.

228. **Deruelle MJ, De Corte N, Englebienne J, Nauwynck HJ, Favoreel HW.** 2010. Pseudorabies virus US3-mediated inhibition of apoptosis does not affect infectious virus production. J Gen Virol **91:**1127-1132.

229. **Kato A, Arii J, Shiratori I, Akashi H, Arase H, Kawaguchi Y.** 2009. Herpes simplex virus 1 protein kinase Us3 phosphorylates viral envelope glycoprotein B and regulates its expression on the cell surface. J Virol **83:**250-261.

230. **Eaton HE, Saffran HA, Wu FW, Quach K, Smiley JR.** 2014. Herpes Simplex Virus Protein Kinases US3 and UL13 Modulate VP11/12 Phosphorylation, Virion Packaging, and Phosphatidylinositol 3-Kinase/Akt Signaling Activity. J Virol **88:**7379-7388.

231. **Wilkinson GW, Kelly C, Sinclair JH, Rickards C.** 1998. Disruption of PML-associated nuclear bodies mediated by the human cytomegalovirus major immediate early gene product. J Gen Virol **79 (Pt 5):**1233-1245.

232. **Negorev DG, Vladimirova OV, Ivanov A, Rauscher F, 3rd, Maul GG.** 2006. Differential role of Sp100 isoforms in interferon-mediated repression of herpes simplex virus type 1 immediate-early protein expression. J Virol **80:**8019-8029.

233. **Tavalai N, Papior P, Rechter S, Stamminger T.** 2008. Nuclear domain 10 components promyelocytic leukemia protein and hDaxx independently contribute to an intrinsic antiviral defense against human cytomegalovirus infection. J Virol **82:**126-137.

234. **Korioth F, Maul GG, Plachter B, Stamminger T, Frey J.** 1996. The nuclear domain 10 (ND10) is disrupted by the human cytomegalovirus gene product IE1. Exp Cell Res **229:**155-158.

235. **Salsman J, Zimmerman N, Chen T, Domagala M, Frappier L.** 2008. Genome-wide screen of three herpesviruses for protein subcellular localization and alteration of PML nuclear bodies. PLoS Pathog **4:**e1000100.

236. **Salsman J, Wang X, Frappier L.** 2011. Nuclear body formation and PML body remodeling by the human cytomegalovirus protein UL35. Virology **414:**119-129.

237. **Schierling K, Stamminger T, Mertens T, Winkler M.** 2004. Human Cytomegalovirus Tegument Proteins ppUL82 (pp71) and ppUL35 Interact and Cooperatively Activate the Major Immediate-Early Enhancer. J Virol **78:**9512-9523.

238. **Tsai K, Chan L, Gibeault R, Conn K, Dheekollu J, Domsic J, Marmorstein R, Schang LM, Lieberman PM.** 2014. Viral reprogramming of the Daxx histone H3.3 chaperone during early Epstein-Barr virus infection. J Virol **88:**14350-14363.

239. **Hwang J, Kalejta RF.** 2009. Human cytomegalovirus protein pp71 induces Daxx SUMOylation. J Virol **83:**6591-6598.

240. **Sewatanon J, Ling PD.** 2014. Murine Gammaherpesvirus 68 Encodes a Second PML-Modifying Protein. J Virol **88:**3591-3597.

241. **Tsai K, Thikmyanova N, Wojcechowskyj JA, Delecluse HJ, Lieberman PM.** 2011. EBV tegument protein BNRF1 disrupts DAXX-ATRX to activate viral early gene transcription. PLoS Pathog **7:**e1002376.

242. **Saffert RT, Kalejta RF.** 2006. Inactivating a cellular intrinsic immune defense mediated by Daxx is the mechanism through which the human cytomegalovirus pp71 protein stimulates viral immediate-early gene expression. J Virol **80:**3863-3871.

243. **Everett RD, Maul GG.** 1994. HSV-1 IE protein Vmw110 causes redistribution of PML. The EMBO Journal **13:**5062-5069.

244. **Lee HR, Kim DJ, Lee JM, Choi CY, Ahn BY, Hayward GS, Ahn JH.** 2004. Ability of the human cytomegalovirus IE1 protein to modulate sumoylation of PML correlates with its functional activities in transcriptional regulation and infectivity in cultured fibroblast cells. J Virol **78:**6527-6542.

245. **Adamson AL, Kenney S.** 2001. Epstein-barr virus immediate-early protein BZLF1 is SUMO-1 modified and disrupts promyelocytic leukemia bodies. J Virol **75:**2388-2399.

246. **Everett RD, Boutell C, McNair C, Grant L, Orr A.** 2010. Comparison of the biological and biochemical activities of several members of the alphaherpesvirus ICP0 family of proteins. J Virol **84:**3476-3487.

247. **Nojima T, Oshiro-Ideue T, Nakanoya H, Kawamura H, Morimoto T, Kawaguchi Y, Kataoka N, Hagiwara M.** 2009. Herpesvirus protein ICP27 switches PML isoform by altering mRNA splicing. Nucleic Acids Res **37:**6515-6527.

248. **Mu ZM, Le XF, Glassman AB, Chang KS.** 1996. The biologic function of PML and its role in acute promyelocytic leukemia. Leuk Lymphoma **23:**277-285.

249. **Chen SJ, Wang ZY, Chen Z.** 1995. Acute promyelocytic leukemia: from clinic to molecular biology. Stem Cells **13:**22-31.

250. **Brand P, Lenser T, Hemmerich P.** 2010. Assembly dynamics of PML nuclear bodies in living cells. PMC Biophysics **3**.

251. **Bischof O, Kim S-H, Irving J, Beresten S, Ellis NA, Campisi J.** 2001. Regulation and Localization of the Bloom Syndrome Protein in Response to DNA Damage. J Cell Bio **153:**367-380.

252. **Falini B, Flenghi L, Fagioli M, Coco FL, Cordone I, Diverio D, Pasqualucci L, Biondi A, Riganelli D, Orleth A.** 1997. Immunocytochemical diagnosis of acute promyelocytic leukemia (M3) with the monoclonal antibody PG-M3 (anti-PML). Blood **90:**4046-4053.

253. **Berube NG, Smeenk CA, Picketts DJ.** 2000. Cell cycle-dependent phosphorylation of the ATRX protein correlates with changes in nuclear matrix and chromatin association. Hum Mol Genet **9:**539-547.

254. **Hsu KS, Guan BJ, Cheng X, Guan D, Lam M, Hatzoglou M, Kao HY.** 2016. Translational control of PML contributes to TNFα-induced apoptosis of MCF7 breast cancer cells and decreased angiogenesis in HUVECs. Cell Death Differ **23:**469-483.

255. **Chen Y, Wright J, Meng X, Leppard KN.** 2015. Promyelocytic Leukemia Protein Isoform II Promotes Transcription Factor Recruitment To Activate Interferon Beta and Interferon-Responsive Gene Expression. Mol Cell Biol **35:**1660-1672.

256. **Ishov AM, Sotnikov AG, Negorev D, Vladimirova OV, Neff N, Kamitani T, Yeh ET, Strauss JF, 3rd, Maul GG.** 1999. PML is critical for ND10 formation and recruits the PML-interacting protein daxx to this nuclear structure when modified by SUMO-1. J Cell Biol **147:**221-234.

257. **Nisole S, Maroui MA, Mascle XH, Aubry M, Chelbi-Alix MK.** 2013. Differential Roles of PML Isoforms. Frontiers in Oncology **3:**1-17.

258. **Geng Y, Monajembashi S, Shao A, Cui D, He W, Chen Z, Hemmerich P, Tang J.** 2012. Contribution of the C-terminal regions of promyelocytic leukemia protein (PML) isoforms II and V to PML nuclear body formation. J Biol Chem **287:**30729-30742.

259. **Ohsaki Y, Kawai T, Yoshikawa Y, Cheng J, Jokitalo E, Fujimoto T.** 2016. PML isoform II plays a critical role in nuclear lipid droplet formation. J Cell Biol **212:**29-38.

260. **Regad T, Saib A, Lallemand-Breitenbach V, Pandolfi PP, de The H, Chelbi-Alix MK.** 2001. PML mediates the interferon-induced antiviral state against a complex retrovirus via its association with the viral transactivator. EMBO J **20:**3495-3505.

261. **Shimada N, Shinagawa T, Ishii S.** 2008. Modulation of M2-type pyruvate kinase activity by the cytoplasmic PML tumor suppressor protein. Genes Cells **13:**245-254.

262. **Maroui MA, Kheddache-Atmane S, El Asmi F, Dianoux L, Aubry M, Chelbi-Alix MK.** 2012. Requirement of PML SUMO interacting motif for RNF4- or arsenic trioxide-induced degradation of nuclear PML isoforms. PLoS One **7:**e44949.

263. **Negorev DG, Vladimirova OV, Maul GG.** 2009. Differential functions of interferon-upregulated Sp100 isoforms: herpes simplex virus type 1 promoter-based immediate-early gene suppression and PML protection from ICP0-mediated degradation. J Virol **83:**5168-5180.

264. **Sternsdorf T, Jensen K, Reich B, Will H.** 1999. The nuclear dot protein sp100, characterization of domains necessary for dimerization, subcellular localization, and modification by small ubiquitin-like modifiers. J Biol Chem **274:**12555-12566.

265. **Negorev D, Ishov AM, Maul GG.** 2001. Evidence for separate ND10-binding and homo-oligomerization domains of Sp100. J Cell Sci **114:**59-68.

266. **Seeler J-S, Marchio A, Sitterlin D, Transy C, Dejean A.** 1998. Interaction of SP100 with HP1 proteins: A link between the promyelocytic leukemia-associated nuclear bodies and the chromatin compartment. Proc Natl Acad Sci USA **95:**7316-7321.

267. **Seeler J-S, Marchio A, Losson R, Desterro JMP, Hay RT, Chambon P, Dejean A.** 2001. Common Properties of Nuclear Body Protein SP100 and TIF1α Chromatin Factor: Role of SUMO Modification. Mol Cell Biol **21:**3314-3324.

268. **Negorev DG, Vladimirova OV, Kossenkov AV, Nikonova EV, Demarest RM, Capobianco AJ, Showe MK, Rauscher FJ, 3rd, Showe LC, Maul GG.** 2010. Sp100 as

a potent tumor suppressor: accelerated senescence and rapid malignant transformation of human fibroblasts through modulation of an embryonic stem cell program. Cancer Res **70:**9991-10001.

269. **Isaac A, Wilcox KW, Taylor JL.** 2006. SP100B, a repressor of gene expression preferentially binds to DNA with unmethylated CpGs. J Cell Biochem **98:**1106-1122.
270. **Org T, Chignola F, Hetényi C, Gaetani M, Rebane A, Liiv I, Maran U, Mollica L, Bottomley MJ, Musco G, Peterson P.** 2008. The autoimmune regulator PHD finger binds to non-methylated histone H3K4 to activate gene expression. EMBO Reports **9:**370-376.
271. **Sanchez-Giraldo R, Acosta-Reyes FJ, Malarkey CS, Saperas N, Churchill ME, Campos JL.** 2015. Two high-mobility group box domains act together to underwind and kink DNA. Acta Crystallogr D Biol Crystallogr **71:**1423-1432.
272. **Koschmann C, Calinescu AA, Nunez FJ, Mackay A, Fazal-Salom J, Thomas D, Mendez F, Kamran N, Dzaman M, Mulpuri L, Krasinkiewicz J, Doherty R, Lemons R, Brosnan-Cashman JA, Li Y, Roh S, Zhao L, Appelman H, Ferguson D, Gorbunova V, Meeker A, Jones C, Lowenstein PR, Castro MG.** 2016. ATRX loss promotes tumor growth and impairs nonhomologous end joining DNA repair in glioma. Sci Transl Med **8:**328ra328.
273. **Voon HP, Wong LH.** 2016. New players in heterochromatin silencing: histone variant H3. 3 and the ATRX/DAXX chaperone. Nucleic acids research **44:**1496-1501.
274. **He Q, Kim H, Huang R, Lu W, Tang M, Shi F, Yang D, Zhang X, Huang J, Liu D, Songyang Z.** 2015. The Daxx/Atrx Complex Protects Tandem Repetitive Elements during DNA Hypomethylation by Promoting H3K9 Trimethylation. Cell Stem Cell **17:**273-286.
275. **Slatter TL, Hsia H, Samaranayaka A, Sykes P, Clow WB, Devenish CJ, Sutton T, Royds JA, Pc P, Cheung AN, Hung NA.** 2015. Loss of ATRX and DAXX expression identifies poor prognosis for smooth muscle tumours of uncertain malignant potential and early stage uterine leiomyosarcoma. J Pathol Clin Res **1:**95-105.

276. **Liau JY, Lee JC, Tsai JH, Yang CY, Liu TL, Ke ZL, Hsu HH, Jeng YM.** 2015. Comprehensive screening of alternative lengthening of telomeres phenotype and loss of ATRX expression in sarcomas. Mod Pathol **28:**1545-1554.

277. **Shao LW, Pan Y, Qi XL, Li YX, Ma XL, Yi WN, Zhang J, Zhong YF, Chang Q.** 2016. ATRX loss in adult supratentorial diffuse astrocytomas correlates with p53 over expression and IDH1 mutation and predicts better outcome in p53 accumulated patients. Histol Histopathol **31:**103-114.

278. **Dhayalan A, Tamas R, Bock I, Tattermusch A, Dimitrova E, Kudithipudi S, Ragozin S, Jeltsch A.** 2011. The ATRX-ADD domain binds to H3 tail peptides and reads the combined methylation state of K4 and K9. Hum Mol Gen **20:**2195-2203.

279. **Yadav R, Kakkar A, Sharma A, Malik PS, Sharma MC.** 2016. Study of clinicopathological features, hormone immunoexpression, and loss of ATRX and DAXX expression in pancreatic neuroendocrine tumors. Scand J Gastroenterol **51:**994-999.

280. **Kurihara S, Hiyama E, Onitake Y, Yamaoka E, Hiyama K.** 2014. Clinical features of ATRX or DAXX mutated neuroblastoma. J Pediatric Surgery **49:**1835-1838.

281. **Tavalai N, Stamminger T.** 2009. Interplay between Herpesvirus Infection and Host Defense by PML Nuclear Bodies. Viruses **1:**1240-1264.

282. **Wang L, Oliver SL, Sommer M, Rajamani J, Reichelt M, Arvin AM.** 2011. Disruption of PML nuclear bodies is mediated by ORF61 SUMO-interacting motifs and required for varicella-zoster virus pathogenesis in skin. PLoS Pathog **7:**e1002157.

283. **Delboy MG, Siekavizza-Robles CR, Nicola AV.** 2010. Herpes Simplex Virus Tegument ICP0 Is Capsid Associated, and Its E3 Ubiquitin Ligase Domain Is Important for Incorporation into Virions. J Virol **84:**1637-1640.

284. **Burkham J, Coen DM, Weller SK.** 1998. ND10 protein PML is recruited to herpes simplex virus type 1 prereplicative sites and replication compartments in the presence of viral DNA polymerase. J Virol **72:**10100-10107.

285. **Everett RD, Murray J.** 2005. ND10 components relocate to sites associated with herpes simplex virus type 1 nucleoprotein complexes during virus infection. J Virol **79:**5078-5089.

286. **Loret S, Guay G, Lippé R.** 2008. Comprehensive characterization of extracellular herpes simplex virus type 1 virions. J Virol **82:**8605-8618.

287. **Tang Q, Li L, Ishov AM, Revol V, Epstein AL, Maul GG.** 2003. Determination of minimum herpes simplex virus type 1 components necessary to localize transcriptionally active DNA to ND10. J Virol **77:**5821-5828.

288. **Everett RD, Sourvinos G, Orr A.** 2003. Recruitment of herpes simplex virus type 1 transcriptional regulatory protein ICP4 into foci juxtaposed to ND10 in live, infected cells. J Virol **77:**3680-3689.

289. **Carpenter DE, Misra V.** 1991. The most abundant protein in bovine herpes 1 virions is a homologue of herpes simplex virus type 1 UL47. J Gen Virol **72:**3077-3084.

290. **Zhang K, Afroz S, Brownlie R, Snider M, van Drunen Littel-van den Hurk S.** 2015. Regulation and function of phosphorylation on VP8, the major tegument protein of bovine herpesvirus 1. J Virol **89:**4598-4611.

291. **Burkham J, Coen DM, Hwang CBC, Weller SK.** 2001. Interactions of Herpes Simplex Virus Type 1 with ND10 and Recruitment of PML to Replication Compartments. J Virol **75:**2353-2367.

292. **Everett RD, Sourvinos G, Leiper C, Clements JB, Orr A.** 2004. Formation of nuclear foci of the herpes simplex virus type 1 regulatory protein ICP4 at early times of infection: localization, dynamics, recruitment of ICP27, and evidence for the de novo induction of ND10-like complexes. J Virol **78:**1903-1917.

293. **Lukonis CJ, Burkham J, Weller SK.** 1997. Herpes simplex virus type 1 prereplicative sites are a heterogeneous population: only a subset are likely to be precursors to replication compartments. J Virol **71:**4771-4781.

294. **Everett RD, Murray J, Orr A, Preston CM.** 2007. Herpes simplex virus type 1 genomes are associated with ND10 nuclear substructures in quiescently infected human fibroblasts. J Virol **81:**10991-11004.

295. **Lukonis CJ, Weller SK.** 1996. Characterization of nuclear structures in cells infected with herpes simplex virus type 1 in the absence of viral DNA replication. J Virol **70:**1751-1758.

296. **Everett RD, Meredith M, Orr A, Cross A, Kathoria M, Parkinson J.** 1997. A novel ubiquitin-specific protease is dynamically associated with the PML nuclear domain and binds to a herpesvirus regulatory protein. The EMBO Journal **16:**1519-1530.

297. **Gu H, Roizman B.** 2003. The degradation of promyelocytic leukemia and Sp100 proteins by herpes simplex virus 1 is mediated by the ubiquitin-conjugating enzyme UbcH5a. Proc Natl Acad Sci U S A **100:**8963-8968.

298. **Gaudreault N, Jones C.** 2011. Regulation of promyelocytic leukemia (PML) protein levels and cell morphology by bovine herpesvirus 1 infected cell protein 0 (bICP0) and mutant bICP0 proteins that do not localize to the nucleus. Virus Res **156:**17-24.

299. **Chelbi-Alix MK, de The H.** 1999. Herpes virus induced proteasome-dependent degradation of the nuclear bodies-associated PML and Sp100 proteins. Oncogene **18:**935-941.

300. **Perusina Lanfranca M, Mostafa HH, Davido DJ.** 2013. Two overlapping regions within the N-terminal half of the herpes simplex virus 1 E3 ubiquitin ligase ICP0 facilitate the degradation and dissociation of PML and dissociation of Sp100 from ND10. J Virol **87:**13287-12396.

301. **Zhong S, Salomoni P, Pandolfi PP.** 2000. The transcriptional role of PML and the nuclear body. Nat Cell Biol **2:**E85-90.

302. **Maul GG, Everett RD.** 1994. The nuclear location of PML, a cellular member of the C3HC4 zinc-binding domain protein family, is rearranged during herpes simplex virus infection by the C3HC4 viral protein ICP0. J Gen Virol **75 (Pt 6):**1223-1233.

303. **Lukonis CJ, Weller SK.** 1997. Formation of herpes simplex virus type 1 replication compartments by transfection: requirements and localization to nuclear domain 10. J Virol **71:**2390-2399.

304. **Maul GG, Ishov AM, Everett RD.** 1996. Nuclear domain 10 as preexisting potential replication start sites of herpes simplex virus type-1. Virology **217:**67-75.

305. **Everett RD, Rechter S, Papior P, Tavalai N, Stamminger T, Orr A.** 2006. PML contributes to a cellular mechanism of repression of herpes simplex virus type 1 infection that is inactivated by ICP0. J Virol **80:**7995-8005.

306. **Catez F, Picard C, Held K, Gross S, Rousseau A, Theil D, Sawtell N, Labetoulle M, Lomonte P.** 2012. HSV-1 genome subnuclear positioning and associations with host-cell PML-NBs and centromeres regulate LAT locus transcription during latency in neurons. PLoS Pathog **8:**e1002852.

307. **Lomonte P.** 2016. The interaction between herpes simplex virus 1 genome and promyelocytic leukemia nuclear bodies (PML-NBs) as a hallmark of the entry in latency. Microb Cell **3:**569-572.

308. **Maroui MA, Calle A, Cohen C, Streichenberger N, Texier P, Takissian J, Rousseau A, Poccardi N, Welsch J, Corpet A, Schaeffer L, Labetoulle M, Lomonte P.** 2016. Latency Entry of Herpes Simplex Virus 1 Is Determined by the Interaction of Its Genome with the Nuclear Environment. PLoS Pathog **12:**e1005834.

309. **Chee AV, Lopez P, Pandolfi PP, Roizman B.** 2003. Promyelocytic leukemia protein mediates interferon-based anti-herpes simplex virus 1 effects. J Virol **77:**7101-7105.

310. **Chelbi-Alix MK, Pelicano L, Quignon F, Koken MH, Venturini L, Stadler M, Pavlovic J, Degos L, de The H.** 1995. Induction of the PML protein by interferons in normal and APL cells. Leukemia **9:**2027-2033.

311. **Stadler M, Chelbi-Alix MK, Koken MH, Venturini L, Lee C, Saib A, Quignon F, Pelicano L, Guillemin MC, Schindler C, et al.** 1995. Transcriptional induction of the PML growth suppressor gene by interferons is mediated through an ISRE and a GAS element. Oncogene **11:**2565-2573.

312. **Masroori N, Merindol N, Berthoux L.** 2016. The interferon-induced antiviral protein PML (TRIM19) promotes the restriction and transcriptional silencing of lentiviruses in a context-specific, isoform-specific fashion. Retrovirology **13:**19.

313. **Fuchsová B, Novák P, Kafková J, Hozák P.** 2002. Nuclear DNA helicase II is recruited to IFN-α–activated transcription sites at PML nuclear bodies. J Cell Biol **158:**463-473.

314. **Mentec H, Leport C, Leport J, Marche C, Harzic M, Vilde JL.** 1994. Cytomegalovirus colitis in HIV-1-infected patients: a prospective research in 55 patients. Aids **8:**461-467.

315. **Sunnetcioglu A, Sunnetcioglu M, Emre H, Soyoral L, Goktas U.** 2016. Cytomegalovirus pneumonia and pulmonary haemorrhage in a patient with polyarteritis nodosa. J Pak Med Assoc **66:**1484-1486.

316. **Ahn JH, Jang WJ, Hayward GS.** 1999. The human cytomegalovirus IE2 and UL112-113 proteins accumulate in viral DNA replication compartments that initiate from the periphery of promyelocytic leukemia protein-associated nuclear bodies (PODs or ND10). J Virol **73:**10458-10471.

317. **Ahn JH, Hayward GS.** 1997. The major immediate-early proteins IE1 and IE2 of human cytomegalovirus colocalize with and disrupt PML-associated nuclear bodies at very early times in infected permissive cells. J Virol **71:**4599-4613.

318. **Ahn JH, Hayward GS.** 2000. Disruption of PML-associated nuclear bodies by IE1 correlates with efficient early stages of viral gene expression and DNA replication in human cytomegalovirus infection. Virology **274:**39-55.

319. **Ahn JH, Brignole EJ, 3rd, Hayward GS.** 1998. Disruption of PML subnuclear domains by the acidic IE1 protein of human cytomegalovirus is mediated through interaction with PML and may modulate a RING finger-dependent cryptic transactivator function of PML. Mol Cell Biol **18:**4899-4913.

320. **Tavalai N, Adler M, Scherer M, Riedl Y, Stamminger T.** 2011. Evidence for a dual antiviral role of the major nuclear domain 10 component Sp100 during the immediate-early and late phases of the human cytomegalovirus replication cycle. J Virol **85:**9447-9458.

321. **Scherer M, Otto V, Stump JD, Klingl S, Muller R, Reuter N, Muller YA, Sticht H, Stamminger T.** 2015. Characterization of Recombinant Human Cytomegaloviruses Encoding IE1 Mutants L174P and 1-382 Reveals that Viral Targeting of PML Bodies Perturbs both Intrinsic and Innate Immune Responses. J Virol **90:**1190-1205.

322. **Scherer M, Klingl S, Sevvana M, Otto V, Schilling EM, Stump JD, Muller R, Reuter N, Sticht H, Muller YA, Stamminger T.** 2014. Crystal structure of cytomegalovirus IE1 protein reveals targeting of TRIM family member PML via coiled-coil interactions. PLoS Pathog **10:**e1004512.

323. **Sourvinos G, Tavalai N, Berndt A, Spandidos DA, Stamminger T.** 2007. Recruitment of human cytomegalovirus immediate-early 2 protein onto parental viral genomes in association with ND10 in live-infected cells. J Virol **81:**10123-10136.

324. **Adler M, Tavalai N, Muller R, Stamminger T.** 2011. Human cytomegalovirus immediate-early gene expression is restricted by the nuclear domain 10 component Sp100. J Gen Virol **92:**1532-1538.

325. **Kim YE, Lee JH, Kim ET, Shin HJ, Gu SY, Seol HS, Ling PD, Lee CH, Ahn JH.** 2011. Human cytomegalovirus infection causes degradation of Sp100 proteins that suppress viral gene expression. J Virol **85:**11928-11937.

326. **Groth A, Rocha W, Verreault A, Almouzni G.** 2007. Chromatin challenges during DNA replication and repair. Cell **128:**721-733.

327. **Argentaro A, Yang J-C, Chapman L, Kowalczyk MS, Gibbons RJ, Higgs DR, Neuhaus D, Rhodes D.** 2007. Structural consequences of disease-causing mutations in the ATRX-DNMT3-DNMT3L (ADD) domain of the chromatin-associated protein ATRX. Proc Natl Acad Sci USA **104:**11939-11944.

328. **Cantrell SR, Bresnahan WA.** 2005. Interaction between the human cytomegalovirus UL82 gene product (pp71) and hDaxx regulates immediate-early gene expression and viral replication. J Virol **79:**7792-7802.

329. **Ishov AM, Vladimirova OV, Maul GG.** 2002. Daxx-mediated accumulation of human cytomegalovirus tegument protein pp71 at ND10 facilitates initiation of viral infection at these nuclear domains. J Virol **76:**7705-7712.

330. **Huang H, Deng Z, Vladimirova O, Wiedmer A, Lu F, Lieberman PM, Patel DJ.** 2016. Structural basis underlying viral hijacking of a histone chaperone complex. Nat Commun **7:**12707.

331. **Frappier L.** 2012. Contributions of Epstein-Barr nuclear antigen 1 (EBNA1) to cell immortalization and survival. Viruses **4:**1537-1547.

332. **Amon W, White RE, Farrell PJ.** 2006. Epstein-Barr virus origin of lytic replication mediates association of replicating episomes with promyelocytic leukaemia protein nuclear bodies and replication compartments. J Gen Virol **87:**1133-1137.

333. **Ling PD, Peng RS, Nakajima A, Yu JH, Tan J, Moses SM, Yang WH, Zhao B, Kieff E, Bloch KD, Bloch DB.** 2005. Mediation of Epstein-Barr virus EBNA-LP transcriptional coactivation by Sp100. Embo J **24:**3565-3575.

334. **Sides MD, Block GJ, Shan B, Esteves KC, Lin Z, Flemington EK, Lasky JA.** 2011. Arsenic mediated disruption of promyelocytic leukemia protein nuclear bodies induces ganciclovir susceptibility in Epstein-Barr positive epithelial cells. Virology **416:**86-97.

335. **Bell P, Lieberman PM, Maul GG.** 2000. Lytic but not latent replication of epstein-barr virus is associated with PML and induces sequential release of nuclear domain 10 proteins. J Virol **74:**11800-11810.

336. **Johannsen E, Luftig M, Chase MR, Weicksel S, Cahir-McFarland E, Illanes D, Sarracino D, Kieff E.** 2004. Proteins of purified Epstein-Barr virus. Proc Natl Acad Sci U S A **101:**16286-16291.

337. **Sivachandran N, Sarkari F, Frappier L.** 2008. Epstein-Barr nuclear antigen 1 contributes to nasopharyngeal carcinoma through disruption of PML nuclear bodies. PLoS Pathog **4:**e1000170.

338. **Sivachandran N, Cao JY, Frappier L.** 2010. Epstein-Barr virus nuclear antigen 1 Hijacks the host kinase CK2 to disrupt PML nuclear bodies. J Virol **84:**11113-11123.

339. **Echendu CW, Ling PD.** 2008. Regulation of Sp100A subnuclear localization and transcriptional function by EBNA-LP and interferon. J Interferon Cytokine Res **28:**667-678.

340. **Szekely L, Pokrovskaja K, Jiang WQ, de The H, Ringertz N, Klein G.** 1996. The Epstein-Barr virus-encoded nuclear antigen EBNA-5 accumulates in PML-containing bodies. J Virol **70:**2562-2568.

341. **Everett RD, Freemont P, Saitoh H, Dasso M, Orr A, Kathoria M, Parkinson J.** 1998. The disruption of ND10 during herpes simplex virus infection correlates with the Vmw110- and proteasome-dependent loss of several PML isoforms. J Virol **72:**6581-6591.

342. **Schilling EM, Scherer M, Reuter N, Schweininger J, Muller YA, Stamminger T.** 2017. The Human Cytomegalovirus IE1 Protein Antagonizes PML Nuclear Body-

Mediated Intrinsic Immunity via the Inhibition of PML De Novo SUMOylation. J Virol **91:**e02049-02016.

343. **Bowling BL, Adamson AL.** 2006. Functional interactions between the Epstein-Barr virus BZLF1 protein and the promyelocytic leukemia protein. Virus Res **117:**244-253.
344. **Yu X, Li W, Liu L, Che Y, Cun W, Wu W, He C, Shao C, Li Q.** 2008. Functional analysis of transcriptional regulation of herpes simplex virus type 1 tegument protein VP22. Sci China C Life Sci **51:**966-972.
345. **Potel C, Elliott G.** 2005. Phosphorylation of the herpes simplex virus tegument protein VP22 has no effect on incorporation of VP22 into the virus but is involved in optimal expression and virion packaging of ICP0. J Virol **79:**14057-14068.
346. **Morrison EE, Wang Y-F, Meredith DM.** 1998. Phosphorylation of structural components promotes dissociation of the herpes simplex virus type 1 tegument. J Virol **72:**7108-7114.
347. **Ottosen S, Herrera FJ, Doroghazi JR, Hull A, Mittal S, Lane WS, Triezenberg SJ.** 2006. Phosphorylation of the VP16 transcriptional activator protein during herpes simplex virus infection and mutational analysis of putative phosphorylation sites. Virology **345:**468-481.
348. **Geiss BJ, Tavis JE, Metzger LM, Leib DA, Morrison LA.** 2001. Temporal regulation of herpes simplex virus type 2 VP22 expression and phosphorylation. J Virol **75:**10721-10729.
349. **Pomeranz LE, Blaho JA.** 1999. Modified VP22 localizes to the cell nucleus during synchronized herpes simplex virus type 1 infection. J Virol **73:**6769-6781.
350. **Saffert RT, Penkert RR, Kalejta RF.** 2010. Cellular and viral control over the initial events of human cytomegalovirus experimental latency in CD34+ cells. J Virol **84:**5594-5604.
351. **Everett R, O'Hare P, O'Rourke D, Barlow P, Orr A.** 1995. Point mutations in the herpes simplex virus type 1 Vmw110 RING finger helix affect activation of gene expression, viral growth, and interaction with PML-containing nuclear structures. J Virol **69:**7339-7344.

352. **Cuchet-Lourenco D, Vanni E, Glass M, Orr A, Everett RD.** 2012. Herpes simplex virus 1 ubiquitin ligase ICP0 interacts with PML isoform I and induces its SUMO-independent degradation. J Virol **86:**11209-11222.

353. **Komis G, Takac T, Bekesova S, Vadovic P, Samaj J.** 2014. Affinity-based SDS PAGE identification of phosphorylated Arabidopsis MAPKs and substrates by acrylamide pendant Phos-Tag. Methods Mol Biol **1171:**47-63.

354. **Marks F.** 2008. Protein phosphorylation. Chapter 10.6, Page 292. ISBN: 978-3-527-61502-5.

355. **Ross-Thriepland D, Harris M.** 2014. Insights into the complexity and functionality of hepatitis C virus NS5A phosphorylation. J Virol **88:**1421-1432.

356. **Hizli AA, Chi Y, Swanger J, Carter JH, Liao Y, Welcker M, Ryazanov AG, Clurman BE.** 2013. Phosphorylation of Eukaryotic Elongation Factor 2 (eEF2) by Cyclin A–Cyclin-Dependent Kinase 2 Regulates Its Inhibition by eEF2 Kinase. Mol Cell Biocham **33:**596-604.

357. **Eblen ST, Slack-Davis JK, Tarcsafalvi A, Parsons JT, Weber MJ, Catling AD.** 2004. Mitogen-activated protein kinase feedback phosphorylation regulates MEK1 complex formation and activation during cellular adhesion. Mol Cell Biol **24:**2308-2317.

358. **Benetti L, Roizman B.** 2004. Herpes simplex virus protein kinase US3 activates and functionally overlaps protein kinase A to block apoptosis. Proc Natl Acad Sci U S A **101:**9411-9416.

359. **Chuluunbaatar U, Roller R, Feldman ME, Brown S, Shokat KM, Mohr I.** 2010. Constitutive mTORC1 activation by a herpesvirus Akt surrogate stimulates mRNA translation and viral replication. Genes Dev **24:**2627-2639.

360. **Joughin BA, Liu C, Lauffenburger DA, Hogue CW, Yaffe MB.** 2012. Protein kinases display minimal interpositional dependence on substrate sequence: potential implications for the evolution of signalling networks. Philos Trans R Soc Lond B Biol Sci **367:**2574-2583.

361. **Rihs H-P, Jans D, Fan H, Peters R.** 1991. The rate of nuclear cytoplasmic protein transport is determined by the casein kinase II site flanking the nuclear localization sequence of the SV40 T-antigen. The EMBO Journal **10:**633-639.

362. **Bosse JB, Virding S, Thiberge SY, Scherer J, Wodrich H, Ruzsics Z, Koszinowski UH, Enquist LW.** 2014. Nuclear herpesvirus capsid motility is not dependent on F-actin. MBio **5:**e01909-01914.

363. **Shen S, Jia X, Guo H, Deng H.** 2015. Tegument protein ORF33 of a gammaherpesvirus is associated with intranuclear capsids at an early stage of tegumentation process. J Virol doi:10.1128/jvi.00079-15.

364. **Schulz KS, Klupp BG, Granzow H, Passvogel L, Mettenleiter TC.** 2015. Herpesvirus nuclear egress: Pseudorabies Virus can simultaneously induce nuclear envelope breakdown and exit the nucleus via the envelopment-deenvelopment-pathway. Virus Res.

365. **Shaw AM, Braun L, Frew T, Hurley DJ, Rowland RR, Chase CC.** 2000. A role for bovine herpesvirus 1 (BHV-1) glycoprotein E (gE) tyrosine phosphorylation in replication of BHV-1 wild-type virus but not BHV-1 gE deletion mutant virus. Virology **268:**159-166.

366. **Bashour A-M, Bloom GS.** 1998. 58K, a microtubule-binding Golgi protein, is a formiminotransferase cyclodeaminase. J Bio Chem **273:**19612-19617.

367. **Schindelin J, Arganda-Carreras I, Frise E, Kaynig V, Longair M, Pietzsch T, Preibisch S, Rueden C, Saalfeld S, Schmid B.** 2012. Fiji: an open-source platform for biological-image analysis. Nature methods **9:**676-682.

368. **Mettenleiter TC.** 2002. Herpesvirus assembly and egress. J Virol **76:**1537-1547.

369. **Visalli RJ, van Zeijl M.** 2003. DNA encapsidation as a target for anti-herpesvirus drug therapy. Antiviral Research **59:**73-87.

370. **Kawana K, Yoshikawa H, Taketani Y, Yoshiike K, Kanda T.** 1998. In vitro construction of pseudovirions of human papillomavirus type 16: incorporation of plasmid DNA into reassembled L1/L2 capsids. J Virol **72:**10298-10300.

371. **Henaff D, Remillard-Labrosse G, Loret S, Lippe R.** 2013. Analysis of the early steps of herpes simplex virus 1 capsid tegumentation. J Virol **87:**4895-4906.

372. **Fuchs W, Klupp BG, Granzow H, Osterrieder N, Mettenleiter TC.** 2002. The interacting UL31 and UL34 gene products of pseudorabies virus are involved in egress from the host-cell nucleus and represent components of primary enveloped but not mature virions. J Virol **76:**364-378.

373. **Granzow H, Klupp BG, Mettenleiter TC.** 2004. The pseudorabies virus US3 protein is a component of primary and of mature virions. J Virol **78:**1314-1323.

374. **Donnelly M, Elliott G.** 2001. Fluorescent tagging of herpes simplex virus tegument protein VP13/14 in virus infection. J Virol **75:**2575-2583.

375. **Zhang K, Brownlie R, Snider M, van Drunen Littel-van den Hurk S.** 2016. Phosphorylation of Bovine Herpesvirus 1 VP8 Plays a Role in Viral DNA Encapsidation and Is Essential for Its Cytoplasmic Localization and Optimal Virion Incorporation. J Virol **90:**4427-4440.

376. **Biswas A, Mukherjee S, Das S, Shields D, Chow CW, Maitra U.** 2011. Opposing Action of Casein Kinase 1 and Calcineurin in Nucleo-cytoplasmic Shuttling of Mammalian Translation Initiation Factor eIF6. J Bio Chem **286:**3129-3138.

377. **Miluzio A, Beugnet A, Volta V, Biffo S.** 2009. Eukaryotic initiation factor 6 mediates a continuum between 60S ribosome biogenesis and translation. EMBO Reports **10:**459-465.

378. **Alonzo F, Mayzaud P.** 1999. Spectrofluorometric quantification of neutral and polar lipids in zooplankton using Nile red. Marine Chem **67:**289-301.

379. **Feng G-D, Zhang F, Cheng L-H, Xu X-H, Zhang L, Chen H-L.** 2013. Evaluation of FT-IR and Nile red methods for microalgal lipid characterization and biomass composition determination. Bioresource Technology **128:**107-112.

380. **Rohwedder A, Zhang Q, Rudge SA, Wakelam MJ.** 2014. Lipid droplet formation in response to oleic acid in Huh-7 cells is mediated by the fatty acid receptor FFAR4. J Cell Sci **127:**3104-3115.

381. **Gotoh O.** 1990. Consistency of optimal sequence alignments. Bulletin of Mathematical Biology **52:**509-525.

382. **Gao YS, Alvarez C, Nelson DS, Sztul E.** 1998. Molecular cloning, characterization, and dynamics of rat formiminotransferase cyclodeaminase, a Golgi-associated 58-kDa protein. J Biol Chem **273:**33825-33834.

383. **Burman JL, Hamlin JN, McPherson PS.** 2010. Scyl1 regulates Golgi morphology. PLoS One **5:**e9537.

384. **Gao Y, Sztul E.** 2001. A novel interaction of the Golgi complex with the vimentin intermediate filament cytoskeleton. J Biol Chem **152:**877-894.

385. **Hennig D, Scales SJ, Moreau A, Murley LL, De Mey J, Kreis TE.** 1998. A formiminotransferase cyclodeaminase isoform is localized to the Golgi complex and can mediate interaction of trans-Golgi network-derived vesicles with microtubules. J Biol Chem **273:**19602-19611.

386. **Asante D, Maccarthy-Morrogh L, Townley AK, Weiss MA, Katayama K, Palmer KJ, Suzuki H, Westlake CJ, Stephens DJ.** 2013. A role for the Golgi matrix protein giantin in ciliogenesis through control of the localization of dynein-2. J Cell Sci **126:**5189-5197.

387. **Katayama K, Sasaki T, Goto S, Ogasawara K, Maru H, Suzuki K, Suzuki H.** 2011. Insertional mutation in the Golgb1 gene is associated with osteochondrodysplasia and systemic edema in the OCD rat. Bone **49:**1027-1036.

388. **Lan Y, Zhang N, Liu H, Xu J, Jiang R.** 2016. Golgb1 regulates protein glycosylation and is crucial for mammalian palate development. Development **143:**2344-2355.

389. **Chege NW, Pfeffer SR.** 1990. Compartmentation of the Golgi complex: brefeldin-A distinguishes trans-Golgi cisternae from the trans-Golgi network. J Bio Chem **111:**893-899.

390. **Bejarano E, Cabrera M, Vega L, Hidalgo J, Velasco A.** 2006. Golgi structural stability and biogenesis depend on associated PKA activity. J Cell Sci **119:**3764-3775.

391. **Reaves B, Banting G.** 1992. Perturbation of the morphology of the trans-Golgi network following Brefeldin A treatment: redistribution of a TGN-specific integral membrane protein, TGN38. J Cell Biol **116:**85-94.

392. **Nagashima S, Takahashi M, Jirintai S, Tanggis, Kobayashi T, Nishizawa T, Okamoto H.** 2014. The membrane on the surface of hepatitis E virus particles is derived from the intracellular membrane and contains trans-Golgi network protein 2. Archives Virol **159:**979-991.

393. **Angius F, Uda S, Piras E, Spolitu S, Ingianni A, Batetta B, Pompei R.** 2015. Neutral lipid alterations in human herpesvirus 8-infected HUVEC cells and their possible involvement in neo-angiogenesis. BMC Microbiol **15:**74.

394. **Boncompain G, Perez F.** 2013. The many routes of Golgi-dependent trafficking. Histochem and Cell Bio **140:**251-260.

395. **Papanikou E, Glick BS.** 2014. Golgi compartmentation and identity. Current Opinion of Cell Biololgy **29:**74-81.

396. **Li T, You H, Zhang J, Mo X, He W, Chen Y, Tang X, Jiang Z, Tu R, Zeng L, Lu W, Hu Z.** 2014. Study of GOLPH3: a potential stress-inducible protein from Golgi apparatus. Mol Neurobiol **49:**1449-1459.

397. **Hollinshead M, Johns HL, Sayers CL, Gonzalez-Lopez C, Smith GL, Elliott G.** 2012. Endocytic tubules regulated by Rab GTPases 5 and 11 are used for envelopment of herpes simplex virus. The EMBO Journal **31:**4204-4220.

398. **Johns HL, Gonzalez-Lopez C, Sayers CL, Hollinshead M, Elliott G.** 2014. Rab6 dependent post-Golgi trafficking of HSV1 envelope proteins to sites of virus envelopment. Traffic **15:**157-178.

399. **Hagemann D, Xiao RP.** 2002. Dual site phospholamban phosphorylation and its physiological relevance in the heart. Trends Cardiovasc Med **12:**51-56.

400. **Byeon I-JL, Li H, Song H, Gronenborn AM, Tsai M-D.** 2005. Sequential phosphorylation and multisite interactions characterize specific target recognition by the FHA domain of Ki67. Nature structural & molecular biology **12:**987-993.

401. **Fujii H, Mugitani M, Koyanagi N, Liu Z, Tsuda S, Arii J, Kato A, Kawaguchi Y.** 2014. Role of the nuclease activities encoded by herpes simplex virus 1 UL12 in viral replication and neurovirulence. J Virol **88:**2359-2364.

402. **Li L, Li Y, Dai Z, Liu M, Wang B, Liu S, Wang L, Chen L, Tan Y, Wu G.** 2016. Lipid Metabolism in Vascular Smooth Muscle Cells Infuenced by HCMV Infection. Cell Physiol Biochem **39:**1804-1812.

403. **Seo JY, Cresswell P.** 2013. Viperin regulates cellular lipid metabolism during human cytomegalovirus infection. PLoS Pathog **9:**e1003497.

404. **Hwang KY, Choi YB.** 2015. Modulation of Mitochondrial Antiviral Signaling by Human Herpesvirus 8 Interferon Regulatory Factor 1. J Virol **90:**506-520.

405. **Raghu H, Sharma-Walia N, Veettil MV, Sadagopan S, Caballero A, Sivakumar R, Varga L, Bottero V, Chandran B.** 2007. Lipid rafts of primary endothelial cells are essential for Kaposi's sarcoma-associated herpesvirus/human herpesvirus 8-induced phosphatidylinositol 3-kinase and RhoA-GTPases critical for microtubule dynamics and

nuclear delivery of viral DNA but dispensable for binding and entry. J Virol **81:**7941-7959.

406. **Leppard KN, Emmott E, Cortese MS, Rich T.** 2009. Adenovirus type 5 E4 Orf3 protein targets promyelocytic leukaemia (PML) protein nuclear domains for disruption via a sequence in PML isoform II that is predicted as a protein interaction site by bioinformatic analysis. J Gen Virol **90:**95-104.

407. **Hoppe A, Beech SJ, Dimmock J, Leppard KN.** 2006. Interaction of the adenovirus type 5 E4 Orf3 protein with promyelocytic leukemia protein isoform II is required for ND10 disruption. J Virol **80:**3042-3049.

408. **Carvalho T, Seeler JS, Ohman K, Jordan P, Pettersson U, Akusjärvi G, Carmo-Fonseca M, Dejean A.** 1995. Targeting of adenovirus E1A and E4-ORF3 proteins to nuclear matrix-associated PML bodies. J Cell Bio **131:**45-56.

409. **Bontems S, Di Valentin E, Baudoux L, Rentier B, Sadzot-Delvaux C, Piette J.** 2002. Phosphorylation of varicella-zoster virus IE63 protein by casein kinases influences its cellular localization and gene regulation activity. J Biol Chem **277:**21050-21060.

410. **Habran L, Bontems S, Di Valentin E, Sadzot-Delvaux C, Piette J.** 2005. Varicella-zoster virus IE63 protein phosphorylation by roscovitine-sensitive cyclin-dependent kinases modulates its cellular localization and activity. J Biol Chem **280:**29135-29143.

411. **Mueller NH, Graf LL, Orlicky D, Gilden D, Cohrs RJ.** 2009. Phosphorylation of the nuclear form of varicella-zoster virus immediate-early protein 63 by casein kinase II at serine 186. J Virol **83:**12094-12100.

412. **Zuranski T, Nawar H, Czechowski D, Lynch JM, Arvin A, Hay J, Ruyechan WT.** 2005. Cell-type-dependent activation of the cellular EF-1alpha promoter by the varicella-zoster virus IE63 protein. Virology **338:**35-42.

413. **Baiker A, Bagowski C, Ito H, Sommer M, Zerboni L, Fabel K, Hay J, Ruyechan W, Arvin AM.** 2004. The immediate-early 63 protein of Varicella-Zoster virus: analysis of functional domains required for replication in vitro and for T-cell and skin tropism in the SCIDhu model in vivo. J Virol **78:**1181-1194.

414. **Fujii H, Kato A, Mugitani M, Kashima Y, Oyama M, Kozuka-Hata H, Arii J, Kawaguchi Y.** 2014. The UL12 Protein of Herpes Simplex Virus 1 Is Regulated by Tyrosine Phosphorylation. J Virol **88:**10624-10634.

415. **Malik P, Clements JB.** 2004. Protein kinase CK2 phosphorylation regulates the interaction of Kaposi's sarcoma-associated herpesvirus regulatory protein ORF57 with its multifunctional partner hnRNP K. Nucleic Acids Res **32:**5553-5569.

416. **Banfield DK.** 2011. Mechanisms of protein retention in the Golgi. Cold Spring Harb Perspect Biol **3:**a005264.